

DYNA

Journal of the Facultad de Minas, Universidad Nacional de Colombia - Medellín Campus
DYNA 92 (239), October- December, 2025 - ISSN 0012-7353



Facultad de Minas
Sede Medellín



UNIVERSIDAD
NACIONAL
DE COLOMBIA

DYNA is an international journal published by the Facultad de Minas, Universidad Nacional de Colombia, Medellín Campus since 1933. DYNA publishes peer-reviewed scientific articles covering all aspects of engineering. Our objective is the dissemination of original, useful and relevant research presenting new knowledge about theoretical or practical aspects of methodologies and methods used in engineering or leading to improvements in professional practices. All conclusions presented in the articles must be based on the current state-of-the-art and supported by a rigorous analysis and a balanced appraisal. The journal publishes scientific and technological research articles, review articles and case studies.

DYNA publishes articles in the following areas:

Organizational Engineering

Civil Engineering

Materials and Mines Engineering

Geosciences and the Environment

Systems and Informatics

Chemistry and Petroleum

Mechatronics

Bio-engineering

Other areas related to engineering

Publication Information

DYNA (ISSN 0012-73533, Printed; 2346-2183, online).

Is published by the Facultad de Minas, Universidad Nacional de Colombia, with a quarterly periodicity (January - March, April - June, July - September and October - December).

Circulation License Resolution 000584 de 1976 from the Ministry of the Government.

Contact information:

Web page: <https://revistas.unal.edu.co/index.php/dyna>

E-mail: dyna@unal.edu.co

Mail address:

Revista DYNA

Facultad de Minas

Universidad Nacional de Colombia - Medellín Campus

Carrera 80 No. 65-223 Bloque M9 - Of.:107

Telephone: (574) (604) 4255343

Medellín - Colombia

© Copyright 2025. Universidad Nacional de Colombia

The complete or partial reproduction of texts with educational ends is permitted, granted that the source is duly cited. Unless indicated otherwise.

Notice

All statements, methods, instructions and ideas are only responsibility of the authors and not necessarily represent the view of the Universidad Nacional de Colombia. The publisher does not accept responsibility for any injury and/or damage for the use of the content of this journal.

The concepts and opinions expressed in the articles are the exclusive responsibility of the authors.

Institutional Exchange Request

DYNA may be requested as an institutional exchange through the e-mail: canjebib_med@unal.edu.co or to the postal address:

Biblioteca Central "Efe Gómez"

Universidad Nacional de Colombia, Sede Medellín

Calle 59A No 63-20

Teléfono: (574) (604) 430 97 86

Medellín - Colombia

Indexing and Databases

DYNA is admitted in:

The National System of Indexation and Homologation of Specialized Journals CT+I-PUBLINDEX, Category C

Science Citation Index Expanded

SCImago Journal & Country Rank - SJR

SCOPUS

SciELO Scientific Electronic Library Online

Chemical Abstract - CAS

Scientific Electronic Library on Line - SciELO

GEOREF

PERIÓDICA Data Base

Latindex

Actualidad Iberoamericana

Redalyc - Scientific Information System

Directory of Open Acces Journals - DOAJ

PASCAL

CAPEP

UN Digital Library - SINAB

EBSCO Host Research Databases

Publisher's Office

Luz Alexandra Montoya Restrepo, Director

Mónica del Pilar Rada T., Editorial Coordinator

Catalina Cardona A., Editorial Assistant

Manuela González C., Editorial Assistant

Todograficas Ltda., Diagramming

Reduced Postal Fee

Tarifa Postal Reducida # 2014-287 4-72.

La Red Postal de Colombia, expires Dec. 31st, 2025



UNIVERSIDAD
NACIONAL
DE COLOMBIA

DYNA

COUNCIL OF THE FACULTAD DE MINAS

Dean

Eva Cristina Manotas, PhD

Vice-Dean

Néstor Ricardo Rojas Reyes, PhD

Vice-Dean of Research and Extension

Jorge Eliécer Córdoba Maquilón, PhD

Director of University Services

Camilo Alberto Suárez Méndez, PhD

Academic Secretary

Maria Constanza Torres Madroñero, PhD

Representative of the Curricular Area Directors

John Robert Ballesteros Parra, PhD

Representative of the Curricular Area Directors

Claudia Helena Muñoz Hoyos, PhD

Representative of the Basic Academic Units

Álvaro Jesús Castro Caicedo, PhD

Representative of the Basic Academic Units

Albeiro Rendón Rivera, PhD

Professor Representative

Luis Hernán Sánchez Arredondo, PhD

Student representative at the Faculty Council

Bleidys Thamara Valderrama Casas

Student representative at the Faculty Council

Sara Daniela Coronado Maju

JOURNAL EDITORIAL BOARD

Editor-in-Chief

Luz Alexandra Montoya Restrepo,
PhD. Universidad Nacional de Colombia, Colombia

Editors

Raúl Ocampo Pérez,
PhD. Universidad Autónoma de San Luis Potosí, Mexico

Vladimir Alvarado,
PhD. Universidad de Wyoming,
USA

Francisco Carrasco Marin,
PhD. Universidad de Granada, Spain

Sergio Velastin,
PhD, University of London, England

Hans Christian Öttinger,
PhD. Swiss Federal Institute of Technology (ETH),
Switzerland

Jordi Payá Bernabeu,
PhD. Instituto de Ciencia y Tecnología del Hormigón
(ICITECH), Universitat Politècnica de València, Spain

Javier Belzunce Varela,
PhD. Universidad de Oviedo, Spain

Henrique Lorenzo Cimadevila,
PhD. Universidad de Vigo, Spain

Carlos Palacio,
PhD. Universidad de Antioquia, Colombia

Oscar Jaime Restrepo Baena,
PhD. Universidad Nacional de Colombia,
Colombia

FACULTY EDITORIAL BOARD

Dean

Eva Cristina Manotas, PhD

Vice-Dean of Research and Extension

Jorge Eliécer Córdoba Maquilón, PhD

Members

Luz Alexandra Montoya Restrepo, PhD
Néstor Ricardo Rojas Reyes, PhD
Enrique Posada Restrepo, MSc
Mónica del Pilar Rada Tobón, MSc

Support members

Francisco Montaña Ibáñez, MSc
Director Editorial UN
Diana Carolina Martínez Santos, MSc.
Directora Nacional de Bibliotecas UN

CONTENTS

Impact of printing strategies and thermal debinding atmosphere on the microstructure and mechanical properties of M2 tool steel produced via fused filament fabrication	9
Theylor Andres Amaya-Villabon, Andres Fernando Gil-Plazas, Julián David Rubiano-Buitrago & Liz Karen Herrera-Quintero	
A mathematical model for optimizing the milk and cheese production chain in southern Nariño, Colombia	19
Rigoberto Rosero-Benavides & Carlos Julio Vidal-Holguín	
Experimental analysis and computational simulation of heat transfer in a radiator	27
Juan Mauricio Trenado-Herrera, Crisanto Mendoza-Covarrubias, Alicia Aguilar-Corona & Hugo Cuauhtémoc Gutiérrez-Sánchez	
Methodology for evaluating the effectiveness of clay inhibition treatments in injection wells: a case study in a colombian field	38
Jeimy Alejandra Peña-Mateus, María Paula Mosquera-González, Eduardo Alfredo Gómez-Cepeda, Franklin Iván Archer-Martínez & Jaqueline Jaimes-Barajas	
Proposals for improving acoustic comfort at the Be Live Experience Tuxpan hotel	49
Juan Lázaro Acosta-Prieto, Yoel Almeda-Barrios, Yosmil Lázaro Peña-Pérez & Juan Carlos Peña-Ramírez	
ADKT: a support tool for reducing architectural knowledge evaporation in software projects	56
Santiago Hyun-Dorado, Julio Ariel Hurtado-Alegria, Enrique Moguel, & Jose Garcia-Alonso	
Effectiveness of 2-Layered grounding grids in high voltage GIS substations and new design considerations using FEM	66
Asaad Shemshadi, Mitra Kamal Abadi, Vahid Sourí, Ali Safari, & Ali Fathi	
Governance and participatory strategies in sustainable water management: a systematic analysis	72
Rossember Saldaña-Escorcia	
Synthesis of surfactants based on alkyl glyceryl ester /ether and evaluation as wax inhibitor	82
Denise Gentili Nunes, Giovani Cavalcanti Nunes, Elizabeth Roditi Lachter, Agatha Oliveira Santos, Rita de Cássia Pessanha Nunes & Elizabete Fernandes Lucas	
Mapping the evolution of drone-based last-mile delivery: a bibliometric analysis with field insights from Colombia	91
Luz Maribel Guevara-Ortega, Juan Enrique Hidalgo-Urrea, Luz Mireya Candil-Parra & William Rafael Navarro-Zúñiga	
Improvement of the efficiency of hospital care: a simulation-based approach	101
Katherine Tatiana Osorio-Canchig, John Paúl Reyes-Vásquez & Darwin Santiago Aldás-Salazar	
Safety competency model for drillers in open-pit mines: application of functional analysis and developing a curriculum in Mexican mining	111
Graciela Rodríguez-Vega, María Alejandra Valenzuela-Soto & Dora Aydee Rodríguez-Vega	
Technical and economic analysis of alternatives for the construction of tertiary roads in Colombia	118
Zully Palomeque-Sánchez, Juan Gabriel Bastidas-Martínez & Jessica Rincón-Esteva	
Dam break analysis in Andean mountainous areas using numerical simulation in Iber	130
Paulina Elizabeth Suárez-Naranjo, Patricio Rubén Ortega-Lara & Patricia Lorena Haro-Ruiz	
Methods for determining the structural strength of reinforced concrete beams with hybrid nodes	139
Yordy Míeles-Bravo & Gema Zambrano-Baque	

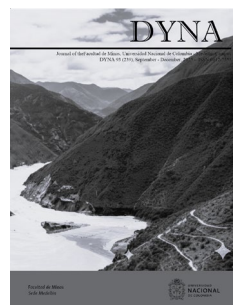
Our Cover

Image: *Discharge of the Cuenca River due to the breach of the artificial dam*, by: Barreto et al, 2008.

In the article "Analysis of dam breaks in Andean mountain areas using numerical simulation in Iber"
Image manipulated and enhanced with Artificial Intelligence in:
<https://gemini.google.com/app>.

Authors

Paulina Elizabeth Suárez-Naranjo, Patricio Rubén Ortega-Lara & Patricia Lorena Haro-Ruiz.



CONTENIDO

Impacto de las estrategias de impresión y de la atmósfera de despolimerización térmica en la microestructura y las propiedades mecánicas del acero de herramientas M2 producido mediante fabricación por fusión de filamentos	9
Theylor Andres Amaya-Villabon, Andres Fernando Gil-Plazas, Julián David Rubiano-Buitrago & Liz Karen Herrera-Quintero	
Un modelo matemático para optimizar la cadena de producción de leche y queso en el sur de Nariño, Colombia	19
Rigoberto Rosero-Benavides & Carlos Julio Vidal-Holguín	
Análisis experimental y simulación computacional de la transferencia de calor en un radiador	27
Juan Mauricio Trenado-Herrera, Crisanto Mendoza-Covarrubias, Alicia Aguilar-Corona & Hugo Cuauhtémoc Gutiérrez-Sánchez	
Metodología para la evaluación de la eficacia de tratamientos de inhibición de arcilla en pozos inyectoros: caso de estudio en un campo colombiano	38
Jeimy Alejandra Peña-Mateus, María Paula Mosquera-González, Eduardo Alfredo Gómez-Cepeda, Franklin Iván Archer-Martínez & Jaqueline Jaimes-Barajas	
Propuestas para la mejora del confort acústico en el hotel Be Live Experience Tuxpan	49
Juan Lázaro Acosta-Prieto, Yoel Almeda-Barrios, Yosmil Lázaro Peña-Pérez & Juan Carlos Peña-Ramírez	
ADKT: una herramienta para la reducción de la evaporación del conocimiento arquitectónico en proyectos software	56
Santiago Hyun-Dorado, Julio Ariel Hurtado-Alegría, Enrique Moguel, & Jose Garcia-Alonso	
Eficacia de redes de puesta a tierra de dos capas en subestaciones GIS de alta tensión y consideraciones de diseño mediante FEM	66
Asaad Shemshadi, Mitra Kamal Abadi, Vahid Souri, Ali Safari, & Ali Fathi	
Gobernanza y estrategias participativas en la gestión sostenible del agua: un análisis sistemático	72
Rossember Saldaña-Escordia	
Síntesis de surfactantes basados en ésteres/éteres de alquil glicerilo y evaluación como inhibidores de ceras	82
Denise Gentili Nunes, Giovani Cavalcanti Nunes, Elizabeth Roditi Lachter, Agatha Oliveira Santos, Rita de Cássia Pessanha Nunes & Elizabete Fernandes Lucas	
Evolución de la entrega con drones en la última milla: análisis bibliométrico con enfoque en Colombia	91
Luz Maribel Guevara-Ortega, Juan Enrique Hidalgo-Urrea, Luz Mireya Candil-Parra & William Rafael Navarro-Zúñiga	
Mejora de la eficiencia de la atención hospitalaria: un enfoque basado en la simulación	10
Katherine Tatiana Osorio-Canchig, John Paúl Reyes-Vásquez & Darwin Santiago Aldás-Salazar	
Modelo de competencias de seguridad para perforistas en minas a cielo abierto: aplicación de análisis funcional y desarrollo de un curriculum en la minería Mexicana	111
Graciela Rodríguez-Vega, María Alejandra Valenzuela-Soto & Dora Aydee Rodríguez-Vega	
Análisis técnico y económico de alternativas para la construcción de vías terciarias en Colombia	118
Zully Palomeque-Sánchez, Juan Gabriel Bastidas-Martínez & Jessica Rincón-Esteva	
Análisis de rotura de presas en zonas montañosas Andinas mediante simulación numérica en Iber	130
Paulina Elizabeth Suárez-Naranjo, Patricio Rubén Ortega-Lara & Patricia Lorena Haro-Ruiz	
Métodos para determinar la resistencia estructural en vigas de hormigón armado con nudos híbridos	139
Yordy Mielles-Bravo & Gema Zambrano-Baque	

Nuestra Carátula

Imagen: *Desfogue del río Cuenca por rotura del dique artificial*, por: Barreto et al, 2008.

En el artículo "Análisis de rotura de presas en zonas montañosas Andinas mediante simulación numérica en Iber"

Imagen manipulada y mejorada con Inteligencia Artificial en: <https://gemini.google.com/app>.

Autores

Paulina Elizabeth Suárez-Naranjo, Patricio Rubén Ortega-Lara & Patricia Lorena Haro-Ruiz.



Carta de la Decana

2025 sido un año de retos y desafíos, ante los que la Facultad de Minas de la Universidad Nacional de Colombia, ha logrado proponer desde la articulación de sus capacidades para la ejecución de sus fines misionales, estrategias de trabajo colaborativo para responder a las necesidades de la región y el país.

Entre las ceremonias de junio y noviembre de este año, graduamos a 918 personas: 617 en nuestros pregrados y 301 en nuestros posgrados. Hemos recibido visitas de pares evaluadores de 5 de nuestros programas académicos para la reacreditación de los mismos y creamos un nuevo programa de posgrado, la especialización en gestión de proyectos de inversión pública.

Cada año educamos con Trabajo y Rectitud a los nuevos líderes que transformarán y le darán desarrollo y esperanza a Colombia. Nuestros egresados, afirman su compromiso con un ejercicio profesional dedicado y responsable, ejerciendo de manera idónea la ingeniería, de acuerdo a los estándares académicos y técnicos de calidad, conscientes de que la ingeniería constituye un poderoso factor de transformación de las comunidades humanas y del entorno natural. En cada decisión y en su actuar reconocen y cuidan el valor de la vida: Personas íntegras con aprecio por el trabajo colaborativo y multidisciplinario, líderes de los procesos de cambio social e innovación tecnológica.

En investigación y extensión, nuestra Facultad actualmente ejecuta cerca de 114 proyectos, y después de 5 años logramos finalizar el proyecto del diseño y construcción de una embarcación híbrida para la comunidad de pescadores de Guapi, Cauca.

Y promovemos la apropiación social del conocimiento a través del trabajo responsable y comprometido de la comunicación de los aportes en el campo de la ingeniería, a través de nuestras publicaciones científicas DYNA y el

Boletín de Ciencias de la Tierra, y nuestra revista de divulgación Ingeniería y Organizaciones. El reto de seguir imprimiendo el rigor de la investigación y asegurar que nuestros artículos lleguen a la audiencia correcta, y todo lo anterior, en presencia de la rápida evolución tecnológica, el manejo de la competencia de fábricas de artículos y la gestión del proceso de publicación en sí mismo, hoy me hacen destacar y felicitar a nuestro equipo editorial DYNA, por lograr esta maravillosa publicación. Reuniendo temas diversos pero pertinentes que nos invitan a disfrutar de una lectura nutrida y llena de aprendizajes.

Finalmente, invito a nuestros lectores a seguir acompañándonos y hacer parte de nuestra comunidad, bien sea como espectadores a través de la lectura y análisis de nuestras publicaciones, o como colaboradores directos de nuestros fines misionales. En 138 años, hemos mantenido una posición de liderazgo en el contexto de las facultades de ingeniería de la región y el país, cultivando una identidad colectiva basada en nuestros valores institucionales y en el convencimiento del papel que juega la ingeniería como fuente de bienestar para la sociedad.

Los invitamos a que nos acompañen en la construcción de un nuevo camino, una nueva plataforma para desarrollar una “Ingeniería para la vida, pero siempre conectados con el territorio y el mundo”.

Eva Cristina Manotas Rodríguez
Decana Facultad de Minas
Profesora Titular
Universidad Nacional de Colombia
E-mail: ecmanota@unal.edu.co
ORCID: 0000-0002-5078-278X

Impact of printing strategies and thermal debinding atmosphere on the microstructure and mechanical properties of M2 tool steel produced via fused filament fabrication

Theylor Andres Amaya-Villabon ^a, Andres Fernando Gil-Plazas ^b, Julián David Rubiano-Buitrago ^a
& Liz Karen Herrera-Quintero ^a

^a Universidad Nacional de Colombia – Sede Bogotá, Facultad de Ingeniería, Departamento de Ingeniería Mecánica y Mecatrónica, Grupo de Investigación AFIS, Laboratorio de Fundición y Pulvimetalurgia, Bogotá, Colombia. taamayav@unal.edu.co, judrubianobu@unal.edu.co, lherreraq@unal.edu.co

^b SENA, Centro de Materiales y Ensayos - Regional Distrito Capital, Grupo de Investigación GIMES, Bogotá, Colombia. agilp@sena.edu.co

Received: August 14th, 2024. Received in revised form: November 13th, 2024. Accepted: December 2nd, 2024.

Abstract

This research investigates the effects of printing strategies and thermal debinding atmosphere on the microstructure and mechanical properties of M2 tool steel samples obtained by Fused Filament Fabrication. A comparative analysis was conducted between concentric and linear printing patterns. Printed samples were subjected to different thermal debinding heating rates in nitrogen and vacuum atmospheres to evaluate their effects on mechanical properties, such as microhardness and Transverse Rupture Strength (TRS). The assessment of the results showed a consistent correlation between microstructure and mechanical properties, confirmed by metallography and ANOVA statistical test studies. The study concluded that a nitrogen atmosphere enhances densification and strength by retaining higher carbon content, whereas a vacuum atmosphere leads to increased porosity and reduced strength. Finally, these findings offer valuable insights for optimizing sintering processes to improve material properties.

Keywords: thermal debinding; additive manufacturing; M2 steel.

Impacto de las estrategias de impresión y de la atmósfera de despolimerización térmica en la microestructura y las propiedades mecánicas del acero de herramientas M2 producido mediante fabricación por fusión de filamentos

Resumen

Esta investigación indaga el efecto de la estrategia de impresión y de la atmósfera de despolimerizado térmico en la microestructura y las propiedades mecánicas de muestras de acero M2 obtenido mediante fabricación con filamento fundido. Se realizó un análisis comparativo entre patrones de impresión concéntricos y lineales. Las muestras impresas se sometieron a diferentes velocidades de despolimerizado térmico en atmósferas de nitrógeno y vacío para evaluar sus efectos sobre las propiedades mecánicas, como la microdureza y la resistencia a la ruptura transversal (TRS). La evaluación de los resultados mostró una correlación continua entre la microestructura y las propiedades mecánicas, confirmada mediante metalografía y pruebas estadísticas ANOVA. El estudio concluyó que una atmósfera de nitrógeno mejora la densificación y la resistencia mecánica al retener un mayor contenido de carbono; mientras que una atmósfera de vacío aumenta la porosidad y reduce la resistencia. Estos hallazgos ofrecen información valiosa para optimizar los procesos de sinterización para mejorar las propiedades de los materiales.

Palabras clave: despolimerizado térmico; manufactura aditiva; acero M2.

How to cite: Amaya-Villabon, T.A., Gil-Plazas, A.F., Rubiano-Buitrago, J.D., and Herrera-Quintero, K., Impact of printing strategies and thermal debinding atmosphere on the microstructure and mechanical properties of M2 tool steel produced via fused filament fabrication, DYNA, (92)239, pp. 9-18, October - December, 2025.

1 Introduction

Nowadays, additive manufacturing has become a widely studied process with significant advancements over the last decade [1]. Additive manufacturing in metals has had a great impact on the industry, leading to the development of various techniques such as Directed Energy Deposition (DED) [2], Wire Arc Additive Manufacturing (WAAM) [3], Laser Metal Deposition (LMD) [4], Electron Beam Additive Manufacturing (EBAM) [5] and Laser-Powder-based DED (LP-DED) [6]. These techniques offer significant advantages, including high-speed deposition rates. However, the layer-by-layer approach creates a molten pool, which can lead to anisotropic behavior in the final product. Despite this, heat treatment can homogenize the microstructure and mitigate these effects [7-9].

Now being applied to metals, Fused Filament Fabrication (FFF) technology is a variant of the Shaping-Debind-Sintering (SDS) processes, which has been used in Powder Injection Molding (PIM) for over five decades [10]. This approach is significantly more cost-effective than Directed Energy Deposition (DED) techniques. As a result, many research efforts focus on FFF for shaping due to its lower costs and practical applications.

PIM feedstocks are available in the form of pellets with a powder material content of about 55 Vol% to 65 Vol%, whereas FFF feedstocks are in the form of filaments with a powder material content of about 45 Vol% to 55 Vol% [11], [12]. The main difference lies in the fact that pellets require a vehicle solely for transportation, which is provided by polyolefins, waxes, and surfactants. In the case of filaments, the powder content is lower because the polymers acting as the vehicle tend to exhibit brittle behavior in filament form. To mitigate this issue, part of the powder is replaced with a thermoplastic elastomer to enhance elasticity [12].

Like PIM, FFF can process a wide range of materials including oxides [13] [14], metals [15], [16], and composites [17], among others. FFF offers an advantage in producing parts with minimal or reduced anisotropic behavior compared to the DED process. However, it is important to note that FFF exhibits relatively slow deposition rates. The quality of the printed parts can be compared to techniques such as Powder Bed Fusion (PBF) and Binder Jetting (BJ) [1].

In FFF, the filament is fed through a mechanism that transports the material into a heated zone where it melts. The molten material is then applied layer by layer to complete the desired geometry. The geometry is first modeled and then sliced to calculate the machine's movements (strategies). The mechanical strength of parts produced by FFF is influenced by these strategies, as the bonding between layers is crucial to the overall strength of the part [18].

M2 tool steel, also known as high-speed steel, derives its name from its ability to machine materials at high speeds. It is an alloy of steel that includes elements, which promote the alpha phase of iron, such as tungsten, molybdenum, and vanadium. M2 is characterized by high hardness and excellent abrasion resistance [19]. These properties make it commonly used in the manufacture of cutting tools and punching tools. Its microstructure provides high resistance to

deformation and fatigue, making it particularly suitable for maintaining sharp edges in precise geometries. Therefore, ensures high tool durability.

One of the main advantages of using M2 tool steel in the fabrication of parts via the FFF process is its ability to reproduce complex geometries and designs for specific applications [20]. This includes specialized tools or components that require high hardness and excellent abrasion resistance properties that may be difficult to obtain through conventional manufacturing processes due to the complexity of their form and function.

The aim of this study is to provide insights into the behavior of printed parts produced via FFF, focusing on strategies to produce dense parts suitable for wear applications. It analyzes how different thermal debinding rates influence densification and mechanical properties. The findings of this research serve as a valuable resource for the tool manufacturing industry, including applications such as punching and other specialized tooling.

2 Materials and Methods

2.1 Raw materials

The M2 tool steel powders used in this study (Fig. 1) are nitrogen-atomized powders supplied by Chengdu Huarui Industrial CO., LTD. These powders possess a particle size ranging from 17 μm to 50 μm , with a chemical composition listed in Table 1. The powders were mixed with two polymers: a polyolefin-based backbone comprising polypropylene random-copolymer (PP) (Essentia, Cartagena, Colombia) and polypropylene grafted with maleic anhydride (PPMA), as well as a thermoplastic elastomer (TPE) (Sungallon, Shenzhen, China). The combination of these materials serves as feedstock to create a composite filament for the FFF process [16-17,21-27].

The feedstock was mixed using a shear-based machine to achieve the composition of 50 vol.% powders and 50 vol.% binder. This specific ratio was selected after testing several powder-to-binder mixtures, including 60/40 and 55/45. It was noticed that higher powder contents (e.g., 60 vol.% and 55 vol.%) increased the fragility of the filament, leading to breakage during handling and the FFF process. The 50/50 composition provided an optimal balance between powder

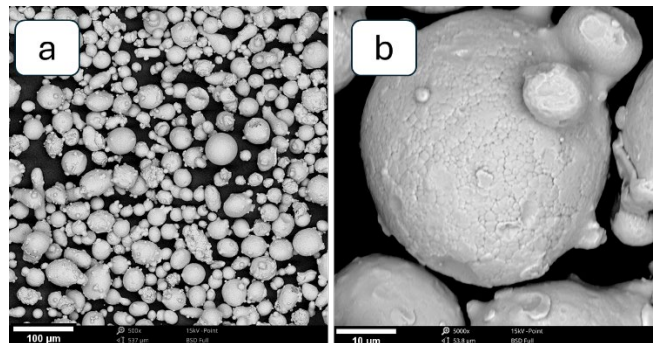


Figure 1. (a) SEM image of M2 tool steel powders, (b) detail of particles in M2 tool steel.

Source: Authors.

Table 1.
Chemical composition of M2 tool steel.

Element	Weight %
C	0.819
Si	0.43
Cr	3.99
W	5.68
Mo	4.56
V	1.76
Mn	0.27
S	0.007
P	0.013

Source: CHENGDU HUARUI INDUSTRIAL CO., LTD.

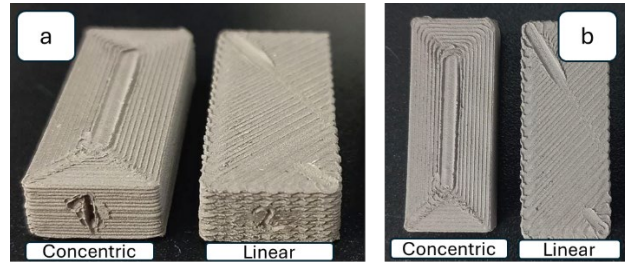


Figure 2. Concentric and linear printed samples, (a) Front view of green TRS samples(b) Top view of green TRS samples.
Source: Authors.

Table 2.
Printing parameters.

Parameter	Concentric pattern	Linear pattern
Printing flow	102 %	102 %
Infill overlap	50 %	50 %
Retraction	None	None
Nozzle temperature	225 °C	225 °C
Cooling fan	Off	Off
Printing speed	7.5 mm/s	7.5 mm/s

Source: Authors.

loading and filament flexibility, ensuring successful filament fabrication and printing. Finally, the selected binder composition for this study consisted of 60 wt.% of TPE and 40 wt.% of backbone (PP and PPMA).

After mixing, the material was cut into squares smaller than 5 mm. The filaments were produced using a single-screw extruder at temperatures ranging from 150°C to 180°C and spooled to obtain a diameter of 1.75 ± 0.08 mm. The final filament was found to have a real density of 4.73 g/cm^3 and a linear density of 11.38 g/m . These properties are crucial for maintaining a steady and reliable material feed throughout the Fused Filament Fabrication (FFF) process.

2.2 Printing

Two different patterns were studied in this work: a linear pattern and a concentric pattern, the printing parameters are shown in Table 2. Sixteen TRS (Transverse Rupture Strength) samples were printed using an Ender 3 V2 FFF printer for each pattern, following the geometry specified in ASTM standard B528. Fig. 2 illustrates the obtained samples.

2.3 Debinding and sintering

The printed samples were subjected to solvent debinding

using cyclohexane for 72 hours at 60 °C and 250 rpm. This step is crucial to dissolve the TPE, thereby promoting a porous network that helps in the removal of gases produced during thermal debinding.

Thermal debinding was examined by varying the heating rate: 0.5 °C/min, 1 °C/min, and 2 °C/min. In each case, the material was heated up to 200 °C with a plateau of 60 minutes, then heated up to 350 °C with a plateau of 120 minutes, and finally to 600 °C with a plateau of 60 minutes. These temperatures were selected based on TGA results, which showed plateaus corresponding to polymer pyrolysis. For each heating rate, two debinding atmospheres were selected vacuum at 10 Pa and nitrogen (N₂) atmospheric pressure.

After thermal debinding, sintering was conducted by switching the atmosphere to an active gas mixture, specifically H₂N₂ (75 vol% H₂ – 25 vol% N₂), at a temperature of 1350 °C. At this temperature, Super Solidus Liquid Phase Sintering occurs, where the sintering temperature is above the alloy's solidus but below its liquidus point. This results in a small fraction of the material melting and forming a liquid phase while the majority remains solid. The presence of this liquid phase promotes better densification by enhancing particle rearrangement and atomic diffusion [28–30].

2.4 Characterization

The thermal degradation temperatures of the polymers were studied using thermogravimetric analysis (TGA) with a Mettler Toledo TGA 1 STARe System. The analysis was conducted in a nitrogen (N₂) atmosphere with a heating rate of 10 °C/min, ranging from 25 °C to 1000 °C. This procedure was performed in accordance with ASTM E1131-08, which outlines the standard test method for compositional analysis by thermogravimetry.

The density of the printed and sintered samples was determined using the Archimedes method, following ASTM B962-17, the standard test method for the density of compacted or sintered powder metallurgy (PM) products using Archimedes' principle. A Sartorius analytical balance equipped with a density determination kit was employed to measure the mass of the samples in air and submerged in distilled water at room temperature. The densities were calculated considering the buoyancy effect of water and correcting for air bubbles adhering to the sample surfaces.

For the metallographic analysis, samples were prepared following ASTM E3-11, 'Standard Guide for Preparation of Metallographic Specimens.' The sintered samples were sectioned using a metallographic cutter to obtain cross-sectional specimens without inducing significant mechanical deformation and then mounted in thermosetting epoxy resin for ease of handling during grinding and polishing. The mounted samples were sequentially ground with silicon carbide (SiC) abrasive papers of grit sizes 240, 400, 600, 800, and 1200 under water lubrication to prevent heat generation and microstructural alteration. Following grinding, the samples were polished using diamond suspensions of 6 µm, 3 µm, and 1 µm particle sizes on a polishing cloth to achieve a mirror-like surface finish. All polishing steps were

performed using a rotating polishing wheel at controlled speeds and pressures, adhering to ASTM E3-11 guidelines.

To reveal the microstructure, the polished samples were chemically etched with a 2 % Nital solution (2 ml nitric acid in 98 ml ethanol) for 10–15 seconds. This etchant selectively attacks the grain boundaries and carbide phases in M2 tool steel, enhancing the contrast between different microstructural features under microscopic examination.

Microstructural observations were performed using optical microscopy (Zeiss Axio Observer Z1.m) to assess the general microstructure, grain size, phase distribution, and porosity. High-resolution imaging was conducted using scanning electron microscopy (SEM) (Phenom XL), coupled with Energy-Dispersive X-ray Spectroscopy (EDS) for elemental analysis and phase identification.

Mechanical properties were evaluated through microhardness testing and transverse rupture strength (TRS) testing. Microhardness measurements were conducted using a Vickers microhardness tester according to ASTM E384-17, 'Standard Test Method for Microindentation Hardness of Materials.' A load of 500 gf was applied with a dwell time of 10 seconds, and several indentations were performed at both the edge and center of the sintered samples to assess hardness homogeneity. TRS tests were made on sintered specimens using a Shimadzu UH-50A universal testing machine at a crosshead speed of 1 mm/min, following ASTM B528, 'Standard Test Method for Transverse Rupture Strength of Powder Metallurgy (PM) Specimens.' Tests were performed at room temperature to determine the transverse rupture strength and deformation behavior of the material.

3 Results Analysis and Discussion

3.1 Green density

Initially, the study analyzed the influence of fill patterns on the green density of M2 tool steel specimens produced via Fused Filament Fabrication (FFF). As shown in the boxplot (Fig. 3), the green density of the samples varied depending on whether concentric or linear fill patterns were used. Notably, the linear fill pattern showed a higher median green density compared to the concentric fill pattern.

A closer examination of the nature of the fill patterns reveals that the linear pattern likely provides more consistent layer overlap, which may result in fewer gaps and a more uniform density throughout the sample.

In contrast, the concentric pattern, which follows the part's contour in concentric circles or ellipses, creates variable overlaps between layers. These variations can introduce inconsistencies in packing density, potentially causing differential shrinkage during the debinding and sintering processes.

To evaluate the differences observed in Fig. 3 a statistical analysis was made outlined in Table 3. According to the ANOVA results, the fill pattern has a statistically significant impact on the green density (p -value = 0.000068).

The statistical variability is attributed to the accumulation of defects produced by the printing strategy. The concentric pattern shows a higher presence of defects compared to the linear pattern, some observed

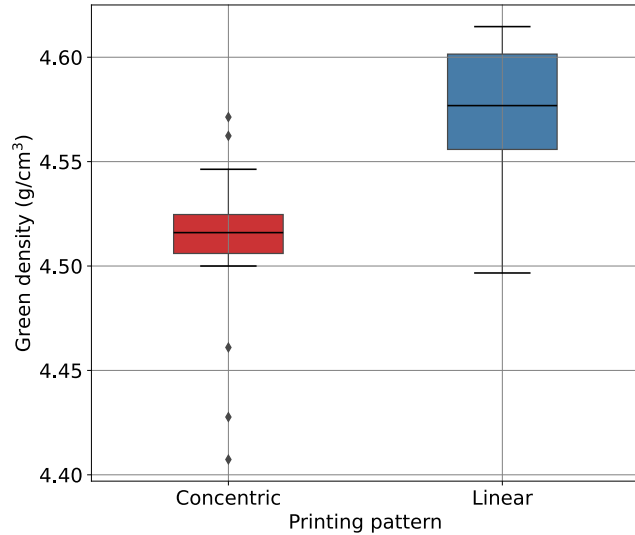


Figure 3. Green density of printed samples.
Source: Authors.

Table 3.
Results of the one-way ANOVA of green density.

Source	Sum sq	Df	F	P-value
Pattern	0.033800	1.0	21.332498	0.000068
Residual	0.47533	30		

Source: Authors

concentric samples have a presence of porosity in area of 2.7 % compared to the linear pattern with a porosity of 1.9 %. Fig. 4 illustrates the transverse rupture of the samples in the green state, showing voids resulting from a lack of material between fill lines. This lack of material could be a consequence of insufficient printing flow; however, if the flow exceeds the amount, could lead to other defects such as “mountain-type” [17]. Nevertheless, the observed defects could be associated with variability in the filament diameter which is assumed to be randomly distributed all over the extruded filament. The resultant green density also reflects the capacity of each infill strategy to avoid this random effect.

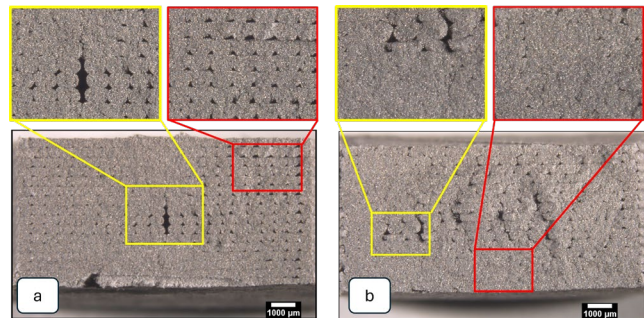


Figure 4. Transverse fracture of green samples, (a) Concentric pattern, (b) linear pattern.

Source: Authors.

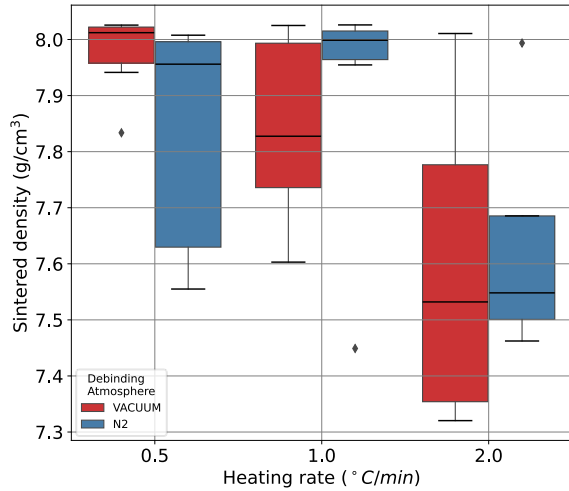


Figure 5. Sintered density of printed samples.
Source: Authors.

3.2 Thermal debinding and Sintering

Once the green samples were solvent debinded and considering the behavior of the composite material at TGA, ten TRS samples were thermally debinded for each heating rate (0.5 °C/min, 1 °C/min, and 2 °C/min) and finally sintered by the mechanism of SLPS (Super solidus Liquid Phase Sintering) [16,28,31].

After sintering, the density of the samples was measured. Density is a critical indicator of the final product's mechanical properties and overall quality. The accompanying box-and-whisker plot (Fig. 5) depicts the sintered density across different heating rates during the debinding process, under two distinct atmospheres: nitrogen (N₂) and vacuum.

With the aim to identify how the parameters of the process interact in the final density a multilevel ANOVA was made, considering the parameters: HR: Heating rate, ATM: Thermal debinding atmosphere, PAT: Infill Pattern.

The three-way ANOVA analysis shown in Fig. 6, indicates that the heating rate holds a statistically significant influence on the sintered density with a p-value of 0.03276, which highlights its role as a critical parameter in the sintering process. The plot reveals that samples processed at a 0.5 °C/min heating rate generally exhibit a higher density, regardless of the atmosphere. The data suggest that slower heating rates facilitate a more effective release of the polymer decomposition gases, which may result in fewer defects during the sintering process. This is because, at higher heating rates, the rapid expansion of gases from the polymers could create flaws in the final pieces. Such control over the heating rate is crucial, as it can significantly enhance the integrity of the sintered parts by reducing porosity and cracks that compromise the material's mechanical properties.

Conversely, the sintered density does not appear to be significantly affected by either the nitrogen atmosphere or the vacuum environment, as their results overlap substantially at each heating rate.

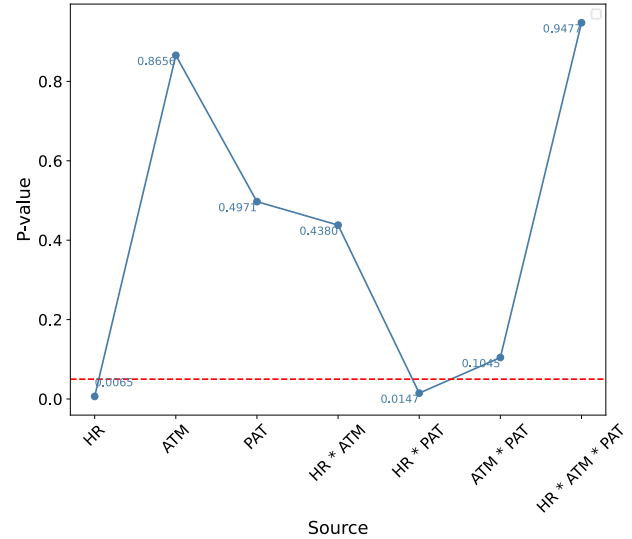


Figure 6. Three-way ANOVA of sintered density.
Source: Authors.

Whereas the fill pattern was a significant factor in the green density of the parts, it does not seem to exert a considerable influence on the sintered density. This observation may occur since any initial differences in green density are mitigated or overshadowed by the dominant effects of the heating rate during sintering. This emphasizes the importance of optimizing the heating rate in the debinding process to achieve the desired material properties in the final sintered product.

To complement the analysis of sintered density, porosity measurements were conducted using image analysis on the cross-sectional area of the specimens, quantifying the pore area relative to the total area of the sample. The attached results illustrate these findings. According to ANOVA analysis with a p-value of 0.0057, the heating rate during debinding significantly affects porosity, with slower heating rates yielding lower porosity.

This correlation is depicted in the boxplot (Fig. 7), where it is evident that specimens subjected to slower heating rates exhibit significantly reduced porosity. This observation aligns with the previous discussion: slower heating rates allow the gases from the polymer decomposition to escape more gradually, diminishing the likelihood of pore formation which can occur due to rapid gas expansion at higher heating rates. This reinforces the conclusion that careful control of the heating rate is crucial for minimizing defects and ensuring the structural integrity of the sintered parts. Samples with lower porosity are better for withstanding internal pressures during thermal debinding, which is influenced by heating rates. This explains the results shown in Fig. 5 and the interaction between HR*PAT in Fig. 6.

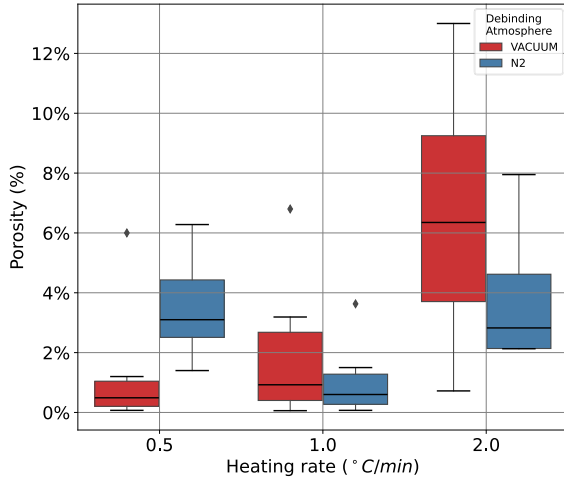


Figure 7. Final porosity.
Source: Authors.

3.2 Microstructure

A cross-sectional analysis of the sintered samples was conducted to identify the final microstructure. The samples did not exhibit differences between them, despite variations in parameters such as the printed pattern, heating rate, and debinding atmosphere. All the samples analyzed revealed a martensitic matrix surrounded by carbides, positioned intergranularly and at the grain boundaries, forming an

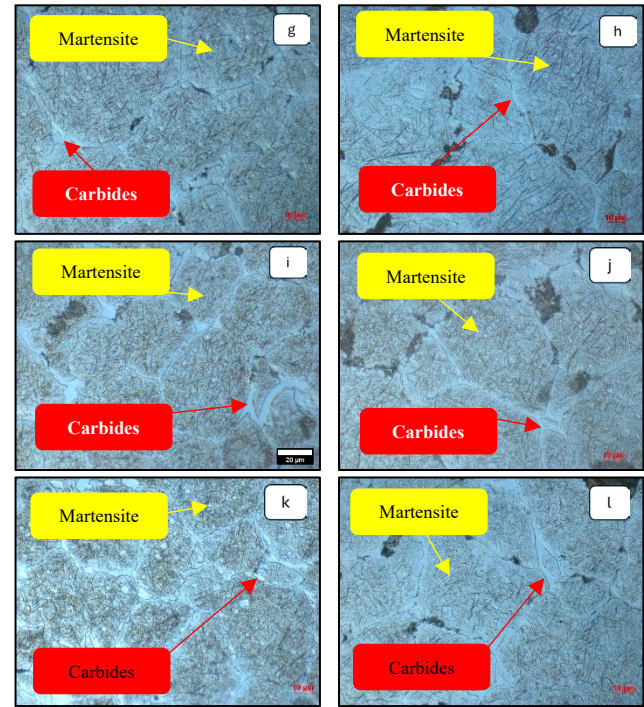
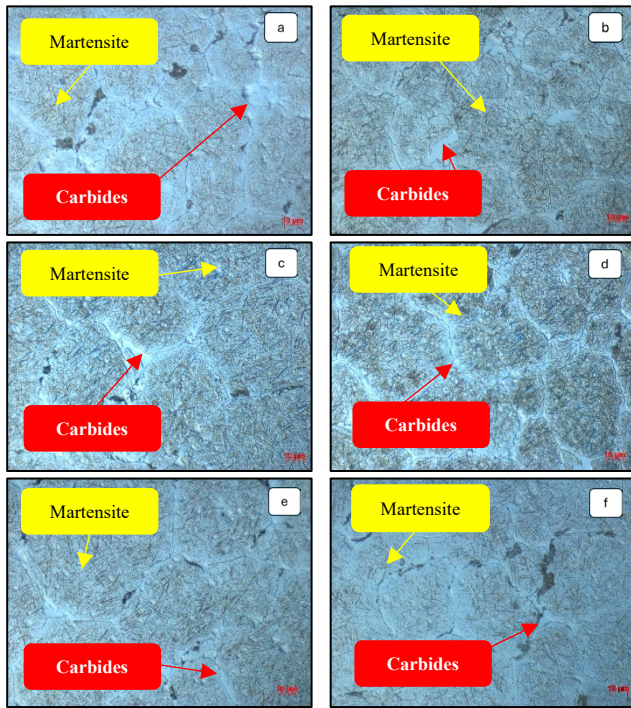


Figure 8. Metallography sections of printed and sintered samples. (a,c,e,g,i,k) Concentric patterns sintered at N2-0.5°C/min (a), N2-1°C/min (c), N2-2°C/min (e), Vacuum-0.5°C/min (g), Vacuum-1°C/min (i), Vacuum-2°C/min (k). (b,d,f,h,j,l) Linear pattern sintered at N2-0.5°C/min (b), N2-1°C/min (d), N2-2°C/min (f), Vacuum-0.5°C/min (h), Vacuum-1°C/min (j), Vacuum-2°C/min (l).
Source: Authors.



intergranular network, as shown in Fig. 8. The formation of martensite occurred despite the cooling taking place in the furnace, rather than through rapid quenching. This is due to the high alloy content of M2 steel, which significantly increases its hardenability, allowing the transformation of austenite to martensite at the slower cooling rates typical of furnace cooling. Regarding the carbides, they are predominantly secondary carbides that precipitated during the cooling stage, influenced by the steel's chemical composition. The microstructure of the material remains unaffected by the process parameters because the SLPS mechanism is governed primarily by the temperature and the chemical composition of the steel [31].

3.4 Mechanical properties

To evaluate the mechanical properties of the sintered materials, microhardness measurements were conducted at two positions on the samples: the edge and the center. These positions were chosen to assess the homogeneity achieved during the sintering process using the SLPS mechanism. The results, shown in Fig. 9, indicate a mean value of 727 HV for the linear strategy and 703 HV for the concentric strategy at the edge, while at the center, the values were 628 HV and 634 HV, respectively. However, some measurements deviated significantly from the mean, likely due to samples with higher porosity.

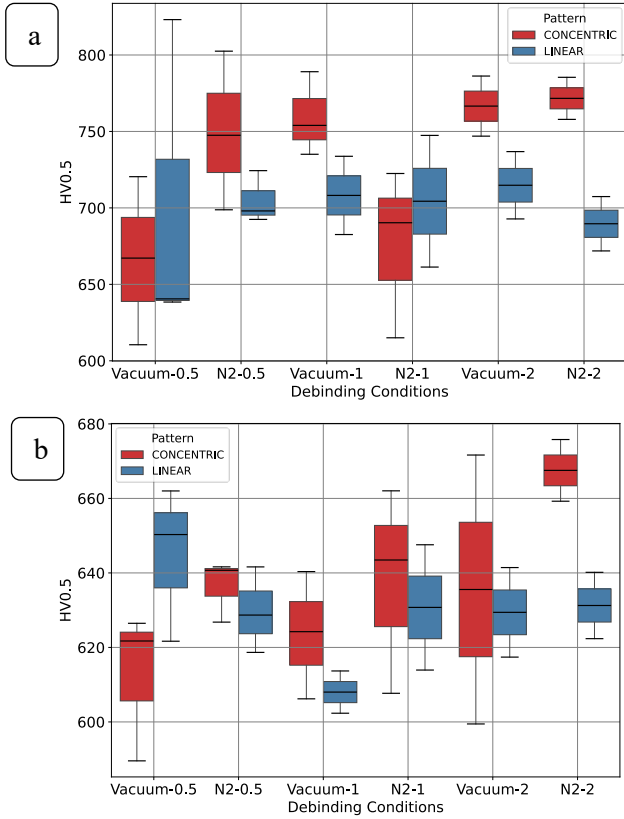


Figure 9. Microhardness of the sintered samples.
(a) Edge zone. (b) Center zone.
Source: Authors.

A three-way ANOVA confirmed these hardness observations, showing that the obtained values are not significantly influenced by parameters such as the printed pattern, heating rate, debinding atmosphere, or their interactions, as evidenced by the p-values in Fig. 10.

The TRS test results are presented in Figure 11. Samples subjected to thermal debinding in a nitrogen atmosphere exhibited the highest strength compared to those debinded in a vacuum atmosphere. This behavior correlates with the previously observed density (Fig. 1) and porosity (Fig. 7). Samples debinded in nitrogen retain more carbonaceous residues (from polymers), leading to a higher carbon content in the material. This increased carbon content enhances the formation of a liquid phase at high temperatures, promoting better densification, reduced porosity, and improved mechanical strength.

In contrast, samples debinded in a vacuum atmosphere may be exposed to oxygen, which can lead to oxide formation during thermal debinding. In such cases, the carbon residues from backbone degradation act as reducing agents for oxides in the initial stages of sintering, reducing the overall carbon content in the vacuum-debound samples [32], as shown in the carbon content measurements in Fig. 12. This reduction in carbon content significantly affects densification. Furthermore, the porosity introduced by high heating rates exacerbates this effect, resulting in lower mechanical strength.

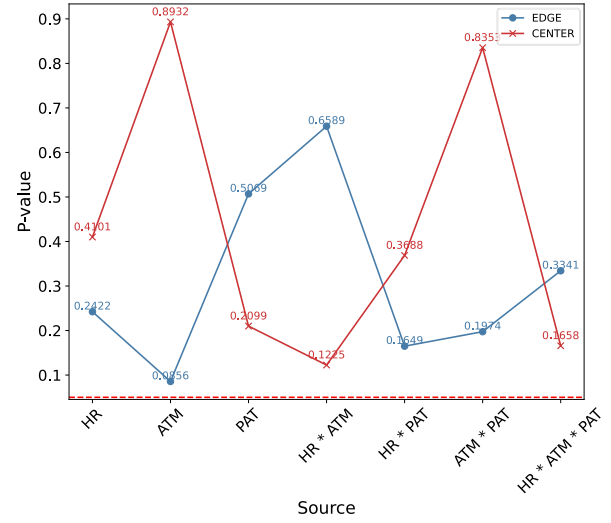


Figure 10. Three-way ANOVA of microhardness.
Source: Authors.

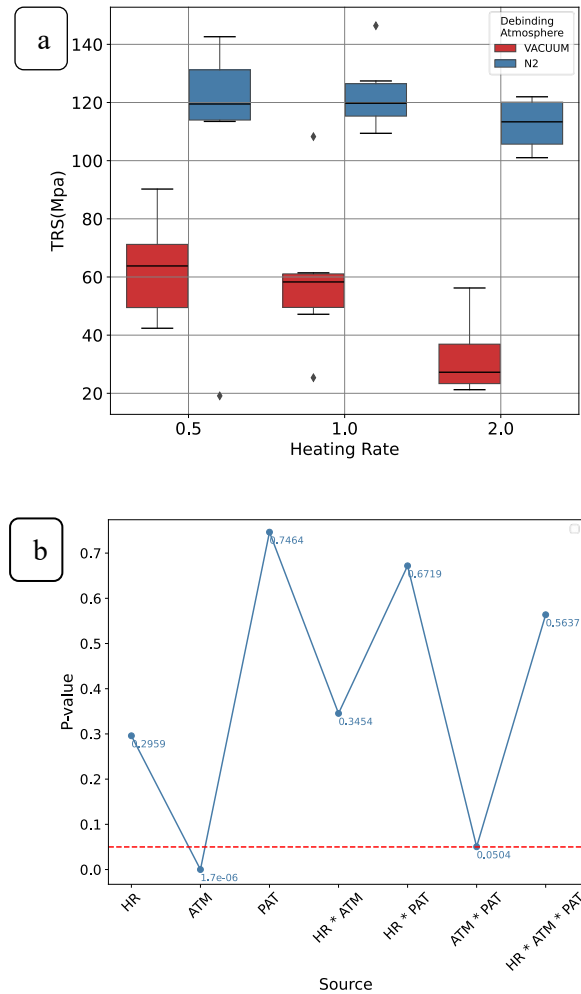


Figure 11. TRS results.
(a) Mechanical strength. (b) Three-way ANOVA of TRS.
Source: Authors.

Optical Emission Spectrometry confirms the final percentage of carbon: 1.33% in the nitrogen atmosphere and 1.27% in the vacuum atmosphere (Fig. 12). Based on the ANOVA results (Fig. 11b), it is demonstrated that the thermal debinding atmosphere significantly impacts the mechanical strength of the samples. This effect is compounded by the previously discussed printing strategy, which produces a greater presence of pores.

It is important to mention that the final material has a higher carbon content percentage than the initial material. Therefore, using active agents like hydrogen in thermal debinding could enhance the reduction of the residual carbonaceous products.

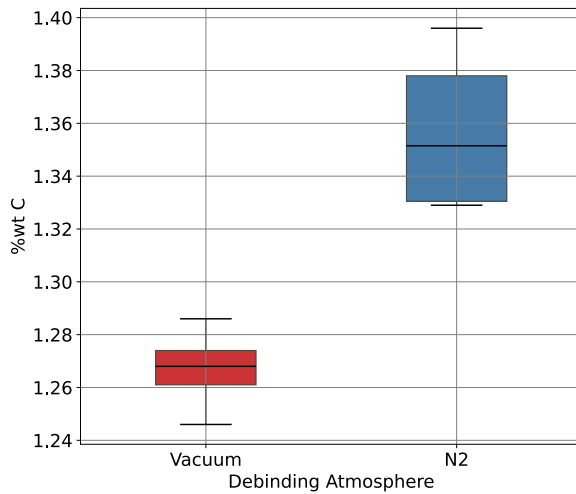


Figure 12. Final carbon weight percentage of the sintered samples. Source: Authors.

Optical observations of the TRS samples reveal the presence of defects that persist after the debinding process (indicated by yellow arrows), demonstrating that the partial formation of liquid is insufficient to address these defects (Fig. 13).

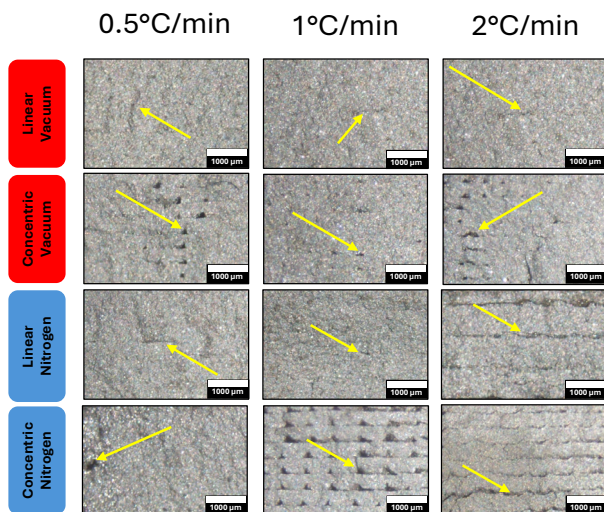


Figure 13. Optical micrographs of the transversal fracture of TRS samples. Source: Authors.

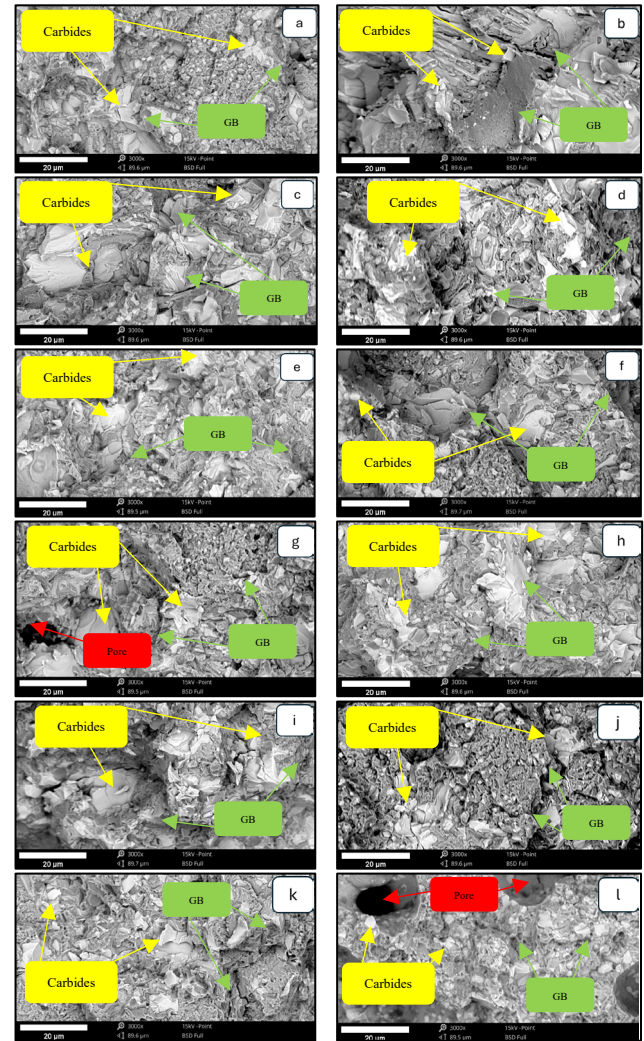


Figure 14. SEM micrographs of the transversal fracture of TRS samples. (a,c,e,g,i,k) Concentric patterns sintered at N2-0.5°C/min (a), N2-1°C/min (c), N2-2°C/min (e), Vacuum-0.5°C/min (g), Vacuum-1°C/min (i), Vacuum-2°C/min (k). (b,d,f,h,j,l) Linear pattern sintered at N2-0.5°C/min (b), N2-1°C/min (d), N2-2°C/min (f), Vacuum-0.5°C/min (h), Vacuum-1°C/min (j), Vacuum-2°C/min (l). Source: Authors.

SEM micrographs (Fig. 14) of the fracture surfaces of TRS samples reveal the failure mode and mechanism, indicating predominantly brittle behavior in all cases. The brittle fracture is characterized by intergranular boundaries, where carbides precipitate during the sintering process, as shown in Fig. 8. These carbides are present both at the grain boundaries (GB) and intergranular, with some exhibiting cleavage. In the martensitic matrix, fractures exhibit a mixed mode of dimples and cleavage. However, the fracture surfaces observed by SEM are insufficient to explain the mechanical behavior of TRS, except when considering the influence of porosity.

4 Conclusions

Two different printing strategies were studied using a composite material for the FFF process, providing a foundation for future research to determine the optimal

parameters for producing functional parts. The main findings of this study are as follows:

Concentric strategies tended to result in more defects, which persisted through the SLPS process.

Higher heating rates during thermal debinding promoted defects due to internal pressure caused by the decomposition of polymeric products.

The findings indicate that the thermal debinding atmosphere has a significant impact on the final carbon content and, consequently, on the mechanical properties of the material. It is suggested to investigate the use of active atmospheres rich in hydrogen (H_2) during debinding and sintering. These atmospheres could facilitate the removal of carbonaceous residues and allow for more precise control of the carbon content, improving densification and reducing porosity in the sintered parts.

Based on the results obtained, it is possible to produce tools such as hot punching tools through the Fused Filament Fabrication (FFF) technique. This advancement allows us to perform real tests to evaluate the performance of these tools under high-temperature and wear conditions.

Acknowledgements

The authors thank the Powder Metallurgy Laboratory of “Universidad Nacional de Colombia, Sede Bogotá” and the “Centro de Materiales y Ensayos de SENA, Regional Distrito Capital SGPS-12351-2024 and SGPS-13030-2024” for the logistical, technical, human, and financial support of the project. The project funded this research, “Technological development for the manufacture of metal tools using additive manufacturing techniques based on extrusion for high temperature and wear applications used by the Colombian auto parts industry” with the code 82305 - 110189082305 and contingent recovery financing contract number 2021-1012 of 2021 celebrated between the Colombian institute of educational credit and technical studies abroad, “Mariano Ospina Pérez”—ICETEX, the Ministry of Science, Technology and Innovation, and the National University of Colombia.

References

- [1] Zhou, L., et al., Additive manufacturing: a comprehensive review sensor. Multidisciplinary Digital Publishing Institute (MDPI), 24(9), art. 2668, 2024. DOI: <https://doi.org/10.3390/s24092668>
- [2] Imran, M.M., Che-Idris, A., De-Silva, L.C., Kim, Y.B., and Abas, P.E., Advancements in 3D printing: directed energy deposition techniques, defect analysis, and quality monitoring. Technologies (Basel), 12(6), art. 0086, 2024. DOI: <https://doi.org/10.3390/technologies12060086>
- [3] Shah, A., Aliyev, R., Zeidler, H., and Krinke, S., A review of the recent developments and challenges in wire arc additive manufacturing (WAAM) process. Journal of Manufacturing and Materials Processing, 7(3), art. 0097, 2023. DOI: <https://doi.org/10.3390/jmmp7030097>
- [4] Ghanadi, N., and Pasebani, S., A review on wire-laser directed energy deposition: parameter control, process stability, and future research paths. Journal of Manufacturing and Materials Processing, Multidisciplinary Digital Publishing Institute (MDPI), 8(2), art. 0084, 2024. DOI: <https://doi.org/10.3390/jmmp8020084>
- [5] Gong, X., Anderson, T., and Chou, K., Review on powder-based electron beam additive manufacturing technology. Manufacturing Review, EDP Sciences, (1), art. 4001, 2014. DOI: <https://doi.org/10.1051/mfreview/2014001>
- [6] Li, Z., et al., High deposition rate powder-and wire-based laser directed energy deposition of metallic materials: a review. International Journal of Machine Tools and Manufacture, (181), art. 103942, 2022. DOI: <https://doi.org/10.1016/j.ijmachtools.2022.103942>
- [7] Jorge, V.L., Teixeira, F.R., Wessman, S., Scotti, A., and Henke, S.L., The impact of multiple thermal cycles using CMT® on microstructure evolution in WAAM of Thin walls made of AlMg5. Metals (Basel), 14(6), art. 0717, 2024. DOI: <https://doi.org/10.3390/met14060717>
- [8] Heo, S., Lim, Y., Kwak, N., Jeon, C., Choi, M., and Jo, I., Impact of heat treatment and building direction on tensile properties and fracture mechanism of Inconel 718 produced by SLM process. Metals (Basel), 14(4), art. 0440, 2024. DOI: <https://doi.org/10.3390/met14040440>
- [9] Honu, E., Emanet, S., Chen, Y., Zeng, C., and Mensah, P., Effects of low-temperature heat treatment on mechanical and thermophysical properties of Cu-10Sn alloys fabricated by laser powder bed fusion. Materials, 17(12), art. 2943, 2024. DOI: <https://doi.org/10.3390/ma17122943>
- [10] Banerjee, S., and Joens, C.J., Debinding and sintering of metal injection molding (MIM) components. Handbook of Metal Injection Molding, pp. 133–180, 2012. DOI: <https://doi.org/10.1533/9780857096234.1.133>
- [11] Kukla, C., Duretek, I., Schuschnigg, S., Gonzalez-Gutierrez, J., and Holzer, C., Properties for PIM feedstocks used in fused filament fabrication. World PM 2016 Congress and Exhibition, 2016.
- [12] Kukla, C., Gonzalez-Gutierrez, J., Cano, S., and Hampel, S., Fused filament fabrication (FFF) of PIM feedstocks. Proceedings of VI Congreso Nacional de Pulvimetalurgia y I Congreso Iberoamericano de Pulvimetalurgia, 2017.
- [13] Cano, S., et al., Additive manufacturing of Zirconia parts by fused filament fabrication and solvent debinding: selection of binder formulation. Additive Manufacturing, 26(11), pp. 117–128, 2019. DOI: <https://doi.org/10.1016/j.addma.2019.01.001>
- [14] Tirado-González, J.G., Esguerra-Arce, J., Esguerra-Arce, A., and Herrera-Quintero, L.K., 3D printing Iron/Iron oxide composites by metal material extrusion from an industrial waste. JOM, 76(4), pp. 1924–1936, 2024. DOI: <https://doi.org/10.1007/s11837-024-06371-2>
- [15] Gil-Plazas, A.F., Villamil Galindo, A.D., Rubiano Buitrago, J.D., Viloria Estrada, A., y Herrera-Quintero, L.K., La industria 4.0 en tu casa: impresión de prototipos de herramientas de punzonado para trabajo en caliente con impresoras de modelado por deposición fundida de bajo coste. Reto, pp. 23–35, 2021.
- [16] Gil-Plazas, A.F., Rubiano-Buitrago, J.D., Boyacá-Mendivelso, L.A., and Herrera-Quintero, L.K., Solid-state and super solidus liquid phase sintering of 4340 Steel SLM powders shaped by fused filament fabrication. Revista Facultad de Ingeniería, 31(60), art. 13913, 2022. DOI: <https://doi.org/10.19053/01211129.v31.n60.2022.13913>
- [17] Rubiano-Buitrago, J.D., Gil-Plazas, A.F., Boyacá-Mendivelso, L.A., and Herrera-Quintero, L.K., Fused filament fabrication of WC-10Co Hardmetals: a study on binder formulations and printing variables. Journal of Manufacturing and Materials Processing, 8(3), art. 30118, 2024 DOI: <https://doi.org/10.3390/jmmp8030118>
- [18] Costa, J.M., Sequeiros, E.W., and Vieira, M.F., Fused filament fabrication for metallic materials: a brief review. Materials, Multidisciplinary Digital Publishing Institute (MDPI), 16(24), art. 7505, 2023. DOI: <https://doi.org/10.3390/ma16247505>
- [19] Myers, N.S., and Heaney, D.F., Metal Injection Molding (MIM) of high-speed tool steels. Handbook of Metal Injection Molding, pp. 516–525, 2012. DOI: <https://doi.org/10.1533/9780857096234.4.516>
- [20] Naranjo, J.A., Berges, C., Gallego, A., and Herranz, G., A novel printable high-speed steel filament: Towards the solution for wear-resistant customized tools by AM alternative. Journal of Materials Research and Technology, 11(3), pp. 1534–1547, 2021. DOI: <https://doi.org/10.1016/j.jmrt.2021.02.001>
- [21] Thompson, Y., Gonzalez-Gutierrez, J., Kukla, C., and Felfel, P., Fused filament fabrication, debinding and sintering as a low-cost additive manufacturing method of 316L stainless steel. Additive Manufacturing, 30(5), art. 100861, 2019. DOI: <https://doi.org/10.1016/j.addma.2019.100861>
- [22] Gonzalez-Gutierrez, J., Arbeiter, F., Schlauf, T., Kukla, C., and Holzer, C., Tensile properties of sintered 17-4PH stainless steel fabricated by material extrusion additive manufacturing. Materials letters, (248), pp. 165–168, 2019. DOI: <https://doi.org/10.1016/j.matlet.2019.04.024>

- [23] Gonzalez-Gutierrez, J., Kukla, C., Schuschnigg, S., Duretek, I., and Holzer, C., Fused Filament Fabrication for Metallic Parts. 2016.
- [24] Abel, J., et al., Fused Filament Fabrication (FFF) of metal-ceramic components. *Journal of Visualized Experiments*, 2019(143), pp. 1–13, 2019. DOI: <https://doi.org/10.3791/57693>
- [25] Kukla, C., Gonzalez-Gutierrez, J., Burkhardt, C., Weber, O., and Holzer, C., The production of magnets by FFF-Fused Filament Fabrication. *Proceedings Euro PM 2017: International Powder Metallurgy Congress and Exhibition*, 2017.
- [26] Gonzalez-Gutierrez, J., Godec, D., Kukla, C., Schlauf, T., Burkhardt, C., and Holzer, C., Shaping, debinding and sintering of steel components via fused filament fabrication. *16th International Scientific Conference on Production Engineering - CIM2017*, 2017.
- [27] Lengauer, W., et al., Fabrication and properties of extrusion-based 3D-printed hardmetal and cermet components. *International Journal of Refractory Metals and Hard Materials*, 82(2), pp. 141–149, 2019. DOI: <https://doi.org/10.1016/j.ijrmhm.2019.04.011>.
- [28] German, R.M., Suri, P., and Park, S.J., Review: liquid phase sintering. *Journal of Materials Science*, 44(1), pp. 1–39, 2009. DOI: <https://doi.org/10.1007/s10853-008-3008-0>.
- [29] German, R.M., Densification of prealloyed tool steel powders: sintering model. *International Journal of Powder Metallurgy*, pp. 49–61, 1986.
- [30] German, R.M., Computer model for the sintering densification of injected molded M2 tool steel. *International Journal of Powder Metallurgy*, pp. 57–67, 1999.
- [31] German, R.M., Liquid phase sintering. Ed. Tongfang CNKI Technology Co., Ltd. Beijing. China, 1985. DOI: <https://doi.org/10.16309/j.cnki.issn.1007-1776.2003.03.004>
- [32] Herranz, G., Control of carbon content in metal injection molding (MIM). En: *Handbook of Metal Injection Molding*, Ed. Elsevier Inc., 2012, pp. 265–304. DOI: <https://doi.org/10.1533/9780857096234.2.265>.

T.A Amaya Villabón, is BSc. Eng in Mechanical Engineering from the Universidad Nacional de Colombia. He is currently working on additive manufacturing of ceramic materials to obtain a bachelor's degree in Mechatronics Engineering.
ORCID: 0009-0004-4871-8780.

A.F Gil Plazas, is a MSc.in Materials and Processes from the Universidad Nacional de Colombia and a BSc. Eng. in Mechanical Engineering from ECCI University. He is currently working on additive manufacturing using Wire Arc Additive Manufacturing (WAAM) at SENA and serves as the SENNOVA leader of the Materials and Testing Center.
ORCID: 0000-0001-6585-9121.

J.D Rubiano Buitrago, is a MSc. in Materials and Processes from the Universidad Nacional de Colombia, and a Mechanical Engineer from Universidad Distrital, Colombia. He is currently pursuing a PhD. in Materials and Science Engineering, focusing on additive manufacturing using Fused Filament Fabrication (FFF) in hard metals.
ORCID: 0000-0003-3491-8373.

L.K Herrera Quintero, is an Associate Professor in the Mechanical and Mechatronics programs at the School of Engineering, Universidad Nacional de Colombia. Holds a PhD. in Materials Science from Universidad de Sevilla, Spain, and has completed two postdoctoral positions in materials and advanced manufacturing technologies. Serves as the Academic Coordinator of the Doctorate Program in Science and Technology of Materials and Coordinator of the Laboratory University Division (UNALab). Strategic promoter of Digital Transformation at the National University of Colombia, he focuses on promoting capacities and empowering the community to tackle challenges related to a human-centered society, sustainability, and resilience. He works to reduce barriers to incorporating competitive ecosystems and generating solutions aligned with the university's mission goals.
ORCID: 0000-0003-2002-4336.

A mathematical model for optimizing the milk and cheese production chain in southern Nariño, Colombia

Rigoberto Rosero-Benavides ^a & Carlos Julio Vidal-Holguín ^b

^a Centro de Investigación y Desarrollo Tecnológico en Ciencias Aplicadas – CIDTCA. Pasto, Nariño, direcciontecnica@cidtca.com

^b Universidad del Valle, Escuela de Ingeniería Industrial, Cali, Colombia. carlos.vidal@correounivalle.edu.co

Received: May 8th, 2025. Received in revised form: July 28th, 2025. Accepted: August 19th, 2025.

Abstract

This study analyzes the milk production and processing chain in the southern region in Nariño, Colombia, through an optimization model aimed at improving the profitability of small-scale producers. Currently, about 44% of the region's milk is sent to collection centers and transported to large processing companies, resulting in frequent losses and reduced prices due to the product's perishability. The proposed model evaluates the creation of processing plants managed by local associations under a solidarity economy approach, for transforming a part of surplus milk and increasing producer income. The optimization model suggests establishing a plant in Guachucal, one of the region's top milk-producing municipalities, which could potentially double profits through the production of dairy derivatives such as cheese. Various scenarios were analyzed, supporting the feasibility of this strategy as a means to economically reactivate and strengthen the regional dairy sector.

Keywords: production chain; milk; supply chain optimization; Nariño.

Un modelo matemático para optimizar la cadena de producción de leche y queso en el sur de Nariño, Colombia

Resumen

Este estudio analiza la cadena de producción y transformación de leche en la región sur de Nariño, Colombia, mediante un modelo de optimización orientado a mejorar la rentabilidad de pequeños productores. Actualmente, cerca del 44% de la leche producida se envía a centros de acopio y luego a grandes transformadoras, generando pérdidas y bajos precios debido a la alta perecibilidad del producto. Se analiza la apertura de plantas de procesamiento gestionadas por asociaciones locales bajo un modelo de economía solidaria, con el fin de transformar parte del excedente de leche y mejorar los ingresos del productor. El modelo de optimización sugiere la instalación de una planta en Guachucal, uno de los municipios con mayor producción, lo que permitiría duplicar las utilidades al producir derivados como quesos. Además, se exploran diversos escenarios que respaldan la viabilidad de esta estrategia como mecanismo de reactivación económica y fortalecimiento del sector lechero regional.

Palabras clave: cadena productiva; leche; optimización de cadenas de abastecimiento; Nariño.

1 Introduction

The milk supply chain in Nariño is one of the most representative chains in the region due to the number of direct and indirect jobs that it generates. Nariño is the third-largest milk producer in Colombia, behind Antioquia and Cundinamarca, and accounts for 6-10 percent of the country's total milk production. According to the development plan

2024-2027 of Nariño, the milk supply chain contribution to the gross domestic product of the agricultural sector was about 27 percent in 2023. The milk supply chain included 39,862 direct producers and 159,448 indirect workers, yielding an estimated milk production of 1,009,747 liters per day based on statistics for the last semester of 2024 [1, 2].

The department of Nariño presents an important case study for the optimization of the milk and cheese supply

How to cite: Rosero-Benavides, R. and Vidal-Holguín, C.J., A mathematical model for optimizing the milk and cheese production chain in southern Nariño, Colombia. DYNA, (92)239, pp. 19-26, October - December, 2025.

Universidad Nacional de Colombia.

Revista DYNA, (92)239, pp. 19-26, October - December, 2025, ISSN 0012-7353

DOI: <https://doi.org/10.15446/dyna.v92n239.120278>



chain in Colombia due to its significant role in national dairy production, its challenging geography, and the socioeconomic profile of its producers.

Specifically, most producers are small-scale farmers. Dairy production is dispersed across multiple small rural settlements (veredas) within municipalities, which complicates the collection and centralization of the product. Many producers form associations or cooperatives to sell their milk collectively, which gives them greater bargaining power. However, these organizations often face management and logistical challenges.

The department's topography, characterized by access roads in poor condition and frequent road blockades due to landslides or strikes, complicates timely milk collection, thereby increasing transportation costs and the risk of product loss. The milk is often collected in milk cans (cantinas) and transported in small vehicles, without the necessary cold chain, which can affect its quality. Many small producers lack access to refrigeration technology on their farms, forcing them to sell and transport the milk immediately after milking. Consequently, a portion of the milk must be transported warm, posing a risk to the quality of both the raw milk and its derived products.

All the above factors make the milk and cheese supply chain network design and optimization crucial to improving competitiveness and sustainability in Nariño. Any disruption or inefficiency in the supply chain not only affects the regional economy, but also directly translates into widespread economic vulnerability and a considerable social impact, which supports the design and application of optimization initiatives. The results of this paper suggest that an effective strategy for small producers would be to enhance their associative capacity to establish their own cheese production plants, thereby creating value-added products using a portion of the milk that would otherwise be sold to external companies.

A recent comprehensive review of the network design of agri-food supply chains, which includes milk and cheese, concludes that agri-food perishable-product supply chains remain understudied. The authors also highlight the need for not only considering location-allocation decisions, but also for including supplier selection in the models. In addition, the authors consider perishability as a key factor that can affect product life due to deterioration, supply chain disruptions, and quality problems of the initial raw products. Also, seasonality is considered as a key factor for supply chain design [3].

Guarnaschelli, Salomone and Méndez (2020) [4] apply a stochastic optimization model for integrating production and distribution in a dairy supply chain in Argentina. This chain consists of one manufacturing complex that produces 42 dairy products and has nine distribution centers. The model includes a single milk supplier in the formulation. The solution to the model requires a significant computational effort and therefore the authors divided the solution into two stage decisions. The results showed that considering randomness in the model can improve profitability, but at a significant computational effort.

An adequate structure of a supply chain allows for improved quality, good logistics performance, better

response capacity, efficiency, and demand satisfaction [5]. A perishable supply chain has additional complexities, such as keeping the cold chain, controlling production time, optimizing transportation modes, and using the required storage of the product. In addition, biophysical and organoleptic characteristics of the product must be analyzed and considered to design the supply chain [6].

According to García, García and Cárdenas (2013) [7], to establish improvement processes throughout the supply chain, it is initially necessary to identify the variables that affect the system, and then to establish a set of logical mathematical and probabilistic relationships that integrate the behavior of the system, which is known as supply chain modeling. This is considered as a tool that supports decision making, since it provides an approximation of what would happen under certain conditions that affect the system, thus reducing risks and costs (which would be incurred) by not making the right decision.

Despite the importance of the dairy supply chain in Colombia, few studies to date have conducted a cross-cutting analysis of this sector, particularly in Nariño. Consequently, clear deficiencies and opportunities for improvement have not been systematically identified to inform interventions aimed at optimizing the chain's structure.

Tordecillas-Madera, Polo, Muñoz, and González-Rodríguez (2017) [8] present a binary optimization model to design a milk storage and refrigeration logistics system for a dairy cooperative in Ubaté, Colombia. This model includes cooling tank location, the allocation of producers to tanks (clusters), and system capacity calculation. The authors included supply chain robustness analysis in their publication by generating eight configurations and considering three supply scenarios (low, medium, or high). No production plans are included in the model.

Finally, an associativity scheme for the dairy chain in the department of Atlántico, Colombia, is presented in [9]. The authors analyzed variables such as Logistics, Quality, Production, and Associativity. The study showed that the associativity factor has a very low index compared to the other factors, and therefore it suggests the creation of new cooperatives to strengthen the sector's relationships. This study is fundamentally descriptive, and no optimization models are presented.

Modeling facilitates the management of a supply chain since, in addition to building a model of a complex system, its greatest advantage lies in the different applications that the model can have. In addition, it allows studying how the entire system is affected by small and large changes without having to implement them. This study performs an analysis of the fresh cheese production chain to identify key optimization points. Specifically, it presents the current structure and strategies that can improve the efficiency of the cheese production chain in associative enterprises in the department of Nariño. Modeling the most influential variables makes it possible to evaluate different scenarios, supporting well-informed decisions regarding the chain's improvement and competitiveness. This serves as a management tool for both private companies and territorial entities, which contributes to defining resource investment criteria to achieve better results for the chain.



Figure 1. Distribution of municipalities with the highest milk production in the Department of Nariño.

Source: DANE

The geographical distribution of the producing municipalities considered in this article is shown in Fig. 1. This region corresponds to the southern zone of the department, whose municipalities produce approximately 94 percent of the department's total milk. In the north of Nariño, while other municipalities do have livestock farming, their focus is on the production of meat or dual-purpose livestock, as the agroclimatic conditions are not suitable for milk production. For this reason, the southern zone in Nariño is a representative region of its total milk production.

In Nariño, approximately 56 percent of the milk produced in municipalities is converted into value-added milk products and 44 percent is sold to collection centers that transport the milk to large producers located in northern zones of the country (Table 1).

Table 1.
Milk availability for processing in existing plants or eventually new plants.

No	Municipality	Total (liters/day)	Milk for existing plants (liters/day)	Milk for collection centers (liters/day)
1	Guachucal	154,797	86,686	68,111
2	Cumbal	191,334	107,147	84,187
3	Pupiales	158,469	88,743	69,726
4	Pasto	105,699	59,191	46,508
5	Túqueres	96,630	54,113	42,517
6	Ipiales	88,359	49,481	38,878
7	Sapuyes	70,539	39,502	31,037
8	Tangua	59,031	33,057	25,974
9	Aldana	62,694	35,109	27,585
10	Cuaspu	53,277	29,835	23,442
11	Potosí	28,569	15,999	12,570
12	Iles	23,418	13,114	10,304
13	Gualmatán	20,493	11,476	9,017
14	Contadero	21,060	11,794	9,266
15	Guaitarilla	19,506	10,923	8,583
	Subtotal	1,153,875	646,170	507,705
	Percentage	100%	56%	44%

Source: Author's elaboration based on primary data collected through direct interviews with legal association representatives, municipal governments, and agricultural government officials in selected municipalities and collection centers. Specific source data cannot be released due to confidentiality agreements.

Based on the above considerations and the references reviewed, the specific contributions of this paper, not found in the literature, are the following:

- Modeling the southern Nariño dairy supply chain, including its main municipalities as milk suppliers
- Identifying the optimal location for one or more new plants to produce value-added products and performing sensitivity analyses for alternative locations
- Identifying the potential of producer associations to benefit small-scale milk producers
- Considering the transportation of both cold and warm milk throughout the supply chain

Section 2 presents the optimization model. In Section 3, the model results are discussed, and some key sensitivity analyses are conducted. Finally, Section 4 presents the conclusions of the article.

2 Methodology

2.1 Milk supply chain characterization and echelon identification

Collection centers: Collection centers are facilities where milk is collected from several producers and cooled in stainless steel tanks with modular systems that are easy to install. The cooling process conducted at collection centers allows the milk to be transported in a cooling network over long distances minimizing product deteriorating.

Milk from the collection centers is purchased by companies in the north of the country, such as Colanta and Alpina, which have a presence in Nariño's milk-producing municipalities. These companies have large collection centers where milk is consolidated and shipped in 10,000- or 20,000-liter tanks to their processing plants.

Existing processing plants: The processing plants, as well as the collection centers, are in areas of high milk production to reduce freight and transportation time. Once the milk arrives at the plant, there is no further transportation; the milk is only stored for processing during the day.

The existing plants produce a variety of products, the most processed being fresh farmer's cheese and curd cheese, and to a lesser extent other derivative such as heavy cream cheese, mozzarella, and fermented beverages such as yogurt.

Since the plants are small with processing ranges mostly between 5,000 and 15,000 liters of milk/day, they do not have solid commercial logistics. Their marketing channel depends on intermediaries who end up setting sales prices according to supply/demand variations. These marketers mostly buy products at the processing plants and transport products to the main cities in the north of the country.

Considering the above situation, it has become evident that, for the producer/processor organizations, the process of marketing to intermediaries is not competitive, since there is no fair relationship between the parties and the commercial alliances are not agreed under contracts that allow stabilizing sales prices. Therefore, with a growing demand for fresh cheese consumption, one alternative that has been proposed for the department is to implement new processing plants on an associative basis, so that they manage their own transportation and marketing of their product to final consumers, trying to shorten intermediation in the supply chain.

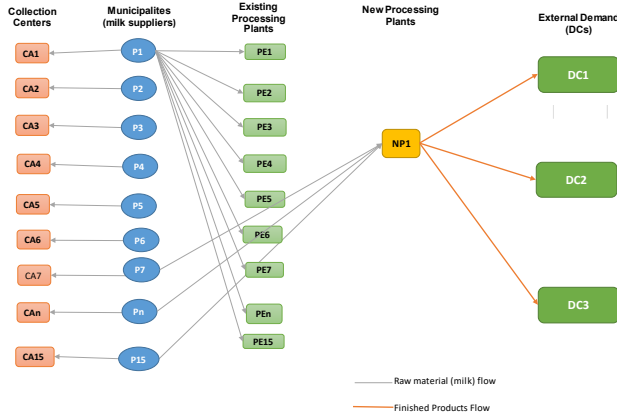


Figure 2. Fresh cheese supply chain in Nariño

Source: Source: Author's elaboration based on primary data collected through direct interviews with legal association representatives, municipal governments, and agricultural government officials in selected municipalities and collection centers. Specific source data cannot be released due to confidentiality agreements.

The milk that is considered available for the implementation of new processing plants is that which is sent to collection centers destined for plants in the north of the country. On the other hand, the milk that goes to existing processing plants, for the purposes of mathematical modeling, is maintained as a demand to be satisfied in terms of milk consumption, since these companies have a market segment of internal demand that they already serve in the department and the milk they receive is of a lower physicochemical and microbiological quality than that received at the collection centers. Accordingly, the profit made by existing plants from their finished product sales is not considered here as a supply chain profit; only the milk sales from municipalities are included in the supply chain profit.

There is a growing demand for fresh cheese in the north of the country, which needs to be met by cheese produced in Nariño. There are several small plants (existing plants) in the department that are not efficient enough to meet the demand at competitive prices, and most of them are managed by private, non-associative companies. Therefore, this study proposes the implementation of new cheese production plants. However, the factors associated with this process, such as location, volume to be processed, raw material supply routes, and distribution routes, among others, are unknown. An illustrative diagram of the supply chain for milk and its derivatives in the Department of Nariño is shown in Fig. 2. We next formulate the mathematical optimization model for the shown supply chain.

2.2 Sets and indexes

CA: Set of existing collection centers, indexed by n
CD: Set of distribution centers (DCs) where the external demand is located, indexed by q
NP: Set of new plants or potential locations to open a plant, indexed by k
P: Set of finished products, indexed by p
PE: Set of existing plants, indexed by j
PROV: Set of municipalities that supply milk, indexed by i

2.3 Parameters

AMORT = Fixed daily amortization of civil construction and equipment when investing in a new plant (it is assumed that this amortization does not depend on the location where a new plant is to be opened) (COP/day)

CENF = Cost of milk cooling (COP/liter)

CLF = Transportation cost of cold milk (COP/liter per hour)

CLT = Transportation cost of warm milk (COP/liter per hour)

CPAST_k = Transportation cost from the new plant k to the municipality of Pasto where consolidation takes place to ship finished products to external customers' DCs in the northern part of the country (COP/kg)

CPL = Production cost of milk in farms (COP/liter)

CTCD_q = Average transportation cost from the municipality of Pasto to external DC q (COP/kg)

CTRANSF_p = Conversion cost of product p in new plants (COP/kg)

DEME_{pq} = External demand of product p at the external DC q (kg/day)

DEMLE_j = Milk demand at existing plant j (liters/day)

PROD_i = Production capacity of milk at each municipality i (liters/day)

PV_p = Selling price of product p (COP/kg)

PVCA = Buying Price of milk at collection centers, assumed to be the same for all of them (COP/liter)

PVPE = Buying Price of milk at existing plants, assumed to be the same for all of them (COP/liter)

R_p = Finished product yield when converting milk into a finished product p (liters of milk/kg of finished product)

RUTAE_{ij} = Binary parameter equal to 1 if milk supplier i is located at a place where the transportation time to the existing plant j is more than 180 min, so that the milk must be cold to be transported; 0, otherwise.

RUTAN_{ik} = Binary parameter equal to 1 if milk supplier i is located at a place where the transportation time to the new plant k is more than 180 min, so that the milk must be cold to be transported; 0, otherwise.

TE_{ij} = Estimated travel time from municipality supplier i to existing plant j (min).

TN_{ik} = Estimated travel time from municipality supplier i to a new plant k (min).

VMIN = Minimum milk volume to be processed so that a new plant would be profitable (liters/day)

2.4 Decision and auxiliary variables

FPNDE_{pkq} = Flow of product p from new plant k to external distribution center q (kg/day)

varl_{pk} = Amount of product p to be produced in new plant k (kg/day)

W_i = Amount of milk to be sent from municipality supplier i to its associated collection center (it is assumed that each municipality that produces milk has only one associated collection center located in the same municipality) (liters/day)

X_k = Binary variable equal to 1 if a new plant is opened at the potential site k ; 0 otherwise.

Y_{ik} = Amount of milk that is transported from municipality supplier i to new plant k (liters/day).

Z_{ij} = Amount of milk that is transported from municipality supplier i to existing plant j (liters/day).

The above variables are illustrated in Fig. 3.

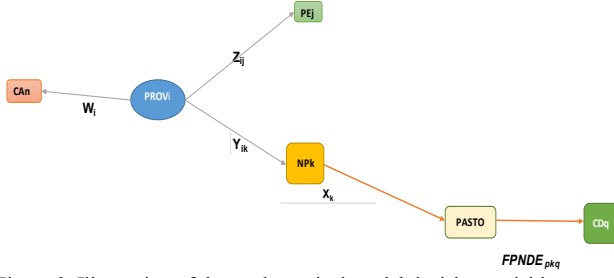


Figure 3. Illustration of the mathematical model decision variables
Source: Own elaboration

2.5 Constraints

1. Municipality supplier i will supply all the daily amount of milk to new plants, existing plants, or collection centers:

$$\sum_k Y_{ik} + \sum_j Z_{ij} + W_i = PROD_i \quad (\forall i) \quad \left(\frac{\text{liters}}{\text{day}} \right) \quad (1)$$

2. A municipal supplier i will transport milk to a new plant only if it is open:

$$Y_{ik} \leq PROD_i X_k \quad (\forall i, k) \quad \left(\frac{\text{liters}}{\text{day}} \right) \quad (2)$$

3. External demand satisfaction constraint. The flow of finished products from new plants must satisfy the external demand (if this is profitable) by product p and by external distribution center q :

$$\sum_k FPNDE_{pkq} \leq DEME_{pq} \quad \forall p, q \quad \left(\frac{\text{kg}}{\text{day}} \right) \quad (3)$$

4. Minimum milk volume to be processed for profitable conversion at new plants:

$$\sum_i Y_{ik} \geq VMIN X_k \quad \forall k \quad \left(\frac{\text{liters}}{\text{day}} \right) \quad (4)$$

5. Milk demand satisfaction at existing plants. The milk coming from all municipalities to each existing plant must satisfy its demand:

$$\sum_i Z_{ij} = DEMLE_j \quad \forall j \quad \left(\frac{\text{liters}}{\text{day}} \right) \quad (5)$$

6. Balance of milk at each new plant:

$$\sum_t Y_{ik} = \sum_{p,q} FPNDE_{pkq} R_p \quad \forall k \quad \left(\frac{\text{liters}}{\text{day}} \right) \quad (6)$$

7. Auxiliary variable. Production of each finished product at each new plant k :

$$varl_{pk} = \sum_q FPNDE_{pkq} \quad \forall p, k \quad \left(\frac{\text{kg}}{\text{day}} \right) \quad (7)$$

8. Flow control of finished products from new plants when either they are closed or open (by product, external distribution center and new plant):

$$FPNDE_{pkq} \leq DEME_{pq} X_k \quad \forall p, k, q \quad \left(\frac{\text{kg}}{\text{day}} \right) \quad (8)$$

9. Flow control of finished products from new plants when either they are closed or open (by product and new plant):

$$varl_{pk} \leq M X_k \quad \forall p, k \quad \left(\frac{\text{kg}}{\text{day}} \right) \quad (9)$$

10. Variable definition:

$$FPNDE_{pkq}, varl_{pk}, W_i, Y_{ik}, Z_{ij} \geq 0; X_k \text{ binary} \quad \forall i, j, k, p, q \quad (10)$$

2.6 Objective function

Three sources of profit have been identified according to the route taken by daily milk production estimated by the mathematical model:

- Profit from milk sales to collection centers (UCA)
- Profit from milk sales to existing plants (UPE)
- Profit from the conversion of milk and sale of finished products from new plants (UPN)

$$Max Z = \text{Overall profit of the milk and cheese supply chain} \left(\frac{COP}{\text{day}} \right) \quad (11)$$

Total profit of milk sales at collection centers (UCA):

$$UCA = \text{Income from sale of milk at collection centers} \\ - \text{Cost of milk production on farm} \quad (12)$$

$$UCA = \sum_i W_i (PVCA - CPL)$$

It is important to note that transportation costs are not considered in this part of the objective function because farms located in each municipality can only send milk to the associated collection center located at the same municipality, which is usually close to the farms to avoid the deterioration of milk properties.

Total profit of milk sales to existing plants (UPE):

$$UPE = \text{Income from sale of milk to existing plants} \\ - \text{Cost of milk production on farm} \\ - \text{Transportation cost (i, j)}$$

$$UPE = \sum_{i,j} Z_{ij} (PVPE - CPL) \\ - \sum_{i,j} Z_{ij} CLT \left(\frac{TE_{ij}}{60} \right) (1 - RUTAE_{ij}) \\ - \left(\sum_{i,j} Z_{ij} CLF \left(\frac{TE_{ij}}{60} \right) RUTAE_{ij} \right) \\ + \sum_{i,j} Z_{ij} CENF RUTAE_{ij} \quad (13)$$

Total profit from milk conversion and sales of finished products from new plants (UPN):

UPN

- = Income from finished product sales sent by new plants
- Milk transportation costs from municipalities (i, k)
- Production costs at new plants
- Transportation costs from new plants to Pasto and from here to northern cities (Popayán, Cali, Pereira)
- Amortized cost from the investment in new plants.

$$\begin{aligned}
 UPN = & \sum_{p,k} var l_{pk} PV_p \\
 & - \sum_{i,k} Y_{ik} CLT \left(\frac{TN_{ik}}{60} \right) (1 - RUTAN_{ik}) \\
 & - \left(\sum_{i,k} Y_{ik} CLF \left(\frac{TN_{ik}}{60} \right) RUTAN_{ik} \right. \\
 & \left. + \sum_{i,k} Y_{ik} CENF RUTAN_{ik} \right) \\
 & - \sum_{i,k} CPL Y_{ik} \\
 & - \sum_{p,k} var l_{pk} CTRANSFN_p \\
 & - \sum_{p,k,q} FPND E_{pkq} CTCD_q \\
 & - \sum_{p,k,q} FPND E_{pkq} CPAST_k \\
 & - \sum_k AMORT X_k
 \end{aligned} \quad (14)$$

Note that the income from milk sales from municipalities to new plants is not considered here because this item is an income for municipalities, but it is also a cost for new plants and thus it vanishes for the supply chain.

$$Max Z = UCA + UPE + UPN \quad (15)$$

3 Results and discussion

3.1 Optimal solution to the original model

The above model was run in the *neos server*, using the *gurobi solver*. The first significant result is that the optimal solution opens a single plant located in the municipality of Guachucal, with a maximum daily profit of 373,800,805 COP/day. The optimal configuration of the supply chain is shown in Fig. 4. The milk suppliers that would supply the new plant with their associated volume are shown in Table 2 and the milk suppliers that would supply the existing plants are shown in Table 3.

Table 2.
Milk suppliers of the new plant to be opened in Guachucal.

Municipality	Milk volume (liters/day)
Aldana	27,525
Cumbal	14,118
Guachucal	154,797
Total Flow of milk	196,440

Source: Own elaboration

Table 3.
Milk suppliers of existing plants.

Origin municipality	Destination municipality	Milk volume (liters/day)
Túquerres	Túquerres	54,113
	Guachucal	16,617
Contadero	Contadero	11,794
Cuaspud	Cuaspud	29,835
Guaitarilla	Guaitarilla	10,923
Aldana	Aldana	35,109
Gualmatán	Gualmatán	11,476
Iles	Iles	13,114
Guachucal	Guachucal	70,069
Ipiales	Ipiales	49,481
Pasto	Pasto	59,191
Cumbal	Guachucal	70,069
	Cumbal	107,147
Potosí	Potosí	15,999
Pupiales	Pupiales	88,743
Sapuyes	Sapuyes	39,502
Tangua	Tangua	33,057
Total		716,239

Source: Own elaboration

The flows of milk to the collection centers are shown in Table 4. This result shows that the municipalities that feed the new plant stop supplying milk to the collection centers, because, for the entire supply chain, it is more profitable to sell the milk to the new plant. This confirms the fact that it can be more profitable to add value to the milk and sell the finished products than to sell it entirely to external production plants. However, there is still a significant flow of milk to the collection centers and therefore the external plants could continue to be supplied.

Another result to highlight is that the expected external demand in the northern cities of the department of Nariño is fully satisfied by the mathematical model, demonstrating the profitability of the current estimated sales prices. Regarding the profit components in the objective function, it is interesting to observe the result in Table 5, which shows that profit can double if the chain processes its own milk instead of selling it to collection centers.

Table 4.
Milk supplies to collection centers located in each municipality.

Municipality	Volume to be sent to collection centers (liters/day)
Túquerres	25,900
Contadero	9,266
Cuaspud	23,442
Guaitarilla	8,583
Aldana	0
Gualmatán	9,017
Iles	10,304
Guachucal	0
Ipiales	38,878
Pasto	46,508
Cumbal	0
Potosí	12,570
Pupiales	69,726
Sapuyes	31,037
Tangua	25,974
Total	311,205

Source: Own elaboration

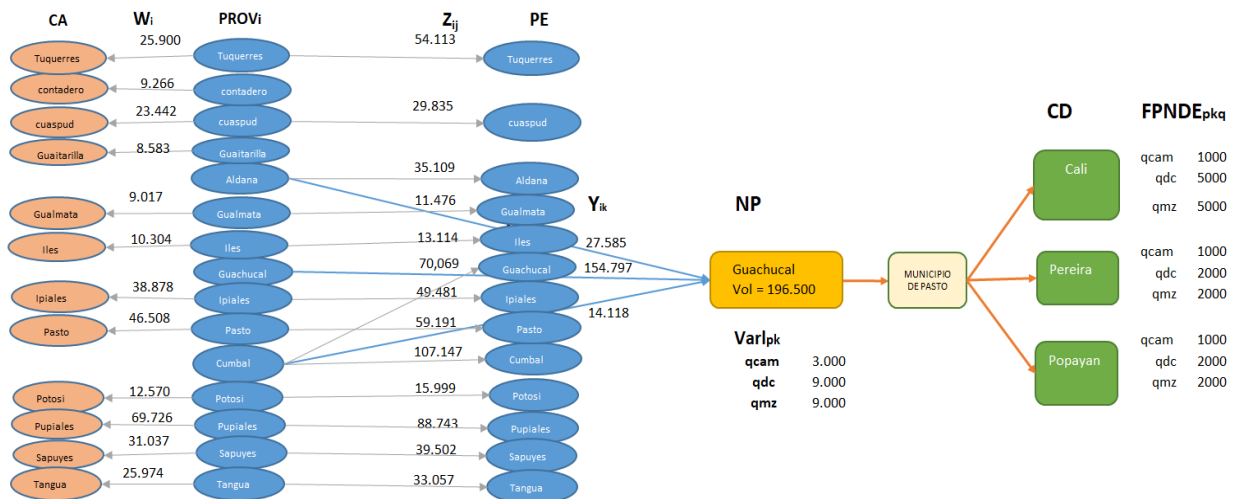


Figure 4. Optimal solution to the original mathematical model (qcam = farmer's cheese, qdc = double cream cheese, qmz = mozzarella cheese). Source: Own elaboration.

Table 5. Relative percentage of the objective function components.

Component in the objective function	Optimal value (COP/day)	Relative percentage
Profit of milk sales at collection centers (UCA)	93,361,500	25%
Profit of milk sales to existing plants (UPE)	99,164,900	27%
Profit from production and sales of finished products at new plants (UPN)	181,274,405	48%

Source: Own elaboration

3.1 Sensitivity analyses

3.2.1. Scenarios about changes in new processing plant location

To analyze the effect of opening the plant in another municipality, with the use of configuration constraints, the change in the profit generated shown in Table 6 was evaluated. It can also be concluded that, although the municipality of Pasto is a good milk producer in Nariño, locating a plant in this municipality is not ideal considering that it is in another sub-region where there is low milk production and therefore it is necessary to collect milk from distant municipalities. If the plant is opened in this municipality, profits would decrease by 3.18 percent.

Table 6. Maximum profit when a single plant is open in each municipality.

Municipality to open the plant	Maximum profit (COP/day)
Guachucal	373,800,805
Cumbal	373,686,029
Ipiales	373,144,012

Municipality to open the plant	Maximum profit (COP/day)
Pupiales	373,006,334
Aldana	373,000,628
Cuaspud	372,245,850
Túquerres	372,137,288
Sapuyes	371,618,242
Potosí	371,501,884
Contadero	371,305,093
Gualmatán	371,174,225
Tangua	369,844,279
Guaitarilla	369,656,158
Iles	368,140,691
Pasto	361,911,674

Source: Own elaboration

3.2.2. Scenarios about demand variation

Table 7 shows the results for fluctuating demand, by decreasing or increasing it with respect to the value originally considered. A reasonable decrease in external demand does not modify the original optimal location in the municipality of Guachucal. Likewise, when demand increases up to 20 percent, the optimal location does not change. When the demand increases by 25 percent, two new plants are open, including Guachucal. However, if we force the model to open a single plant in Guachucal, then the optimal profit decreases only by 0.016 percent. When the demand increases by 30 percent, the model opens two plants different from Guachucal. Nevertheless, if in this case we force the model to open a single plant in Guachucal, the optimal profit decreases only by 0.043 percent. We consider both profit decreases negligible. Therefore, the option to open a plant in the municipality of Guachucal is satisfactory for the demand changes shown in Table 7.

Table 7.

Effects of demand variation on the optimal location and the objective function.

% external demand variation	New plant optimal location	Total supply chain profit (COP/day)	Volume of milk processed (liters/day)
-20	Cumbal	349,603,430	157,200
-15	Guachucal	355,636,542	167,025
-10	Guachucal	361,725,183	176,850
-5	Guachucal	367,774,368	186,675
0	Guachucal	373,800,805	196,500
+5	Guachucal	379,827,243	206,325
+10	Guachucal	385,853,680	216,150
+15	Guachucal	391,880,118	225,975
+20	Guachucal	397,906,555	235,800
+25 ^a	Guachucal Pupiales	403,996,000	245,625
+25 ^b	Guachucal	403,932,993	245,625
+30 ^a	Cumbal Pupiales	410,087,199	255,450
+30 ^c	Guachucal	409,911,390	255,450

Source: Own elaboration

^a In these cases, two new plants are opened in the optimal solution.

^b This is the optimal solution when the model is forced to open a single plant.

^c This is the optimal solution when a single new plant is forced to be opened in Guachucal.

4 Conclusions

In this work, it has been possible to identify the economic importance of the dairy supply chain for the Department of Nariño, Colombia. The structure of the network has facilitated the analysis of its current behavior and the possible points of improvement for the benefit of small producers in the Department of Nariño.

In relation to the results generated from the location of the new processing plant in the municipality of Guachucal, it can be concluded that the results are consistent in the sense that it is a highly milk-producing region surrounded by other producing municipalities at short distances, which optimizes transportation costs in the different scenarios proposed.

The generation of agro-industrial transformation processes for milk generates positive effects in terms of higher profit margins for small producers. Considering the physicochemical characteristics of milk, it is better for the chain to transport cheese with added value than to transport milk as a raw material. Further research in this area may include the more precise consideration of the distribution channels of finished products, the inclusion of warehousing and holding inventory costs, and the analysis of the cold supply chain of finished products, among others.

References

- [1] Sociedad de Agricultores y Ganaderos de Nariño (SAGAN). Encuesta de leche (Producción Diaria), [online] 2024. Available at: <https://sagan.com.co/informacion-estadistica/>
- [2] Ponce-Córdoba, G., Crisis en la cadena lechera del departamento de Nariño, [online] 2023, 10 P. Available at: <https://pagina10.com/web/crisis-en-la-cadena-lechera-del-departamento-de-narino/> Published. Consulted in August 2025.

- [3] Chokri, H., Nouaouri, I., Allaoui, H., and Lasram, F.B.R., Agri-food supply chain network design: a comprehensive review and future research directions. *Computers & Industrial Engineering* (207), art. 111203, 2025. DOI: <https://doi.org/10.1016/j.cie.2025.111203>
- [4] Guarnaschelli, A., Salomone, H.E., and Méndez, C.A., A stochastic approach for integrated production and distribution planning in dairy supply chains. *Computers and Chemical Engineering* (140), art. 106966, 2020. DOI: <https://doi.org/10.1016/j.compchemeng.2020.106966>
- [5] Aramyan, L.C., Ondersteijn, C., Van Kooten, O., and Lansink, A.O., Performance indicators in agri-food production chains in: Ondersteijn, C.J.M., J.H.M. Wijnands, R.B.M. Huirne, and O. Van Kooten (eds.). *Quantifying the agri-food supply chain*, Springer, 2006, pp. 47-64. DOI: https://doi.org/10.1007/1-4020-4693-6_5
- [6] Lyons, A.C., and Ma'aram, A., An examination of multi-tier supply chain strategy alignment in the food industry. *International Journal of Production Research*, 52(7), pp. 1911-1925, 2014. DOI: <https://doi.org/10.1080/00207543.2013.787172>
- [7] García, E., García, H., and Cárdenas, L.E., Simulación y análisis de sistemas con ProModel. 2 ed., Pearson, México, 2013.
- [8] Tordecillas-Madera, R., Polo, A., Muñoz, D., and González-Rodríguez, L., A robust design for a Colombian dairy cooperative's milk storage and refrigeration logistics system using binary programming. *International Journal of Production Economics* (183), pp. 710-720, 2017. DOI: <http://dx.doi.org/10.1016/j.ijpe.2016.09.019>
- [9] Salas-Navarro, K., Obredor-Baldovino, T., González-Laverde, G., and Mercado-Caruso, N., Diseño de esquema de asociatividad para la cadena de suministro del Clúster Lácteo en el Departamento del Atlántico de Colombia. *Revista Espacios* 39(50), 11P, 2018.

R. Rosero-Benavides, is a BSc. Eng. in Agro-Industrial Engineer, Sp. in Project Management, and MSc. in Engineering with an emphasis in Industrial Engineering, currently serves as the Technical Director of the Center for Research and Technological Development in Applied Sciences – CIDTCA. He has approximately 15 years of experience as a consultant in the management and execution of research and technological development projects, as well as productive and social projects across various fields of knowledge, working with both public and private sector entities at the national level.

ORCID: 0000-0002-8340-4697

C.J. Vidal-Holguín, is a BSc. Eng. in Mechanical Engineer and MSc. in Industrial and Systems Engineering from the Universidad del Valle, Cali, Colombia. He also holds a MSc. in industrial engineering and a PhD. in Industrial Engineering from the Georgia Institute of Technology (Georgia Tech) in Atlanta, USA. He has been a full professor at the School of Industrial Engineering at the Universidad del Valle since 1986, specializing in the areas of Industrial Logistics, Supply Chain Planning and Optimization, Inventory Management and Control, Operations Research and Applied Mathematical Modeling. He was the director of the Research Group on Logistics and Production at Universidad del Valle, now called the Research Group on Logistics and Analytics for a Sustainable Society (LASSOS). Since 1997, he has authored several articles published in both national and international journals, taught various international courses, and served as a consultant for multiple companies.

ORCID: 0000-0002-4774-9591

Experimental analysis and computational simulation of heat transfer in a radiator

Juan Mauricio Trenado-Herrera, Crisanto Mendoza-Covarrubias, Alicia Aguilar-Corona,
& Hugo Cuauhtémoc Gutiérrez-Sánchez

Faculty of Mechanical Engineering, Michoacán University of San Nicolás de Hidalgo (UMSNH), Morelia, Michoacán, Mexico, 1597281H@umich.mx, cmendoza@umich.mx, alicia.aguilar@umich.mx, hcgsan@umich.mx

Received: February 28th, 2025. Received in revised form: July 31st, 2025. Accepted: August 19th, 2025.

Abstract

This study analyzes the thermal performance of a 4.1 dm³ engine radiator through experimental tests and CFD simulations using ANSYS Fluent. The effects of materials, tube geometry, and flow conditions on heat transfer and thermal efficiency were evaluated. The results show that copper tubes enhance heat transfer by 18% but increase pressure drop by 4.44%. Additionally, increasing air velocity improves thermal efficiency by 3.74%, suggesting that specific improvements in fin design could enhance performance without increasing energy consumption. The study validates the use of CFD as a reliable tool for analyzing cooling systems in engines, benefiting the automotive industry with more efficient radiators. These improvements can be extended to hybrid and electric vehicles, as well as industrial heat exchangers, contributing to more sustainable thermal management. The main scientific contributions of this work are: (i) the experimental validation of a CFD model applied to an automotive radiator under transitional flow regime, (ii) the quantitative evaluation of the effects of copper tubes on thermal efficiency and pressure drop, and (iii) the detailed analysis of air velocity impact on heat transfer and its implications for radiator thermal design.

Keywords: radiator; heat transfer; CFD (Computational Fluid Dynamics); thermal efficiency; thermal design.

Análisis experimental y simulación computacional de la transferencia de calor en un radiador.

Resumen

Este estudio analiza el rendimiento térmico de un radiador de motor de 4.1 dm³ mediante pruebas experimentales y simulaciones CFD en ANSYS Fluent. Se evaluaron los efectos de materiales, geometría de tubos y condiciones de flujo en la transferencia de calor y eficiencia térmica. Los resultados muestran que los tubos de cobre mejoran la transferencia de calor en un 18%, pero aumentan la caída de presión en un 4.44%. Además, incrementar la velocidad del aire mejora la eficiencia térmica en un 3.74%, lo que sugiere que ciertas mejoras en el diseño de las aletas podrían aumentar el desempeño sin afectar el consumo energético. El estudio valida el uso de CFD como herramienta confiable para el análisis de sistemas de enfriamiento en motores, beneficiando a la industria automotriz con radiadores más eficientes. Estas mejoras pueden extenderse a vehículos híbridos y eléctricos, así como a intercambiadores de calor industriales, contribuyendo a una gestión térmica más sostenible. Las principales contribuciones científicas de este trabajo son: (i) la validación experimental de un modelo CFD aplicado a un radiador automotriz en régimen de flujo transitorio, (ii) la evaluación cuantitativa del efecto de los tubos de cobre sobre la eficiencia térmica y la caída de presión, y (iii) el análisis detallado del impacto de la velocidad del aire en la transferencia de calor y sus implicaciones en el diseño térmico del radiador.

Palabras clave: radiador; transferencia de calor; CFD (Dinámica de Fluidos Computacional); eficiencia térmica; diseño térmico.

1 Introduction

The thermal performance of internal combustion engines

is a critical factor in ensuring their efficiency, reliability, and compliance with increasingly strict environmental regulations. An efficient cooling system is essential to

How to cite: Trenado-Herrera, J.M., Crisanto Mendoza-Covarrubias, C., Aguilar-Corona, A., and Gutiérrez-Sánchez, H.C., Experimental analysis and computational simulation of heat transfer in a radiator. DYNA, (92)239, pp. 27-37, October - December, 2025.

Universidad Nacional de Colombia.
Revista DYNA, (92)239, pp. 27-37, October - December, 2025, ISSN 0012-7353
DOI: <https://doi.org/10.15446/dyna.v92n239.119111>



maintain the engine temperature within an optimal range, preventing overheating and reducing fuel consumption. Among these systems, radiators play a key role by facilitating heat exchange between the coolant and the ambient air. However, radiator design faces a significant challenge: improving heat transfer without generating excessive pressure losses that could affect the performance of the cooling system. Over the past decades, research on heat transfer applied to radiators has evolved from classical theoretical models, such as the Dittus-Boelter correlations [5], to advanced simulations using computational fluid dynamics (CFD). Previous studies have shown that parameters such as tube geometry, fin distribution, and air velocity directly influence radiator thermal efficiency [1], [2]. Nevertheless, many of these investigations have relied solely on numerical simulations without detailed experimental validation, limiting their applicability in real systems. This means that, although numerical models predict thermal behavior with good approximation, the lack of experimental data hinders their practical implementation in the industry. In particular, research by Patel et al. [3] and Vajjha et al. [4] has explored heat transfer in conventional radiators but has not thoroughly evaluated the impact of pressure drop in different geometric configurations. Similarly, studies such as those by Olier et al. [13] have analyzed thermal performance based on air velocity and tube geometry without validating their models with experimental data to confirm the accuracy of their results. These limitations leave a gap in the understanding of real radiator behavior under operational conditions. Recent literature has continued to emphasize the importance of CFD and experimental methods in enhancing radiator design. Chen et al. (2022) evaluated plate-fin compact radiators under varying inlet conditions and highlighted the role of airflow optimization in improving thermal efficiency [18]. Likewise, Kumar et al. (2021) demonstrated the accuracy of the $k-\omega$ SST model for simulating multi-tube radiators in transitional regimes, supporting its selection in this study [19]. Zhang et al. (2020) combined wind tunnel experiments with CFD simulations to validate pressure and temperature predictions in crossflow radiators [20]. These recent advances confirm the relevance of the methodological approach adopted in the present work. To address this issue, this study aims to bridge this gap by combining experimental analysis and CFD simulations to evaluate the thermal performance of a 4.1 dm³ internal combustion engine radiator. Unlike previous research, this work focuses on a detailed analysis of the influence of tube geometry and air velocity on system efficiency, validating numerical models with experimental tests conducted in a test bench. The results obtained not only provide a better understanding of radiator thermal behavior but also offer guidelines for improving its design, reducing pressure losses without compromising heat dissipation. This research is particularly relevant to the automotive industry, as it contributes to the development of more efficient cooling systems with lower energy losses and greater thermal dissipation capacity, which could reduce the environmental impact of internal combustion engines. Moreover, the proposed design improvements can be applied to the development of radiators for high-performance applications,

as well as cooling systems for hybrid and electric engines, expanding their impact on the industry. The main scientific contributions of this study are: (i) the experimental validation of a CFD model applied to an automotive radiator under transitional flow regime, (ii) the quantitative evaluation of copper tube effects on thermal efficiency and pressure drop, and (iii) the detailed analysis of airflow velocity on heat transfer and its implications for radiator thermal design. Based on these contributions, the specific objectives of this study are:

- (i) to evaluate the thermal behavior of an automotive radiator segment using CFD and experimental methods,
- (ii) to analyze the influence of copper tube material and airflow velocity on heat transfer and pressure drop,
- (iii) to validate the CFD simulation results through experimental data obtained from a custom test bench,
- (iv) and to generate design recommendations based on performance indicators such as thermal efficiency and pressure loss.

2 Methodology

This section describes the experimental procedures and numerical simulations used to evaluate the thermal performance of a three-tube radiator with fins through computational fluid dynamics (CFD) simulations and experimental tests. The methodology focused on a detailed study of the thermal behavior of three radiator tubes, aiming to identify configurations that improve heat transfer and minimize pressure losses [16], [17]. To ensure the validity of the models and the applicability of the results, simulations were combined with experimental validation, providing a solid foundation for the research findings.

2.1 System selection and analysis

A 4.1 dm³ inline six-cylinder engine with a copper-tube, aluminum-fin radiator was selected (see Fig. 1). Three tubes were analyzed to study the fluid-air interaction. Using ANSYS Fluent, the thermal behavior was modeled, and the results were validated with experimental tests, recording the coolant flow rate and temperatures (inlet: 89°C, outlet: 76°C) and air temperatures (inlet: 28°C, outlet: 39°C).



Figure 1. Radiator in the test bench.
Source: Own elaboration.

2.2 Simulation and validation process

The methodological process was carried out in nine key stages. First, the problem was defined by selecting the radiator, its geometry, and establishing the operating conditions. Next, geometric modeling was developed in ANSYS, creating the computational domain. Then, the mesh was generated, with refinement in critical areas to accurately capture thermal and velocity effects. Boundary conditions were set by assigning appropriate velocities, temperatures, and thermal coefficients. The turbulence model was then selected, implementing the $k-\omega$ SST model due to its ability to handle flows with high-pressure gradients. The CFD simulation was executed by solving the conservation equations of mass, momentum, and energy. A mesh sensitivity analysis was performed to verify its independence and ensure numerical stability.

Subsequently, experimental validation was conducted by comparing the CFD results with experimental data from the test bench. Finally, a results analysis was performed, evaluating thermal efficiency, pressure drop, and proposing improvements in the radiator design.

Table 1 presents the experimental results, highlighting the cooling of the water as it flows through the radiator, contributing to maintaining the engine's ideal temperature. Additionally, a slight decrease in water pressure was observed, as well as an increase in air temperature due to heat absorption during the heat exchange process.

2.3 Geometric model for the radiator CFD Simulation

The CFD model of the radiator includes three parallel tubes (6.18 mm in diameter, 748 mm in length) and zigzag fins (6 mm spacing) to maximize heat transfer. Simulated in ANSYS Fluent, it considers steady-state flow, conduction, and convection. The analysis identifies critical zones and evaluates the influence of airflow on thermal dissipation (see Fig. 2).

The selected computational domain consists of three flat tubes with their corresponding fins, which represent a simplified yet representative section of the actual radiator, which contains 84 tubes arranged in three columns of 28 tubes each.

This simplification was chosen to maintain representative thermal and aerodynamic behavior while significantly reducing computational cost. Key geometric features such as fin spacing, tube arrangement, and boundary conditions were preserved.

The inlet velocity and mass flow rate per tube were scaled to match those of the full radiator, ensuring comparable Reynolds numbers and heat transfer characteristics.

Table 1.

Experimental data on the thermal performance of the radiator in the test bench.

Water Inlet Temperature °C	Water Outlet Temperature °C	Water Inlet Pressure, Pa	Water Outlet Pressure, Pa	Air Inlet Temperature °C	Air Outlet Temperature °C
89	76	23248.4	19950.7	28	39

Source: Own elaboration.

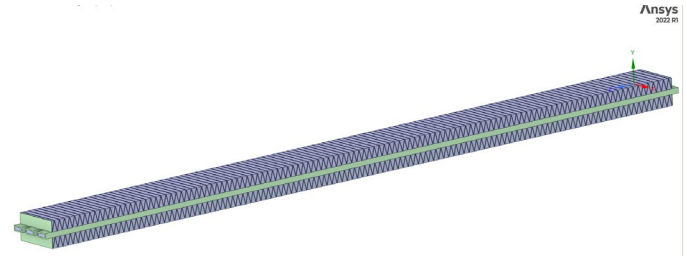


Figure 2. Geometry of the three tubes simulated using CFD. Source: Own elaboration using ANSYS Fluent®.

This strategy has been successfully applied in previous studies [3], [17], where reduced domains were used to capture local thermal behavior with acceptable accuracy.

2.3.1 Selection of the turbulence model

For the numerical simulation, the $k-\omega$ SST turbulence model was used due to its accuracy in flows with separation and high-pressure gradients, better resolution of the thermal boundary layer, and greater numerical stability. Additionally, it offers lower computational cost compared to LES and better performance than $k-\epsilon$ in recirculation zones.

3 CFD meshing of the three-tube radiator model with fins

The CFD meshing of the radiator included 6560221 elements and 4524309 nodes, with regular hexahedral elements for numerical stability. Refinements were applied at the tube-fin interfaces to capture thermal and velocity gradients accurately. The dense mesh on the fins precisely represents the air-surface interaction. Smooth transitions minimize numerical errors, ensuring a reliable thermal analysis (see Fig. 3).

3.1 Mesh sensitivity analysis

A mesh sensitivity analysis was conducted by modifying the number of elements and evaluating its impact on the coolant outlet temperature and pressure drop. It was determined that with more than 6.5 million elements, variations in the results were less than 1%, ensuring accuracy without significantly increasing computational cost. This guarantees a balance between numerical accuracy and simulation efficiency.

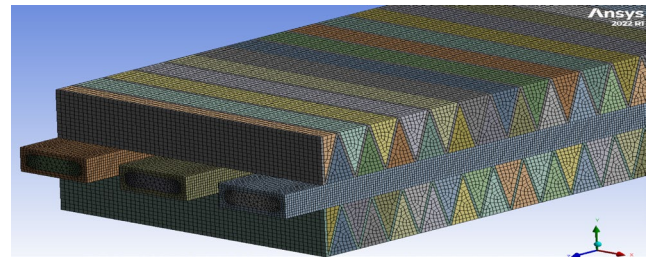


Figure 3. CFD mesh of the complete radiator, showing the three tubes and their respective fins.

Source: Own elaboration using ANSYS Fluent®.

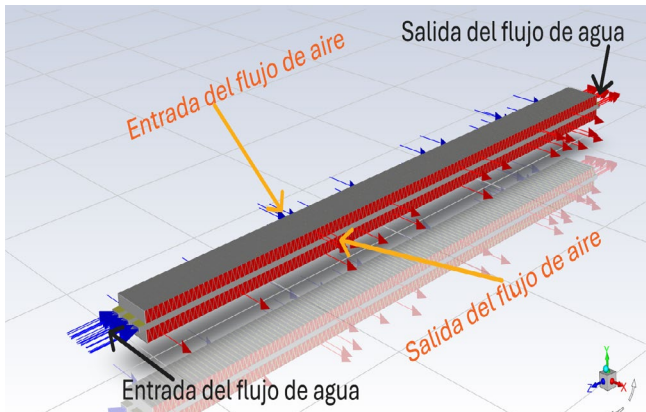


Figure 4. CFD schematic of the radiator's boundary conditions (inlet and outlet). Source: Own elaboration using ANSYS Fluent®.

3.1.1 Boundary conditions

Once the mesh was generated, boundary conditions for the simulation were established. The tube and fin surfaces were modeled as thermal solids interacting with the environment, allowing heat transfer. For the water flow, an initial velocity of 0.682 m/s and an inlet temperature of 89°C were imposed. For the airflow, an initial velocity of 15.47 m/s and an inlet temperature of 28°C were assigned (see Fig. 4).

Tables 2, 3, and 4 present the inlet and outlet parameters of the water and air flow, as well as the thickness of the tubes and fins. These data are essential to ensure the accuracy of the CFD analysis.

Table 2.
Input specifications for the water flow.

WATER FLOW INLET CONDITIONS	
Initial Water Temperature	89°C
Water Velocity Through The Tube	0.682 m/s
Water Inlet Pressure	23248.4 Pa
Water Mass Flow Rate	0.01916 kg/s
Water Convective Heat Transfer Coefficient (H)	6447.0758 W/m ² *K
Hydraulic Diameter	0.0046153 m

Source: Own elaboration.

Table 3.
Input specifications for the airflow.

AIR FLOW INLET CONDITIONS	
Initial Air Temperature	28°C
airflow velocity	15.47 m/s
Air Mass Flow Rate	0.09298 kg/s
Air Convective Heat Transfer Coefficient (H)	7447.45 W/m ² *K
Hydraulic Diameter	0.0044843 m

Source: Own elaboration.

Table 4.
Thickness specifications for the tube and fin.

TUBE AND FIN THICKNESSES	
Tube Wall Thickness	0.001 m
Fin Thickness	0.0005 m

Source: Own elaboration.

Table 5.

Thermophysical properties: density, viscosity, thermal conductivity, and specific heat of water.

THERMOPHYSICAL PROPERTIES OF WATER	
Density [kg/m ³]	965.86
Cp (Specific Heat) [J/(kg - °C)]	4205
Thermal Conductivity [W/(m - °C)]	0.6746
Viscosity [kg/(m - s)]	0.0003187

Source: Own elaboration.

Table 6.

Thermophysical properties: density, viscosity, thermal conductivity, and specific heat of air.

THERMOPHYSICAL PROPERTIES OF AIR	
Density [kg/m ³]	1.225
Cp (Specific Heat) [J/(kg - °C)]	1006.43
Thermal Conductivity [W/(m - °C)]	0.0242
Viscosity [kg/(m - s)]	0.000017894

Source: Own elaboration.

3.1.2 Thermophysical properties

The thermophysical properties of water and air used in the simulations are summarized in Tables 5 and 6, which include parameters such as density, viscosity, thermal conductivity, and specific heat.

Table 5 presents the properties of water, while Table 6 details the corresponding values for air.

3.1.3 Conservation equations

The governing equations for the analysis domain are the conservation of mass (Eq. 1), conservation of momentum (Eqs 2 and 4), and conservation of energy (5) [17].

$$\frac{\partial u}{\partial x} + \frac{\partial v}{\partial y} + \frac{\partial w}{\partial z} = 0 \quad (1)$$

$$\rho \left(u \frac{\partial u}{\partial x} + v \frac{\partial u}{\partial y} + w \frac{\partial u}{\partial z} \right) = -\frac{\partial p}{\partial x} + \mu \nabla^2 u \quad (2)$$

$$\rho \left(u \frac{\partial v}{\partial x} + v \frac{\partial v}{\partial y} + w \frac{\partial v}{\partial z} \right) = -\frac{\partial p}{\partial y} + \mu \nabla^2 v \quad (3)$$

$$\rho \left(u \frac{\partial w}{\partial x} + v \frac{\partial w}{\partial y} + w \frac{\partial w}{\partial z} \right) = -\frac{\partial p}{\partial z} + \mu \nabla^2 w \quad (4)$$

$$\rho c_p \left(u \frac{\partial T}{\partial x} + v \frac{\partial T}{\partial y} + w \frac{\partial T}{\partial z} \right) = k \nabla^2 T \quad (5)$$

3.1.4 CFD simulation parameters

In ANSYS Fluent, the k- ω SST model was used to capture flow interactions, the SIMPLE numerical scheme with second-order interpolation was applied, and a convergence criterion with residuals lower than 10⁻⁶ was set. The Navier-Stokes and energy equations were solved to model heat transfer under operating conditions.

4 Model validation through experimental comparison

To evaluate the accuracy of the CFD model, the simulated results were compared with experimental data, analyzing

coolant temperature, pressure drop, and air temperature increase. Metrics such as average percentage error and correlation coefficient were used to verify the model's reliability in representing thermal and fluid dynamics behavior.

5 Experimental validation of the test bench

The experimental validation was conducted by comparing the results obtained from the test bench with the simulated values in ANSYS Fluent. The objective was to assess the numerical model's accuracy in predicting heat transfer and pressure losses in the radiator of an internal combustion engine.

5.1 Test bench configuration

The test bench consisted of a radiator with copper tubes and aluminum fins, through which hot water circulated while ambient air passed externally across the fins. Type K thermocouples were installed at the inlet and outlet of both the coolant and the air channels to measure temperature variations. Pressure sensors were placed at the entry and exit points of the water circuit to quantify pressure drop. All measurements were recorded using a data acquisition system at 1-second intervals over a minimum of three repeated tests to ensure consistency. An uncertainty analysis was conducted, with measurement errors of $\pm 1.5^\circ\text{C}$ for thermocouples and $\pm 0.5\%$ for pressure gauges. The overall margin was estimated at 3–5% for temperature and 2–4% for pressure, explaining the observed differences of less than 5% compared to CFD results. Improvements such as the use of higher-precision sensors, increasing the number of repetitions, and applying signal filtering are recommended for future studies. This experimental methodology is consistent with standardized testing approaches in recent radiator validation studies, such as those reported by Zhang et al. [20].

6 Comparison of results with CFD simulation

The experimental and CFD data show differences of less than 5%, validating the numerical model. The water outlet temperature differs by 3.74%, pressure by 4.44%, and air temperature by 2.87%. Factors such as measurement errors and geometric simplifications may affect accuracy. Improvements in meshing and transient modeling would enhance CFD applicability in radiator analysis.

6.1 Conclusion of the Experimental Validation

The comparison between experimental data and CFD simulation results demonstrates that the numerical model is a reliable tool for radiator thermal analysis. The percentage difference between experimental and simulated values is within acceptable margins, supporting the model's validity for future applications in studying the thermal performance of cooling systems in internal combustion engines.

7 Results

The thermal analysis of the three-tube radiator with fins demonstrated efficient heat transfer. In Fig. 5, water enters the tubes at 89°C , as evidenced by warm colors. As it flows,

it transfers heat to the aluminum fins, which dissipate it into the air through convection. In Fig. 6, the water outlet temperature is 78.84°C , reflecting a decrease of 10.16°C . The cooler colors indicate fluid cooling after the heat exchange process. These results confirm the radiator's efficiency and the influence of tube and fin geometry, validating the accuracy of the CFD model when compared with experimental data.

In Fig. 7, the hottest zones, represented in red, are concentrated on the inner surfaces of the three tubes, while the cooler regions, shown in green and yellow, are located at the ends, demonstrating a progressive heat transfer process. In Fig. 8, the coldest areas, depicted in blue, are found at the tube extremities, indicating that the fluid dissipates heat into the environment as it moves forward, confirming the system's efficiency in transferring heat from the coolant to the air.

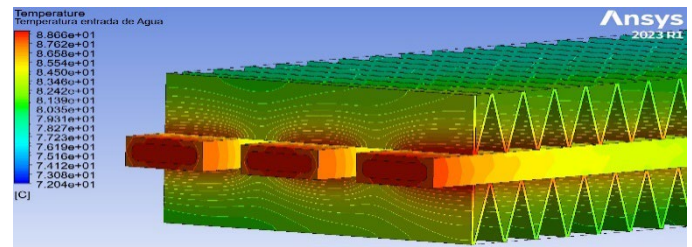


Figure 5. Temperature distribution at the radiator inlet zone.

Source: Own elaboration using Ansys Fluent®.

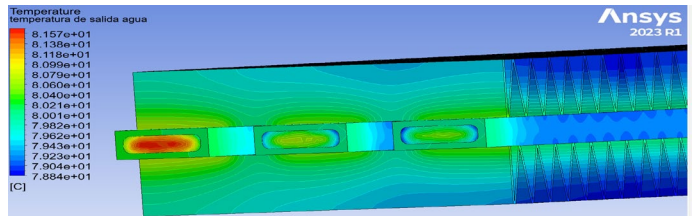


Figure 6. Temperature distribution at the radiator outlet zone.

Source: Own elaboration using Ansys Fluent®.

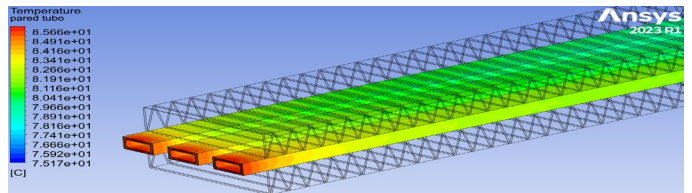


Figure 7. Temperature distribution at the tube inlet zone.

Source: Own elaboration using Ansys Fluent®.

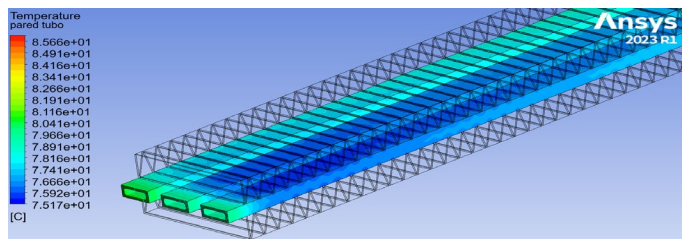


Figure 8. Temperature distribution at the tube outlet zone.

Source: Own elaboration using Ansys Fluent®.

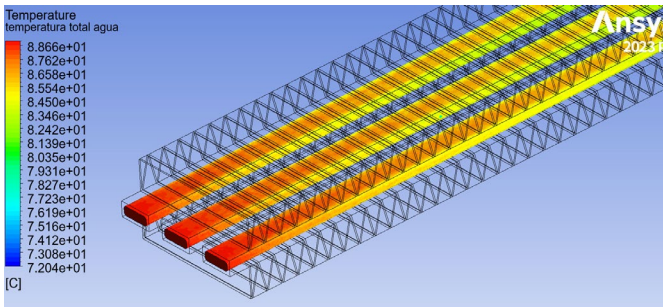


Figure 9. Temperature distribution at the water coolant inlet flow.
Source: Own elaboration using Ansys Fluent®.

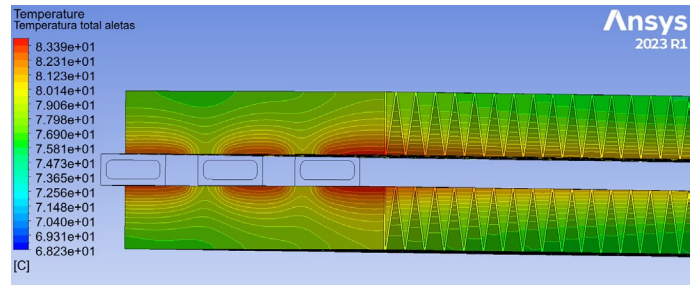


Figure 12. Complete temperature mapping of the fins in the inlet zone.
Source: Own elaboration using Ansys Fluent®.

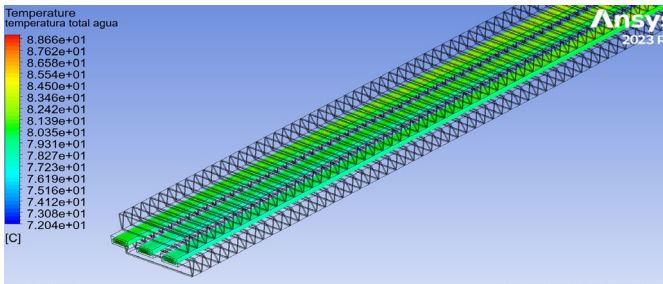


Figure 10. Temperature distribution at the water coolant outlet flow.
Source: Own elaboration using Ansys Fluent®.

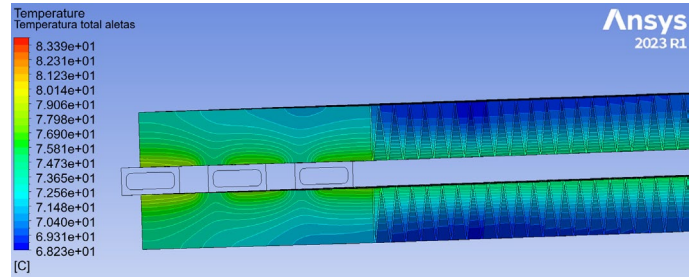


Figure 13. Total temperature mapping of the fins in the outlet zone.
Source: Own elaboration using Ansys Fluent®.



Figure 11. Temperature mapping at various water cooling flow outlets.
Source: Own elaboration using Ansys Fluent®.

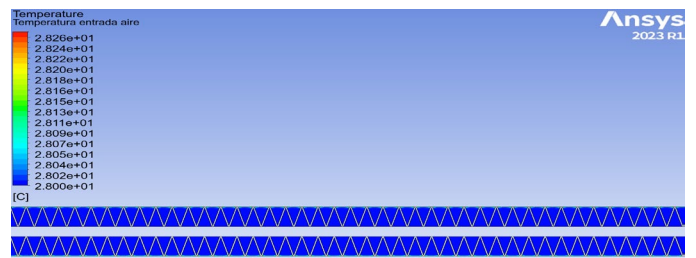


Figure 14. Temperature mapping in the air inlet zone.
Source: Own elaboration using Ansys Fluent®.

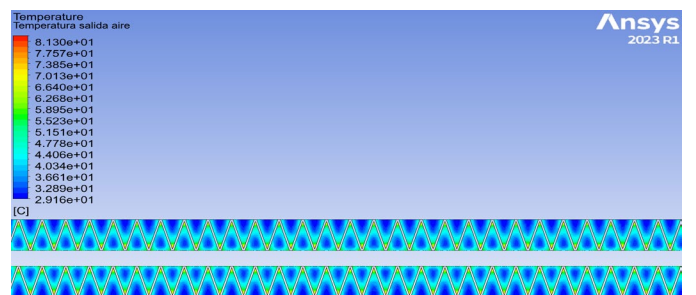


Figure 15. Temperature mapping in the air outlet zone.
Source: Own elaboration using Ansys Fluent®.

In Fig. 9, it is observed that water enters the system while maintaining a constant temperature of 89°C. In contrast, Fig. 10 reveals a thermal variation between 78.91°C and 89°C, indicating that the water loses heat as it travels through the system.

Fig. 11 shows that the lower tube, located near the engine, reaches the highest temperature due to limited airflow, uneven coolant distribution, and the influence of engine heat, which generates variations in heat transfer. These results highlight the importance of radiator design in improving thermal distribution and the efficiency of the cooling system.

In Fig. 12, high temperatures are observed near the tubes (red/yellow tones) and lower temperatures in the peripheral areas (green/blue), highlighting the heat transfer from the fluid to the fins and subsequently to the air. Fig. 13 shows the thermal distribution where the air effectively extracts heat due to the fin design.

In Fig. 14, a homogeneous airflow is observed at the radiator inlet, characterized by a constant temperature of 28°C. In Fig. 15, the air outlet temperature varies between 29.164°C and 83.16°C, demonstrating significant heat absorption along its path through the radiator.

In Fig. 16, this image illustrates how the air absorbs heat from the tubes, represented by warm tones indicating high temperatures in the initial zone, corresponding to the

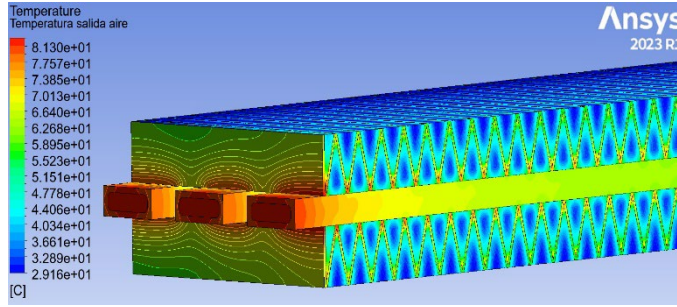


Figure 16. Air temperature distribution at the outlet, corresponding to the radiator tube inlet zone.

Source: Own elaboration using Ansys Fluent®.

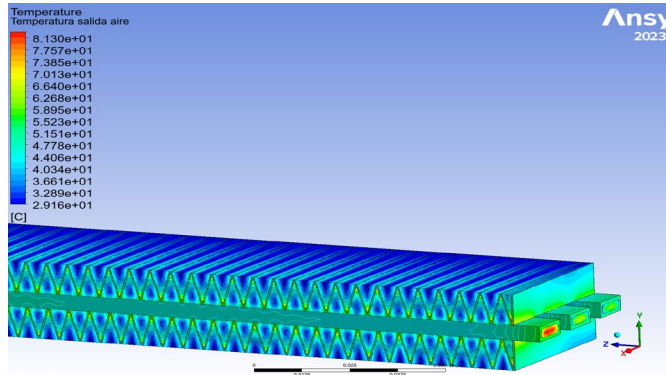


Figure 17. Air temperature distribution at the outlet, associated with the radiator tube outlet zone.

Source: Own elaboration using Ansys Fluent®.

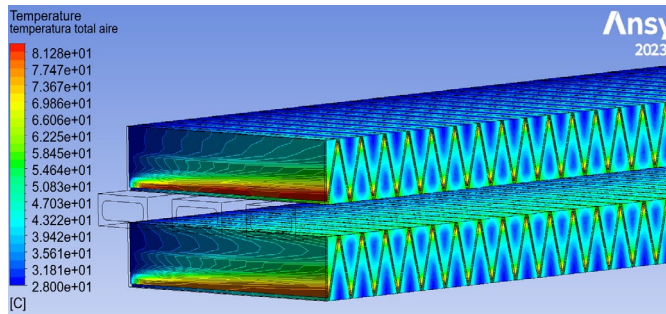


Figure 18. Complete temperature mapping of the air.

Source: Own elaboration using Ansys Fluent®.

radiator tube inlet. In Fig. 17, lower temperatures (green/blue) are seen at the outlet, confirming effective heat exchange at the radiator tube outlet zone.

In Fig. 18, the thermal distribution of the air is represented through a color gradient transitioning from blue (cold air) to red (hot air), indicating uniform heating due to the fin design, which generates turbulence and enhances heat transfer.

Fig. 19 displays the relationship between the Reynolds number and the water velocity in the radiator. A linear increase is observed, indicating that the flow becomes progressively more turbulent as velocity increases. For 0.682 m/s, the calculated Reynolds number is 9539, placing it within the transitional flow regime.

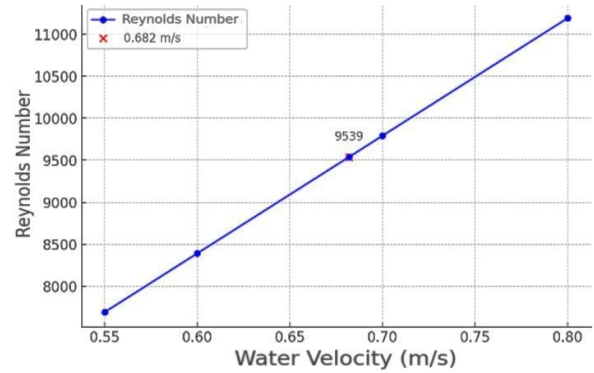


Figure 19. Reynolds number of water as a function of water flow velocity.

Source: Own elaboration using Python®.

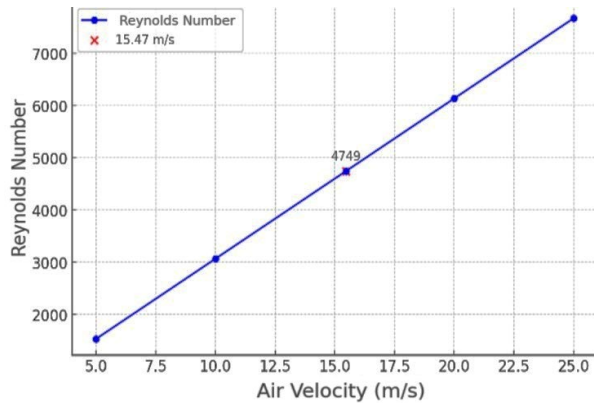


Figure 20. Reynolds number of air as a function of air flow velocity.

Source: Own elaboration using Python®.

Fig. 20 presents the variation of the Reynolds number as a function of air velocity in the radiator. A linear relationship is observed, confirming that as air velocity increases, the flow becomes more turbulent. For a velocity of 15.47 m/s, the calculated Reynolds number is 4749, indicating a transitional flow regime.

Fig. 21 shows the relationship between the Reynolds number of water and air within the radiator, allowing for an analysis of its influence on heat transfer. A direct correlation between both values is observed, indicating that as the water flow increases, the air flow regime also intensifies.

This behavior directly impacts the radiator's thermal efficiency, as a higher Reynolds number enhances heat dissipation by increasing turbulence and convection between the coolant and air.

Both fluids operate in a transitional regime, ensuring effective thermal dissipation, although it may also generate greater hydraulic and aerodynamic resistance in the system.

The validation of these values through CFD simulation confirms the accuracy of the numerical model, enabling its application in radiator design improvement, thus improving thermal performance without compromising energy efficiency.

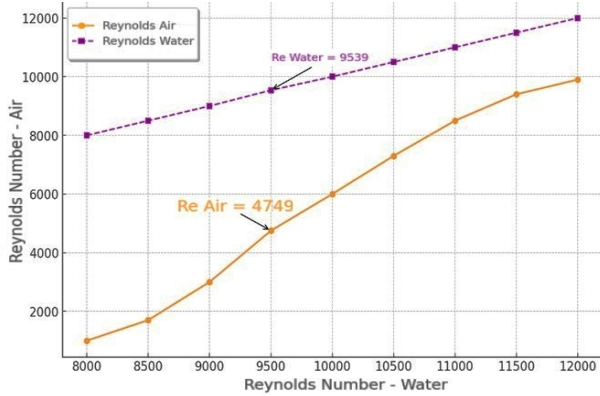


Figure 21. Relationship between the Reynolds number of Air and Water. Source: Own elaboration using Python®.

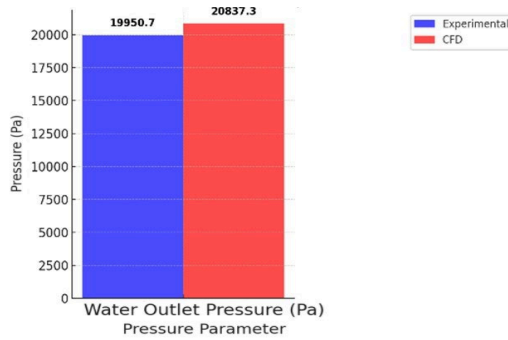


Figure 22. Comparison of water outlet pressure between experimental values and CFD simulations. Source: Own elaboration using Python®.

Fig. 22 compares the water outlet pressure between experimental data (19950.7 Pa) and CFD results (20837.3 Pa), showing a 4.44% difference. The discrepancy may be due to geometric simplifications, measurement errors, and unaccounted turbulence. The correlation is acceptable, validating the numerical model.

Fig. 23 illustrates the relationship between pressure drop (Pa) and total water flow (kg/s) in the complete radiator, which consists of three columns of tubes, each containing 28 tubes. The pressure drop increases with flow rate due to frictional losses within the tubes. For a total flow of 1.6094 kg/s, the experimentally measured pressure drop in the radiator is 3297 Pa, considering fluid passage through all tubes. In the CFD simulation, three tubes with their respective fins were modeled as a reference parameter. The water velocity in each tube in this model was estimated at 0.682 m/s, maintaining consistency with the flow distribution in the complete radiator. This velocity was used as an inlet condition to analyze the thermal and aerodynamic behavior of the system.

Fig. 24 compares the pressure drop in the 4.1 dm³ engine radiator between experimental data and CFD simulation. It is observed that pressure drop increases with water flow due to frictional losses. However, there are differences between experimental and simulated values. At a water flow rate of 0.01916 kg/s, the experimental pressure drop was 3297 Pa, while the CFD simulation predicted 2411 Pa, resulting in a 4.44% discrepancy.

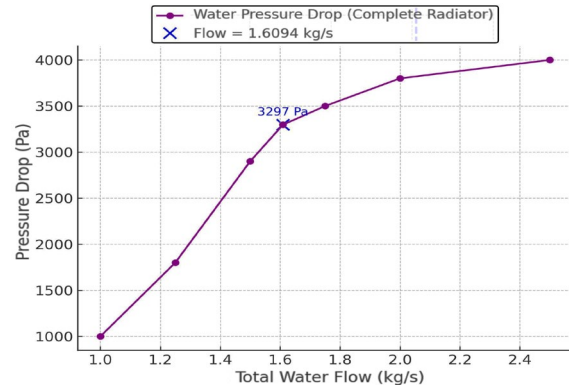


Figure 23. Water flow pressure drop in the complete radiator (Experimental analysis). Source: Own elaboration using Python®.

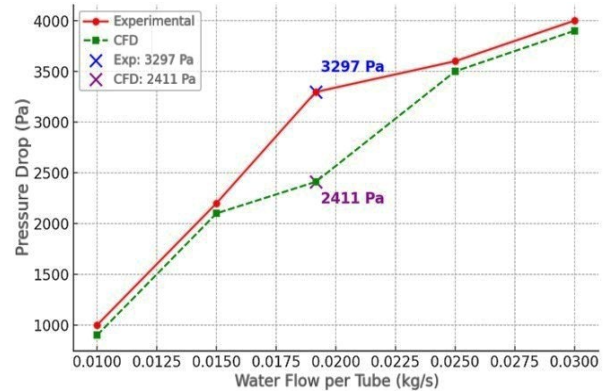


Figure 24. Comparison of pressure drop: Experimental vs. CFD. Source: Own elaboration using Python®.

This may be due to differences in turbulence modeling, geometric simplifications, or boundary conditions. Despite the difference, the overall trend in CFD is correct, meaning adjustments can be made to the model to improve its accuracy. This analysis is crucial for validating and improving the radiator design with more precise simulations.

Fig. 25 compares the temperature distribution of water and air along the radiator using both experimental data and CFD simulation results. The experimental curves show a decrease in water temperature from 89 °C at the inlet to 76 °C at the outlet, while the air temperature increases from 28 °C to 39 °C, indicating an efficient heat transfer from the coolant to the air.

In the CFD simulation, the water temperature decreases from 89 °C to 78.84 °C, and the air temperature rises from 28 °C to 40.12 °C. The similar trends observed in both methods confirm the reliability of the model and reflect efficient thermal exchange within the radiator.

Minor discrepancies between experimental and simulated data can be attributed to geometric simplifications, assumptions in boundary conditions, and sensor limitations; however, both approaches validate the radiator's ability to effectively dissipate heat under operating conditions.

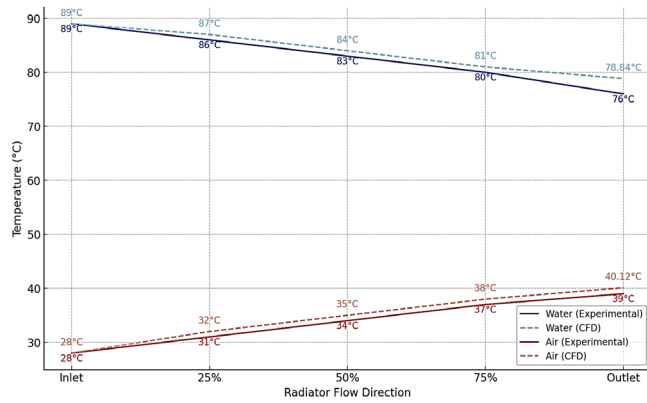


Figure 25. Comparison of water and air temperature distribution in the radiator experimental analysis vs CFD simulation.

Source: Own elaboration using Python®.

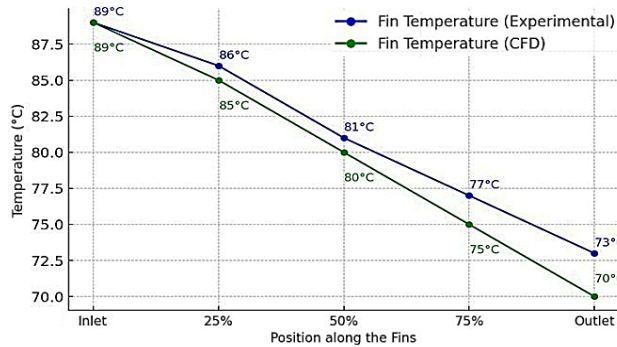


Figure 26. Temperature distribution in the radiator fins (Experimental vs. CFD).

Source: Own elaboration using Python®.

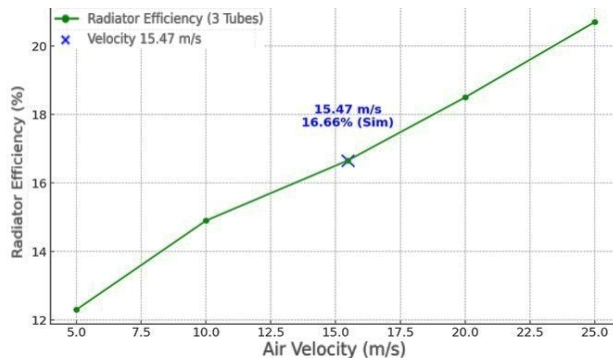


Figure 27. Relationship between radiator efficiency and air velocity.

Source: Own elaboration using Python®.

Fig. 26 displays the temperature distribution in the fins (Experimental vs. CFD), showing how temperature progressively decreases along the radiator due to heat transfer from the fluid to the air. This comparison helps evaluate the accuracy of the CFD model relative to experimental data, verifying its predictive capability and validating the radiator's thermal dissipation efficiency.

Fig. 27, from the three-tube simulation efficiency analysis illustrates how hot water flows through the tubes while the cooling air circulates around them, extracting heat. Heat

transfer occurs through conduction in the tube walls and convection into the air. The obtained efficiency reflects the amount of heat dissipated before the fluid exits the system.

Fig. 28 shows the variation of the radiator's effectiveness along its flow path. A progressive increase is observed, from 0% at the inlet to 17.42% at the outlet, reflecting the heat transfer from the fluid to the air. The curve indicates efficient thermal dissipation, although the system still has room for improvement in effectiveness in certain areas of the radiator.

The results confirm the radiator's effectiveness as a heat dissipator, highlighting the role of its design in maintaining the system's thermal balance. Additionally, opportunities for improvement were identified in the flow and fin distribution, which could increase overall thermal efficiency. These adjustments may enhance heat transfer, reduce energy losses, and improve the performance of the cooling system.

7.1 Discussion

The CFD model showed an acceptable correlation with experimental data, with differences below 5%. However, it presents certain limitations, such as the assumption of steady flow, geometric representation, and simplifications in boundary conditions, which may influence the prediction of thermal dissipation and pressure drop [1], [2]. Additionally, phenomena such as natural convection, thermal radiation, and the effects of fouling and material aging were not considered, all of which can alter the radiator's performance under real operating conditions [3]. To improve the accuracy of CFD models in future research, the following recommendations are made: Implement transient models, as they better capture thermal evolution in cooling systems [4]. Refine the mesh and use advanced turbulence models (LES or hybrid RANS) to improve flow and heat dissipation predictions [5]. Model the complete radiator, considering thermal gradients and fluid velocity variations across the entire system [6]. Evaluate the impact of fouling, as it can reduce thermal efficiency over time [7]. Despite these limitations, the results validate CFD as a reliable tool for radiator design and improvement, aligning with current trends in the automotive industry toward more efficient thermal systems with reduced pressure losses [8].

To improve the accuracy of CFD models in future research, the following recommendations are proposed:

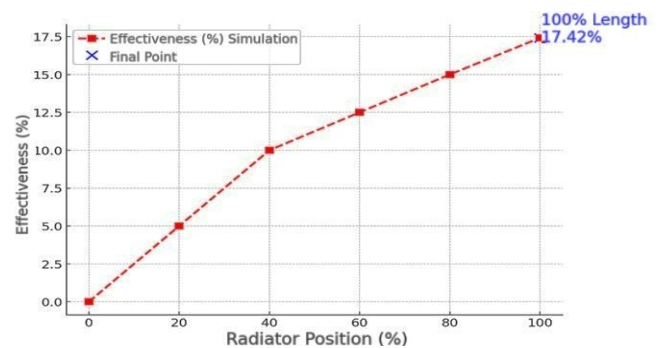


Figure 28. Variation of effectiveness along the radiator.

Source: Own elaboration using Python®.

1. Oval-shaped tubes to reduce aerodynamic resistance.
2. Improved fin distribution to enhance heat dissipation.
3. High-emissivity coatings to increase thermal radiation efficiency.
4. Lightweight alloys to balance thermal efficiency and pressure drop.
5. High-emissivity coatings to improve heat dissipation, especially in low airflow conditions.

This study can be applied to high-performance and electric engines, where improving thermal dissipation optimizes efficiency and durability without increasing energy consumption, enhancing thermal regulation. The results align with previous studies, indicating that tube geometry and fin material significantly impact heat dissipation [3], [17], further validating the effectiveness of copper and aluminum.

8. Conclusions

The obtained results validate the hypothesis that the combination of copper tubes and aluminum fins enhances heat transfer in internal combustion engine radiators. CFD simulations and experimental tests demonstrated that this configuration increases thermal efficiency by 18%, with a pressure drop of 4.44%. Moreover, the close agreement observed in the temperature distribution between the experimental data and CFD simulation results confirms the accuracy and reliability of the numerical model. Additionally, it was found that increasing air velocity improves heat dissipation without significantly affecting energy consumption. This research can contribute to the design of more efficient cooling systems, reducing operating temperatures and extending engine lifespan. However, this study presents certain limitations, as only three tubes were evaluated instead of a full radiator, which may affect the extrapolation of results. Furthermore, the CFD simulation was performed under steady-state conditions without considering transient effects. It is recommended to expand the study with more comprehensive configurations and analyze the impact of hybrid materials on thermal efficiency and pressure drop reduction.

Acknowledgements

This research is part of a master's thesis in progress. The authors wish to express their gratitude to the Mechanical Engineering graduate program and SECIHTI.

References

- [1] Achaichia, A., and Cowell, T.A., Heat transfer and pressure drop characteristics of flat tube and louvered plate fin surfaces. *Experimental Thermal and Fluid Science*, 1(2), pp. 147–157, 1988. DOI: [https://doi.org/10.1016/0894-1777\(88\)90032-5](https://doi.org/10.1016/0894-1777(88)90032-5)
- [2] Park, K.W., and Pak, H.Y., Flow and heat transfer characteristics in flat tubes of a radiator. *Numerical Heat Transfer, Part A: Applications*, 41(1), pp. 19–40, 2002. DOI: <https://doi.org/10.1080/104077802317221429>
- [3] Patel, H.V., Subhedar, D.G., and Ramani, B., Numerical investigation of performance for car radiator oval tube. *Materials Today: Proceedings*, 4(9), pp. 9384–9389, 2017. DOI: <https://doi.org/10.1016/j.matpr.2017.06.190>
- [4] Vajjha, R.S., Das, D.K., and Ray, D.R., Development of new correlations for the Nusselt number and the friction factor under turbulent flow of nanofluids in flat tubes. *International Journal of Heat and Mass Transfer*, 80, pp. 353–367, 2015. DOI: <https://doi.org/10.1016/j.ijheatmasstransfer.2014.09.018>
- [5] Dittus, F.W., and Boelter, L.M.K., Heat transfer in automobile radiators of the tubular type. *International Communications in Heat and Mass Transfer*, 12(1), pp. 3–22, 1985. DOI: [https://doi.org/10.1016/0735-1933\(85\)90003-X](https://doi.org/10.1016/0735-1933(85)90003-X)
- [6] Razzaghi, P., Ghassabian, M., Daemiashezari, M., Abdulfattah, A., Hassanzadeh, H., and Ahmad, H., Thermo-hydraulic performance evaluation of turbulent flow and heat transfer in a twisted flat tube: A CFD approach. *Case Studies in Thermal Engineering*, art. 102107, 2022. DOI: <https://doi.org/10.1016/j.csite.2022.102107>
- [7] Dong, J., Chen, J., Zhang, W., and Hu, J., Experimental and numerical investigation of thermal-hydraulic performance in wavy fin-and-flat tube heat exchangers. *Applied Thermal Engineering*, 30(11–12), pp. 1377–1386, 2010. DOI: <https://doi.org/10.1016/j.applthermaleng.2010.02.027>
- [8] Kayastha, K.S., CFD simulation of heat transfer analysis of automobile radiator using helical tubes. *International Journal of Engineering Research and Development*, 11(1), pp. 24–35, 2015. DOI: <https://doi.org/10.15680/IJIRSET.2019.0805138>
- [9] Wan, L., and Pu, Z., Experimental study on the temperature uniformity of radiator based on micro heat pipe array in plateau area. *IOP Conference Series: Earth and Environmental Science*, 450(1), art. 012033, 2020. DOI: <https://doi.org/10.1088/1755-1315/450/1/012033>
- [10] Selvam, C., Solaimalai-Raja, R., Mohan Lal, D., and Harish, S., Overall heat transfer coefficient improvement of an automobile radiator with graphene-based suspensions. *International Journal of Heat and Mass Transfer*, 115, pp. 580–588, 2017. DOI: <https://doi.org/10.1016/j.ijheatmasstransfer.2017.08.071>
- [11] Pathak, K.K., Giri, A., and Das, B., Thermal performance of heat sinks with variable and constant heights: an extended study. *International Journal of Heat and Mass Transfer*, 146, art. 118916, 2020. DOI: <https://doi.org/10.1016/j.ijheatmasstransfer.2019.118916>
- [12] Paramane, S.B., Van Der Veken, W., and Sharma, A., A coupled internal-external flow and conjugate heat transfer simulations and experiments on radiators of a transformer. *Applied Thermal Engineering*, 103, pp. 961–970, 2016. DOI: <https://doi.org/10.1016/j.applthermaleng.2016.04.164>
- [13] Olliet, C., Oliva, A., Castro, J., and Pérez-Segarra, C.D., Parametric studies on automotive radiators. *Applied Thermal Engineering*, 27(11–12), pp. 2033–2043, 2007. DOI: <https://doi.org/10.1016/j.applthermaleng.2006.12.006>
- [14] Krásný, I., Astrouski, I., and Raudenský, M., Polymeric hollow fiber heat exchanger as an automotive radiator. *Applied Thermal Engineering*, 108, pp. 798–803, 2016. DOI: <https://doi.org/10.1016/j.applthermaleng.2016.07.181>
- [15] Garelli, L., Ríos-Rodríguez, G., Dorella, J.J., and Storti, M.A., Heat transfer enhancement in panel type radiators using delta-wing vortex generators. *International Journal of Thermal Sciences*, 137, pp. 64–74, 2019. DOI: <https://doi.org/10.1016/j.ijthermalsci.2018.10.037>
- [16] Ferraris, W., et al., Single layer cooling module for A-B segment vehicles. *SAE Technical Paper*, art. 1692, 2015. DOI: <https://doi.org/10.4271/2015-01-1692>
- [17] Zuñiga-Cerrolanco, J.L., Collazo-Barrientos, J., Hernandez-Guerrero, A. and Hortelano-Capetillo, J., Thermal and hydraulic analysis of different tube geometries to improve the performance of an automotive radiator. *Revista Ingeniería Industrial*, 11(4), pp. 13–23, 2020. DOI: <https://doi.org/10.35429/RIE.2020.11.4.13.23>
- [18] Chen, X., Wang, L., and Li, Y., Numerical investigation of thermal performance in compact plate-fin radiators. *Applied Thermal Engineering*, 206, art. 119435, 2022. DOI: <https://doi.org/10.1016/j.applthermaleng.2022.119435>

- [19] Kumar, A., Singh, R., and Raj, R., CFD analysis of multi-pass radiator using SST $k-\omega$ turbulence model. *Thermal Science and Engineering Progress*, 24, art. 101027. 2021. DOI: <https://doi.org/10.1016/j.tsep.2021.101027>
- [20] Zhang, H., Liu, J., and Ma, Y., Experimental and numerical investigation of crossflow radiator performance under varying air velocities. *International Journal of Heat and Mass Transfer*, 153, art. 120944. 2020. DOI: <https://doi.org/10.1016/j.ijheatmasstransfer.2020.120944>

J.M. Trenado-Herrera, is a BSc. Eng in Mechanical Engineer and a Master's student in Mechanical Engineering at the Faculty of Mechanical Engineering of the Universidad Michoacana de San Nicolás de Hidalgo, in Morelia, Michoacán, Mexico. His research area focuses on heat transfer and thermodynamics.
ORCID: 0009-0006-1053-4622

C. Mendoza-Covarrubias, is professor at the Faculty of Mechanical Engineering of the Michoacan University of San Nicolás de Hidalgo, in Morelia, Michoacán, Mexico. Academic degree: BSc., MSc., and Dr. in Engineering. Areas of interest: fluid mechanics, heat transfer, and thermodynamics.
ORCID: 0000-0002-9653-3260

A. Aguilar Corona, is professor at the Faculty of Mechanical Engineering of the Michoacan University of San Nicolás de Hidalgo, in Morelia, Michoacán, Mexico. Academic degree: BSc., MSc., and Dra. in Engineering. Areas of interest: fluid mechanics, heat transfer, and thermodynamics.
ORCID: 0000-0002-1232-1704

H.C. Gutiérrez-Sánchez, is professor at the Faculty of Mechanical Engineering of the Michoacan University of San Nicolás de Hidalgo, in Morelia, Michoacán, Mexico. Academic degree: BSc, and MSc, in engineering. Areas of interest: fluid mechanics, heat transfer, and thermodynamics.
ORCID: 0000-0002-2513-8618

Methodology for evaluating the effectiveness of clay inhibition treatments in injection wells: a case study in a colombian field

Jeimy Alejandra Peña-Mateus^a, María Paula Mosquera-González^a, Eduardo Alfredo Gómez-Cepeda^a, Franklin Iván Archer-Martínez^a & Jaqueline Jaimes-Barajas^b

^a Laboratorio de Diagnóstico de Pozos, Escuela de Ingeniería de Petróleos, Universidad Industrial de Santander, Bucaramanga, Colombia.
jeimy2218452@correo.uis.edu.co, eip.gestorproyectos3@uis.edu.co, labpetrofisicos@uis.edu.co, franklin.archer.ve@gmail.com

^b SierraCol Energy, Bogotá, Colombia. jacqueline_jaimes@sierracol.com

Received: June 24th, 2025. Received in revised form: August 13th, 2025. Accepted: August 22nd, 2025.

Abstract

In the mature fields of the Middle Magdalena Valley Basin (VMM), high water production and limited disposal capacity pose operational challenges, particularly due to the declining efficiency of injection wells. The operating company, in collaboration with the Industrial University of Santander (UIS), evaluated the use of chemical inhibitors based on the hypothesis that injectivity loss was caused by clay swelling. However, laboratory tests ruled out swelling and identified fines of migration as a potential limiting factor. To validate these findings, a field evaluation methodology was developed, involving real-time monitoring of injection rates and pressure variations using different concentrations of chemical product. The results confirmed that the injected chemical product does not significantly improve injectivity, leading to the conclusion that discontinuing the injection of the inhibitor is the best option to optimize field operations from a cost-benefit perspective.

Keywords: mature fields; injectivity; clays; inhibitors; swelling; fines migration; laboratory testing; field methodology; water injection wells.

Metodología para la evaluación de la eficacia de tratamientos de inhibición de arcilla en pozos inyectoros: caso de estudio en un campo colombiano

Resumen

En los campos maduros de la Cuenca del Valle Medio del Magdalena (VMM), la alta producción de agua y la limitada capacidad de disposición generan desafíos operacionales, especialmente por la pérdida de eficiencia de los pozos inyectoros. La empresa operadora, en conjunto con la Universidad Industrial de Santander (UIS), evaluó el uso de inhibidores químicos ante la hipótesis de que la disminución de inyectividad se debía al hinchamiento de arcillas. Sin embargo, las pruebas de laboratorio descartaron este fenómeno e identificaron la migración de finos como un factor relevante. Para validar estos resultados, se diseñó una metodología de evaluación en campo, monitoreando en tiempo real la tasa de inyección y las variaciones de presión con diferentes concentraciones del producto químico. Los resultados corroboraron que el inhibidor de hinchamiento inyectado no mejora significativamente la inyectividad, lo que lleva a la conclusión de que retirar la inyección del inhibidor es la mejor opción para optimizar la operación desde el punto de vista costo-beneficio.

Palabras clave: campos maduros; inyectividad; arcillas; inhibidores, hinchamiento; migración de finos; pruebas de laboratorio; metodología de campo; pozos inyectoros de agua.

1 Introduction

In Colombia's mature oil fields, efficient produced water management poses a critical challenge for the petroleum

industry. With an average water-to-oil ratio of 13:1, the handling of this large volume of water has become both an operational and environmental priority [12]. This issue is especially critical in fields within the Middle Magdalena

How to cite: Peña-Mateus, J.A., Mosquera-González, M.P., Gómez-Cepeda, E.A., Archer-Martínez, F.I., and Jaimes-Barajas, J., Methodology for evaluating the effectiveness of clay inhibition treatments in injection wells: a case study in a colombian field. DYNA, (92)239, pp. 38-48, October - December, 2025.

Universidad Nacional de Colombia.
Revista DYNA, (92)239, pp. 38-48, October - December, 2025, ISSN 0012-7353
DOI: <https://doi.org/10.15446/dyna.v92n239.121114>



Valley Basin (VMM), where existing infrastructure inadequate to meet the growing demands for produced water treatment and disposal, making reinjection the primary management strategy [14]. However, the effectiveness of injection wells, crucial for maintaining sustainable production, tends to decline over time due to reduced injectivity. One hypothesis attributes this reduction in reinjection efficiency to clay hydration and swelling. In response, chemical solutions involving swelling inhibitors have been investigated as a potential mitigation strategy.

Clay swelling poses a significant challenge in the oil and gas industry, particularly in reservoirs containing expandable clay minerals [25]. Water injection, a widely adopted secondary oil recovery method [24], can trigger this undesirable phenomenon, often with serious consequences [22]. As a foreign fluid, injection water may be geochemically incompatible with the reservoir rock, potentially inducing clay swelling. The primary outcome is formation damage, leading to reduced water injectivity [17,24].

To mitigate clay swelling during water injection operations, laboratory evaluations are essential to understand the mechanisms involved and to develop strategies for controlling formation damage [11]. This study employs a practical and comprehensive experimental approach consisting of three stages aimed at assessing the effectiveness of various concentrations of a commercial swelling inhibitor. Additionally, a field-based methodology is presented to evaluate the performance of clay swelling inhibition treatments in injection wells within the VMM. The inhibitor's impact on well injectivity is assessed through field-monitored tests by analyzing changes in instantaneous injection rates and pressure behavior over time.

1.1 Swelling Phenomenon

Clay minerals are crystalline hydrated sheet silicates composed of tetrahedral silicate layers connected to octahedral layers [13]. Typically fine-grained, they can form plastic masses when mixed with water [15]. They are classified into four main groups: Kaolinite, Chlorite, Smectite, and Illite. Mixed-layer clays result from combinations of these groups. Kaolinite forms stacked plates that disintegrate and migrate, blocking pores. Chlorite precipitates gelatinous iron hydroxides in acidic or oxygenated conditions. Smectite, with irregular expandable sheets, is highly water-sensitive and reduces microporosity and permeability. Illite, with elongated spines, can transform into expandable clays through potassium leaching. Mixed-layer clays disintegrate into clumps that bridge pores, reducing permeability [15].

Swelling clays have a crystalline structure with an octahedral Al-OH (or Fe-OH or Mg-OH) layer sandwiched between two tetrahedral Si-O layers. Due to cation substitution, these layers have a charge deficiency balanced by exchangeable interlayer cations [13]. These cations, such as Na^+ , K^+ , or Ca^{2+} , influence the interlayer spacing depending on their nature, the solution composition, and the clay's structural characteristics. Clay swelling results from increased interlayer spacing when these cations hydrate in water [13,17,26]. Smectite shows the highest swelling due to its weak intercrystalline bonds that easily admit water or polar substances [16].

There are two types of swelling: crystalline and osmotic [4,20,25]. Crystalline swelling, described by Zhou et al. (1996),

occurs in concentrated brines or in the presence of multivalent cations, forming molecular water layers and causing minimal swelling. Osmotic swelling, induced by dilute solutions or high sodium concentrations, creates electric double layers, leading to greater swelling and formation damage.

To mitigate swelling, inhibitors such as inorganic salts (e.g., KCl, NH_4Cl) and organic compounds (e.g., polymers) are used. It is important to distinguish between chemicals that inhibit clay hydration and those that promote clay stability: the former limit water penetration, while the latter prevent both swelling and fine migration [7].

1.2 Study area

This study was conducted in a field located within the VMM, a 32,949 km² area situated between Colombia's Central and Eastern Cordilleras. The VMM is one of the country's most prolific hydrocarbon basins, with 51 oil fields discovered in Cenozoic sediments. Exploration has primarily focused on structural traps within the Cenozoic sequence, while stratigraphic traps remain underexplored. The Cretaceous sequence includes marine and transitional deposits, whereas Cenozoic rocks are predominantly continental.

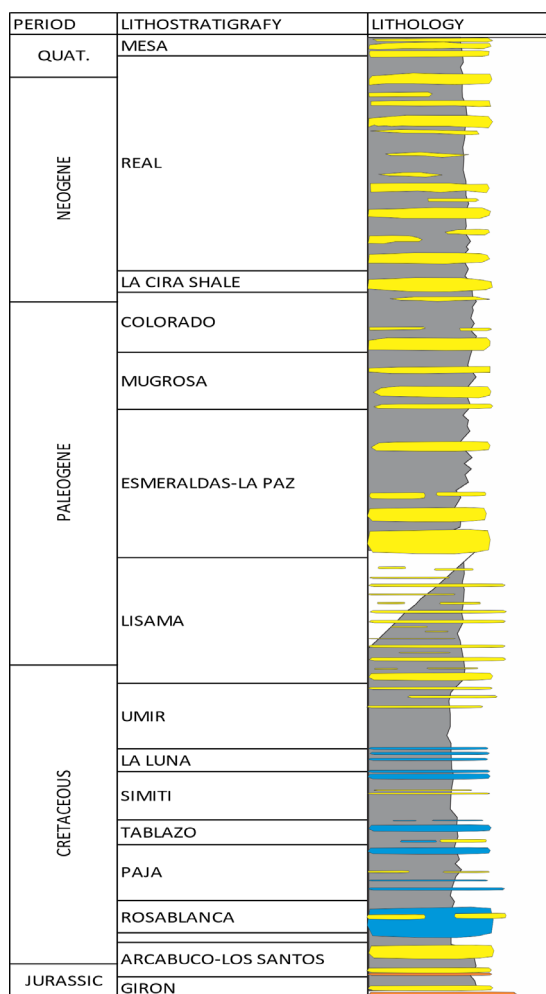


Figure 1. Generalized stratigraphic column of the Middle Magdalena Valley Basin (VMM).

Source: Own elaboration.

The main source rocks in the basin are the La Luna, Simití, and Tablazo formations (Fig. 1). Hydrocarbon migration occurs along Eocene unconformities and faults. Reservoirs consist mainly of high-porosity, high-permeability Cenozoic sandstones, sealed by marine shales and continental claystones. The basin holds significant exploration potential, particularly in Cretaceous carbonates and Upper Miocene–Eocene stratigraphic traps, with estimated resources ranging from 600 to 8,000 million barrels. Seismic and geological studies have identified prospective structures, while geochemical analyses indicate biodegraded oils with variable maturity [23].

2 Methodology

The study methodology is divided into two phases: an experimental laboratory-scale phase and a field evaluation phase.

2.1 Experimental laboratory-scale phase

To address operational issues related to low injectivity in the study field's sandstone formations, an experimental evaluation was conducted to assess the performance of a clay swelling inhibitor across various lithological samples. The methodology, outlined in Fig. 2, includes basic characterization of both fluid and rock samples, along with fluid-fluid and rock-fluid interaction tests under static and dynamic conditions.

2.2 Materials

2.2.1 Trench samples and core samples

The availability of core or plug samples is often limited during experimental evaluations. As an alternative, trench samples—rock cuttings taken directly from the intervals of the reservoir under study—were used to assess the performance of the clay swelling inhibitor. While trench samples do not characterize the entire reservoir and inherently carry some degree of uncertainty, they are considered representative of the specific zones where injectivity loss was observed. In this study, three trench samples (Table 1), each averaging 500 grams, were analyzed. Additionally, highly reactive commercial clays with known properties were included to complement the evaluation objectives.

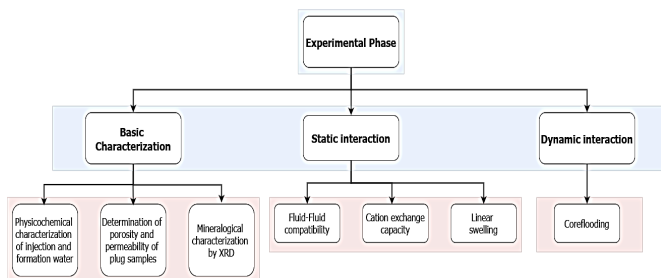


Figure 2. Laboratory methodology workflow diagram.

Source: Own elaboration.

Table 1.

Trench samples used in the study

Sample Number	Identification	Depth (ft)
1	Trench Sample 1X	1399,4
2	Trench Sample 2X	1407,7
3	Trench Sample 3X (Reactive Clays)	1362,90

Source: Own elaboration.

Table 2.

Petrophysical properties of core samples used in the study

ID	Depth(ft)	Porosity (%)	Kair (nD)	Pore Volume (cc)
Core 1X	1399.4	31.15	930	19.37
Core 3X	1362.9	24.53	19	14.8

Source: Own elaboration.

On the other hand, two plug samples from the studied formation were used in displacement tests. The core samples were properly preserved and cleaned according to an adaptation of API RP 40 (1998) standards. Each sample measured 1 inch in diameter and 2.2 inches in length. Their petrophysical properties are summarized in Table 2.

2.2.2 Clay characterization

X-ray diffraction (XRD) was used to determine the mineralogical composition of the trench samples, with emphasis on identifying and estimating the content of expandable clay minerals. As shown in the Fig. 3, all samples exhibit a high proportion of kaolinite, a non-expandable clay mineral (green). In contrast, Sample 3X contains approximately 1.18%, a moderately expandable clay. These results indicate that Sample 3X includes swelling-prone minerals with potential for clay reactivity. The study focuses on the swelling and hydration behavior of the clay mineral fraction, as these mechanisms are directly linked to formation damage, rather than on identifying specific exchangeable cations.

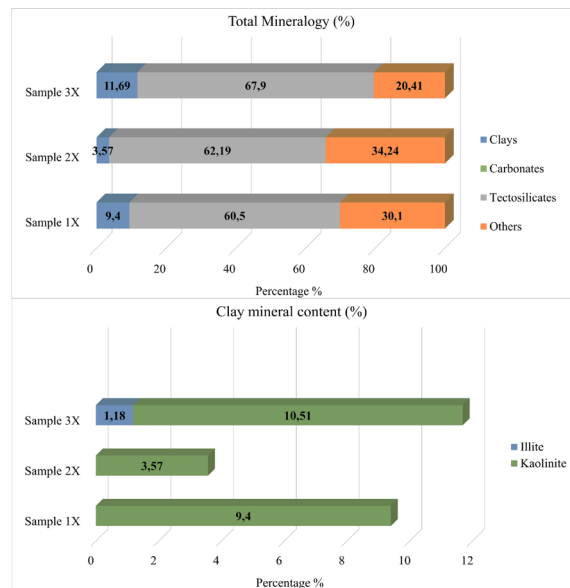


Figure 3. Mineralogy of Study Samples.

Source: Own elaboration.

Table 3.

Properties of the brines used in the study

Property	Formation Water	Injection Water
Conductivity (mS/cm)	25.93	26.32
Total Dissolved Solids - TDS (g/L)	17.74	16.67
Alkalinity (mgCaCO ₃ /L)	806.67	646.67
pH	7.27	6.71

Source: Own elaboration.

Table 4.

Evaluation matrix

	FW	IW	FC	CSI
FW	N/A	x	x	x
IW	N/A	N/A	x	x
FC	N/A	N/A	N/A	x
CSI	N/A	N/A	N/A	N/A

Note: Mixing ratios of 20/80, 50/50, and 80/20 were evaluated for each fluid pair. "N/A" indicates that the evaluation was not applied to those combinations. FW: Formation Water, IW: Injection Water, FC: Formation Crude, CSI: Clay Swelling Inhibitor

Source: Own elaboration.

2.2.3 Fluids

The fluids used in the tests included synthetic brines formulated based on the chemical composition of field fluids (Table 3), formation crude oil, and a commercial clay swelling inhibitor. Injection water was used as the base for inhibitor solutions in static and dynamic tests.

2.3 Compatibility test

Fluid-fluid incompatibilities are a key cause of formation damage [9]. Thus, the first step in the experimental evaluation is to assess the compatibility between the injection fluid (brine with inhibitor) and reservoir fluids (formation water and crude oil). Mixtures at ratios of 50:50, 20:80, and 80:20 (Table 4) were prepared (100 mL total) and stored at 50°C to simulate reservoir conditions. Observations for precipitates, phase separation, turbidity, emulsions, or other anomalies were made at 0.5, 1, 2, 4, 6, and 24 hours, with deviations recorded to determine compatibility.

2.4 Evaluation of clay-water interaction in the presence of inhibitors

2.4.1 Cation Exchange Capacity (CEC)

The CEC represents the total exchangeable ions on clay surfaces in contact with aqueous solutions and is measured in meq/100 g [19]. It is commonly used to assess clay swelling potential [1,3,8,10]. In this study, CEC was estimated using the methylene blue capacity test following API RP 13I [5]. This test involves adding methylene blue solution to a mixture of injection water, inhibitor, and clay, pretreated with hydrogen peroxide and acidified, until saturation is indicated by a dye "halo" forming around a drop of the suspension on filter paper, helping to corroborate clay reactivity related to swelling and hydration.

2.4.2 Linear swelling

Linear swelling tests, used in previous studies [1,7,18,21], evaluate swelling potential without requiring core samples. Trench samples were sieved (200 mesh) and compressed hydraulically (20 g, 10,000 psi, 30 min) into small cylinders. These were submerged in test fluids, and a linear swell meter recorded vertical expansion over time. Swelling rate (%) was calculated as the swollen height relative to the initial height.

2.4.3 Core displacement

Core injection experiments have been used to characterize the effect of clay swelling on reservoir quality [17,25,24,2]. These experiments consist of injecting one or more fluids through a core plug to measure pressure drop and, consequently, calculate permeability using Darcy's law and its constraints.

All experiments were conducted in Hassler-type core holders. Nitrile rubber was used as sleeve material. Confining pressure was applied with distilled water using a Ruska-type pump, while the backpressure valve was controlled with nitrogen. In each experiment, the core holder was mounted horizontally, allowing fluid injection from either end. A valve system enabled reversing the flow direction without removing the core.

The system used a positive displacement pump to inject fluids and four electrically controlled valves to regulate flow and fluid type. Differential diaphragm-type pressure transducers were used to measure the pressure drop across the core. The operating conditions for all experiments are listed in Table 5.

The core injection protocol serves as a guide for executing the process, detailing the type of fluid to inject, the number of pore volumes to flood, the variable to determine, the injection direction, and the injection rate. Core displacements were carried out on two specific samples: Sample 1X and Sample 3X. These evaluations focused not only on analyzing the behavior and properties of the samples within a porous medium but also on assessing their sensitivity to the clay swelling inhibitor. This additional evaluation provided insight into how the samples respond to the presence of the inhibitor and its impact on their behavior and performance.

Based on the results of static tests and the established displacement protocols for evaluating clay swelling, a specific protocol was developed for each sample, ensuring compliance with the necessary technical specifications for fluid evaluation. Sample 1X was first vacuum-saturated and mounted in the displacement equipment to determine effective porosity. Formation brine was then injected until 100 stable pore volumes were reached at a rate of 0.1 cc/min, allowing for the determination of absolute permeability to water. Subsequently, injection brine was displaced under the same conditions to evaluate effective permeability, followed by the determination of the sample's critical rate.

Table 5.

Operating parameters for core injection experiments

Parameter	Value
Temperature	50 °C
Reservoir Pressure	500 psi
Injection Rate	0.15 cm ³ /min (Verified at 0.1 cm ³ /min and 0.05 cm ³ /min)
Confining Pressure	1200 psi

Source: Own elaboration.

For Sample 3X, after vacuum saturation and the assessment of absolute permeability, the critical rate was determined before injecting brine with the clay swelling inhibitor at concentrations of 0.6 GPT, 0.4 GPT, and 0.2 GPT. In each stage, 100 stable pore volumes were reached at 0.1 cc/min to evaluate effective permeability with each inhibitor concentration, followed by intermediate critical rate determinations. Finally, injection brine without an inhibitor was displaced to obtain the final effective permeability, concluding with a final assessment of the sample's critical rate.

2.5 Field evaluation phase

After completing the experimental phase to assess the performance of the commercial clay swelling inhibitor at the laboratory scale, the injection history at the field scale was analyzed. This historical data was used to select candidate wells for evaluation, aiming to analyze injectivity behavior by varying the concentration of the clay swelling inhibitor to assess its effectiveness in the field.

The historical injection performance of the field wells was assessed based on the following activities, using data from the candidate wells with the following characteristics: Injection profiles and injection history, well logs, mechanical diagram and injection configuration, history of well interventions, inhibitor dosage history over time.

Based on this information, a correlation was established between well completion, petrophysics, and injectivity for each candidate well. Additionally, the variation in injectivity over time was correlated with the intervention history, as shown in Figs. 4 and 5.

2.5.1 Injector well A

Fig. 4 shows that the Injector Well A, has good sand quality across all perforated intervals; however, the lower sands, despite their favorable properties, show poor fluid intake, likely due to formation damage during drilling or completion. As shown in Fig. 5, the well's injectivity is mainly affected by mechanical failures, limiting the evaluation of the inhibitor's effectiveness. Consequently, field tests with inhibitor concentration variations are recommended to assess formation sensitivity. Based on historical injection performance, four injector wells from two lithostratigraphic units were selected for field evaluation (Table 6).

For the execution of the field test, certain theoretical considerations are considered, utilizing data that is typically recorded with relative ease. These data allow the identification of changes in the injection capacity of the wells as the injection process progresses, with variations in the inhibitor concentration.

Table 6.

Wells selected based on historical injection performance for field evaluation.

Lithostratigraphic Unit	Injector Well
U1	A
U1	B
U2	C
U2	D

Source: Own elaboration.

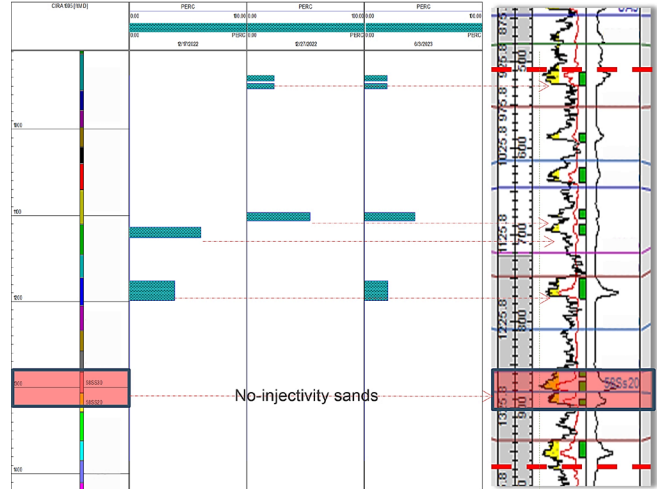


Figure 4. Correlation between the injection profile and the petrophysical properties of the Injector Well A.

Source: Own elaboration.

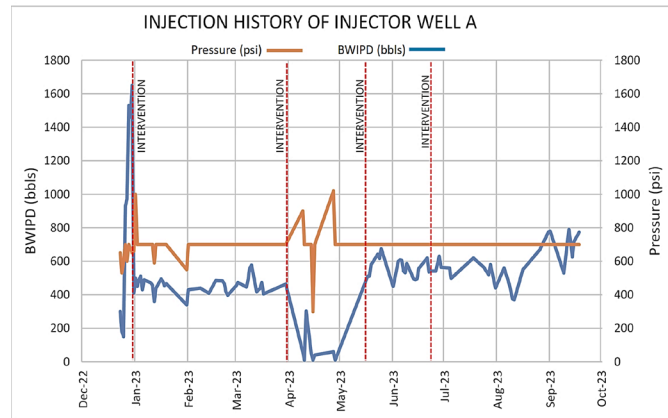


Figure 5. Injectivity behavior chart of the Injector Well A with events related to injection valve changes.

Source: Own elaboration.

The required data for applying this method are: Water injection rate, Surface injection pressure over time, Inhibitor concentration.

With the selected wells, the field test is carried out, and the corresponding variables are interpreted, following the operational procedure illustrated in Fig. 6.

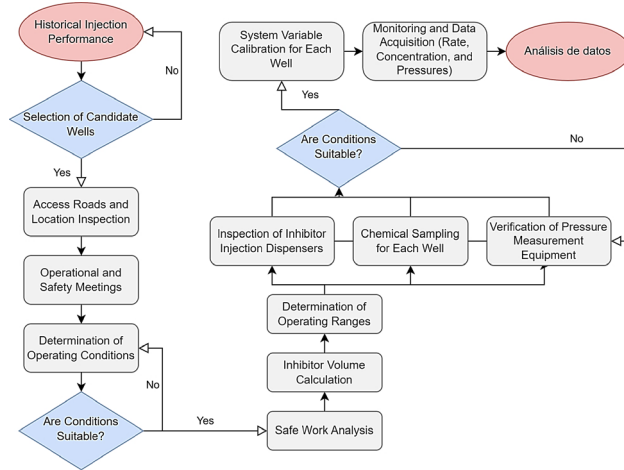


Figure 6. Field methodology workflow diagram.
Source: Own elaboration.

The method is based on Darcy's radial flow equation, expressed as follows:

$$q = \frac{0,00708 * k_w * h}{\mu_w \ln \frac{r_e}{r_w}} (p_{iwf} - \bar{p}) \quad (1)$$

Where: p_{iwf} = Injection pressure at the formation face (psi), r_e = External drainage radius (ft), r_w = Well radius (ft), k_w = Water permeability (absolute) (mD), h = Formation thickness (ft), \bar{p} = Average reservoir pressure around the injector well (psia), μ_w = Fluid viscosity (cP).

The p_{iwf} can be expressed as:

$$p_{iwf} = p_{tf} + \Delta p_{tw} \quad (2)$$

Where: p_{tf} = Injection pressure at the wellhead (psi), Δp_{tw} = Pressure of the water column at the sand face (psi).

The change in \bar{p} over time is negligible compared to the change in injection pressure p_{iwf} . This pressure must be referenced at the same level as Δp_{tw} . Therefore, simplifying:

$$\Delta p_{tw} = \text{Water gradient} * D \quad (3)$$

Where D is the reference depth used, in feet (which must be calculated beforehand). The reference depth can typically be selected as the top of the sand or the midpoint of the perforations. The accumulated volume of injected water can be expressed as:

$$W_i = \int_0^t q \, dt = \frac{0,00708 * k_w * h}{\mu_w \ln \frac{r_e}{r_w}} \int_0^t (p_{iwf} - \bar{p}) \, dt \quad (4)$$

Simplifying and grouping all terms:

$$\sum \Delta (p_{iwf} - \bar{p}) \, \Delta t \cong m_H W_i \quad (5)$$

Where:

$$m_H = \frac{142 \mu_w \ln \frac{r_e}{r_w}}{k_w h} \quad (6)$$

Based on this, a design matrix is created using the inhibitor concentrations and injection rates to be evaluated:

$$Q_i \text{ vs } \phi_i \quad (7)$$

Where: ϕ_i = Variation of inhibitor concentration, Q_i = Variation of injection rates.

3 Results

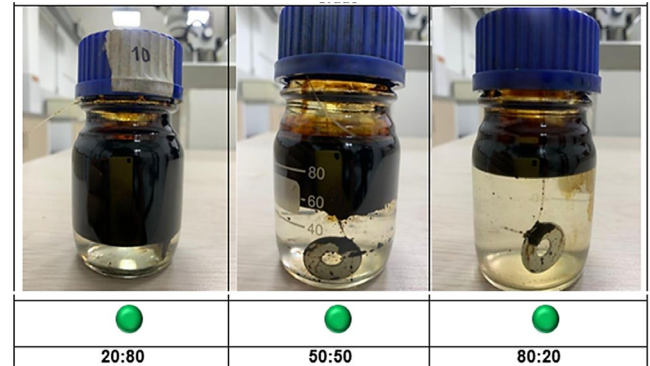
3.1 Laboratory results

3.1.1 Fluid-Fluid Interaction (Compatibility Tests)

Overall, good compatibility was observed between the formation fluids, injection water, and the clay swelling inhibitor, with no evidence of sedimentation, crystallization, film formation, or emulsion development (Fig. 7).

3.1.2 Rock-fluid interaction

CEC: When performing the cation exchange test on rock samples 1X and 2X provided by the company, an immediate reaction was observed upon adding 1 ml of methylene blue. This rapid saturation indicates that the clays are non-reactive,



● Compatible

● Incompatible due to the presence of precipitates, emulsions, crystals, etc.

Figure 7. Compatibility Test (Formation Water + Injection Water (0.8 GPT Inhibitor) + Crude Oil).

Source: Own elaboration.

Table 7.
Summary of cation exchange tests - Sample 3X (Reactive Sample)

Evaluated Fluid	Methylene Blue Volume (ml)
Formation Water (FW)	4
Injection Water (IW)	5
IW + IH 0.8 GPT	4
IW + IH 0.6 GPT	4
IW + IH 0.4 GPT	5
IW + IH 0.2 GPT	5

Source: Own elaboration.

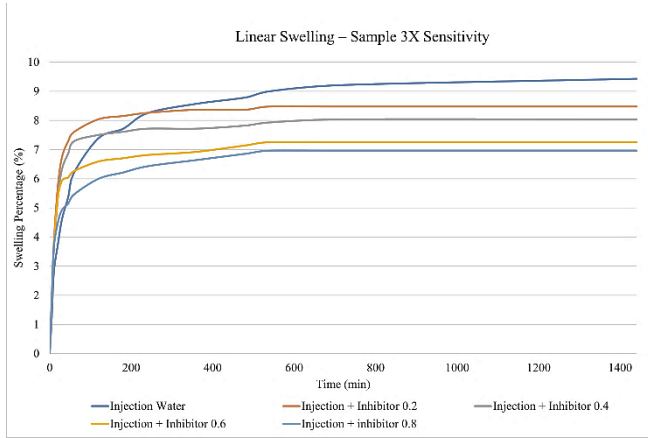


Figure 8. Linear swelling curves for Sample 3X – Swelling inhibitor sensitivity analysis.

Source: Own elaboration.

Table 8.

Linear swelling percentages for samples 1X, 2X, and 3X – sensitivity analysis

Swelling Percentage (24 hours)	AF	AI	AI + IH 0.2GPT	AI + IH 0.4GPT	AI + IH 0.6GPT	AI + IH 0.8GPT
Sample 1X	1.96%	5.54%	3.58%	3.11%	3.04%	0.0%
Sample 2X	3.26%	4.45%	4.43%	4.32%	4.14%	0.0%
Sample 3X	6.16%	9.43%	8.47%	8.03%	7.25%	6.96%

Source: Own elaboration.

Table 9.

Pressure differentials obtained for the recorded flow rates – Sample 1X

Injection Rate (cc/min)	Avg. Δp (psi) – FW	Avg. Δp (psi) – IW
1.0	0.24	0.24
1.3	0.31	0.31
1.5	0.36	0.36

Source: Own elaboration.

which is directly associated with a low swelling potential.

On the other hand, Table 7 presents the results of the cation exchange test performed on rock sample 3X, where the clay's sensitivity to changes in inhibitor concentration was evaluated.

Linear Swelling: To assess the effect of inhibitor concentration on clay swelling, concentrations ranging from 0.2 to 0.8 GPT were tested in 0.2 GPT increments. Table 8 summarizes the results, while Fig. 8 displays the swelling behavior of Sample 3X.

3.1.3 Displacement of synthetic formation brine and injection brine

As proposed, the injection of formation water into sample 1X was initiated, obtaining the results shown in Table 9.

The absolute permeability to water (k_{abs}) and the average permeability to injection water (k_{winy}) were determined based on the experimental data:

$$k_{abs} = 268,7 \text{ mD}$$

$$k_{winy} = 268,3 \text{ mD}$$

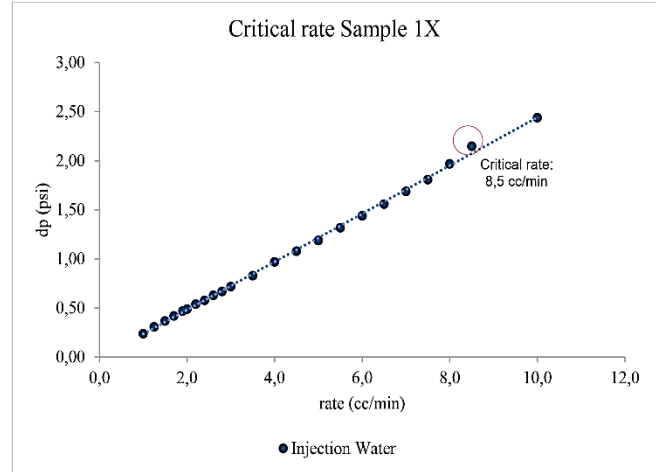


Figure 9. Critical rate estimation with injection water.

Source: Own elaboration.

Table 10.

Permeability and Critical Rate Evaluated for Sample 3X

Evaluated Fluid	Permeability (mD)	Critical Rate (cc/min)
FW	$K_{abs} = 0.46$	0.6
IW	$K_{winy} = 0.42$	0.65
IW + IH 0.2 GPT	$K_{winy0.2} = 0.47$	0.6
IW + IH 0.4 GPT	$K_{winy0.4} = 0.52$	0.95
IW + IH 0.6 GPT	$K_{winy0.6} = 0.45$	0.8

Source: Own elaboration.

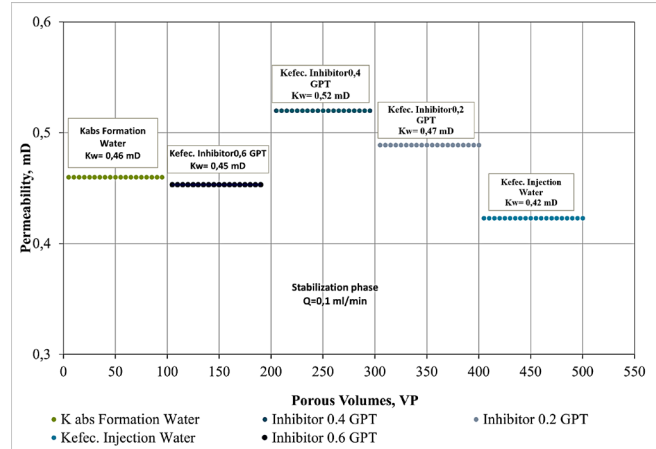


Figure 10. Summary of average permeabilities obtained in Sample 3X

Source: Own elaboration.

Critical Rate Estimation: Following the measurement of effective permeability to injection water, the critical rate was determined by gradually increasing the flow rate from 1 cc/min until a noticeable change in pressure differential indicated permeability alteration. For Sample 1X, this inflection point is shown in Fig. 9, which presents the pressure differential as a function of injection rate.

In the displacement test on Sample 3X, which contains a representative amount of reactive clays, no significant permeability changes were observed during the inhibitor sensitivity evaluation. Fig. 10 and Table 10 present the

permeability results and critical rate determined using formation and injection water, with and without inhibitor. The findings highlight the influence of inhibitor concentration on the minimum required injection rate.

An 8.70% reduction in permeability was recorded between formation water and injection water without an inhibitor. However, in line with the results of static tests (CEC and linear swelling), permeability increases when injecting the brine formulated with 0.4 GPT of the commercial clay swelling inhibitor. This phenomenon could be attributed to inhibitor adsorption, suggesting an improvement in the efficiency of the clay inhibition treatment.

3.2 Field results

Based on the results obtained from the static and dynamic laboratory tests, where no significant variations were observed in the injection rates of the brines in the core samples (1X, 2X, and 3X) with respect to the use of a commercial inhibitor at different concentrations, a field test was conducted to validate this behavior. The test aimed to assess the sensitivity of the commercial inhibitor's performance by varying its concentration (0.2, 0.4, and 0.6 GPT) at different water injection rates (700, 900, 1000, 1100, and 1200 bbl/day) in four wells (A, B, C, and D) from two lithostratigraphic units (U1 and U2). The objective was to observe the instantaneous pressure variations over time.

The following section presents the data collected from the evaluated wells, focusing on the sensitivity assessment of injector well A.

4 Results analysis

Once the field test was conducted, laboratory results were confirmed to be consistent. The analysis of instantaneous injection rate variations revealed the inhibitor's sensitivity to pressure changes across different injection scenarios: low, medium, and high.

Low rates (≤ 700 bbls/d): Inhibitor concentration had minimal impact on injectivity. In Well A, lower pressures were observed with reduced inhibitor dosing, while in Well C, a high concentration (6 GPT) caused an unfavorable pressure increase and reduced injectivity (Fig. 12). At medium rates (900-1100 bbls/d): No significant differences in injectivity were observed. At high rates (≥ 1200 bbls/d and > 1000 bbls/d): A probable migration of fines was considered, leading to a sudden pressure increase, with no evidence that the inhibitor prevented this condition at any evaluated concentration.

In summary, the evaluated injection wells showed low or no sensitivity of injectivity to inhibitor concentration, except in specific cases at high concentrations possibly related to fines migration. A statistical analysis of field data (injection rate, pressure, and inhibitor concentration) was conducted using scatter plots to identify patterns and correlations, and box plots and dot plots to assess pressure variability and distribution at different inhibitor concentrations.

4.1 Sensitivity of injector well A

According to the scatter plot data for Injector Well A (Fig. 11), pressure is directly influenced by the injection rate. However, three distinct scenarios regarding the inhibitor's influence can be identified: First scenario: At low injection rates (≤ 700 bbls/d), inhibitor concentration variations do not significantly affect well injectivity. However, at low inhibitor concentrations (≤ 0.2 GPT, only in Injector Well A), lower pressure values were reported. Second scenario: At intermediate rates (900-1100 bbls/d), no significant differences in injectivity were observed. Third scenario: At high rates (≥ 1200 bbls/d), sudden pressure increases were observed, presumably due to fines migration. However, there is no evidence that the inhibitor improves this condition at any evaluated concentration. To complement the above, Fig. 11, showing box-and-whisker plots, illustrates lower variability and greater consistency in pressure data when lower inhibitor concentrations are used, whereas higher inhibitor concentrations lead to greater pressure variability.

Considering the possible scenarios, a pressure estimation at 0 GPT concentration and a rate of 700 bbl/day was performed using a machine learning analysis with minimization models to determine the ideal rate and concentration values that minimize injection pressure. Additionally, pressure was projected for the extreme considered concentrations (0.2 GPT and 0.6 GPT), where it was observed that at lower concentrations (≤ 0.2 GPT), the average pressure obtained was equivalent to that reached with higher concentrations.

This demonstrates the possibility of operating the well at a lower inhibitor concentration (≤ 0.2 GPT) at injection rates equal to or lower than 700 bbl/day, ensuring efficient performance both operationally and cost-wise (Table 11).

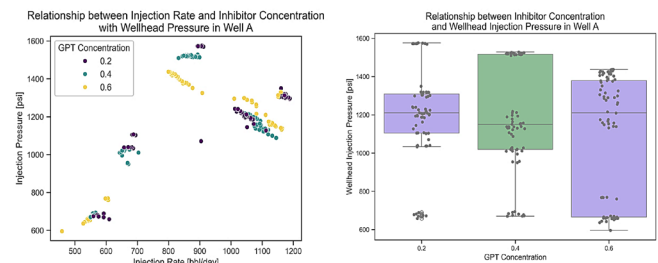


Figure 11. Scatter plot of pressure data in relation to injection rate and inhibitor concentration in the Injector Well A and Pressure variability and dispersion for each concentration used in Injector Well A.

Source: Own elaboration.

Table 11.

Prediction of pressure in Injector Well A using machine learning methods:

Injection Rate [bbl/day]	Inhibitor Concentration GPT	Predicted Pressure [psi]
700	0	1296
700	0.2	933
700	0.6	933

Source: Own elaboration.

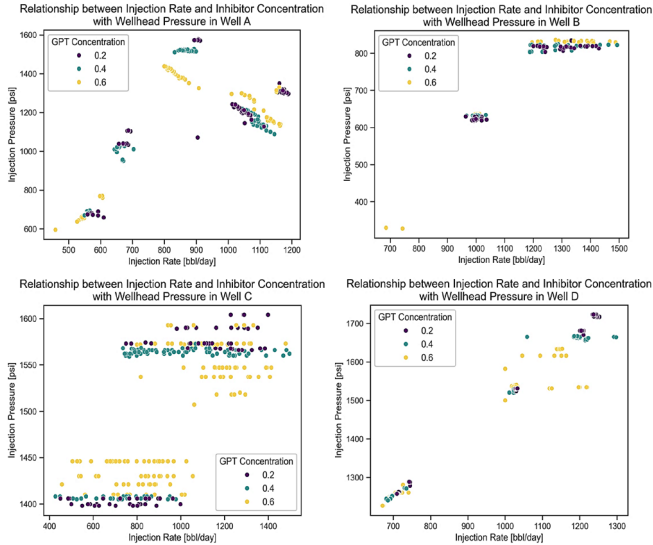


Figure 12. Scatter plot of pressure data considering its relationship with the injection rate and inhibitor concentration in the evaluated wells.
Source: Own elaboration.

Table 12.

Prediction of Injector Well C's injection rate based on operating pressure and different commercial inhibitor concentrations.

Injection Rate [bbl/day]	Inhibitor Concentration GPT	Predicted Pressure [psi]
700	0	1296
700	0.2	933
700	0.6	933

Source: Own elaboration.

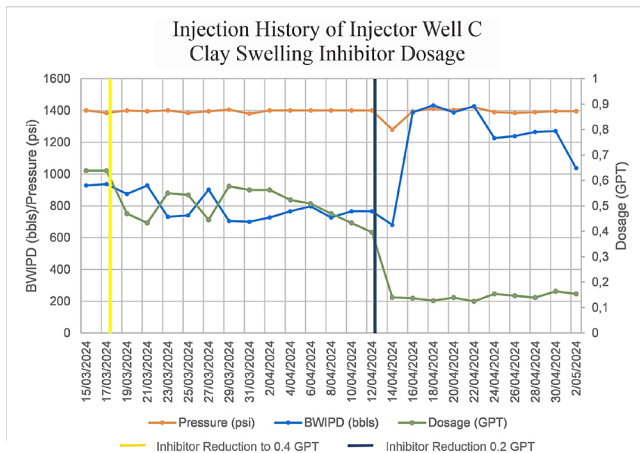


Figure 13. Injectivity history during the follow-up stage of Injector Well C vs. inhibitor concentration.
Source: Own elaboration.

Scatter plots in Fig. 12, show that inhibitor concentration does not affect injectivity in Injector Well B. In Injector Well C, two pressure behaviors are observed: pressure remains constant for injection rates below or near 1000 BWIPD, while at higher rates, pressure increases.

Increasing inhibitor concentration to 6 GPT raises pressure at low rates but reduces it at higher rates. Similarly, in Injector Well D, inhibitor concentration has no effect

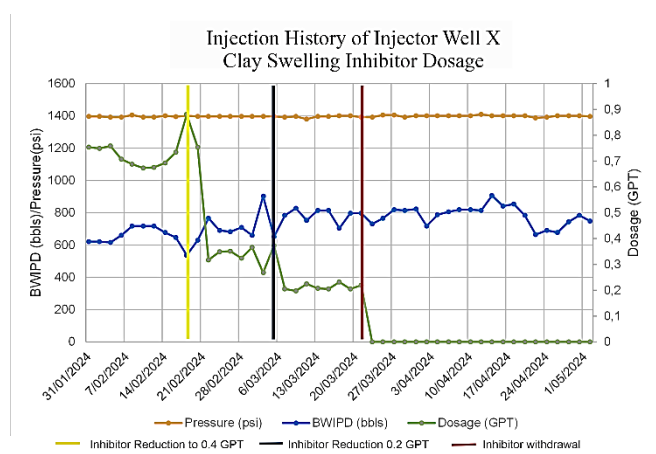


Figure 14. Injectivity history during the monitoring stage of Injector Well X vs. clay swelling inhibitor dosage.
Source: Own elaboration.

below 1000 BWIPD, but at higher pressures, 6 GPT reduces injection pressure. An injection rate prediction was performed for an operating pressure of 1400 psi, which is the controlled variable in Injector Wells C and D.

As shown in Table 12, results indicate that injection rates do not exceed 1000 BWIPD for any inhibitor concentration, with predicted values close to 700 BWIPD at 1400 psi.

4.2 Field Evaluation Follow-Up

A subsequent long-term evaluation of the field's injection wells demonstrated that reducing the inhibitor concentration (Fig. 13) or even eliminating it (Fig. 14) does not significantly affect well injectivity.

This follow-up confirmed that injectivity remains stable without the need for high inhibitor levels, suggesting that the inhibitor's presence is not critical for the continuous performance of injection wells. These findings highlight the feasibility of operational management without relying on inhibitors, enabling cost optimization. In summary, the follow-up phase confirmed the low sensitivity of the inhibitor to injectivity changes and emphasized the viability of operating wells with minimal or no inhibitor concentration without compromising injection efficiency.

5 Conclusions

Once the field test was conducted, it was confirmed that the laboratory results were consistent and that by analyzing the instantaneous variation of injection rates, the sensitivity of the inhibitor to pressure changes in the injection wells could be observed.

The results demonstrate that it is feasible to perform an instantaneous evaluation of the rate-pressure relationship in water injection wells based on the use and/or concentration of the commercial swelling-hydration inhibitor. This suggests that it is possible to operate the wells at lower inhibitor concentrations or even eliminate its dosing in some wells where it does not significantly improve

injectivity, especially at low injection rates. This optimization can lead to significant economic savings and improve the injection performance of the reservoir.

Additionally, some instantaneous pressure increases in the wells may be related to variations in the mechanical conditions of the injection system rather than formation-level plugging, highlighting the importance of strict control over operational conditions.

The field methodology implemented to evaluate the influence of the swelling-hydration inhibitor proved effective in establishing cost-effective injectivity scenarios. This provides a solid basis for well-informed technical decisions to enhance economic efficiency by optimizing inhibitor dosing according to each well's specific needs.

Importantly, this methodology is applicable across different lithological sequences and sample types—both consolidated core samples and fragmented trench samples—since it focuses on identifying clay minerals prone to swelling and hydration in depleted reservoirs where injectivity decline is observed. By detecting minerals with swelling potential, this approach can be applied preventively or correctively in any water injection well where produced water is injected, regardless of the mineralogical arrangement in the rock matrix. Thus, it offers a versatile tool for evaluating and managing clay-related formation damage in a broad range of field conditions.

References

- [1] Abbas, A., Flori, R., AL-Anssari, A., and Alsaba, M., Laboratory analysis to assess shale stability for the Zubair Formation, Southern Iraq. *Journal of Natural Gas Science and Engineering* 56, pp. 315-323, 2018. DOI: <https://doi.org/10.1016/j.jngse.2018.05.041>
- [2] Abbasi, S., Shahrabadi, A., and Golghanddashti, H., Experimental investigation of clay mineral effects on the permeability. *Society of Petroleum Engineers, Art.* 4248, 2011. DOI: <https://doi.org/10.2118/144248-MS>
- [3] Alsaba, M., Al-Marshad, A., Abbas, A., Abdulkareem, T., Al-Shammari, A., Al-Ajmi, M., and Kebeish, E., Laboratory evaluation to assess the effectiveness of inhibitive nano-water-based drilling fluids for Zubair shale formation. *Journal of Petroleum Exploration and Production Technology* 10, pp. 419-428, 2019. DOI: <https://doi.org/10.1007/s13202-019-0737-3>
- [4] Anderson, R., Ratcliffe, I., Greenwell, H., Williams, P., Cliffe, S., and Coveney, P., Clay swelling a challenge in the oilfield. *Earth-Science Reviews*, 98(3-4), pp. 201-216, 2010. DOI: <https://doi.org/10.1016/j.earscirev.2009.11.003>
- [5] API Methylene blue test for drill solids and commercial bentonites. Section 12 in: *API RP 131: Laboratory Testing of Drilling Fluids*, 7th ed., ISO 10416:2002. American Petroleum Institute, 2004.
- [6] API 1998 Porosity determination and permeability determination. sections 5 and 6 in: *API RP 40: Core Analysis*, 2nd ed., American Petroleum Institute, 1998.
- [7] Balaban, R.C., Ferreira, E., and Rodrigues, M., Design of experiments to evaluate clay swelling inhibition by different combinations of organic compounds and inorganic salts for application in water base drilling fluids. *Applied Clay Science*, pp. 124-130, 2015. DOI: <https://doi.org/10.1016/j.clay.2014.12.029>
- [8] Bailey, L., Keall, M., Audibert, A., and Lecourtier, J., Effect of clay/polymer interactions on shale stabilization during drilling. *IFP Langmuir* 10, pp. 1544-1549, 1994. DOI: <https://doi.org/10.1021/la00017a037>
- [9] Bishop, S.R., The experimental investigation of formation damage due to the induced flocculation of clays within a sandstone pore structure by a high salinity brines. Paper presented at the SPE European Formation Damage Conference, The Hague, Netherlands, June 1997. DOI: <https://doi.org/10.2118/38156-MS>
- [10] Cheng, K., and Heidari, Z., A new method for quantifying cation exchange capacity in clay minerals. *Applied Clay Science* 161, pp. 444-455, 2018. DOI: <https://doi.org/10.1016/j.clay.2018.05.006>
- [11] Civan, F., *Reservoir formation damage: fundamentals, modeling, assessment, and mitigation*, 1st ed., Gulf Publishing Company, Houston, Texas, USA, 2000. DOI: <https://doi.org/10.1016/C2020-0-03547-4>
- [12] Ecopetrol., *Reporte integrado de gestión sostenible* [online]. 2015. Bogotá. Available at: <https://www.ecopetrol.com.co/wps/portal/Home/es/ResponsabilidadEtiqueta/InformesGestionSostenibilidad/Informesdegestion>
- [13] Fink, J.K., *Hydraulic fracturing chemicals and fluids technology*. Gulf Professional Publishing, Oxford, UK, 2013. DOI: <https://doi.org/10.1016/C2012-0-02544-6>
- [14] Instituto de Hidrología, Meteorología y Estudios Ambientales (IDEAM), [online]. 2015. *Estudio Nacional del Agua 2014*. Bogotá. Available at: <https://www.ideam.gov.co/sala-de-prensa/informes/Estudios%20nacionales%20del%20agua>
- [15] Karpinski, B., and Szkodo, M., Clay minerals mineralogy and phenomenon of clay swelling in oil and gas industry. *Advances in Materials Science*, 15(1) pp. 37-55, 2015. DOI: <https://doi.org/10.1515/adms-2015-0006>
- [16] Laird, D.A., Influence of layer charge on swelling of smectites. *Appl. Clay Sci.* 34, pp. 74-87, 2006. DOI: <https://doi.org/10.1016/j.clay.2006.01.009>
- [17] Leone, J.A., and Scott, E.M., Characterization and control of formation damage during waterflooding of a high-clay-content reservoir. *Society of Petroleum Engineers - SPE Res Eng.* 3(4), pp. 1279-1286, 1988. DOI: <https://doi.org/10.2118/16234-PA>
- [18] Liu, S., Mo, X., Zhang, C., Sun, D., and Mu, C., Swelling inhibition by polyglycols in montmorillonite dispersions. *Journal of Dispersion Science and Technology* 25, pp. 63-66, 2004. DOI: <https://doi.org/10.1081/DIS-120027669>
- [19] Kleven, R., and Alstad, J., Interaction of Alkali, Alkaline-Earth and Sulphate Ions with clay minerals and sedimentary rocks. *Journal of Petroleum Science and Engineering*, 15(1996), pp. 181-200, 1996. DOI: [https://doi.org/10.1016/0920-4105\(95\)00085-2](https://doi.org/10.1016/0920-4105(95)00085-2)
- [20] Norrish, K., The swelling of Montmorillonite, *Discussions Faraday Soc.*, 18, pp. 120-134, 1954. DOI: <https://doi.org/10.1039/DF9541800120>
- [21] Ramos, N., Cabrera, M., Liberti, I., Cevalco, C., Dibilio, J., Belén, M., y Renta, D., Utilización de ensayos de expansión de arcillas para el análisis de inhibidores en la cuenca del Golfo San Jorge, [online], 2017. Available at: https://www.researchgate.net/publication/318040185_utilizacion_de_ensayos_de_expansion_de_arcillas_para_el_analisis_de_inhibidores
- [22] Sarkisyan, S.G., Origin of authigenic clay minerals and their significance in petroleum geology. *Sedimentary Geology*, 7, pp. 1-22, 1972. DOI: [https://doi.org/10.1016/0037-0738\(72\)90050-4](https://doi.org/10.1016/0037-0738(72)90050-4)
- [23] Valle Medio del Magdalena—Agencia Nacional de Hidrocarburos. [online], 2024. Available at: <https://www.anh.gov.co/es/hidrocarburos/oportunidades-disponibles/procesosde-seleccion/ronda-colombia-2010/tipo-1/valle-medio-del-magdalena/>
- [24] Yang, R., Zhang, J., Chen, H., Jiang, R., Sun, Z., and Rui, Z., The injectivity variation prediction model for water flooding oilfields sustainable development. *Energy*, 189, Art. 116317, 2019. DOI: <https://doi.org/10.1016/j.energy.2019.116317>
- [25] Zhou, Z., Gunter, W.D., Kadatz, B., and Cameron, S., Effect of clay swelling on reservoir quality. *Petroleum Society of Canada*, art. 96-07-02, 1996. DOI: <https://doi.org/10.2118/96-07-02>
- [26] Zhou, Z.J., Cameron, S., Kadatz, B., and Gunter, W.D., Clay swelling diagrams: their applications in formation damage control. Paper presented at the SPE Formation Damage Control Symposium, Lafayette, Louisiana, February, 1996. DOI: <https://doi.org/10.2118/31123-MS>

J.A. Peña-Mateus, received the BSc. Eng in Petroleum Engineering in 2021, the MSc. in Hydrocarbon Engineering in 2024, both from the Universidad Industrial de Santander (UIS), Bucaramanga, Colombia, where her studies focused on geomechanics and molecular dynamics. Between 2023 and 2024, she worked for the Laboratorio de Diagnóstico de Pozo, Escuela de Ingeniería de Petróleos, UIS. Currently, she is involved in energy transition projects at UIS, with a focus on geothermal energy, including topics such as geothermal well integrity, estimation of geothermal gradient, heat flow, and electric power potential based on data from the oil and gas industry.

ORCID: 0009-0004-5182-308X

M.P. Mosquera-González, received the BSc. Eng in Chemical Engineering in 2018 from the Industrial University of Santander (UIS), Colombia. She currently works as a service and laboratory professional at the Well Diagnostics Laboratory, affiliated with the School of Petroleum Engineering. Her research interests include formation damage and reservoir engineering.
ORCID: 0009-0009-6232-707X

F.I. Archer-Martínez, received the BSc. Eng in Petroleum Engineering in 2004 from the Universidad Central de Venezuela, and the MSc. in Petroleum Engineering in 2011 from the IFP School, Rueil-Malmaison, France. From 2004, he worked for consulting companies within the power and O&G sector. Nowadays, he is Chief Operating Officer (COO) y Co-Founder of Bonpland Energy y Chief Executive Officer (CEO) of EOR Wave S.A.S. His research interests include chemical enhanced/improve oil recovery, well stimulation, and numerical reservoir simulation.
ORCID: 0009-0003-3670-064X

E.A. Gómez-Cepeda, received the BSc. Eng in Petroleum Engineering in 2016, and the MSc. in Hydrocarbon Engineering in 2020, all of them from the Universidad Industrial de Santander, Bucaramanga, Colombia. From 2023, he has worked as Extension Laboratories Coordinator of the School of Petroleum Engineering for Universidad Industrial de Santander. Nowadays, he is Chief Executive Officer (CEO) of LOGOZ SAS. His research interests include chemical enhanced/improve oil recovery, reservoir engineering, well stimulation, and numerical reservoir simulation.
ORCID: 0000-0002-4580-3654

Y. Jaimes-Barajas, received the BSc. and MSc. in Chemistry from Universidad Industrial de Santander, Bucaramanga, Colombia. She has worked at Occidental de Colombia since 2004, holding roles such as Laboratory Supervisor, Facilities Engineer, and currently Mechanical Integrity Engineer. Her experience includes produced water treatment, asset integrity, corrosion control, crude measurement, environmental compliance, and risk management in oil and gas operations.
ORCID: 0009-0005-8786-5510

Proposals for improving acoustic comfort at the Be Live Experience Tuxpan hotel

Juan Lázaro Acosta-Prieto^a, Yoel Almeda-Barrios^b, Yosmil Lázaro Peña-Pérez^a & Juan Carlos Peña-Ramírez^a

^a Facultad de Ingeniería Industrial, Universidad de Matanzas, Matanzas, Cuba. acostaprietojuanlazar@gmail.com, yosmil.pena@est.umcc.cu, juan.carlospe@est.umcc.cu

^b Instituto Superior Politécnico do Moxico, Angola. yoelalmedabarrios@gmail.com

Received: July 29th, 2025. Received in revised form: October 1st, 2025. Accepted: October 9th, 2025.

Abstract

This research was carried out at the Be Live Experience Tuxpan hotel due to effects caused by noise. The objective is to design intervention solutions that guarantee regulatory standards for acoustic comfort in the facilities of the Be Live Experience Tuxpan Hotel. Design and modeling tools such as AutoCAD 2021 and SketchUp 2021 were used. The use of absorbent materials and their correct selection constitute the basis for the application of acoustic treatment of premises as a measure for noise control, and to achieve pleasant spaces, both aesthetically and functionally, as well as acoustically. Elements of graphic acoustics were used to propose solutions for noise control in the propagation media. The results showed a reduction in the sound pressure level of up to 11.7 dB in the rooms and a decrease in the reverberation time from 1.33 seconds to 0.089 seconds, complying with regulatory standards.

Keywords: acoustic comfort; design; effects; graphic acoustics; noise.

Propuestas para la mejora del confort acústico en el hotel Be Live Experience Tuxpan

Resumen

La presente investigación se desarrolló en el Hotel Be Live Experience Tuxpan debido a afectaciones provocadas por el ruido. El objetivo es diseñar soluciones de intervención que garanticen los estándares normativos para el confort acústico en las instalaciones del Hotel Be Live Experience Tuxpan. Se emplearon herramientas de diseño y modelación como AutoCAD 2021 y SketchUp 2021. El empleo de materiales absorbentes y la correcta selección de los mismos, constituyen la base para la aplicación del tratamiento acústico de locales como medida para el control del ruido, y lograr espacios agradables, tanto estética y funcional, como acústicamente. Se utilizaron elementos de acústica gráfica para proponer soluciones para el control del ruido en los medios de propagación. Los resultados mostraron una reducción del nivel de presión sonora de hasta 11.7 dB en las habitaciones y una disminución del tiempo de reverberación de 1.33 segundos a 0.089 segundos, cumpliendo con los estándares normativos.

Palabras claves: acústica gráfica; afectaciones; confort acústico; diseño; ruido.

1 Introduction

With the development of society, noise has become one of the factors contributing to environmental pollution. Today, we can speak of noise pollution, which affects human health and the environment, making it necessary to counteract its effects.

In most countries, noise is the most common harmful agent in the workplace. Its presence in industrial activities is

compounded by its widespread use in urban and social environments, especially during leisure activities. This almost universal spread of noise in social and work environments becomes even more significant when considering that hearing damage is irreversible, and that exposure produces other disorders—organic, physiological, and psycho-emotional—that translate into a clear reduction in the quality of life and health of workers [1].

How to cite: Acosta-Prieto, J.L., Almeda-Barrios, Y., Peña-Pérez, Y.L., and Peña-Ramírez, J.C., Proposals for improving acoustic comfort at the Be Live Experience Tuxpan hotel. DYNA, (92)239, pp. 49-55, October - December, 2025.

Various construction companies and businesses have conceived noise reduction as one of the strategies to ensure competitiveness in the market by preserving worker health, customer satisfaction, and environmental integrity paying particular attention to technologies and materials that are capable of keeping noise levels below the standards established in each country, since these factors are currently evaluated by consumers, especially those in demanding markets [2].

Architects and contractors must make a space as aesthetically pleasing and functional as it is acoustically pleasing; this has been framed under the term: architectural acoustics. The design must take into account the acoustic absorption properties of materials to create a desired interior sound environment in the design of buildings, performance halls, recording studios, etc., to achieve favorable moods in a particular enclosed space, which is what is known as acoustic comfort. Acoustic comfort constitutes a state of satisfaction with acoustic conditions, with the opportunity to perform acoustic activities without disturbing other people [3].

In order to comply with this parameter, when designing a work, the materials must be correctly selected according to the purpose and objective of the work. Over time, the materials used in construction have been diversified and improved to achieve better environments, aesthetic, acoustically comfortable, durable and adaptable to the needs of man and the functions for which they are conceived. For the treatment and acoustic conditioning of premises, different types of noise absorbing materials are used, which control interior noises, reverberation time and eliminate echoes; according to the classification of acoustic materials reported in [4], for this research porous absorbent materials (mineral wool panels, polyester fiber) and panel resonators (EchoPanel) were selected, considering their shape, structure and energy absorption coefficient ($\alpha \geq 0.45$) to ensure acoustic comfort in the intervened spaces.

To control the reverberation of a room, it is essential to know the behavior of the materials that form or cover the room, defined by the sound absorption coefficient of the material for the different frequencies of the octave band (63 Hz, 125 Hz, 250 Hz, 500 Hz, 1000 Hz, 2000 Hz and 4000 Hz. [5].

Internationally, each country has its own noise regulations where the admissible limits are established. The most generalized criterion is the exposure limit of 85 dBA. In Cuba, the following standards stand out: NC 26 (2007), NC 871 (2011) and Law 81 of the Environment, related to noise. NC 871 (2011) [6], a reference standard for the evaluation of occupational noise, proposes a maximum permissible of 85 dBA (Leq-noise not constant) and 80 NdB (Criterion N-noise constant). Noise is a disturbing agent of city life, especially in large cities and tourist areas. Noise impacts have become a worldwide inconvenience and its effects are not limited to a specific sphere, but affect a wide range of sectors that is increasing every day; its scope is not limited to the manufacturing industry and other traditional sectors, but also to services.

For indoor spaces such as hotel rooms and restaurants, NC 26:2007 - 'Residential areas and public spaces' - sets stricter limits (e.g., 50 dB(A) for the nighttime period in

bedrooms) than the occupational limits of NC 871:2011. Furthermore, Law 81/97 'On the Environment' provides the legal framework to protect citizens from noise pollution, reinforcing the need for these interventions.

The parameter of acoustic comfort has a significant value in the service sector and specifically in tourism activities where customer satisfaction is a determining factor. This is evidenced by [7], when expressing that acoustic comfort has become one of the main demands for hotel customers.

At present, Cuban tourism is very demanding, demanding privacy, a quiet and silent space where they can rest and disconnect from their daily tasks and the stress of work, so hotels must have acoustic solutions to avoid uncomfortable situations. However, the tourism sector in Cuba faces an environment of noise pollution due to a reality that ranges from problems of technological obsolescence to social indiscipline according to [8]. Many times, the lack of materials, resources and even culture and knowledge, have caused buildings to be destined or conceived for certain purposes, without studying if they comply with all the established quality and safety requirements. The design of hotels and the culture of their workers have a decisive influence on the presence of noise [9].

In addition to the identified structural problems, the proposal is based on decision-making criteria such as the hotel management's interest in improving customer satisfaction, the feasibility of investing in sustainable acoustic solutions, and legal compliance under Environmental Law 81/97 and Cuban regulations NC 26:2007 and NC 871:2011, which is crucial in a competitive tourist destination like Varadero.

The tourist destination of Varadero is one of the most affected by noise. The Be Live Experience Tuxpan Hotel, which has been in operation for 31 years, stands out as one of the most affected by noise pollution. Acoustic measurements made by [10] yielded values of 89.0 dB(A) in the pool snack bar during show hours, 87.3 dB(A) in the Cristal buffet restaurant, 68.5 dB(A) in rooms 313, 315, 317 and 319 during the hours of the La Bamba discotheque, which exceed the normed limits in all cases and have repercussions on the image of the identity. Therefore, this hotel was selected as the object of study of this research.

Hence, the objective was: to design intervention solutions that guarantee regulatory standards for acoustic comfort in the facilities of the Be Live Experience Tuxpan Hotel.

2 Materials and Method

In order to meet the objective of the research, this section presents the procedure to diagnose the acoustic comfort in the affected areas of the Be Live Experience Tuxpan hotel with the purpose of designing feasible solutions with suitable noise absorbing materials. A methodology based on the one proposed by [8] is elaborated, with modifications that allow its application in these spaces.

The characterization of the premises is carried out taking into account the following criteria:

1. Description of the materials covering the premises.
2. Explanation of the activities that take place in each room.
3. Identification of the type of noise and the source.

4. Measurement of existing noise levels using a certified sound level meter, recording continuous equivalent levels (Leq) by frequency.
5. Define permissible noise levels according to NC 871 (2011).
6. Basis of the constructive state of the premises.
7. Explanation of the relationship between the constructive technical condition and the generation of noise.

For the acoustic treatment of premises, the following procedure is proposed, taken from [8], with some modifications given by the inclusion of the calculation of the reverberation time before and after the design as a parameter of effectiveness of the measure.

Step # 1: calculation of reverberation time.

From a search of the expressions for the calculation of the reverberation time, the ones proposed by [11] were detected.

$$Tr = (0.161 * V) / (Atot + 4 * M * V) \quad (1)$$

Where:

Tr: Reverberation time [s]

V: Room volume [m³]

Atot: Total absorption [sabino]

M: Sound attenuation constant in air [m⁻¹].

Sound attenuation in air (M), is calculated as follows:

$$M = \frac{1}{434} \times \gamma \quad (2)$$

Where:

γ : attenuation in air in dB/100 m .

The total absorption is calculated:

$$Atot = \bar{\alpha} \times Stot \quad (3)$$

Where:

$$Stot = \sum Si \quad (4)$$

(Total enclosure area) [m²]

$$\alpha = (\sum \alpha_i \times Si) / Stot \quad (5)$$

(Average absorption coefficient of the enclosure) [sabinos/m²]

α = absorption coefficient of surface “i”

Si = area of surface “i” [m²]

Step # 2: determine the sound pressure level to be attenuated (NR).

$$NR = Lex - Lrec \quad (6)$$

Where:

NR: reduction level [dB].

Lex: existing sound pressure level [dB].

Lrec: recommended sound pressure level [dB].

Step # 3: Determine the material to be used.

$$A2 = St \times \alpha t + Atot - Aat \quad (7)$$

$$\Delta L = 10 \log(A2 / Atot) \quad (8)$$

Where:

A2: equivalent absorption of the room after treatment [sabinos].

St: treated area [m²].

Aat: absorption of the area to be treated before treatment [sabinos].

αt : absorption coefficient required for treatment [sabinos/m²].

In this step, αt is cleared. Its result will tell the material to be selected based on that absorption coefficient.

Step # 4: determine the optimum area to be coated (AOR).

$$AOR = \frac{A2 - Atot}{\alpha r} \quad (9)$$

$$\alpha r = \alpha t - \alpha at \quad (10)$$

Where:

AOR: optimum area to be coated [m²].

αr : reduction absorption coefficient [sabinos/m²].

αat : absorption coefficient of the treated surface material before treatment [sabinos/m²].

The AOR determines the amount of m² that need to be coated with the selected material to comply with the NR.

Highlight in this case that:

When performing the calculation of A2 and Atot all objects in the room must be taken into account.

The absorption coefficient of open windows and doors is 1 sabino/m².

One person absorbs approximately 0.57 sabinos/m².

Step # 5: recalculation of the reverberation time.

Step # 6: calculation of the decrease in reverberation time.

$$\Delta RT = RTa - RTd \quad (11)$$

Where:

ΔRT : decrease in reverberation time [s].

RTa: reverberation time before treatment [s].

RTd: reverberation time after treatment [s].

The software used for the plan and 3D design of the rooms are AutoCAD and SketchUp, both in their 2021 version.

3 Results

Based on the proposed methodology, the areas identified as critical by [10] were characterized. For a clear and systematic comparison, Table 1 consolidates the initial acoustic conditions of each intervened area.

As evidenced in Table 1, all areas studied exhibited sound pressure levels that exceeded the permissible limits established by NC 871:2011, confirming the impact of noise pollution. It should be noted that, although the construction condition of the premises is good, the lack of specific insulating and absorbent elements limits their ability to guarantee acoustic comfort. Furthermore, the reverberation time (Tr) in the rooms (1.33 s) significantly exceeds the value

Table 1.

Comparative acoustic characterization of the study areas prior to the intervention.

Variable	Rooms 313, 315, 317, 319	Snack-bar Pool	Buffet Restaurant Glass
Covering Materials	Concrete walls, sliding door with acoustic duplex glass, concrete ceiling, ceramic floor.	Concrete walls, wooden plateau, tile ceiling with plasterboard false ceiling, columns and wooden beams, ceramic floor.	Concrete walls, glass walls with metal edges, concrete columns, tiled countertops, plasterboard false ceiling, ceramic slab floor.
Function	Standard room (max. 2 clients).	Service of drinks and snacks.	Buffet service (breakfast, lunch, dinner). Handling of crockery/cutlery, verbal communication, kitchen area noise (non-constant).
Noise Source & Type	La Bamba discotheque (non-constant). Located below the rooms.	Audio amplification equipment during shows (non-constant).	
Permissible Level (dB(A))	50	70	50
Existing Level (dB(A))	68.5	89	87.3
Tr Before (s)	1.33	0.26	0.63
Construction Condition	Good	Good	Good

Source: own elaboration.

recommended for residential spaces (<1 s), which worsens noise perception and affects sleep quality.

3.1 Rooms 313, 315, 317 and 319

Covering materials: Enclosed space. Concrete walls, sliding door to the balcony of acoustic duplex glass, concrete ceiling, ceramic floor.

Function: Standard room with a maximum capacity of 2 clients per room.

Type of noise and source: Non-constant noise, which attacks the tranquility and disturbs guests' sleep, caused by the La Bamba discotheque that operates at night from 11:00 pm - 4:00 am, only on Saturdays, and provides services to both hotel guests and external clients. The discotheque is located below these rooms, and the vibrations and sounds are highly perceptible.

Permissible noise levels according to NC 871 (2011): 50 dB

Existing noise levels: The affected frequencies are: 250, 500, 1000 and 2000 Hz with 60 dB, 72 dB, 73 dB respectively. (Most affected rooms 317 and 319). Equivalent continuous noise level: 68.5 dB (A) at La Bamba time.

Construction condition: Good.

Relationship between technical construction condition and noise generation: Despite the building's good technical construction condition, the lack of sound-insulating elements limits its ability to guarantee acoustic comfort.

3.2 Snack-bar pool

Covering materials: Open space outdoors. Concrete walls, wooden plateau, tile ceiling with false ceiling of plasterboard (poorly placed and without acoustic absorbing elements), columns and wooden beams, ceramic floor.

Function: Service of drinks and snacks to take away or enjoy on site.

Type of noise and source: Noise not constant. Recreation with audio amplification equipment in the show area is a source of noise that directly affects the acoustic comfort of the pool snack bar during show and entertainment hours.

Permissible noise levels according to NC 871 (2011): 70 dB(A)

Existing noise levels: The affected frequencies are: 125, 250, 500, 1000, 2000 and 4000 Hz with 72 dB, 80 dB, 85 dB, 87 dB, 85 dB and 74 dB respectively. Equivalent continuous sound level: 89 dB(A).

Construction condition: Good.

Relationship between technical construction condition and noise generation: Although the building is not in a bad technical construction condition, it does not have enough insulating construction elements or good acoustic absorbers, so it does not respond to the activity it performs with the most adequate and comfortable environment that should be ensured to the client.

3.3 Buffet restaurant Glass

Covering materials: Enclosed space. Concrete walls, glass walls with metal edges, concrete columns and walls, tiled countertops, false ceiling of plasterboard, ceramic slab floor.

Function: Buffet service for breakfast, lunch and dinner.

Type of noise and source : Non-constant noise. Handling of crockery and cutlery, verbal communication of customers and the kitchen area whose access is located near the service tables affect the acoustic comfort of the premises.

Permissible noise levels according to NC 871 (2011): 70 dB.

Existing noise levels: The affected frequencies are: 250, 500, 1000, 2000 and 4000 Hz with 74 dB, 83 dB, 93 dB, 90 dB and 86 dB respectively. Equivalent continuous sound level: 87.3 dB(A)

Construction condition: Good.

Relationship between technical construction condition and noise generation: Despite the building's good technical construction condition, the lack of sound-insulating elements limits its ability to guarantee acoustic comfort.

After a study of the different surfaces existing in the area under study, their area and the absorption coefficient of each material, a summary of the results of the calculated reverberation time index is shown in Table 2.

Table 2.

Results of the reverberation time index (Tr).

Areas under study	Result of the index Tr (s)
Rooms 313,315,317,319	1.33
Snack-bar pool (show area)	0.26
Buffet restaurant Glass	0.63

Source: own elaboration.

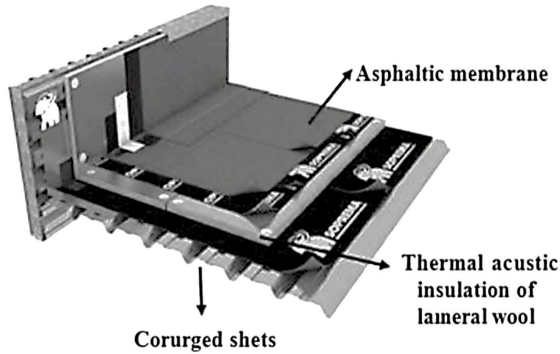


Figure 1. Deck cover for La Bamba nightclub.
Source: own elaboration based on Sketchup 2021 software.

The recommended reverberation times for these premises (residential type building) should be less than 1, but not all the reverberation times obtained in the calculation comply with this condition. In the rooms under study, 1.33 seconds are necessary for the sound pressure level to decrease by 60 db after the noise emission ceases.

Based on the elements analyzed, proposed solutions for noise control of the affected premises are designed.

3.4 Control solution at La Bamba discotheque

To directly control the noise coming from inside La Bamba, a Deck roof is proposed (Fig. 1), on top of the corrugated tiles that make up the exterior roof of the discotheque. This roof will be composed of the existing corrugated tiles, on top of a thermal and acoustic insulation panel of mineral wool covered by a waterproof asphalt blanket. The thermal and acoustic panel will not only act as sound insulation, but will also control the heat from the sun, which hits the roof all day long, so that it does not penetrate the interior of the building and keeps it cool. The drainage of the roof will be with downspouts.

3.5 Control solutions in rooms 313, 315, 317, 319

For the acoustic solution in the rooms located near the discotheque:

Decorative walls with acoustic panels will be placed. On the wall behind the bed, an acoustic panel in the form of mosaic tiles, made of fabric, model CM30E/CM60E/CM120E with an absorption coefficient of 0.8 will be used. The wall in front of the bed will be covered with EchoPanel Empire type panel, composed of polyethylene terephthalate (PET), which is a type of plastic commonly used in containers and bottles, with very good properties of resistance to wear, chemicals, and is fully recyclable, with an absorption coefficient of 0.45.

The back of the bed will be replaced with a wooden headboard.

The chest of drawers will be replaced with a multifunctional wooden cabinet (dresser-luggage cabinet-minibar).

Black out curtains and a net curtain will be installed, which will act as a filter for noise coming from the outside, dampen sound inside the room and control the penetration of daylight.



Figure 2. Design proposal for rooms 313,315,317,319.
Source: own elaboration based on Sketchup 2021 software.

Four sliding windows will be placed on the balcony. This will enable a double filter for the penetration of external noise; if the client wishes, he can keep it open or close it in case the noise bothers him during the discotheque hours.

The above proposals were modeled in Sketchup 2021 software for a more realistic visualization of the results (Fig. 2).

3.6 Control solutions in the pool snack bar

For the acoustic solution of the pool snack bar located in front of the show area:

The design of the false ceiling will be changed to plasterboard, with a central area of false cassette ceiling, made of Cement Board perforated acoustic panel, model Sound BC A-8-15-20. It is a perforated laminated gypsum board, ideal for a multitude of interior applications, cladding, ceilings and partitions. Its dimensions: 2400 mm x 1200 mm, thickness: 12.5 mm and absorption coefficient: 0.8.

Absorbent panels will be placed on the walls of the EchoPanel Frequency model, composed of polyethylene terephthalate (PET). It is recyclable, available in a wide range of neutral, mid-tone and vibrant colors, dowelable, durable, lightweight and easy to cut and install, making it ideal for a multitude of interior applications. Available in 7mm, 12mm and 24mm thicknesses. Its dimensions: 2800mm x 1200mm, thickness: 12mm and absorption coefficient: 0.45.

The plateau and the wall behind it will be covered with IdeaTEC model wood slatted panels; these are slotted panels, separated between pieces, which will help reduce noise and reverberation.



Figure 3. Design proposal for the pool snack bar.
Source: own elaboration based on Sketchup 2021 software.

Dimensions: 1800x600x44mm. Slats of 22(A) x45(B) mm. With separation of 41(C) mm.

Absorption coefficient: 0.8.

Fig. 3 shows the design proposal for the pool snack bar.

3.6 Control solutions in the Cristal buffet restaurant

For the acoustic solution of the Cristal buffet restaurant:

Decorative walls with EchoPanel Frequency acoustic panels will be installed.

A false coffered ceiling will be installed with perforated acoustic panels made of Cement Board, model Sound BC A-8-15-20.

Acoustic totems will be installed as column-shaped elements that function as acoustic absorbers, divide spaces and are aesthetically attractive. Echo Panel Hanging Pendants panels, made of polyethylene terephthalate, were selected for this purpose. It is a space-dividing system, including pendants, freestanding room dividers and workstation screens.

These products allow open plan spaces, typical of modern work and hospitality environments, to be divided with ease and flexibility while reducing reverberant noise to improve both comfort and productivity. It is recyclable, available in a wide range of neutral, mid-tone and vibrant colors. Available in 7mm, 12mm and 24mm thicknesses.

Dimensions: 2400mm x 1200mm

Thickness: 12mm

Absorption coefficient: 0.45

Furniture design will be changed to textile and sponge chairs.

Common wood coverings will be replaced by IdeaTEC pine wood panels and polyester fiber.

The previous proposals were modeled in Sketchup 2021 software for a more realistic visualization of the results.

Then, the materials and coatings that will make up the new proposals are related, with their absorption coefficients, to obtain the total absorption of the enclosure after the proposed treatment, and the recalculation of the reverberation times, in order to compare the effectiveness of the changes made in the design.

Table 3 below shows the comparison of parameters and noise levels before and after the proposed treatment.

Table 3.
Comparison of acoustic parameters before and after treatment.

Parameters	Rooms 313,315,317,319	Snack- bar pool	Buffet restaurant Glass
Absorption of the room before treatment (A1) [m ²]	7.08	44.17	265.29
Absorption of the room after treatment (A2) [m ²]	104.8	175.1	539.44
Tr before [s]	1.33	0.26	0.63
Tr after [s]	0.089	0.058	0.019
Decrease in Tr (ΔRT) [s]	1.23	0.2	0.61
SPL before [dB]	68.5	89	87.3
Decrease in SPL (Δ) [dB]	11.7	6.0	3.5
SPL after [dB]	56.8	83	83.8

Source: own elaboration.

4 Discussion

The tourist destination of Varadero is one of the most affected by noise. Recent research by [8,9,12] proved by measuring sound pressure levels, the existence of noise pollution in certain hotel premises in the tourist pole, in which the most affected areas were reflected in noise maps and coincided with the highest number of complaints reported by customers.

The relevance and scientific novelty of the research in this sense lies in:

The conception of a research that values the analysis of acoustic comfort as an element to be highlighted within the influences on customer satisfaction in the hotel tourism sector.

The use of graphic acoustics for the design of noise control solutions to improve acoustic comfort conditions in tourism facilities, specifically in the Be Live Experience Tuxpan hotel.

The implementation of a group of methodologies that have a novel character in the context of tourism to solve problems related to acoustic comfort.

The calculation of the material absorption coefficients to be used for the diagnosis of the premises of the hotel under study to reduce or eliminate noise levels in tourism facilities and its application in the affected premises of the Be Live Experience Tuxpan hotel.

The analysis of acoustic comfort in the premises of the Be Live Experience Tuxpan hotel reveals the critical importance of designing effective interventions to mitigate noise, especially in a tourist environment where customer welfare is paramount. The results obtained reflect a significant reduction in sound pressure levels (SPL) and a considerably lower reverberation time (Tr) after the implementation of the proposed solutions, aligning with the recommendations of the international literature on acoustic control in similar spaces.

The literature on acoustic design in residential and commercial environments supports the need for adequate sound absorption to ensure occupant comfort. According to [13], optimal reverberation times for lodging premises, such as hotel bedrooms, should be kept below 1 second to avoid noise buildup and interference in verbal communication. In this study, the rooms evaluated had an initial Tr of 1.33 seconds, which exceeds the recommendations. However, the interventions implemented were able to reduce the Tr to 0.089 seconds, meeting the recommended comfort standards. The approach adopted at the Be Live Experience Tuxpan hotel, based on proven methods for sound control and the use of sustainable materials, not only provides a more compassionate and efficient acoustic environment, but also aligns the project with best practices in modern architectural design. This type of innovation can serve as a model for future interventions in similar spaces, promoting a balance between comfort, aesthetics and environmental sustainability.

The significant reduction in SPL, with variations of up to 11.7 dB in the guest rooms, 6.0 dB in the snack bar and 3.5 dB in the restaurant, demonstrates that the proposed modifications not only meet comfort requirements, but also

improve the overall sound experience for guests. This correlation suggests that taking care of acoustic details can result in higher guest satisfaction and thus better ratings for the hotel.

The implementation of a comprehensive acoustic design that encompasses both internal noise control and the prevention of noise transmission from the outside is a novel approach that, to our knowledge, has not been sufficiently explored in the local literature. The use of the SketchUp 2021 tool to model acoustical solutions prior to implementation is another contribution that allows the potential impact of modifications to be visually assessed. This method can serve as a model for future studies and projects, making it easier for designers and architects to visualize and justify proposed acoustic interventions.

5 Conclusions

On the basis of the literature consulted, it was possible to define the main characteristics and parameters for measuring and controlling noise, as well as the related legal framework, and the application of various absorbent materials and methods for its control. The proposed methodology and its deployment procedures for noise management that integrate: the characterization of the premises, the inclusion of acoustic comfort criteria in the evaluation processes based on the levels and indexes established by NTP 503:1998, and a series of control methods selected for application in the facilities affected by noise. The solutions designed for the control of noise in the propagation media and the results presented before the before-after comparison, allow concluding that the objective of the research was met, from the implementation, modeling and/or estimation of the proposed control measures in three noisy areas of the hotel under study, the decrease of the NPS that influenced the rest and satisfaction of customers, as well as improvements in the acoustic comfort parameters. The selection of materials such as mineral wool, polyester fiber (PET), and perforated gypsum board was based not only on their acoustic performance but also on their availability and growing use in the Cuban construction and tourism markets. Their properties, such as recyclability (in the case of PET panels) and local manufacturing potential, make them viable and sustainable options for similar projects in the country's hotel infrastructure.

References

- [1] Carrillo, M., et al., Reducción de ruido industrial en un proceso productivo metalmeccánico: aplicación de la metodología DMAIC de Lean Seis Sigma. *Entre ciencia e ingeniería*, 15(30), pp. 41-48, 2021. DOI: <https://doi.org/10.31908/19098367.1819>
- [2] Mazo-Bermudez, J.C., Atenuación del impacto del ruido causado por actividades de construcción en especies de fauna, caso: ampliación de la frontera urbana del sector Pance de la ciudad de Cali, Colombia, 2021.
- [3] Villegas-Solis, M.A., Análisis del confort acústico en espacios de lavado textil con principios de Neuroarquitectura. Caso de estudio:

lavadora Alexander, Universidad Tecnológica Indoamérica, Pelileo-Ambato, Ecuador, 2024.

- [4] Segura-Alcaraz, M.P., Empleo de textiles en aplicaciones de absorción sonora, Universitat Politècnica de València, España, 2021. DOI: <https://doi.org/10.4995/Thesis/10251/159786>
- [5] Echeverri, C., Evaluación y control del ruido. Ediciones de la U, 2024
- [6] NC 871:2011 Seguridad y salud en el trabajo-ruido en el ambiente laboral-requisitos higiénico sanitarios generales. Oficina Nacional de Normalización, La Habana, Cuba, 2011.
- [7] Campos-Díaz, Y.I., Reyes-Chapman, B., and Sánchez-Espinosa, Y., Diseño de procedimiento para la gestión de ruido en empresas productivas cubanas. *Ciencias Holguín*, 28(3), pp. 1-9, 2022.
- [8] Almeda-Barrios, Y., et al., Tecnología para la gestión de ruido en hoteles de sol y playa en Varadero, Cuba. *Ergonomía, Investigación y Desarrollo*, 4(3), pp. 99-113, 2022. DOI: <https://doi.org/10.29393/EID4-27TGAB40027>
- [9] González-González, L., Estudio de ruido en el hotel Iberostar Varadero, Facultad de Ciencias Empresariales, Universidad de Matanzas, Cuba, 2020.
- [10] Perdomo-Hector, A., Estudio de ruido en el Hotel Be Live Experience Tuxpan, Facultad de Ciencias Empresariales, Universidad de Matanzas, Cuba, 2019.
- [11] Pacheco-Molina, A., Casalin-Maza, Y., and Troncoso-Palacio A., Evaluación teórica del tiempo de reverberación en un aula de enseñanza. *Boletín de Innovación, Logística y Operaciones*, 5(1), pp. 160-169, 2023. DOI: <https://doi.org/https://doi.org/10.17981/bilo.5.1.2023.16>
- [12] González-Falcón, M., Estudio de ruido en el Hotel Meliá Marina Varadero, Facultad de Ciencias Empresariales, Universidad de Matanzas, Cuba, 2019.
- [13] Andrade-Aguilar, V.C., and Gárate-Shinin M.E., La acústica aplicada en el diseño interior de instituciones para niños y niñas sin hogar. Hogar Infantil Tadeo Torres. [en línea], Universidad del Azuay, Cuenca, Ecuador, 2021. Disponible en: <https://dspace.uazuay.edu.ec/handle/datos/10958>

J.L. Acosta-Prieto, is a BSc. Eng. in Industrial Engineer from the University of Matanzas, Cuba, graduated with a degree and scientific merit award. MSc. in Ergonomics and Occupational Health and Safety and MBA, Service Management module. PhD in Technical Sciences of Industrial Engineering in the research line of Cognitive Ergonomics. In 2021 he obtained the CITMA National Award as a student researcher, in 2021 the Seal of Future Shapers. In 2020 he was Vice-Dean of the Faculty of Business Sciences of the University of Matanzas, Cuba, from 2021-2023. Director of the Municipal University Center of Cárdenas, and from 2023-2024 Director of Research and Postgraduate Studies of the University of Matanzas. ORCID: 0000-0003-1390-2380.

Y. Almeda-Barrios, is Bsc. Eng. in Industrial Engineer from the University of Matanzas, Cuba. MSc. in Ergonomics and Occupational Health and Safety and MBA, Service Management module. PhD in Technical Sciences of Industrial Engineering. Actually, he is professor at Instituto Superior Politécnico do Moxico, Angola. ORCID: 0000-0002-8791-5830.

Y.L. Peña-Pérez is a student of Industrial Engineering at the University of Matanzas, Cuba. He is a member of the scientific group Ergoseg of the University of Matanzas, which develops research on ergonomics and its different dimensions. ORCID: 0009-0005-3825-6292.

J.C. Peña-Ramírez is a student of Industrial Engineering at the University of Matanzas, Cuba. He is a member of the scientific group Ergoseg of the University of Matanzas, which develops research on ergonomics and its different dimensions. ORCID: 0009-0003-9649-0058.

ADKT: a support tool for reducing architectural knowledge evaporation in software projects

Santiago Hyun-Dorado^a, Julio Ariel Hurtado-Alegría^a, Enrique Moguel^b & Jose Garcia-Alonso^b

^a *Facultad de Ingeniería Electrónica y Comunicaciones, Universidad del Cauca, Popayán, Colombia. santiagodorado@unicauca.edu.co, ahurtado@unicauca.edu.co*

^b *Quercus Software Engineering Group, Universidad de Extremadura, Cáceres, España. enrique@unex.es, jgaralo@unex.es*

Received: April 4th, 2025. Received in revised form: September 25th, 2025. Accepted: October 9th, 2025.

Abstract

Defining software architecture is a complex task that demands technical expertise and business knowledge. Design decisions drive architectural structures throughout development and maintenance. However, this knowledge often dissipates over time, a phenomenon known as architectural knowledge evaporation, leading to increased costs and maintenance difficulties. This paper presents ADKT, a support tool designed to mitigate architectural knowledge evaporation by enabling the documentation and traceability of design decisions. ADKT was evaluated through a case study involving software engineers of different expertise levels. The evaluation assessed the tool's ease of use, perceived usefulness, and effectiveness in reducing knowledge evaporation. Results indicate that participants found ADKT easy to use and valuable for preserving architectural knowledge. Nonetheless, challenges remain regarding engineers' commitment to consistently documenting decisions and the need for a designated person to oversee this process. These findings highlight the importance of developing advanced tools and fostering a culture of documentation within development teams.

Keywords: architectural design decisions; software architecture; documentation and traceability; software maintenance; architectural knowledge evaporation.

ADKT: una herramienta para la reducción de la evaporación del conocimiento arquitectónico en proyectos software

Resumen

Definir la arquitectura de software es una tarea compleja que exige experiencia técnica y conocimiento del negocio. Las decisiones de diseño impulsan las estructuras arquitectónicas durante el desarrollo y mantenimiento. Sin embargo, este conocimiento a menudo se disipa con el tiempo, un fenómeno conocido como evaporación del conocimiento arquitectónico, lo que genera mayores costos y dificultades de mantenimiento. Este artículo presenta ADKT, una herramienta de apoyo diseñada para mitigar la evaporación del conocimiento arquitectónico al permitir la documentación y trazabilidad de decisiones de diseño. ADKT fue evaluado mediante un estudio de caso con ingenieros de software de distintos niveles de experiencia. La evaluación analizó la facilidad de uso, utilidad percibida y efectividad de la herramienta para reducir la evaporación del conocimiento. Los resultados indican que los participantes encontraron ADKT fácil de usar y valioso para preservar el conocimiento arquitectónico. No obstante, persisten desafíos en el compromiso de los ingenieros para documentar decisiones de manera constante y la necesidad de una persona encargada de supervisar este proceso. Estos hallazgos destacan la importancia de desarrollar herramientas avanzadas y fomentar una cultura de documentación en los equipos de desarrollo.

Palabras clave: decisiones de diseño arquitectónico; arquitectura de software; documentación y trazabilidad; mantenimiento de software; evaporación del conocimiento arquitectónico.

1 Introduction

Software architecture plays a critical role in the development and evolution of software systems. It

encompasses the fundamental structure of a system, defining its components, their relationships, and the guiding principles governing their design and evolution [1]. Architectural design decisions (ADDs) are central to this process, as they

How to cite: Hyun-Dorado, S., Hurtado-Alegría, J.A., Moguel, E., and Garcia-Alonso, J., ADKT: a support tool for reducing architectural knowledge evaporation in Software projects DYNA, (92)239, pp. 56-65, October - December, 2025.

encapsulate the rationale behind the selection of specific patterns, technologies, and organizational structures that shape the software system [2,3].

Despite their importance, ADDs are often poorly documented or entirely omitted from system artifacts [4]. This results in architectural knowledge evaporation, a phenomenon where the rationale and context behind architectural decisions are lost over time [5]. This loss can severely impact software maintainability, increase costs, and hinder future development, as teams struggle to understand the reasons behind existing architectural choices [3,6].

The problem is exacerbated in agile and fast-paced development environments, where teams prioritize rapid delivery over extensive documentation [5,7]. Consequently, architectural decisions are frequently communicated informally through verbal discussions, chat messages, or emails, leaving no traceable record [8]. As the project progresses, team members change, and the context surrounding past decisions dissipates, making it challenging to evolve the architecture without risking architectural drift or degradation [9].

Existing approaches to address architectural knowledge evaporation include both reactive and proactive methods. Reactive approaches focus on mining ADDs from existing artifacts, such as code repositories, emails, and task management systems [10,11]. Proactive methods aim to capture ADDs in real-time through tools like design wikis, decision logs, and chatbots. While these solutions offer valuable contributions, they often lack a unified structure for documenting and tracing ADDs across diverse software artifacts [12].

This work introduces ADKT, a support tool designed to reduce architectural knowledge evaporation by enabling the systematic capture, traceability, and management of ADDs throughout the software development lifecycle. ADKT provides a standardized data model to document ADDs and their relationships with system artifacts, ensuring that architectural knowledge remains accessible and up to date. The tool was validated through a case study with professional software engineers, assessing its ease of use, perceived usefulness, and impact on knowledge preservation.

The rest of the paper is organized as follows: Section 2 reviews related work on architectural knowledge management and traceability. Section 3 presents the ADKT tool and its underlying data model. Section 4 describes the case study methodology and evaluation process. Section 5 discusses the results and their implications. Finally, Section 6 concludes with reflections on the tool's effectiveness and future research directions.

2 Background

The concern about architectural evaporation is not new, and numerous authors have attempted to address it from different angles, some through automated means, others manually. In a previous study [8], we investigated trends to understand the current state of research on approaches for mapping ADDs and how they connect with the various software artifacts involved in the development process. To this end, we conducted a systematic mapping study (SMS) of

the literature, following the method by [13], in which the search string, research questions, inclusion and exclusion criteria were defined, and 34 relevant articles were analyzed. The study concludes that most efforts are focused on reactive approaches for developing software tools driven by artificial intelligence (AI) to extract architectural knowledge from sources such as technical documentation, communication tools, source code, and task management systems. This study underscores the importance of preserving this knowledge to mitigate AK evaporation and future architectural erosion, although it also highlights limitations such as subjectivity in determining relevant elements, artifacts, and ADDs, as well as challenges in validating the proposed approaches.

From this first study, some papers of interest in the scope of this paper were extracted. An example of these reactive approaches for AK preservation is presented by [5], where the challenges of Architectural Knowledge Management in the context of global agile software development are discussed. A concept called AK condensation is introduced to reduce the evaporation of AK stored in Unstructured Textual Electronic Media (UTEM) records. This concept was implemented through a prototype known as ArchiKCo, which includes mechanisms for classifying and searching AK. To evaluate the effectiveness of AK condensation, studies were conducted with professional developers and students, showing promising results in retrieving AK from UTEM records. This is an innovative approach because it allows obtaining architectural knowledge from sources familiar to developers; however, it is limited to a restricted set of technologies such as Skype and Windows. Additionally, the collected information lacks a well-defined structure for ADDs, which could lead to finding knowledge that is not architecturally relevant.

In another vein, [14] suggest a more proactive method with a framework to simplify the real-time recording of software design decisions using instant messaging tools and chatbots commonly used by developers. The core proposal is to integrate a chatbot that guides developers in systematically documenting design decisions through natural language processing (NLP). This chatbot collects information in a data template, stores it in a structured database, and later exports it to a wiki using markdown and version control for future reference. However, there is no option to modify or delete archived decisions, the NLP does not effectively detect synonyms or duplicates, the structure of the decisions is linear with no linking between them, and no empirical user study has been conducted to evaluate its perceived usefulness by professionals. It is restricted to a specific set of technologies, and although it has a defined structure for documenting ADDs, it does not facilitate traceability between them or linking with related software artifacts.

Similarly, [15] present KnoCap, an idea consisting of a note-taking tool with a physical button to record design decisions in the form of voice notes during whiteboard meetings. The goal is to facilitate the capture of design decisions during meetings without distracting attendees from their primary function. They have also developed a web application that allows users to access and review recorded voice notes along with automatically generated transcripts. At the time of writing the article, the proposal includes only

the fundamental aspects. This approach could disrupt the flow of meetings due to the need to record important parts, and it is often challenging to reconstruct what was discussed without additional notes, images, or a visible whiteboard, leading to significant loss of knowledge about decisions and architecture. As with other methods, decisions are not recorded in a well-defined format or structure.

Subsequently, the same authors [16] improves KNOCAP, a set of tools for capturing and delivering important design bits (IDBs) from whiteboard meetings. This proposal incorporates lightweight interfaces for designers to highlight crucial audio segments during meetings, intelligent storage of IDBs through voice recognition, indexing and classification of contribution types, and delivery of relevant previous IDBs for future meetings through reactive conversational agents for queries and proactive agents to suggest pertinent IDBs. Among the main contributions are new capture interfaces, advanced IDB storage techniques, and delivery mechanisms through conversational agents. Challenges include the subjective identification of "important" information, avoiding overwhelming designers with excessive suggestions, developing effective dialogue models, and robust language processing capabilities.

Considering the above, there is a lack of a well-defined structure that can be used by different methods as a basis for representing and tracing these ADDs among the various artifacts generated in software development and the decisions themselves, as well as the possibility of collecting this information independently of the relevant source for each author through a common interface. Traceability, in general terms, is the ability to link each component, decision, or change within a system to the requirements, constraints, or prior decisions that support them [17]. This process allows understanding how and why the system was developed in a specific way, providing a solid foundation for impact analysis and change management. In software architecture, traceability encompasses both ADDs and the artifacts produced, such as models, diagrams, documentation, source code, and other elements mentioned that are fundamental for evaluating the coherence between the architecture and quality goals [12]. This is especially relevant when the system must adapt to new demands or changing conditions, as traceability helps identify affected design elements, promoting controlled evolution of the architecture.

Although there are numerous methods for extracting this AK from various sources, there is still no common standard that ensures adequate traceability of ADDs and software artifacts, resulting in the continuous erosion of software architectures, AK evaporation, and additional efforts by development teams to make informed decisions for system evolution. Next, a complementary proposal to existing studies and its subsequent validation through a case study is presented.

3 ADKT: a tool for tracing architectural design decision knowledge

ADKT is presented as a simple initiative to unify and strengthen the efforts of various authors in mitigating

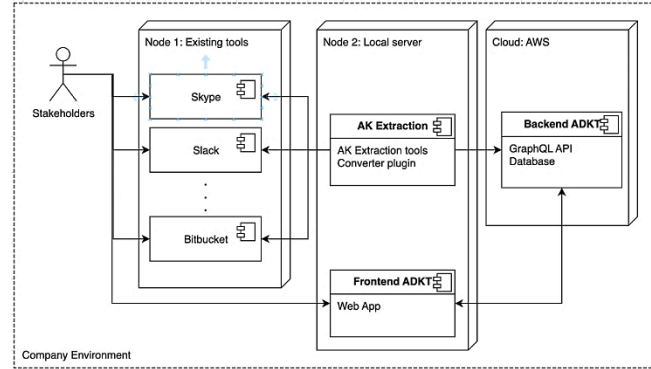


Figure 1. Proposed architecture for the capture from different sources
Source: Own elaboration

architectural knowledge evaporation, a phenomenon previously mentioned that is characterized by the gradual loss of crucial information about ADDs throughout the software lifecycle.

In its initial conception, ADKT was designed as a model to efficiently capture and manage relevant information linked to ADDs. However, its scope expanded upon recognizing the importance of the artifacts generated and used during the software development process. This ensures comprehensive traceability of architectural decisions, linking them to system components and key stakeholders involved, such as developers, software architects, and other interested parties.

The fundamental pillars on which ADKT is built are:

- **Interdisciplinary Collaboration:** Promotes cooperation between authors and teams, fostering a shared vision of the problem.
- **Consensus on Traceability Structure:** Defines a common and standardized structure for documenting, relating, and tracing ADDs coherently.
- **Extensibility through Plugins:** Facilitates the integration of additional plugins to extend the tool's functionality, adapting it to various business contexts and specific needs.

One of the main advantages of ADKT lies in its simplicity, making it accessible to both technical and non-technical teams. Additionally, its ease of integration allows for implementation in any business environment, regardless of size or complexity. This makes it a flexible and practical solution, capable of addressing the challenges associated with managing and preserving architectural knowledge in the software industry.

Below, in the following sections, the ADKT proposal is detailed in descending order of abstraction level: the architecture and its components, implementation aspects, and finally, the defined data model. In Fig. 1, the elements that make up the architecture and their interrelationships can be observed, followed by a detailed description of each.

3.1 Node 1 - existing tools

It represents the execution environment where all the programs commonly used by the stakeholders (analysts, designers, developers, architects, sponsors, managers, or anyone else with an interest in the development of the

project) run, including communication tools such as Slack, WhatsApp, Email, Skype or others; task management tools such as Jira, Trello, Excel, etc; the source code itself hosted on GitHub, GitLab, Bitbucket and others version control systems, technical documentation in Figma, Prototypes, Word, Confluence, Docs, among others.

3.2 Node 2 – Local server

This node represents the execution environment within development organizations where programs developed for extracting and documenting ADDs are executed.

3.2.1 AK extraction

Represents the development of various systems for extracting ADDs from existing tools. As mentioned in the background section, task management tools like Jira, communication tools like Skype, Slack, source code, code repositories like GitHub, Bitbucket, technical documentation, UML, requirements, etc., are frequently used as data sources for extracting ADDs using artificial intelligence techniques

3.2.2 Converter plugin

Additionally, each company can develop an additional subcomponent integrated with the AK extraction systems, responsible for formatting the data to the model proposed in this work to load ADD information into the ADKT Backend, aiming to have a record of these decisions in a common database and allow them to be queried in a single system by different stakeholders.

3.2.3 Converter plugin

Its primary function is the manual registration of ADDs through a data form with instructions and examples to facilitate their documentation. It can also be used to query ADDs captured automatically by AK Extraction tools and manually through the form. It can be installed using Docker commands to facilitate its deployment, with prior installation of the ADKT Backend and configuration of some environment variables. For more information, refer to the official documentation [18].

3.3 AWS cloud

A fully managed Serverless application by AWS Cloud. For its installation, the source code must be requested, and a meeting arranged to install the program directly in the interested company's cloud. This can be done through a contact form available in the official documentation [18]. The application is a GraphQL API in AppSync protected with an API KEY.

To make requests, only the API KEY is required, and the HTTP call documentation available on the official site must be followed [18]. In Fig. 2, the elements of the Backend (AppSync, Lambda, DynamoDB) are detailed, as well as the connection with the Frontend (NextJS, Cognito) and the technologies used to the deployment (Netlify).

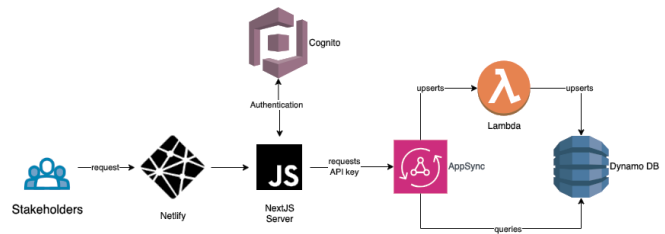


Figure 2. ADKT – Architecture Design
Source: Own elaboration

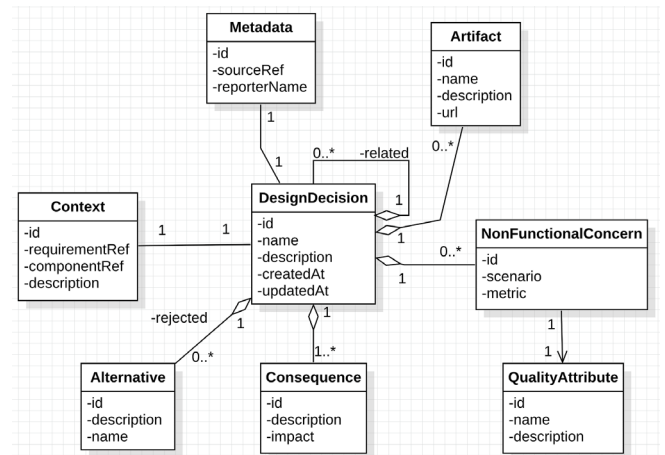


Figure 3. ADKT – Architecture Design
Source: Own elaboration

3.3.1 ADKT model

Data model that represents the knowledge about ADDs, how they relate to each other, and the link with the artifacts generated in the software development process. Below, each of the elements that make up the model is described.

In Fig. 3, you can graphically detail the attributes of each element and the multiplicity of the relationships, which indicates the mandatory nature of each component. This model is an extended version of the design decision metamodel proposed by [14]. Some attributes of the existing entities were modified to make it simpler, and some relationships were added, such as artifacts linked to a specific decision, and a self-relationship that represents the traceability that may exist between certain decisions that depend on previous ones.

- **Design Decision:** The central element of the model, specifies a name for identification, a detailed description of the selected decision, as well as a creation date, update date, and a link to other related design decisions.
- **Metadata:** This element allows knowing who registered the decision and the source of the registration. Depending on the plugin used to register the action, a different source reference will be linked.
- **Context:** As part of each decision, the context is a fundamental element for its understanding as it provides relevant information about the conditions under which a decision is made. Additionally, it links a reference to the requirement motivating the decision. This reference can

be a unique number, a user story code, or any other identifier linking the requirement. Finally, it also links a reference to the component affected by the decision, which can be the name of a service, subsystem, specific class, package, or any other unit or module.

- **Alternatives:** In the analysis for deciding, the different alternatives that will be compared when selecting must always be considered. The alternatives consist of a name for identification and a description of the reasons why they were discarded during the decision-making process.
- **Consequences:** Every decision entails at least one consequence, so it is vital to fully identify these effects when making the decision, as designers will have to address them. These consequences have both negative and positive impacts, so a description of that impact is required.
- **Artifacts:** To maintain the traceability of design decisions, they must not only be captured but also linked to other related documents, resources, or artifacts. These consist of a name for identification, a description indicating the type of artifact, and a URL to locate the resource.
- **Non-Functional Concerns:** Generally, decisions related to architectural aspects are linked to non-functional requirements (NFR). These consist of scenarios that mention: the stimulus and its source, a metric allowing its measurement, and the quality attribute in question. These quality attributes can be managed independently depending on the quality model followed by each organization.
- **Attributes:** These are directly linked to NFRs and, unlike them, do not describe metrics or scenarios. Essentially, they consist of a name and description, and for reference, the web platform advises following the names of the product quality model defined by ISO/IEC 25010 [19].

4 Evaluation of ADKT through a case study

According to the systematic mapping study presented by [8], it is important to note that a large percentage of the proposals presented up to the date of the study do not include a validation method for the proposed approaches, methods, or tools. This may be due to the complexity of the proposals and the time available for conducting empirical validation. However, ADKT presents a simple complementary option that can be integrated with existing works, and its validation can also be straightforward through the proposed tools, the model, and a short case study that allows for quantitative and qualitative conclusions. Below, the design of the case study is described.

4.1 Case study design

For the development of this case study, the guidelines for conducting and presenting case studies in software engineering, proposed by [20], were followed. The work focuses on a holistic explanatory case study, as the goal is to explain the impact of the new ADKT proposal in reducing AK loss within the context of a software development project. Below, the unit of analysis, the study objective, the

research questions to be addressed, the protocol and instruments for data collection, and finally the analysis process to clarify the results are described in detail.

4.1.1 Unit of Analysis

The Quercus Software Engineering Group research group at the University of Extremadura in Spain [21]. This group is responsible for managing research and development projects in quantum computing. Some of its members are dedicated to developing software components to provide traditional and quantum computing services, while others focus on purely administrative and management activities. Currently, they do not follow any specific methodology or framework such as SCRUM, XP, or RUP. However, they do hold weekly planning meetings for task assignment, goal definition, and deliverables, as is common in any software development team. They are currently in the design and construction phase of services, making it an ideal stage for the inclusion and evaluation of the ADKT tool.

4.1.2 Case study objective

The objective of this case study is to explore the impact of ADKT on reducing AK evaporation during the management of ADDs in the context of software component development. On one hand, it quantitatively evaluates whether there is a relationship between the use of the ADKT model and the reduction of architectural evaporation. On the other hand, it qualitatively analyzes the Perceived Usefulness and Perceived Ease of Use of the proposed model along with the provided web tool.

4.1.3 Research questions

The following research questions are aimed at achieving the research objective:

- RQ1: How do engineers document ADDs in their normal workflow before being introduced to ADKT?
- RQ2: How do engineers perceive the ease of use of the ADKT tool?
- RQ3: Do engineers find the ADKT tool useful in their normal development process?
- RQ4: What are the challenges engineers face when introducing new documentation tools into their workflow?
- RQ5: What are the limitations to consider when reducing architectural evaporation?
- RQ6: How does ADKT impact the reduction of AK evaporation?

The main objective of RQ1 is to characterize how engineers manage the documentation of ADDs, including the tools, models, ceremonies, or any other aspect relevant to preserving ADDs. RQ2 and RQ3 are directly related to determining the ease of use and perceived usefulness of the tool by the case study participants. The purpose of RQ4 is to determine the willingness and adoption protocol of new technologies by the development team. Finally, RQ5 allows us to delve deeper into how these limitations can guide new research to overcome them and provide more information to

move closer to the goal of reducing architectural knowledge evaporation. RQ6 provides clarity on the relationship between ADKT and AK evaporation.

4.1.4 Materials

The following documents and tools [22] were developed to support the research objective and were used during the execution of the case study:

- **Architecture Questionnaire:** A Google Form Questionnaire containing relevant questions for the study, divided into two sections: The first section consists of 10 questions about personal and demographic data to characterize the participants. The second section includes 16 questions related to architecture, aiming to provide engineers with a starting point to make the implicit information they have about ADDs explicit and available for documentation in their own artifacts or in the ADKT tool if they prefer.
- **Logbook:** A Google Sheets Document with three tabs to record ADKT usage times, incidents, and any questions that arise during the process. This serves as a record of events throughout the case study.
- **Semi-structured Interview:** Semi-structured interviews are conducted with each participant to extract qualitative data about the model, the tool, and the process carried out during the study. The initial interview questions are listed below. However, additional questions or comments that arise during the interview will also be considered in the study discussion.
- How is the documentation of ADDs currently carried out?
- What difficulties have you encountered when using ADKT?
- What benefits do you find in using ADKT?
- How many and which decisions have been recorded using ADKT?
- What benefits do you find in documenting ADDs?
- Would you use ADKT in the future, and why?
- **TAM Survey:** A Technology Acceptance Model (TAM) [23, 24], is used to measure the perceived usefulness and ease of use of ADKT by engineers. This model is implemented in a Google Form with four sections: the first section includes personal data, the second section consists of 10 questions assessing perceived usefulness, the third section contains 8 questions evaluating perceived ease of use, and the final section includes additional comments from participants.

4.1.5 Protocol

The first step of the protocol involves notifying all case study participants via email about the existence of ADKT, along with a link to the web tool. Following this, a semi-in-person meeting is scheduled with the participants to explain each of the materials in detail. During the meeting, training on the tool is conducted through direct interaction and demonstrations with examples.

Subsequently, participants are asked to complete the Architecture Questionnaire, which is crucial for clarifying

ideas about the current state of the architecture and establishing a foundation for using the tool. Next, the logbook is introduced, where participants can enter any questions that arise during the study, record usage time, and report any incidents with the tool.

A week after the installation and introduction of ADKT, semi-structured interviews are conducted individually with each participant. Once the ADKT trial period concludes, the study is finalized with the TAM survey to determine participants' perceived usefulness and ease of use of the tool.

4.2 Case study execution

4.2.1 Architecture questionnaire

As mentioned earlier, the first part of the questionnaire gathers demographic information about the participants to save time and minimize interruptions to the team's normal workflow with additional questionnaires. The second part consists of architecture-related questions, which can serve as a basis for documenting previously undocumented decisions. The results are described below.

The group consists entirely of six men, researchers, and software developers between the ages of 23 and 38. Their academic levels range from undergraduate to doctoral degrees, with industry experience spanning from six months to 15 years. They work with conventional technologies and programming languages such as Python, Java, NodeJS, AWS, Flask, Kafka, and Azure, as well as libraries like Qiskit and Braket for quantum circuit development. Their domains of expertise include education and research, healthcare, innovation and product development, and communications. Some members are also faculty at the same institution, teaching courses related to computer science and software development.

Below are the responses to some of the most relevant architecture-related questions regarding the documentation and communication of Architectural Design Decisions (ADDs):

- How are architectural changes managed? Architectural change management includes keeping old local versions for recovery, team discussions, and collaborative decision-making. Changes are discussed in weekly meetings iteratively; however, there is no formal process in place.
- Is there a formal process for making architectural design decisions? (If so, please describe it?): No, typically, a team member proposes an idea, and the developer implements it as they see fit, asking colleagues questions to ensure the implementation aligns with previously established guidelines.
- How is the architecture communicated to stakeholders? Verbally in weekly meetings and sometimes through messaging applications like Slack and email.
- What architectural artifacts are used in the project (e.g., diagrams, models, documents, websites, etc.)? Diagrams, some digital and others on paper, as well as code repositories.
- What challenges does the team face regarding the current architecture? There is barely any documentation on changes and architectural components. If I left my job right now, no

one would have access to the code or past versions, nor would they know how it works. The only preserved artifacts would be paper diagrams outlining the architecture at a high level. Process improvements, inherent challenges in quantum computing, and optimization of waiting times and task execution are needed.

- What are the team's priorities for improving the architecture in the future? We function relatively well, but we lack traceability and documentation, which is an area for significant improvement. The main priority is enhancing processes, especially communication workflows.

4.2.2 Logbook

No incidents or additional questions were recorded. However, the usage times shown in Table 1 were logged, documenting the registration of three ADDs by a single participant.

Although the decisions were recorded during the case study, it is impossible to know with certainty whether they had a positive impact at the time of recording, as the usefulness of the tool is usually seen over time. However, according to the comments received in the TAM Survey, these decisions reflected the reasoning behind certain functional and quality characteristics, which can provide greater context when refactoring the architecture proposed for the project in subsequent design and planning meetings of the Quercus research group, even for participants who were not part of the initial design.

4.2.3 Semi-structured interview

The comments received in the semi-structured interview are discussed in the Results section.

4.2.4 TAM survey

Table 2 presents the average scores obtained after administering the TAM survey to study participants. The complete survey results are available in the repository for this article [22]. For a discussion of the results, please refer to the next section.

Table 1.
Decisions and times registered.

Participant	Start	End	Date	Decision
Participant2	12:30PM	12:42PM	24/05/2024	Functionality
Participant2	8:25AM	8:37AM	27/05/2024	Accessibility
Participant2	12:40PM	12:55PM	06/05/2024	Modularity

Source: Own elaboration

Table 2
TAM survey results.

Participant	Perceived Usefulness	Ease of Use
Participant1	4.40	4.00
Participant2	4.20	3.88
Participant3	4.20	3.00
Participant4	4.40	3.63
Participant5	4.70	3.88
Participant6	3.00	3.00
Total	4.15	3.56

Source: Own elaboration

5 Analysis of results

In this section, the results obtained are analyzed both quantitatively and qualitatively, addressing each research question posed in the experiment design. Finally, a discussion on these results and how they contribute to the existing alternatives for traceability of ADDs and artifacts in software development is presented.

5.1 RQ1: How do engineers document ADDs in their regular workflow before being introduced to ADKT?

Due to the informality of the development methodology, there is no specific method, process, ceremony, or technological tool dedicated to documenting ADDs. However, some ADDs are briefly noted in a participant's notebook during planning ceremonies.

When ADDs arise outside meetings, they are not documented and instead are reflected in artifacts such as source code, Slack messages, or emails. Additionally, in many cases, this information is shared verbally without leaving any structured record.

5.2 RQ2: How do engineers find the usability of the ADKT tool?

Based on semi-structured interviews, all participants generally considered the tool easy to use due to its simple interface, which does not require advanced technical knowledge. Below are paraphrased comments from participants: The information indicators for each attribute help understand what data should be associated with each model element. The tool is easy to manage, and the form is intuitive; three design decisions were registered without issues or additional questions. In contrast, the TAM results in Table 2 reveal that most participants perceived the tool as easy to use. However, only one participant performed the registrations, while the others merely observed. Additionally, two of the lowest results were due to participants not using the tool because of lack of time, priority, or because they forgot. This is corroborated in the additional survey comments [22].

5.3 RQ3: Do engineers find the ADKT tool useful in their regular development process?

Overall, all interviewees indicated in the semi-structured interviews that they considered the tool beneficial. Specific comments included: It helps to have a broader view of ongoing activities, improves documentation of decisions that were previously not recorded, is useful to have this information available and centralized when writing a research paper to save time, could be used to document decisions unrelated to architecture, helps preserve knowledge when people leave the project, allows keeping a history of decisions, it is beneficial that one person's decisions are accessible to the entire group, and it is easier to have the information in the tool than to ask someone directly for a summary. These positive aspects align with the TAM results presented in Table 2. However, it is important to note that

only one participant registered design decisions, while the others primarily acted as observers. Additionally, one participant neither used the tool nor perceived its utility.

5.4 RQ4: What challenges do engineers face when introducing new documentation tools into their workflow?

A fast-paced work rhythm, constantly changing goals, lack of a clear direction when updating research project priorities, and team dynamics have hindered the adoption of tools, methods, or work models. Previously, attempts were made to implement the SCRUM methodology; however, ceremonies could not be held, nor could tasks be formally tracked. Additionally, the nature of the research group prevents fully focusing efforts on a single project. Depending on current research needs, some development projects may be temporarily paused while other objectives, such as publishing papers, are achieved. Lightweight tools like Slack have been useful in keeping the team informed outside planning meetings, where information is shared verbally to avoid using other tools and interrupting the meeting flow.

5.5 RQ5: What limitations should be considered when reducing architectural drift?

Time constraints and work dynamics make it difficult to document design decisions. Constant changes in objectives and priorities affect the dedication to this task. Despite recognizing its importance, it is often forgotten or unclear how to perform it. Many details are omitted during the recording process because they are considered self-evident. Although automated tools help, human intervention is required to ensure the relevance of the information.

5.6 RQ6: How does ADKT impact the reduction of AK drift?

Semi-structured interviews, along with a follow-up meeting after the case study, revealed additional ADDs not recorded in ADKT and confirmed that no decisions with architectural impact were made during the study. This indicates that at least three ADDs were documented during the project, which might not have been recorded otherwise, as mentioned earlier and confirmed by participants' comments. However, the amount of information on ADDs may be insufficient for future decisions, as the complete ADKT model was not used. In the Record Calculations [22], it can be observed that for the first decision, 60% of the data was documented, including the name, description, context, a consequence, and an alternative. For the second decision, in contrast to the first, an artifact was included instead of alternatives, reaching 67%. Finally, for the third decision, no artifacts or alternatives were recorded, resulting in 47% of the information being documented.

Beyond the quantitative percentages of documentation, the impact of recording these three decisions (Functionality, Accessibility, and Modularity) is relevant for the project. For instance, the explicit trace of the Functionality decision allows future developers to understand why certain features

were prioritized, reducing the risk of redundant work when new requirements appear. Similarly, the Accessibility decision highlights quality concerns that might otherwise be overlooked in subsequent iterations, helping to align technical improvements with user-centered goals. Finally, documenting Modularity provides a rationale that can guide future refactoring efforts, making it easier for new members of the team to understand the decomposition criteria applied. Although these benefits will be more evident in the medium and long term, the case study shows that even a small number of recorded decisions can provide valuable context for maintaining architectural coherence, supporting onboarding of new developers, and facilitating informed changes during project evolution.

5.7 Discussion

The findings indicate that ADKT effectively helps reduce AK evaporation due to its simplicity and usefulness, as recognized by the stakeholders. Quantitatively, the ADDs collected during the case study were recorded using the tool and prove useful for future stakeholders involved in the project. Qualitatively, participants stated that ADKT is easy to use and expressed their intention to continue using it to document future ADDs. Compared to previously mentioned approaches, it is worth highlighting that this proposal establishes a clear structure for documenting ADDs, including not only the information about the ADD itself but also the traceability between them and the artifacts associated with the decision-making process.

In addition to offering manual data entry, this tool provides a comprehensive architecture designed to integrate with other existing approaches via a well-documented API that runs in the AWS cloud with serverless services that enable automatic scalability of the solution. This allows for the integration of widely used software development tools such as Jira or Confluence, where calls to external APIs can be automated with relevant information from tickets or shared project documentation. It also allows for communication tools such as Slack, where API calls can be made from the definition of specific events in the tool's configuration. The complete installation of this API can be discussed in a scheduled meeting if other developers wish to implement it. This could benefit researchers or developers who gather this knowledge from various artifacts but have yet to develop an application that integrates and visualizes it for all types of stakeholders. The reduction of AK demonstrates that ADKT positively impacts architectural knowledge retention among development teams.

To optimize ADKT, participants provided recommendations, such as adding a notification system to remind users to record ADDs, requesting feedback when completing a record, including a comprehensive example in the field descriptions, and customizing the model according to the specific needs of companies. These suggestions could be implemented in future updated versions of the tool. Meanwhile, delegating the task of reminding team members to record ADDs to one team member or, in the case of a scientific validation, to the experience evaluator, could be considered.

As a recommendation for future research, it is suggested to integrate the proposed architecture into various organizations developing products that extract this information from different artifacts involved in software development. It is necessary to assess whether consolidating this information in a common and easily accessible place significantly impacts time savings and reducing AK loss.

Beyond the specific case study, the applicability of ADKT can extend to organizations that already use tools such as Jira, Confluence, or Slack. In these contexts, ADKT can act as a complementary layer that centralizes architectural decisions automatically extracted from tickets, project documentation, or communication logs, ensuring that rationale is not lost across distributed platforms. Moreover, its serverless design in AWS and the use of a GraphQL API make the solution inherently scalable, enabling adoption both in small research teams and in large, distributed enterprises. This opens the possibility for ADKT to serve not only as a support tool for academic environments but also as a practical solution for industrial software projects where traceability and knowledge retention are critical.

5.8 Limitations of the study

Regarding ADKT: as it is a manual record, it requires the commitment of participants. Likewise, the level of detail required in the forms may discourage frequent use of the tool, leading to temporary and discontinuous use. On the other hand, the system still lacks automatic mechanisms, such as reminders or notifications, that encourage the continuous documentation of ADDs. However, this is mitigated through the development of the API, where this registration can be automated and integrated with existing tools. Additionally, future work aims to integrate periodic notification features to encourage its continuous use and flexible forms for easy completion.

Regarding the design of the case study: it was developed with a single development group (Quercus SEG), which limits the generalization of the results to other organizational contexts. In addition, the duration of the study was relatively short, which prevented the evaluation of whether the observed benefits are maintained in the medium and long term. Finally, longer projects and distributed teams were not considered, so the findings are limited to a controlled and small-scale scenario. To mitigate these limitations, new case studies with other types of organizations and a larger study population are proposed.

Finally, regarding the methodology: although quantitative and qualitative instruments (semi-formal surveys and the TAM model) were used, the evaluation scale was limited, with a small number of participants. Likewise, the study does not allow for verification of the future usefulness of the documented ADDs, as there is no longitudinal analysis that considers their application in subsequent architectural decisions.

To provide greater transparency, the limitations can be grouped into three categories. (1) Tool-related limitations: ADKT still depends on manual registration, does not include reminders or notifications, and its current forms may discourage continuous use. (2) Case study limitations: the evaluation was conducted with a single research group, with a small number of participants and a short observation period, which restricts the generalization of the findings. (3) Methodological limitations:

the instruments applied (semi-structured interviews and TAM survey) provided useful but limited insights, and the absence of a longitudinal analysis prevents confirming the long-term usefulness of the recorded decisions. This categorization clarifies the scope of the study and facilitates future replications or extensions.

6 Conclusions and Future Work

This study examines the issue of architectural knowledge loss, highlighting its significant consequences such as excessive maintenance and additional costs due to the misunderstanding of previous architectural decisions, which may be altered by new decisions that do not consider the original context. It also describes how the scientific community addresses this issue from various perspectives and how different software development artifacts are used as sources of information, with AI tools to extract this knowledge. It is emphasized that these various approaches are innovative and contribute significantly to mitigating the problem; however, there remain certain practical gaps that this research aims to address. These include the lack of a defined structure for ADDs that allows both their registration and traceability, and the absence of a common architecture to integrate existing developments within the scientific community.

In response, ADKT is presented: a tool for the traceability of ADDs and software artifacts. This tool consists of a service-based architecture that facilitates the registration of ADDs through a well-defined API and a user interface, following a data model that connects the ADDs and the involved software artifacts. This approach differs from others because: on the one hand, it is manual, for the use of all the roles involved in the development of a software project, and automatic because it seeks to integrate with existing approaches that use other automated methods for knowledge extraction. Additionally, it includes a consistent data model that standardizes and allows the traceability of the ADDs and artifacts.

To validate this tool, a case study is designed and carried out with the development team of the Quercus SEG group at the University of Extremadura. The study aims to evaluate the perceived usefulness and ease of use of the tool, as well as its relationship to the reduction of architectural knowledge evaporation. The tool is previously installed in the group's development environment, participants are trained, and the study begins. Semi-formal surveys and a TAM are used to quantitatively assess the ease of use and usefulness of the tool. To measure its impact on reducing evaporated architectural knowledge, the ADDs are registered in the tool. This study is a first step in the validation of this proposal. Subsequently, further validations will be carried out with more participants and with longer-term projects.

The results indicate that the tool is perceived as useful and easy to use by participants, and it helps document at least three design decisions that would not have been recorded without ADKT. This suggests that the tool contributes to the reduction of architectural knowledge evaporation, although its effectiveness depends on frequent and correct use by users, which emphasizes the importance of active participation and the need for the tool to provide mechanisms that promote its continuous use.

In conclusion, the development of technologies to document and recover this knowledge is crucial and represents a current concern to avoid excessive maintenance and additional costs in software projects. However, without the habit of recording even the minimal amount of this knowledge, these tools cannot reach their potential as reliable sources for future decisions. Therefore, it is recommended to develop both the necessary technology, and the habit of documenting ADDs, aligned with the tools developed for this purpose. Future work includes the integration of the architecture with existing tools, improvement of features suggested by the study participants, and long-term validation to assess the usefulness of documented ADDs in future decisions.

References

- [1] Bass, L., Clements, P., Kazman, R., Software Architecture in Practice. Second. Addison Wesley; 2003.
- [2] Harrison, N., and Avgeriou, P., How do architecture patterns and tactics interact? a model and annotation. *Journal of Systems and Software*, 83(10), pp. 1735-1758, 2010. DOI: <https://doi.org/10.1016/j.jss.2010.04.067>
- [3] Jansen, A., and Bosch, J., Software architecture as a set of architectural design decisions. 5th Working IEEE/IFIP Conference on Software Architecture (WICSA'05), 2005, pp. 109-120. DOI: <https://doi.org/10.1109/WICSA.2005.61>
- [4] van-der-Ven, J.S., Jansen, A.G.J. and Bosch, J., Design decisions: the bridge between rationale and architecture. In: Dutoit, A.H., McCall, R., Mistrik, I., and Paech, B., eds. *Rationale Management in Software Engineering*. Springer Berlin Heidelberg, 2006, pp. 329-348. DOI: https://doi.org/10.1007/978-3-540-30998-7_16
- [5] Borrego, G., Morán, A., Palacio, R., Vizcaino, A., and García, F., Towards a reduction in architectural knowledge vaporization during agile global software development. *Inf. Softw Technol.*, 112(6), pp. 68-82, 2019. DOI: <https://doi.org/10.1016/j.infsof.2019.04.008>
- [6] Capilla, R., Jansen, A., Tang, A., Avgeriou, P., and Babar, M., 10 years of software architecture knowledge management: practice and future. *Journal of Systems and Software*. (116), pp. 191-205, 2016. DOI: <https://doi.org/10.1016/j.jss.2015.08.054>
- [7] Hadar, I., Sherman, S., Hadar, E., and Harrison, J., Less is more: architecture documentation for agile development, in: 6th International Workshop on Cooperative and Human Aspects of Software Engineering, CHASE, Proceedings, 2013, pp. 121-124.
- [8] Hyun, S., and Hurtado, J., Traceability of architectural design decisions and software artifacts: a Systematic Mapping Study. *Foundations of Computing and Decision Sciences*, 48(4), pp. 401-423, 2023. DOI: <https://doi.org/10.2478/fcds-2023-0018>
- [9] Tofan, D., Understanding and supporting software architectural decisions: for reducing architectural knowledge vaporization. University of Groningen, 2015.
- [10] Dutoit, A.H, McCall, R., Mistrik, I., and Paech, B., Rationale management in software engineering: concepts and techniques. In: Dutoit, A.H., McCall, R., Mistrik, I., Paech, B., eds., *Rationale Management in Software Engineering*. Springer Berlin Heidelberg, 2006, pp. 1-48. DOI: https://doi.org/10.1007/978-3-540-30998-7_1
- [11] Bass, L., Clements, P., Nord, R., and Stafford, J., Capturing and using rationale for a software architecture. In: Dutoit, A.H., McCall, R., Mistrik, I., Paech, B., eds., *Rationale Management in Software Engineering*. Springer Berlin Heidelberg, 2006, pp. 255-272. DOI: https://doi.org/10.1007/978-3-540-30998-7_12
- [12] Kamalabalan, et al., Tool support for traceability of software artefacts. In: *Moratuwa Engineering Research Conference (MERCon)*, 2015, pp. 318-323. DOI: <https://doi.org/10.1109/MERCon.2015.7112366>
- [13] Petersen, K., Vakkalanka, S., and Kuzniarz, L., Guidelines for conducting systematic mapping studies in software engineering: An update. *Inf Softw Technol.*, 64, pp. 1-18, 2015. DOI: <https://doi.org/10.1016/j.infsof.2015.03.007>
- [14] Gilson, F., Annand, S., and Steel, J., Recording software design decisions on the fly. *CEUR Workshop Proc.*, (2799), 2020, pp. 53-66.
- [15] Meza-Soria, A., and Van-Der-Hoeck, A., Collecting design knowledge through voice notes. *Proceedings IEEE/ACM 12th International Workshop on Cooperative and Human Aspects of Software Engineering, CHASE*, 2019, pp. 33-36. DOI: <https://doi.org/10.1109/CHASE.2019.00015>
- [16] Soria, A., KNOCAP: capturing and delivering important design bits in Whiteboard design meetings. *Proceedings ACM/IEEE 42nd International Conference on Software Engineering: Companion, ICSE-Companion*, 2020, pp. 194-197. DOI: <https://doi.org/10.1145/3377812.3381397>
- [17] Souali, K., Rahmaoui, O., and Ouzzif, M., An overview of traceability: definitions and techniques. *Colloquium in Information Science and Technology, CIST.*, 2016, pp. 789-793. DOI: <https://doi.org/10.1109/CIST.2016.7804995>
- [18] Hyun, S., ADKT Documentation web site. Preprint posted [online], 2025. Available at: <https://zahydo.github.io/adkt-docs>
- [19] ISO/IEC. ISO/IEC 25010, Systems and Software Engineering-Systems and Software quality requirements and evaluation (SQuaRE)-System and Software Quality Models. ISO/IEC; 2010.
- [20] Runeson, P., and Höst, M., Guidelines for conducting and reporting case study research in software engineering. *Empir Softw Eng.*, 14, pp. 131-164, 2009. DOI: <https://doi.org/10.1007/s10664-008-9102-8>
- [21] Quercus Software Engineering Group research group. Preprint posted [online], 2025. Available at: <https://quercusseg.unex.es/>
- [22] Hyun-Dorado S., Materiales para la evaluación de ADKT a través de un estudio de caso. Zenodo. Preprint posted, Art. 9845, 2024. DOI: <https://doi.org/10.5281/zenodo.13209845>
- [23] Davis, F., Bagozzi R., and Warshaw P., User acceptance of computer technology: a comparison of two theoretical models. *Management Science*, 35(8), pp. 982-1003, 1989.
- [24] Wang, C., Ahmad SF, Bani Ahmad Ayassrah AYA, et al. An empirical evaluation of technology acceptance model for Artificial Intelligence in E-commerce. *Heliyon*, 9(8), e.18349, 2023. DOI: <https://doi.org/10.1016/j.heliyon.2023.e18349>

S. Hyun-Dorado, is a BSc. Eng. in Systems Engineer from the University of Cauca, Colombia with over 7 years of experience in software development. He is currently finishing his MSc in Computer Science in the University of Cauca. His research interests include Software Engineering, Web Engineering, Software Architecture. ORCID: 0000-0001-7996-7641.

J.A. Hurtado, is a titular professor at the University of Cauca, Colombia. He completed his PhD in Computer Science from the University of Chile, 2012. His research interests include Software Reuse (Model Driven Engineering, Software Product Lines), Software Architecture, Software Process Modeling and Computational Thinking. Currently he is an active member of the IDIS Research Group. ORCID: 0000-0002-2508-0962

J.E. Mogel, is an associate professor from the University of Extremadura, Badajoz, Spain. MSc. in Computer Science in 2011, from the University Carlos III, Spain), and PhD in Computer Science in 2018, from the University of Extremadura Spain. His research interests include Web Engineering, Smart Systems, and Quantum Computing. ORCID: 0000-0002-4096-1282

J. Garcia-Alonso, is currently an associate professor with the Department of Informatics and Telematics System Engineering, University of Extremadura, Badajoz, Spain, and a co-founder of the startups Gloin and Viable. His research interests include quantum software engineering, eHealthCare, eldercare, mobile computing, context-awareness, and pervasive systems. PhD with European Mention in 2014, from the University of Extremadura, Spain. ORCID: 0000-0002-6819-0299

Effectiveness of 2-Layered grounding grids in high voltage GIS substations and new design considerations using FEM

Asaad Shemshadi^a, Mitra Kamal Abadi^a, Vahid Souri^b, Ali Safari^b & Ali Fathi^b

^a Electrical Engineering Department, Arak University of Technology, Arak, Iran. Shemshadi@araut.ac.ir, mitrakamalabadii@gmail.com

^b Bakhtar Regional Electric Company, Tavanir, Arak, Iran. V.souri@brec.ir, a.fathi@brec.ir, a.safari@brec.ir

Received: April 21st, 2025. Received in revised form: September 10th, 2025. Accepted: October 10th, 2025.

Abstract

With the rising demand for electricity and the expansion of power generation facilities, grounding systems have become critical for ensuring human safety and equipment protection. This study employs the finite element method to model single- and double-layer grounding networks, evaluating their effectiveness in mitigating step and touch voltages. Findings reveal that, despite increased complexity and cost, the double-layer configuration does not significantly enhance ground resistance reduction or voltage distribution, indicating that the single-layer network remains a reliable and efficient solution.

Keywords: grounding systems; protection of equipment; high voltage; finite element method; step and touch voltage.

Eficacia de redes de puesta a tierra de dos capas en subestaciones GIS de alta tensión y consideraciones de diseño mediante FEM

Resumen

Con el aumento de la demanda eléctrica y la expansión de las instalaciones de generación, los sistemas de puesta a tierra se han vuelto esenciales para garantizar la seguridad humana y la protección del equipo. Este estudio emplea el método de elementos finitos para modelar redes de puesta a tierra de una y dos capas, evaluando su eficacia en la mitigación de las tensiones de paso y de contacto. Los resultados muestran que, pese a su mayor complejidad y costo, la configuración de doble capa no mejora significativamente la reducción de la resistencia de tierra ni la distribución de voltaje, indicando que la red de capa única sigue siendo una solución confiable y eficiente.

Palabras clave: sistemas de puesta a tierra; protección de los equipos; alto voltaje; método de los elementos finitos; tensión de paso y de contacto.

1. Introduction

Grounding (earthing) systems play a key role in the safety and efficiency of electrical networks. These systems help protect individuals and equipment from voltages caused by electrical faults, lightning, and over voltages [1-5]. Proper grounding network design reduces step and touch voltages, preventing serious damage (Fig. 1). This research aims to examine the performance and effectiveness of single-layer and double-layer grounding networks, comparing them in terms of ground resistance and safety. The finite element method has been employed as an effective approach for the simulation and

analysis of these networks [6-8].

In this study, the finite element method was used to model and simulate single-layer and double-layer grounding networks. First, data related to soil and environmental conditions were collected. Then, the network geometries were designed in COMSOL Multiphysics software, and ground resistance, as well as step and touch voltages, were calculated for each network. Boundary conditions and loading were configured according to industry standards. Simulations were conducted for both types of networks under various conditions to examine their performance in dissipating fault currents and reducing hazardous voltages [9-11].

How to cite: Shemshadi, A., Abadi, M.K., Souri, V., Safari, A., and Fathi, A., Effectiveness of 2-Layered grounding grids in high voltage GIS substations and new design considerations Using FEM DYNA, (92)239, pp. 66-71, October - December, 2025.



Figure 1. A view of high voltage switchgear
Source: Wang, 2020.

2. Single-Layer Network simulation

The single-layer grounding network was simulated by designing its geometry in COMSOL Multiphysics. Soil parameters and environmental conditions were incorporated to ensure realistic modeling. Boundary conditions and loading were set according to relevant standards to assess ground resistance and the distribution of step and touch voltages. The simulation aimed to analyze the network's effectiveness in fault current dissipation and hazardous voltage reduction. The results provided insights into the safety and efficiency of the single-layer design in electrical systems (Figs. 2 and 3).

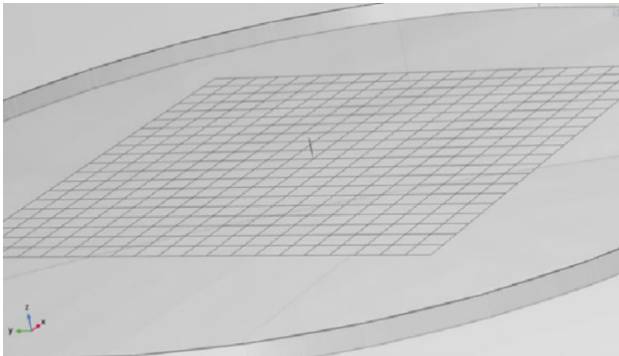


Figure 2. Close-up illustration of the single-layer
Source: Created by the authors

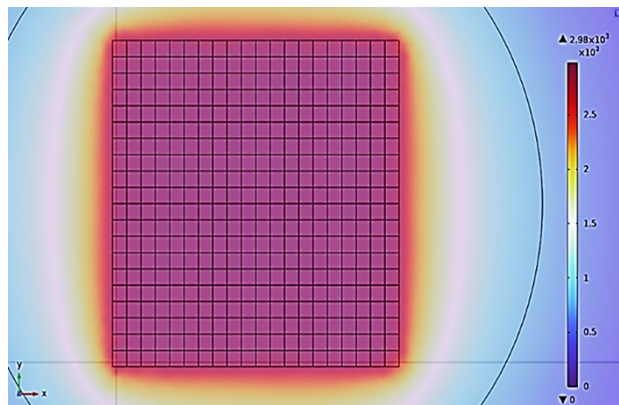


Figure 3. Finite Element Modeling of a Single-Layer Grounding System Using COMSOL Software
Source: Created by the authors

2.1 Step voltage for the Single-Layer Network

Step voltage is the potential difference a person may experience between two points on the ground, typically one step apart, while a fault current is flowing through the grounding system. For the single-layer grounding network, step voltage is calculated based on the current dispersal pattern through the soil and the resistance profile around the grounding electrodes.

In this simulation, step voltage for the single-layer network is measured by analyzing the voltage gradient in the soil around the grounding grid. The aim is to ensure the step voltage stays within safe limits defined by industry standards, minimizing the risk of electrical shock to personnel near the fault location. This analysis helps verify that the single-layer network provides adequate safety during fault conditions by keeping step voltages within acceptable thresholds (Fig. 4).

2.2 Touch voltage for the Single-Layer Network

Touch voltage is the potential difference a person might experience between a point on the ground and a conductive structure or equipment in contact with the grounding network during a fault condition. In a single-layer grounding network, touch voltage is a crucial safety parameter that indicates the level of potential hazard near equipment or structures connected to the ground.

For this network, touch voltage can be evaluated by measuring the voltage difference between the grounding network's metal parts and nearby ground surface points. The goal is to ensure that the touch voltage remains within safe limits as defined by industry standards to prevent electric shock. (Fig. 5).

Through simulation, touch voltage values are analyzed across various points around the network to confirm that the single-layer design effectively reduces potential hazards, keeping touch voltage at safe levels for personnel working near grounded equipment.

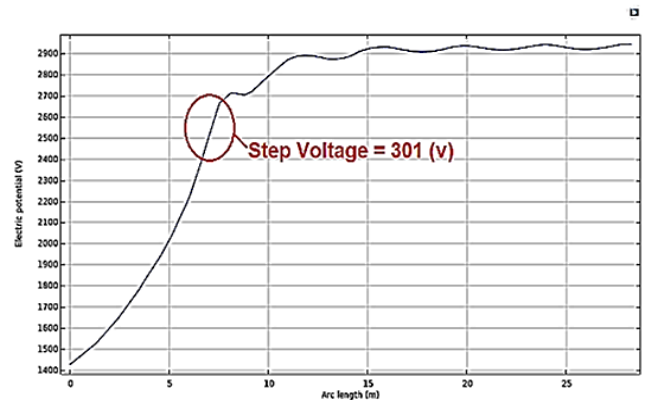


Figure 4. Voltage step diagram for a single-layer network
Source: Created by the authors

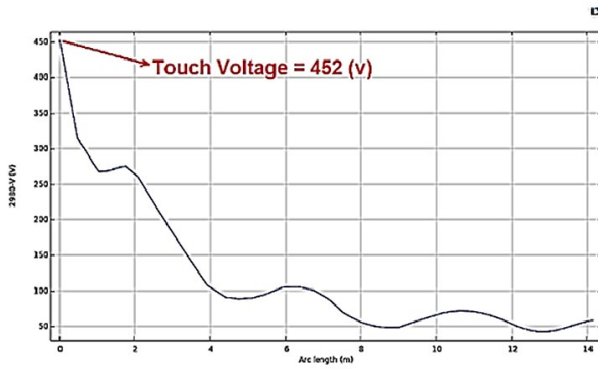


Figure 5. Touch voltage diagram for a single-layer network
Source: Created by the authors

3. Double-Layer grid simulation

The double-layer grounding grid simulation involved creating a detailed geometry in COMSOL Multiphysics, taking into account layered soil characteristics and environmental factors for accurate modeling. Boundary conditions and load settings were applied following industrial standards to calculate ground resistance and evaluate step and touch voltage distributions. This simulation focused on assessing the double-layer network's ability to dissipate fault currents and minimize dangerous voltages. The results helped to determine the added value, if any, of the double-layer configuration in enhancing electrical system safety and reliability compared to the single-layer network (Figs. 6 and 7).

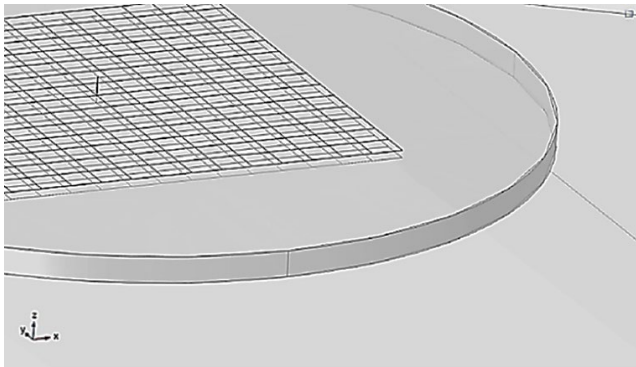


Figure 6. Close-up illustration of the double-layer grounding network
Source: Created by the authors

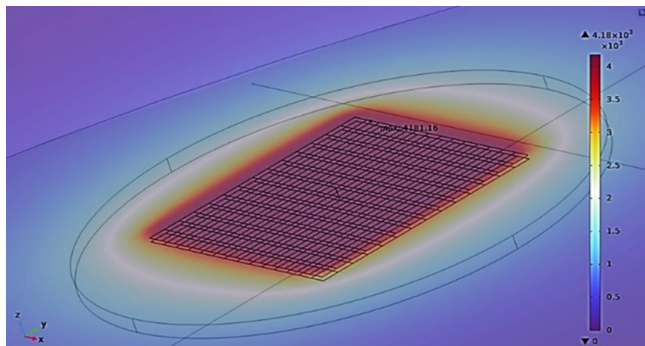


Figure 7. FEM Modeling of a 2-Layer Grounding Grid (COMSOL Software)
Source: Created by the authors

3.1 Step voltage for the Double-Layer Network

Step voltage in a double-layer grounding network refers to the potential difference experienced between two points on the ground surface, typically spaced one step apart, during a fault condition. In this setup, the double-layer design aims to spread fault current more evenly across the soil, potentially reducing step voltages at various points on the surface.

For this network, step voltage is analyzed by simulating voltage gradients around the grounding system (Fig. 8).

The double-layer configuration, with its added complexity, theoretically distributes current over a broader area, potentially achieving lower step voltages compared to a single-layer system. The simulation measures these voltages at various distances from the network to assess compliance with safety standards and to verify the effectiveness of the double-layer design in minimizing step voltage hazards.

3.2 Touch voltage for the Double-Layer Network

In a double-layer grounding network, touch voltage represents the potential difference that a person might experience between a point on the ground and a conductive structure (such as equipment connected to the grounding system) during a fault condition. The double-layer design is intended to distribute fault currents more effectively, which may lower touch voltages in areas surrounding grounded equipment.

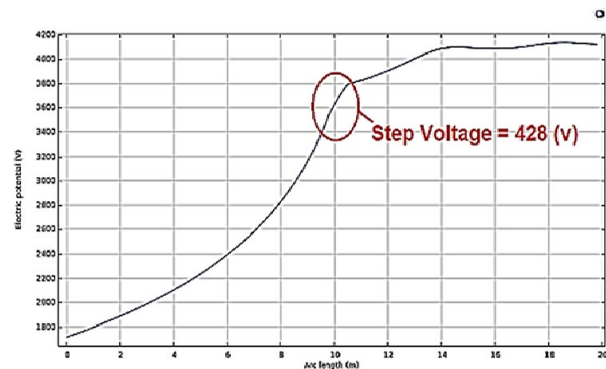


Figure 8. Step Voltage Diagram for the Two-Layer Network
Source: Created by the authors

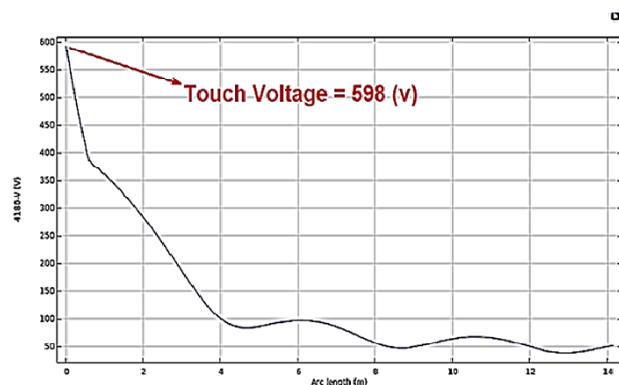


Figure 9. Touch Voltage Diagram for the Two-Layer Network
Source: Created by the authors

To evaluate touch voltage in this network, simulations are conducted to measure the voltage difference between the grounding network components and points on the ground surface nearby (Fig. 9). The double-layer configuration, with its deeper and additional grounding layer, can potentially provide improved voltage distribution and further reduce touch voltage risks.

By analyzing touch voltages at various points, this assessment helps verify that the double-layer network can achieve safer voltage levels, enhancing protection for personnel working near grounded equipment, in line with industry safety standards.

4. Simulations and Results

The simulation results showed that the step and touch voltages in double-layer networks are significantly higher than in single-layer networks. For the single-layer network, the step voltage was measured at 301 volts and the touch voltage at 452 volts, while these values for the double-layer network were 406 volts and 598 volts, respectively. Ground resistance was also higher for the double-layer network compared to the single-layer network (0.418 ohms versus 0.298 ohms).

These results indicate that, despite the increased complexity of the double-layer network, its performance does not significantly improve safety or reduce step and touch voltages.

5. The proposed network

A third network was also modeled, in which the ineffective middle sections of the two-layer configuration were removed (Fig. 10). This modification reduces copper usage, construction delays, and coupling effects, while yielding results comparable to those of the full two-layer network (Figs. 11, 12 and 13).

Comparison among 3 types of investigating grids is briefly obtained as mentioned in Table 1 and Table 2. It can be resulted from this table that in two-layered structure; all technical parameters especially R_g , is increased value and the upper layer is not effectively enough as the commercial designers consider during calculation process.

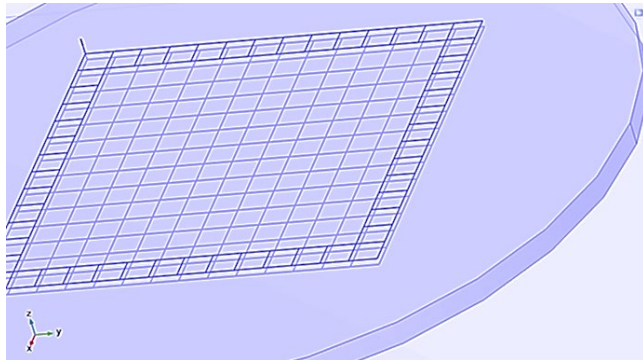


Figure 10. Simulation of the Proposed Network
Source: Created by the authors

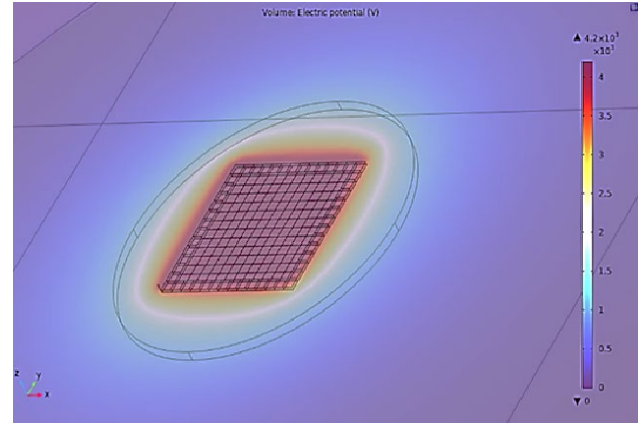


Figure 11. Finite Element Modeling of the Third Proposed Grounding System Using COMSOL Software
Source: Created by the authors

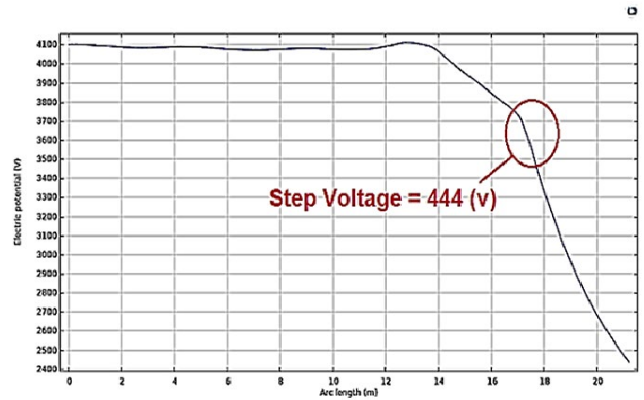


Figure 12. Step Voltage Diagram for the Proposed Network
Source: Created by the authors

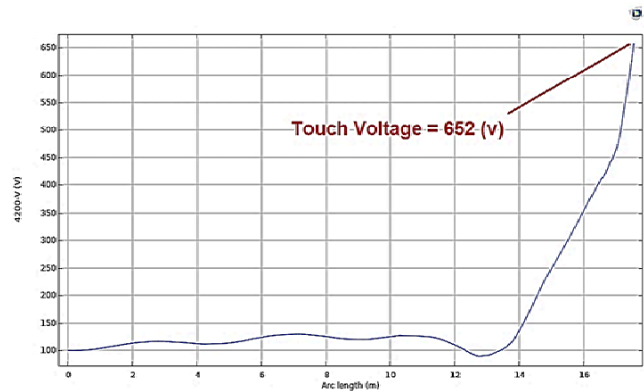


Figure 13. Touch Voltage Diagram for the Proposed Network
Source: Created by the authors

Table.1

Comparison of two-layer and single-layer grounding systems

	R_g	Step-voltage	Touch-voltage	GPR
Single-layer	0.298	492	301	2980
Two-layer	0.418	598	406.4	4180

Source: Created by the authors

Table. 2
Comparison among 3 types of investigating grids

	Rg	Step-voltage	Touch-voltage	GPR
Single-layer	0.298	492	301	2980
Two-layer	0.418	598	406.4	4180
Proposed grounding system	0.42	444	652	4200

Source: Created by the authors

Regarding to proposed grid structure which save about 38% needed copper wire, it is observed that technical parameters variations, especially Rg, are not serious.

6. Discussion and Conclusion

The findings show that two-layer grounding grids, despite their higher complexity and cost, do not outperform single-layer networks in mitigating touch and step voltages. Simulation results confirm that single-layer networks can ensure adequate safety and efficiency, making them the more cost-effective option. Therefore, grounding system designs should prioritize single-layer configurations, optimized according to local and environmental conditions to reduce costs while maintaining safety.

Acknowledge statement

This article is funded and supported by Bakhtar Regional Electric Company (BREC), Tavanir, Arak, Iran.

References

- [1] Gao, Y., Wang, Z., and Liu, J., Application of finite element method in calculation of grounding systems. *IEEE Access*, 8, pp. 10346-10355, 2020, DOI: <https://doi.org/10.1109/ACCESS.2020.xxxxx>
- [2] Sarker, M., et. al., Performance optimization of grounding system for multi-voltage Electrical Installation, *Applied Sciences*, 15(15), pp. 201-210, 2025. DOI: <https://doi.org/10.3390/app15158600>.
- [3] Chen, T., and Smith, A., Use of the finite element method for the modeling of multi-layered power/ground planes. *IEEE Transactions on Power Electronics*, 36(5), pp. 1789-1798, 2021. DOI: <https://doi.org/10.1109/ECTC.2009.5074233>
- [4] Smith, D., and Zhang, L., Finite-element modelling of seism electric and electro seismic waves in frequency Domain. *Geophysical Journal International*, 230(1), pp. 146-157, 2022. DOI: <https://doi.org/10.1093/gji/ggad236>
- [5] Mehri, A., and Ghanizadeh, R., Transient analysis of double-layer ground electrodes under lightning conditions. *Journal of Electrical Engineering*, 50(3), pp. 241-252, 2022. DOI: <https://doi.org/10.1007/s00202-021-01362-x>
- [6] Patel, R., and Kumar, S., Advanced modeling techniques in multilayer grounding systems using FEM. *International Journal of Power Systems*, 29(4), pp. 495-508, 2023. DOI: <https://doi.org/10.1093/gji/ggad236>
- [7] Barich, T., et. al., Modelling grounding systems using the finite element method: the influence of the computational domain size on the accuracy of the numerical calculation, *Technical Gazette*, 30(6), pp. 1717-1727, 2023. DOI: <https://doi.org/10.17559/TV-20220727092344>
- [8] Nahman, J., and Raicevic, N., A novel FEM approach to analyzing grounding systems in multi-layer soils. *Electrical Engineering and Applied Science Journal*, 17(3), art. 007, 2023. DOI: <https://doi.org/10.54554/ijeas.2023.6.02.007>
- [9] Taher, S.A., and Shemshadi, A., Analysis and design of a new method for reduction of touch and step voltages for earthing systems using FEM

approach. *International Journal of Electrical and Power Engineering*, 2(6), pp. 409-416, 2008, DOI: <https://doi.org/10.36478/ijepe>

- [10] Shemshadi, A., and Khorampour P., Research and investigation of high frequency profile of step and touch voltages due to fragmentation of the grounding grid, *Inge Cuc Journal*, 20(1), pp. 68-89, 2024. DOI: <https://doi.org/10.17981/ingecuc.20.1.2024.05>
- [11] Hossinn, M.S., et. al., Design and optimization of substation grounding grid for ensuring the safety of personnel and equipment. *Journal of Electrical Power and Energy Systems*, art. 001, 2021. DOI: <https://doi.org/10.26855/jepes.2021.08.001>.



A. Shemshadi, was born on Nov 1st of 1979. He received the BSc. from the Shiraz University, in 2003. MSc. in 2007, from the Kashan University, Iran, and PhD in 2014, from Khaje Nasir Toosi University of Technology, all of them in Electrical Engineering. His research interests are: Vacuum interrupters design and analysis, high voltage simulations, thermal plasma modeling, high voltage equipment design, transients in vacuum arc quenching, renewable energies and pulsed power.

ORCID: 0000-0002-7271-9933

e-mail: shemshadi@arakut.ac.ir



M. Kamalabadi, was born in Arak, Iran. She is an undergraduate student in Electrical Engineering at Arak University of Technology. Her research interests include grounding systems, electrical safety, and optimization methods in power system design. She is currently working on her

Bachelor's thesis, which focuses on the analysis and comparison of single-layer and double-layer grounding systems.

ORCID: 0009-0002-8807-8875

e-mail: mitrakamalabadii@gmail.com



V. Souri, was born on September 22nd of 1985. He received his BSc. in 2007, from the South Tehran Azad University. MSc. in 2012, from Tehran University of Research Sciences, and PhD. in 2021, from the Kashan University, all of them in Electrical Engineering. He has been employed by Bakhtar Regional Electric Company (BREC) since 2008 and has served in undergraduate and managerial positions, and is currently serving as the project manager for Hamedan Transmission and Sub-Distribution Substations. His research interests are: dynamic design of reactive power compensation systems and design and implementation of transmission and sub-distribution power networks.

ORCID: 0009-0002-2490-9270

e-mail: V.souri@brec.ir



A. Fathi, received the BSc. in Electrical and Electronics Engineering in 1996, from Arak University, Arak, Iran. From 1999 to 2001, he worked at the Shazand Thermal Power Plant and Hyundai Company (Korea) as a Quality Control and Instrumentation Engineer. In 2002, he joined the Bakhtar Regional Electric Company, Arak, Iran, where he has served in different technical and managerial positions. His professional experience includes technical planning, power system operation, and electricity network development. Over more than two decades of activity in the power industry, he has contributed to various projects on grid expansion, operational optimization, and long-term technical planning of regional electricity networks. His research and professional interests include power system planning, network operation, grid development, and power system management.
ORCID: 0009-0002-3323-552X
e-mail: A.Fathi@brec.ir



A. Safari, joined the Bakhtar Regional Electric Company (BREC), Arak, Iran, in 2005, where he has served in different technical and managerial positions and is currently serving as deputy of Planning and Research of Bakhtar Regional Electric Company since 2017. His interest are network operation, grid development, power system restoration and operation.
ORCID: 0009-0008-1330-6793
e-mail: A.Safari@brec.ir

Governance and participatory strategies in sustainable water management: a systematic analysis

Rossember Saldaña-Escorcía

Departamento de Ciencias Ambientales y Sanitaria, Universidad Popular del Cesar, Aguachica, Colombia. rsaldanae@unicesar.edu.co

Received: July 7th, 2025. Received in revised form: September 19th, 2025. Accepted: October 10th, 2025.

Abstract

Sustainable water resources management is increasingly recognized as a critical challenge where effective solutions depend not only on public policies, but also on the active participation of local communities. The review utilized a structured methodology, including the PICOC and PRISMA approaches, to analyze relevant literature published from 2010 to 2024. The findings highlight that community participation empowers local stakeholders, fosters responsibility, and integrates both traditional and scientific knowledge for adaptive water management. Furthermore, inclusive water governance frameworks that promote transparency and cooperation among various stakeholders are critical for equitable and effective resource management. Challenges to implementing these strategies include limited access to information, technical capacity, and resistance from some sectors to relinquish control. The review concludes that overcoming these obstacles requires stronger political commitment, capacity building, and the development of regulatory frameworks that support community rights and inter-institutional cooperation.

Keywords: community water; collaboration; bibliometrics; water governance; water management; stakeholders; participation; water resources; literature review; sustainability water.

Gobernanza y estrategias participativas en la gestión sostenible del agua: un análisis sistemático

Resumen

La gestión sostenible de los recursos hídricos se reconoce cada vez más como un reto crítico cuyas soluciones eficaces dependen no solo de las políticas públicas, sino también de la participación activa de las comunidades locales. La revisión utilizó una metodología estructurada, incluyendo los enfoques PICOC y PRISMA, para analizar la literatura relevante publicada entre 2010 y 2024. Los resultados destacan que la participación de la comunidad empodera a las partes interesadas locales, fomenta la responsabilidad e integra tanto el conocimiento tradicional como el científico para la gestión adaptativa del agua. Además, los marcos inclusivos de gobernanza del agua que promueven la transparencia y la cooperación entre las distintas partes interesadas son fundamentales para una gestión equitativa y eficaz de los recursos. Entre los retos que plantea la aplicación de estas estrategias figuran el acceso limitado a la información, la capacidad técnica y la resistencia de algunos sectores a ceder el control. El estudio concluye que para superar estos obstáculos es necesario un mayor compromiso político, la capacitación y el desarrollo de marcos normativos que apoyen los derechos de las comunidades y la cooperación interinstitucional.

Palabras clave: agua comunitaria; colaboración; bibliometría; gobernanza del agua; gestión del agua; partes interesadas; participación; recursos hídricos; revisión bibliográfica; sostenibilidad del agua.

1 Introduction

Sustainable water resource management is a crucial challenge today, where scarcity, climate change and pollution

generate adverse effects on ecosystems and thus on communities [1]. In this scenario, the participation of local communities in the structuring and implementation of governance strategies is key in the search for solutions

How to cite: Saldaña-Escorcía, R., Governance and participatory strategies in sustainable water management: a systematic analysis DYNA, (92)239, pp. 72-81, October - December, 2025.

adapted to real contexts. These two dimensions are closely related and mutually reinforcing, since sustainable water management depends not only on public policies and technical decisions, but also on the active collaboration of the communities, since they are the most affected by changes in the availability and quality of the resource [2,3].

Community participation in the sustainable management of natural resources is an approach that seeks to include the inhabitants of the communities in decision-making related to conservation and environmental sustainability, especially in water governance processes [4,5]. This type of participation is based on the idea that communities have direct knowledge of their environment and can therefore offer more effective and contextually appropriate solutions [6]. Similarly, the active participation of local communities in decision-making processes stimulates and increases their sense of responsibility and commitment by promoting their involvement in the implementation and monitoring of water policies [7]. In this way, sustainable water management becomes a dynamic and participatory process that integrates the knowledge, skills and experience of the community [8], [9]. On the other hand, water governance includes decision-making processes, regulatory structures and the institutional capacity to regulate water use, as well as resource allocation and conservation [10]. Effective water governance has clear mechanisms for participation and dialogue among key stakeholders, but most of all with local communities [11].

In other words, inclusive and transparent governance ensures that voices are representative within the processes and that the policies structured and implemented respond to the real contexts and situations of the different social groups, especially the most vulnerable. This is why governance should not be understood purely as rules or regulations but as a complex and continuous process of interaction and/or cooperation among key actors [12,13]. However, the implementation of community participation and water governance strategies faces several challenges. Among the most common are the lack of access to relevant information, the limited technical capacity of communities to participate in complex processes, and the resistance of some sectors to cede control of water management [14–16]. Overcoming these obstacles requires not only strong political commitment, but also the strengthening of local capacities through education, training and empowerment of community actors. It is also necessary to develop regulatory frameworks that facilitate effective participation, guarantee community water rights, and promote inter-institutional cooperation [17–19].

The main objective of this review is therefore to identify the governance or community-based strategies that have been applied in sustainable water resources management, but also to describe the main advantages of using governance or community-based strategies for sustainable water resources management. The structure of the document begins with an introduction to the subject followed by a description of the method used to achieve the objective. In addition, the results section highlights the main contexts, followed by a discussion of the impact of community participation and governance strategies on sustainable water resource management. Finally, you will find the conclusions where we

contextualize and/or highlight the gaps in knowledge that can be addressed in another research.

2 Materials and methods

This systematic review seeks to identify participatory strategies in sustainable water management with a governance approach. Therefore, following the PICOC and PRISMA recommendations, this review has three phases: planning, implementation and reporting [20,21]. Likewise, the systematic analysis of the literature was supported by the use of Mendeley (Version 1.19.8) for reference management, Microsoft Excel 365 for the selection and exclusion of studies, and VOSviewer for the structuring of the cooccurrence networks (1.6.19.0) [22–24].

2.1 Planning the review

This part of the review involved structuring the search strategy for specialized information published on the topic in question in order to address the research questions posed for the analysis. Table 1 shows the questions that will guide the review.

Once the questions were defined and the scope of the systematic review of the literature on the subject was defined, we followed the PICOC method approach (see Table 4) [25,26] proposed by Petticrew y Roberts [27].

Table 1.
Questions and objectives of the research work.

	Questions	Objectives
RQ1	What governance or community strategies have been effective for sustainable water resource management?	Identify the governance or community strategies that have been implemented in the sustainable management of water resources.
RQ2	What are the main advantages of using governance or community-based strategies for sustainable water resource management?	Identify the main benefits of using governance or community-based strategies for sustainable water resource management

Source: Created by the author

Table 2.
PICOC method.

Criteria	Descriptions
Population	Publications on participatory strategies in sustainable water management with a governance approach.
Intervention	Available engagement strategies, efficiency of community engagement strategies, approaches to governance strategies.
Comparison	Compare existing community engagement strategies.
Outcome	Understanding and optimizing participatory strategies in sustainable water management from a governance approach.
Context	Conservation of water resources.

Source: Created by the author

Table 3.

List of keywords, synonyms, and relationships

Keyword	Synonyms
Water governance	Community participation, water administration, social involvement,
Water resources	Water sources, water reserves, water supply
water resource management	Water management, water resources management, water use control

Source: Created by the author

In Table 3, the keywords and synonyms were structured under the PICOC criteria, with which the organization of the problem analysed with the search of the documents within the systematic review of the literature was established.

For the search criteria, the search algorithm, inclusion criteria and exclusion criteria were considered (see Table 4). The key words used were water resources, water governance, community participation and water resource management, and the inclusion criteria were English and Spanish language, time range 2010 - 2024, open access and complete document; while the exclusion criteria were related to non-compliance with the time range, publication characteristics, as well as type of document.

The relevant aspects of the scientific articles were determined through the extraction of the information (see Table 5), allowing the effective selection of the documents related to the topic in question.

The specialized Scopus® database was searched for research articles related to the topic. The following search algorithm was used ("Community participation" OR "Social involvement" OR "Water governance" OR "water administration") AND ("water resources" OR "water sources" OR "water reserves" OR "water supply") AND ("water resource management" OR "Water management"). The final search was performed on March 09, 2025 and 1549 studies were found. Each article was evaluated for relevance to the study and articles that did not meet the eligibility requirements were eliminated (see Fig. 1).

Table 4.

Search criteria.

Key	Criteria
Search string	TITLE-ABS-KEY (("Community participation" OR "Social involvement" OR "Water governance" OR "water administration") AND ("water resources" OR "water sources" OR "water reserves" OR "water supply") AND ("water resource management" OR "Water management")) AND PUBYEAR > 2009 AND PUBYEAR < 2025 AND (LIMIT-TO (DOCTYPE , "ar")) AND (LIMIT-TO (LANGUAGE , "English") OR LIMIT-TO (LANGUAGE , "Spanish")) AND (LIMIT-TO (OA , "all"))
Intervention criteria	Academic Journals (Peer-reviewed); Filtering by Keyword: Community water, water governance, water management, water sustainability, water resources, participation and collaboration. Language: English and Spanish; Full Text; Publication Date: 2010–2024.
Exclusion criteria	Documents other than research articles, outside the time range and not fulfilling the objective of the analysis.
Search mode	Apply to title, abstract and keywords.

Source: Created by the author

Table 5.

Relevant fields for data extraction

Fields	Descriptions
Reference	It provides information necessary to locate other original documents, including authors, title, name of the journal or conference, volume, number, pages, year of publication, among other details.
Publication	Specify the medium where the work was published, such as scientific journals, books, conferences, repositories, etc. You may also include details such as the name of the publisher or the volume and number of the publication if relevant.
Year	Indicates the year in which the work was published.
Main idea	Summarizes concisely the main objective or central idea of the research work.
Gaps	This identifies areas not covered or limitations of previous research that the article or study addresses.
Major contributions	Most relevant findings or main contributions of the study
Methodology	Details the methodological approach used to conduct the study. This includes the type of research (qualitative, quantitative, mixed), data collection methods, data analysis, and any models or techniques used in the research.
Results	Provide the results of the research. They may include quantitative findings, patterns, trends, or general conclusions derived from the data analysis.
Limitations	Indicates any constraints that might have influenced the results or the generalization of the findings.

Source: Created by the author

2.2 Selection criteria

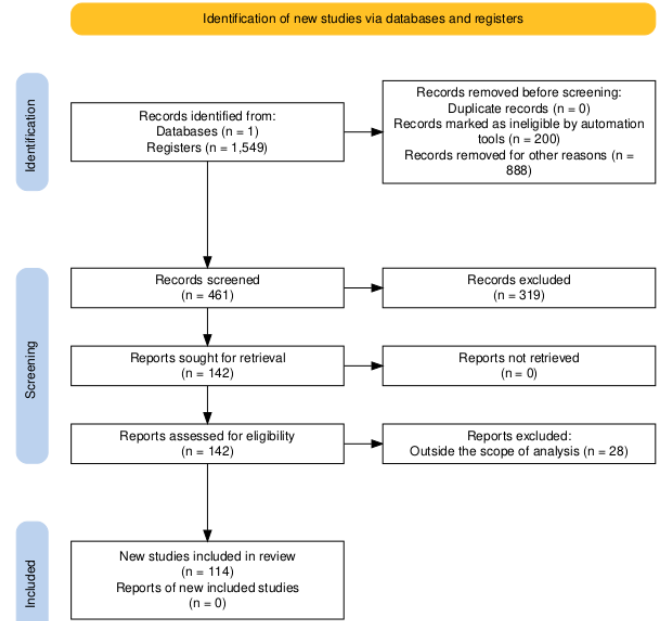


Figure 1. PRISMA 2020 flow chart for systematic reviews.

Source: Own elaboration based on Haddaway et al. [21]

2.3 Performing the review

A structured framework for data extraction was developed to systematically collect relevant information to address the research questions. This framework includes key aspects such as title, year of publication, strategy used, results, country of study,

key concepts, limitations reported, and major findings or gaps identified that require further research (see Table 5). To carry out this process, the researchers reviewed each article individually and used a detailed content analysis to extract the relevant data supported by Excel and VOSviewer (Co-occurrence and density map, which allows the structure, evolution and dynamics of a scientific field to be determined, helping to identify trends, research gaps and opportunities for collaboration).

2.4 Review report

This step corresponds to the process of documenting and presenting the findings of the review in a clear and transparent manner. Its importance lies in ensuring both the reproducibility and reliability of the results, allowing readers to assess the rigor and validity of the study. Details of the findings obtained are presented in the following section.

3 Results and discussion

This section may be divided by subheadings. It should provide a concise and precise description of the experimental results, their interpretation, as well as the experimental conclusions that can be drawn

3.1 Literature review

RQ1: What governance or community strategies have been effective for sustainable water resource management?

Governance and community participation strategies have proven to be fundamental for the sustainable management of water resources, particularly in contexts marked by scarcity and climate change. These practices, in addition to increasing water use efficiency, contribute to strengthening the social fabric and promote equity in access to the resource, which is essential to ensure long-term sustainability.

Within this framework, one of the most effective strategies is collaborative governance, understood as the formation of networks made up of local governments, communities and other relevant stakeholders. Such networks allow the articulation of resources, knowledge and institutional capacities, which favours coordinated and more efficient water management [8,28].

Complementarily, social capital plays a key role in the success of these strategies. The generation and strengthening of bonds of trust and cooperation, both within communities (bridging social capital, this refers to the connections that individuals or social groups with different characteristics or interests have with one another. These links enable them to share information, resources or influence) and between different social and institutional groups (bonding social capital, it refers to close, trusting relationships within a group. These bonds facilitate cooperation and the fulfilment of shared duties, but must be combined with external factors to avoid exclusion and the adoption of innovations by outside actors), promotes greater social cohesion [29, 30].

In governance processes, both types of social capital complement each other, since bonding capital provides cohesion and local legitimacy, while bridging capital broadens the scale of management. This helps to introduce new ideas within groups,

reducing asymmetry with external actors [31,32]. It is also crucial to identify and include central actors within governance networks. Figures such as community leaders, local authorities or key institutions can act as catalysts for dialogue and articulation between sectors [11,13,15]. Their role facilitates the circulation of information, the establishment of alliances, and, consequently, the implementation of more effective management strategies. These actors often engage through specific mechanisms that translate shared objectives into coordinated actions — such as intergovernmental coordination councils, technical development committees, sectoral intergovernmental commissions, basin councils, and water committees — which function as forums for dialogue and consultation, as well as citizen observatories for water conservation [33–35].

On the other hand, the structuring of shared objectives and agreements among key stakeholders allows the efficient allocation of resources, as well as promotes joint solutions to socio-environmental challenges. The existence of these agreements favours the alignment of interests, reinforcing the collective commitment to the integrated management of water resources [36,37]. In this sense, the use of quantitative techniques and tools such as the Water Governance Indicator Framework (36 indicators broken down into four pillars: effectiveness, efficiency, reliability and inclusiveness), the WWAP - Water Governance Score (UNESCO-WWAP; 12 dimensions), the Integrated Water Resources Management Index (33 indicators), geodata, and the Analytic Hierarchy Process for data-based decision-making are essential for monitoring and evaluating the performance of community governance networks [38–40]. These tools can highlight areas for improvement, facilitating the design of precise interventions adapted to the real needs of the territory.

Likewise, it is essential to promote spaces for dialogue and continuous communication among the actors for the creation or strengthening of trust. This continuous communication not only supports relations between institutions, but also promotes the commitment and motivation of the actors in the medium and long term, which generates greater capacity in the implementation of collective actions in sustainable water management. [41–43]. Moreover, it is necessary to adapt the strategies to the specific conditions of each territory, considering the socioeconomic, cultural and environmental factors that allow the structuring and implementation of contextualized and relevant policies that effectively respond to local challenges.

RQ2: What are the main advantages of using governance or community-based strategies for sustainable water resource management?

Water governance strategies, especially community-based ones, offer advantages that contribute to structuring more effective and equitable solutions. In the first instance, such strategies enhance the collaboration and engagement of local communities, government agencies and non-governmental organizations [44,45]. This inclusive approach gathers stakeholder perspectives, resulting in sound decisions that reflect needs and priorities [42,46–48].

In addition, the incorporation of communities provides local knowledge and traditions as a strength within the strategies, since water governance models that are based on indigenous practices, cultural perceptions and historical

conceptions of sustainable water management make solutions more adaptable, relevant to the context and accepted by key stakeholders [38,49–51]. This localized knowledge not only enriches the decision-making process but also promotes more effective and sustainable management practices.

Another key advantage is the strengthening of local actors' technical knowledge [52] and their involvement in planning and decision making generates greater ownership leading to transparent processes between local authorities and local communities [10,53–55]. This approach also increases local leadership capacities, allowing communities to learn to manage their water resources more independently and effectively over time.

Community-based governance and strategies also foster greater adaptive capacity and innovation. These practices support flexible management, enabling governance structures to respond nimbly to environmental changes such as climate variability, pollution or population growth [56–58]. This adaptive capacity is key to facing new challenges and uncertainties. In most of these strategies, the collaborative approach drives innovation, as diverse actors come together to create joint solutions and share ideas that might not emerge in more centralised or vertical management models [50,57,59].

These approaches strengthen the resilience of water systems and communities. By promoting social cohesion and trust among community members, they build stronger support networks that are better able to cope with water-related crises and environmental stresses such as droughts, floods or resource depletion [60–62]. Long-term commitment and the development of lasting relationships with stakeholders also help water management efforts to be sustained over time, favouring the ecological sustainability of water resources.

They also promote transparency and accountability. Community governance systems often have more open decision-making processes, allowing stakeholders to hold decision-makers accountable and ensure that water management is in the public interest [18,63]. This transparency is essential to build trust among stakeholders and ensure the necessary support for successful initiatives [19, 64,65]. Additionally, the collaborative nature of these strategies facilitates early detection and resolution of conflicts, helping to resolve disputes before they escalate.

Taken together, these benefits show how community-based governance and strategies can contribute to more sustainable, resilient and equitable water resources management. By integrating local knowledge, empowering communities, fostering collaboration, and promoting adaptive and innovative solutions, these strategies offer a pathway to long-term sustainable water management, both environmentally and socially.

3.2 Bibliometric analysis

3.2.1 Publication date

Fig. 2 shows the distribution of research articles published annually, reflecting the growing interest in the

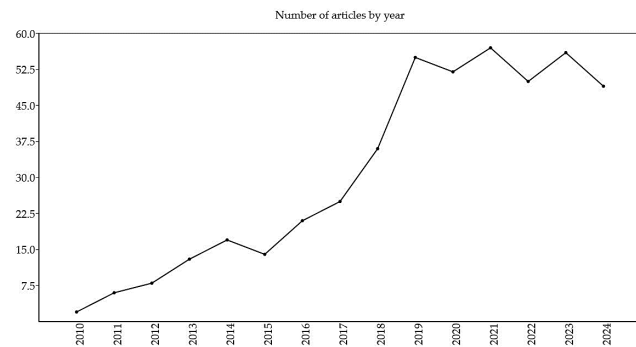


Figure 2. Published studies by year of publication.

Source: Own elaboration based on data retrieved from Scopus. The search was conducted using the keywords listed in 4, in the search string row, covering the period from 2010 to 2024.

formulation and implementation of participatory strategies and/or governance in sustainable water management. The data obtained indicate a progressive increase in publications on the subject between the time range analyzed (2010-2024), with downward peaks in 2015, 2020, 2022 and 2024. This increase in scientific activity related to the topic can be attributed to the management of different governments, as well as to international agreements for the conservation and proper management of water resources. For the year 2020, there will be a lower number of publications, mainly due to the disruption caused by the COVID-19 pandemic, which affected the financing and implementation of multiple strategies worldwide.

Although in 2021, the number of publications increased, this was due to documents and issues held back in journals worldwide as they prioritized pandemic-focused research, however, by 2022 a decrease in publications can be observed due to limitations in data collection needed for community-level water management studies, the shift of interest in the subject matter redirected towards public health and water management issues.

3.2.2 Location of the studies

Fig. 3 shows the distribution of publications by country on the formulation and implementation of participatory strategies and/or governance in sustainable water management, which shows a tendency of concentration in Asian and European countries, although there is an increase in developing countries.

The United States tops the list with 96 studies, representing 12.12% of the total number of publications in the time range analyzed, reflecting the interest in facing the challenges of water resource conservation and management. This is due to changes in climate variability within the territory, specifically in the West, where overexploitation of aquifers and drought have created problems of availability, as well as pollution generated by wastewater discharges, agricultural chemicals and industrial pollutants that affect water quality.

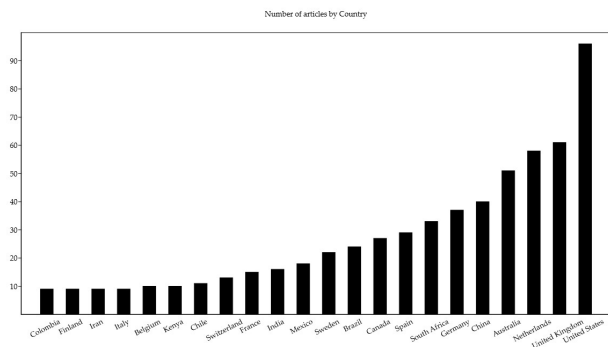


Figure 3. Geographic distribution of studies.

Source: Own elaboration based on data retrieved from Scopus. The search was conducted using the keywords listed in Table 4, in the search string row, covering the period from 2010 to 2024.

The United Kingdom, with 7.7%, faces water resource management in relation to infrastructure modernization, storm drains and agricultural runoff. Netherlands, with 58 studies, has a high dependence on flood control systems and water resources for agriculture. Australia, with 51 studies, has frequent and severe droughts, which directly impacts water availability, as well as an excessive use of water resources in agriculture.

China, with 5.05%, struggles with increasing urban and industrial demand as well as a high percentage of polluted water resources from industrial and agricultural waste. Germany, with 37 publications, is facing the effects of climate change in relation to water availability and water quality, which in turn is caused by the presence of nitrates and chemicals in the water.

South Africa, with 4.17%, has changes in rainfall affecting water availability, especially in rural areas, where access to drinking water is limited. While Spain, Canada and Brazil (more than 3.0% of the publications) present problems to be solved in relation to watershed management and pollution in rivers, especially in urban areas.

Finally, countries such as Sweden, Mexico, India, France, Switzerland, Chile, Belgium, Kenya, Colombia, Finland, Iran, Italy, Indonesia, Nepal, Ethiopia, Japan, Pakistan, Thailand, Austria, Bangladesh, Cambodia, Denmark, Ireland, Malaysia, Philippines, Singapore, Sri Lanka, Argentina, Ecuador, Hong Kong, Peru, South Korea, Bolivia, Ghana, Greece, Mongolia, Portugal, Tanzania, Turkey, Uruguay, Vietnam, Algeria, Botswana, Costa Rica, Czech Republic, Egypt, Laos, Lebanon, Malawi, New Zealand, Nigeria, Norway, Palestine, Saudi Arabia, Slovenia, Uganda, Uzbekistan, Afghanistan, Burkina Faso, Congo, Georgia, Iraq, Kazakhstan, Nicaragua, Poland, Romania, Tonga, Tunisia, Türkiye, Zimbabwe has between 0.13% to 2.78% of the publications; being isolated efforts but significant contributions to the conservation and management of water resources.

3.2.3 Publication by authors

The increasing production of papers suggests a growing interest and an urgent need to address water-related problems (see Fig. 4). Koop, S. stands out as the author with the highest number of papers (8), suggesting a significant contribution to the field.

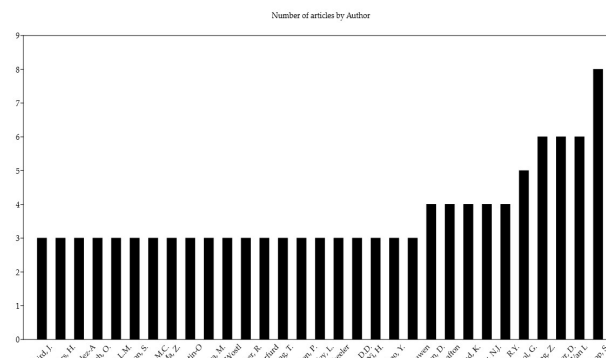


Figure 4. Distribution by authors of the studies.

Source: Own elaboration based on data retrieved from Scopus. The search was conducted using the keywords listed in Table 4, in the search string row, covering the period from 2010 to 2024.

Cheng, Z., Vollmer, D., and van Leeuwen, K. are also prominent authors, each with 6 publications, indicating that they are active in water-related research and strategy development.

Another prominent author with 5 publications is Özerol, G., while authors such as Benson, D., Grafton, R.Q., Shaad, K., Souter, N.J. and Wang, R.Y. each have 4 publications. The published studies reflect trends in specific topics, such as the impact of climate change on water resources or water use efficiency in agriculture.

3.2.4 Co-occurrence network analysis

The co-occurrence map generated with VOSviewer graphically (see Fig. 5) represents the interrelationships between key concepts in the field of water management and governance, allowing the identification of thematic clusters that reflect the main lines of scientific research. In the maps, thematic clusters are formed from co-occurrence networks of keywords, co-authorship, or citations; each node represents an element of analysis, while the size indicates the relative weight (frequency or link strength) [22]. Based on the analysis of the groups, different interconnected approaches that address water resources from technical, social, environmental and institutional dimensions become evident.

One of the core areas is water management, where terms such as water management, climate change, irrigation and water security are articulated to reflect the operational challenges in contexts of growing water pressure, climate variability and the need for efficiency in the use of the resource, particularly in sectors such as agriculture. This technical approach is complemented by a second group focused on water governance, which incorporates terms such as water governance, governance approach, policy making and integrated water resources management. This group reflects the need for robust institutional frameworks, integrated public policies and participatory planning that orients decision making towards sustainability.

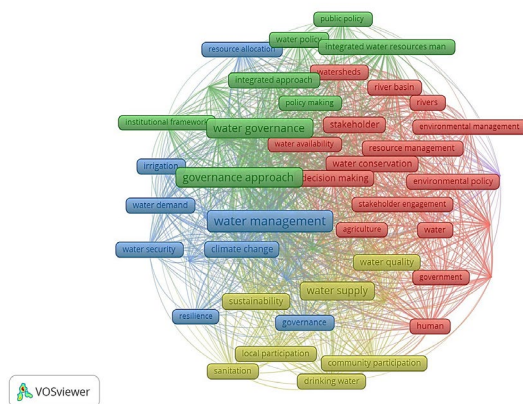


Figure 5. Co-occurrence network map keywords.

Source: Own elaboration based on data retrieved from Scopus. The search was conducted using the keywords listed in Table 4, in the search string row, covering the period from 2010 to 2024.

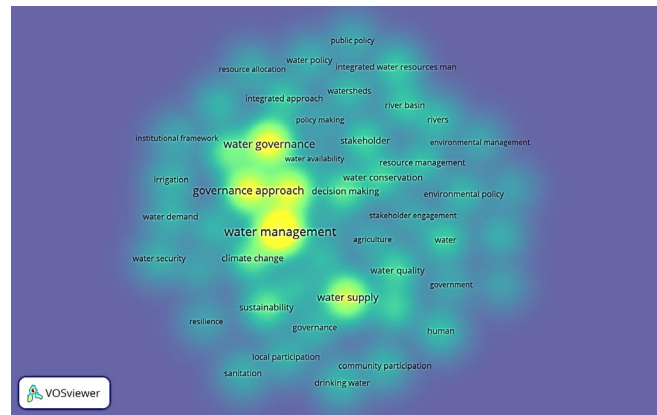


Figure 6. Keyword density map.

Source: Own elaboration based on data retrieved from Scopus. The search was conducted using the keywords listed in Table 4, in the search string row, covering the period from 2010 to 2024.

A third thematic core groups aspects related to the interaction between stakeholders and environmental management. Terms such as stakeholder, resource management, decision making, and environmental policy reflect the importance of considering the various social, economic, and institutional actors in the processes of water conservation and use. Shared decision making and multi-stakeholder participation are presented as strategic elements in the implementation of effective and equitable policies [66–69]. Finally, a group of concepts associated with sustainability, citizen participation and equitable access to water are identified. Terms such as water supply, water quality, community participation, resilience and drinking water show the need to integrate approaches focused on human wellbeing, equity and public health, also considering resilience to extreme climate events and the inclusion of local communities in management processes.

The connectivity between these clusters reveals the multidimensional nature of water governance, highlighting the importance of interdisciplinary approaches that integrate technical, environmental, institutional and social knowledge. The strong co-occurrences between terms from different clusters, such as climate change with sustainability or governance approach with stakeholder engagement, indicate that sustainable solutions require coordinated strategies that consider both management efficiency and legitimacy in decision-making processes [37,70,71]. In this sense, research and policy formulation should be oriented towards integrated models of water governance, with a territorial approach, active participation of stakeholders and a long-term vision focused on sustainability and equity.

On the other hand, in the density map (see Fig. 6) the highest density, indicated by the warmest colours (intense yellow), is concentrated around the terms water management, governance approach and water governance. This grouping reveals a strong scientific interest in the operational and institutional aspects of water resource management, highlighting the need for integrated approaches that articulate public policies, stakeholder participation, institutional frameworks and sustainability strategies [72,73]. The

simultaneous presence of these concepts indicates that current studies are not limited to water use efficiency, but also critically address the governance structures that regulate water use.

The concept of climate change appears very close to the central core, indicating a strong association with water management. This proximity suggests that the impacts of climate change, such as variability in resource availability and increased extreme events, are being addressed in a cross-cutting manner in water governance and planning studies [74–76]. This relationship evidences the need to strengthen the resilience and adaptability of water management systems in the face of uncertain climatic contexts. Also, on the periphery of the main core, there is a technical cluster related to irrigation, water demand, water security, resource allocation and integrated water resources management [77–80]. This grouping points to the interest in optimizing resource allocation, especially in sectors such as agriculture, through integrated planning tools. The connection between these terms and those of the governance cluster suggests a technical-institutional approach that seeks to harmonize operational efficiency with principles of equity and sustainability.

Another thematic cluster is located towards the right side of the map, and includes concepts such as stakeholder, environmental management, resource management, decision making and environmental policy. This cluster reflects the participatory and environmental dimension of water management, in which the involvement of various social actors is crucial to reach consensual and sustainable decisions. The emergence of stakeholder engagement as a point of intersection reaffirms the relevance of the collaborative approach in water governance processes.

In the lower zone, there are terms such as sustainability, resilience, community participation, local participation and drinking water, which form a cluster more focused on the social and human aspects of access to water. This cluster highlights the importance of guaranteeing the human right to water, equity in its distribution and the active participation of local communities in its management.

Moreover, the proximity of these concepts to governance and water supply indicates an interdependence between governance structures and conditions for equitable access.

Therefore, in order to strengthen the capacities of community actors in water governance, it is essential to develop technical, leadership, and participatory planning capacities based on the integration of social, environmental, and cultural dimensions [81]. Likewise, it is necessary to structure alliances with territorial or political entities, and academic institutions, allowing them to participate in spaces such as science committees or water observatories [82]. It is essential to make traditional knowledge visible and integrate it into the dialogue with authorities, adapting it to intercultural approaches and proposing public policies that integrate territorial aspects of the right to water.

Overall, the density map reveals an interrelated thematic structure that articulates the technical, institutional, environmental, and social dimensions of water resources management. The overlapping of densities among groups of actors underscores the need for inter- and transdisciplinary approaches to enhance the integration of scientific knowledge into participatory governance and sustainability processes [83,84]. These findings also highlight the importance of strengthening community participation and multi-stakeholder networks, which has direct implications for public policy formulation. At both local and national levels, it is essential to design more participatory regulatory frameworks that recognize and formalize coordination spaces among communities, authorities, and institutions. Moreover, establishing incentives for inter-institutional collaboration and knowledge exchange is particularly important in diverse territorial contexts. Integrating local knowledge, ensuring effective consultation mechanisms, and supporting community training processes can improve the understanding of complex water systems while contributing to the design of inclusive, legitimate, and context-sensitive water governance strategies.

4 Conclusions

Within the sustainable management of water resources, community governance strategies play a fundamental role since, by promoting collaboration between parties such as local communities, social or environmental non-governmental organizations, as well as governments, it is possible to structure strategies based on integral, transparent processes that are adjusted to realities. The incorporation of ancestral or local knowledge improves relevance and increases the acceptance of sustainable management practices by the communities, promoting ownership and responsibility. Similarly, the strategies promote innovation and adaptability allowing water management systems to be more effective in relation to today's socio-environmental challenges. Ultimately, the integration of technical, institutional and social approaches to these strategies contributes to the long-term sustainability and equity of water resources management.

References

- [1] Latiff, N., and Marimuthu, F., Water-related sustainability reporting practices amongst South African mining and non-mining corporations. *Environmental Economics*, 12(1), pp. 112–123, 2021. DOI: [https://doi.org/10.21511/ee.12\(1\).2021.10](https://doi.org/10.21511/ee.12(1).2021.10)
- [2] River-OfLife, M., Taylor, K.S., and Poelina, A., Living waters, law first: Nyikina and Mangala water governance in the Kimberley, Western Australia. *Australian Journal of Water Resources*, 25(1), pp. 40–56, 2021. DOI: <https://doi.org/10.1080/13241583.2021.1880538>
- [3] Salamanca-Cano, A.K., and Durán-Díaz, P., Stakeholder engagement around water governance: 30 years of decision-making in the Bogotá River Basin. *Urban Science*, 7(3), art. 81, 2023. DOI: <https://doi.org/10.3390/urbansci7030081>
- [4] Salomé, B.O., Torres, J.Z., Sánchez, S.G., Agis, A.J., and González, M.R., Gestión del agua, perspectiva desde la vulnerabilidad socioambiental: área periurbana Acapulco Guerrero México. *Tecnología y Ciencias del Agua*, 15(4), pp. 220–271, 2024. DOI: <https://doi.org/10.24850/j-tyca-2024-04-06>
- [5] Daluwatte, D.D.S., and Sivakumar, S., Community-based water governance for adaptation to water reduction and scarcity in Badulla district of Sri Lanka. *Journal of Water and Climate Change*, 13(2), pp. 451–462, 2022. DOI: <https://doi.org/10.2166/wcc.2021.382>
- [6] Kabogo, J.E., Anderson, E.P., Hyera, P., and Kajanja, G., Facilitating public participation in water resources management: Reflections from Tanzania. *Ecology and Society*, 22(4), art. 26, 2017. DOI: <https://doi.org/10.5751/ES-09739-220426>
- [7] Paerregaard, K., Governing water in the Andean community of Cabanaconde, Peru. *Mountain Research and Development*, 33(3), pp. 207–214, 2013. DOI: <https://doi.org/10.1659/MRD-JOURNAL-D-12-00107.1>
- [8] Tinoco, C., et al., Water resources management in Mexico, Chile and Brazil: Comparative analysis of their progress on SDG 6.5.1 and the role of governance. *Sustainability*, 14(10), art. 14, 2022. DOI: <https://doi.org/10.3390/su14105814>
- [9] Burnham, M., Ma, Z., Endter-Wada, J., and Bardsley, T., Water management decision making in the face of multiple forms of uncertainty and risk. *Journal of the American Water Resources Association*, 52(6), pp. 1366–1384, 2016. DOI: <https://doi.org/10.1111/1752-1688.12459>
- [10] Fernández-Vargas, G., Water governance as an integrating framework for the fulfillment of the sustainable development goals clean in Latin America. *Revista U.D.C.A Actualidad y Divulgación Científica*, 23(2), art. 61, 2020. DOI: <https://doi.org/10.31910/rudca.v23.n2.2020.1561>
- [11] Adom, R.K., and Simatele, M.D., The role of stakeholder engagement in sustainable water resource management in South Africa. *Natural Resources Forum*, 46(4), pp. 410–427, 2022. DOI: <https://doi.org/10.1111/1477-8947.12264>
- [12] Gutenson, J.L., Ernest, A.N.S., Bearden, B.L., Fuller, C., and Guerrero, J., Integrating societal and scientific elements into sustainable and effective water resource policy development. *Journal of Environmental Informatics Letters*, 4(2), pp. 101–108, 2020. DOI: <https://doi.org/10.3808/jeil.202000048>
- [13] Montenegro, L., and Hack, J., A socio-ecological system analysis of multilevel water governance in Nicaragua. *Water (Switzerland)*, 12(6), art. 76, 2020. DOI: <https://doi.org/10.3390/W12061676>
- [14] Chan, N.W., Roy, R., and Chaffin, B.C., Water governance in Bangladesh: An evaluation of institutional and political context. *Water (Switzerland)*, 8(9), art. 3, 2016. DOI: <https://doi.org/10.3390/w8090403>
- [15] Nixon, R., Ma, Z., Khan, B., Birkenholtz, T., Lee, L., and Mian, I., A. Social influence shapes adaptive water governance: empirical evidence from northwestern Pakistan. *Ecology and Society*, 27(3), art. 37, 2022. DOI: <https://doi.org/10.5751/ES-13546-270337>
- [16] Romero-Lankao, P., Gnatz, D.M., Lloyd, S.J., and Bush, K., How urban governance shapes water, sanitation, and hygiene services in informal settlements of Latin America. *Environmental Science and Policy*, 130, pp. 37–46, 2022. DOI: <https://doi.org/10.1016/j.envsci.2021.12.018>

- [17] Jacobi, P.R., Cibim, J., and Souza, T., Governança das águas e os desafios da participação cidadã. *Estudos Avançados*, 30(88), pp. 63–76, 2016. DOI: <https://doi.org/10.1590/S0103-40142016.30880006>
- [18] Rojas, J., and Fernández, R., Participación comunitaria y gestión integral del recurso hídrico en América Latina. *Revista de Estudios Ambientales*, 12(3), pp. 45–62, 2019.
- [19] Li, Z., and Fang, Y., Stakeholder collaboration in watershed governance: evidence from China. *Water Policy*, 25(1), pp. 12–28, 2023. DOI: <https://doi.org/10.2166/wp.2022.216>
- [20] Gómez, A., and Martínez, D., La gobernanza hídrica en territorios rurales de Colombia: desafíos y oportunidades. *Revista Gestión y Ambiente*, 25(1), pp. 87–104, 2022. DOI: <https://doi.org/10.15446/ga.v25n1.94872>
- [21] Molle, F., River-basin planning and management: the social life of a concept. *Geoforum*, 40(3), pp. 484–494, 2009. DOI: <https://doi.org/10.1016/j.geoforum.2009.03.004>
- [22] Boelens, R., and Seemann, M., Forced engagements: water security and local rights formalization in Yanque, Colca Valley, Peru. *Human Organization*, 73(1), pp. 1–12, 2014. DOI: <https://doi.org/10.17730/humo.73.1.v3k744q5q1531350>
- [23] Gutiérrez, R.A., and Portocarrero, J., Comunidades campesinas y gestión del agua en los Andes peruanos. *Revista Latinoamericana de Estudios Rurales*, 6(11), pp. 85–104, 2021.
- [24] Tortajada, C., Water governance: some critical issues. *International Journal of Water Resources Development*, 26(2), pp. 297–307, 2010. DOI: <https://doi.org/10.1080/07900621003683298>
- [25] Hoogesteger, J., Trans-forming social capital around water: water user organizations, water rights, and equity in Ecuador. *Society and Natural Resources*, 28(2), pp. 132–148, 2015. DOI: <https://doi.org/10.1080/08941920.2014.945057>
- [26] Delgado, L.E., and Marín, V.H., Ecosystem governance for sustainability in Chile: Progress and challenges. *Environmental Science and Policy*, 78, pp. 60–69, 2017. DOI: <https://doi.org/10.1016/j.envsci.2017.09.002>
- [27] Villamayor-Tomas, S., and García-López, G., Social movements as key actors in groundwater governance: The case of Spain and Mexico. *Water Alternatives*, 11(3), pp. 725–748, 2018.
- [28] Peña, F.J., and Calizaya, A., Gestión comunitaria del agua en los Andes bolivianos: desafíos frente al cambio climático. *Revista de Geografía Norte Grande*, 73, pp. 123–142, 2019. DOI: <https://doi.org/10.4067/S0718-34022019000200123>
- [29] Bixler, R.P., Dell’Angelo, J., and Mfune, O., The politics of participation in water governance: from theory to practice. *Ecology and Society*, 25(2), art. 4, 2020. DOI: <https://doi.org/10.5751/ES-11425-250204>
- [30] Scott, C.A., and Banister, J.M., The dilemma of water governance in Mexico: Institutional conflicts and sustainability challenges. *Geoforum*, 85, pp. 1–9, 2017. DOI: <https://doi.org/10.1016/j.geoforum.2017.07.018>
- [31] Arias, M.E., and Coello, J., Participatory water governance: Lessons from rural Honduras. *Water International*, 47(3), pp. 332–348, 2022. DOI: <https://doi.org/10.1080/02508060.2022.2068741>
- [32] Wester, P., Hoogesteger, J., and Vincent, L., Local IWRM organizations for groundwater governance in Mexico. *Water Alternatives*, 3(1), pp. 82–101, 2010.
- [33] Calderón, F., and Díaz, P., Conflictos por el agua y participación comunitaria en territorios indígenas de México. *Revista de Estudios Sociales*, 74, pp. 45–59, 2021. DOI: <https://doi.org/10.7440/res74.2021.05>
- [34] Ahlers, R., and Zwartveen, M., The water question in feminism: Water control and gender inequities in Mexico. *Gender, Place & Culture*, 16(4), pp. 415–432, 2009. DOI: <https://doi.org/10.1080/09663690903003945>
- [35] Budds, J., Power, nature and neoliberalism: the political ecology of water in Chile. *Singapore Journal of Tropical Geography*, 25(3), pp. 322–342, 2004. DOI: <https://doi.org/10.1111/j.0129-7619.2004.00189.x>
- [36] Chatterjee, D., and Bhattacharya, P., Participatory water governance and livelihood security: case studies from India. *Water Policy*, 23(4), pp. 1098–1115, 2021. DOI: <https://doi.org/10.2166/wp.2021.020>
- [37] Miranda, L., and Navarrete, M., Gobernanza hídrica y gestión participativa en comunidades rurales del norte de Chile. *Revista de la Facultad de Ciencias Ambientales*, 16(2), pp. 65–79, 2020.
- [38] Rijsberman, F.R., Water scarcity: fact or fiction? *Agricultural water management*, 80(1–3), pp. 5–22, 2006. DOI: <https://doi.org/10.1016/j.agwat.2005.07.001>
- [39] Seemann, M., Inclusive water governance: a framework for integrating community perspectives in water policy. *World Development*, 131, art. 104952, 2020. DOI: <https://doi.org/10.1016/j.worlddev.2020.104952>
- [40] Boelens, R., Hoogesteger, J., and Baud, M., Water reform governmentality in Ecuador: Neoliberalism, centralization, and the restraining of polycentric authority and community rule-making. *Geoforum*, 57, pp. 281–293, 2014. DOI: <https://doi.org/10.1016/j.geoforum.2014.08.020>
- [41] Ostrom, E., A diagnostic approach for going beyond panaceas. *Proceedings of the National Academy of Sciences*, 104(39), pp. 15181–15187, 2007. DOI: <https://doi.org/10.1073/pnas.0702288104>
- [42] Huitema, D., Mostert, E., Egas, W., Moellenkamp, S., Pahl-Wostl, C., and Yalcin, R., Adaptive water governance: assessing the institutional prescriptions of adaptive (co-) management from a governance perspective and defining a research agenda. *Ecology and Society*, 14(1), art. 26, 2009. DOI: <https://doi.org/10.5751/ES-02827-140126>
- [43] Pahl-Wostl, C., Transitions towards adaptive management of water facing climate and global change. *Water Resources Management*, 21(1), pp. 49–62, 2007. DOI: <https://doi.org/10.1007/s11269-006-9040-4>
- [44] Lebel, L., Anderies, J.M., Campbell, B., Folke, C., Hatfield-Dodds, S., Hughes, T.P., and Wilson, J., Governance and the capacity to manage resilience in regional social-ecological systems. *Ecology and Society*, 11(1), art. 19, 2006. DOI: <https://doi.org/10.5751/ES-01606-110119>
- [45] Pahl-Wostl, C., Holtz, G., Kastens, B., and Knieper, C., Analyzing complex water governance regimes: The management and transition framework. *Environmental Science and Policy*, 13(7), pp. 571–581, 2010. DOI: <https://doi.org/10.1016/j.envsci.2010.08.006>
- [46] Van Rijswijk, H.F.M.W., Edelenbos, J., Hellegers, P., Kok, M., and Kuks, S.M.M., Ten building blocks for sustainable water governance: an integrated method to assess the governance of water. *Water International*, 39(5), pp. 725–742, 2014. DOI: <https://doi.org/10.1080/02508060.2014.951828>
- [47] Mukhtarov, F., Dieperink, C., and Driessen, P., The influence of communication on the legitimacy of environmental policy: The case of water governance in Kazakhstan. *Environmental Policy and Governance*, 27(4), pp. 351–367, 2017. DOI: <https://doi.org/10.1002/eet.1754>
- [48] Mccann, E., Urban policy mobilities and global circuits of knowledge: Toward a research agenda. *Annals of the Association of American Geographers*, 101(1), pp. 107–130, 2011. DOI: <https://doi.org/10.1080/00045608.2010.520219>
- [49] Cook, C., and Bakker, K., Water security: Debating an emerging paradigm. *Global Environmental Change*, 22(1), 94–102, 2012. <https://doi.org/10.1016/j.gloenvcha.2011.10.011>
- [50] Biswas, A.K., and Tortajada, C., Future water governance: problems and perspectives. *International Journal of Water Resources Development*, 26(2), pp. 129–139, 2010. DOI: <https://doi.org/10.1080/07900627.2010.488853>
- [51] Bakker, K., The ambiguity of community: debating alternatives for water supply governance. *Water Alternatives*, 1(2), pp. 236–252, 2008.
- [52] Conca, K., Governing water: contentious transnational politics and global institution building. MIT Press, Cambridge, MA, 2006.
- [53] Zeitoun, M., and Allan, J.A., Applying hegemony and power theory to transboundary water analysis. *Water Policy*, 10(S2), pp. 3–12, 2008. DOI: <https://doi.org/10.2166/wp.2008.203>
- [54] Norman, E.S., Bakker, K., and Cook, C., Introduction to the themed section: water governance and the politics of scale. *Water Alternatives*, 5(1), pp. 52–61, 2012.
- [55] Allan, T., Keulertz, M., Sojamo, S., and Warner, J., Handbook of land and water grabs in Africa: foreign direct investment and food and water security. Routledge, London, 2012.
- [56] Woodhouse, P., and Muller, M., Water governance. An historical perspective on current debates. *World Development*, 92, pp. 225–241, 2017. DOI: <https://doi.org/10.1016/j.worlddev.2016.11.014>

- [57] Meijerink, S., and Huitema, D., Policy entrepreneurs and change strategies: lessons from sixteen case studies of water transitions around the globe. *Ecology and society*, 15(2), art. 21, 2010. DOI: <https://doi.org/10.5751/ES-03495-150221>
- [58] Pahl-Wostl, C., The importance of social learning in restoring the multifunctionality of rivers and floodplains. *Ecology and Society*, 11(1), art. 10, 2006. <https://doi.org/10.5751/ES-01542-110110>
- [59] Rogers, P., and Hall, A.W., Effective water governance. TEC Background Papers 7, Global Water Partnership, 2003.
- [60] Castro, J.E., Water governance in the twentieth-first century. *Ambiente & Sociedade*, 10(2), pp. 97–118, 2007. <https://doi.org/10.1590/S1414-753X2007000200007>
- [61] Swyngedouw, E., Dispossessing H2O: the contested terrain of water privatization. *Capitalism Nature Socialism*, 16(1), pp. 81–98, 2005. DOI: <https://doi.org/10.1080/1045575052000335384>
- [62] Bakker, K., Archipelagos and networks: urbanization and water privatization in the South. *The Geographical Journal*, 169(4), pp. 328–341, 2003. DOI: <https://doi.org/10.1111/j.0016-7398.2003.00097.x>
- [63] Budds, J., and Hinojosa, L., Restructuring and rescaling water governance in mining contexts: The co-production of waterscapes in Peru. *Water Alternatives*, 5(1), pp. 119–137, 2012.
- [64] Mehta, L., and Movik, S., Flows and practices: the politics of integrated water resources management (IWRM) in Africa. IDS Working Paper 319, Institute of Development Studies, Brighton, 2011.
- [65] Cleaver, F., and Franks, T., How institutions elude design: river basin management and sustainable livelihoods. BCID Research Paper 12, University of Bradford, 2003.
- [66] Mollinga, P.P., Water, politics and development: framing a political sociology of water resources management. *Water Alternatives*, 1(1), pp. 7–23, 2008.
- [67] Wester, P., Capturing the waters: the hydraulic mission in the Lerma-Chapala Basin, Mexico (1876–1976). PhD Thesis, Wageningen University, 2008
- [68] Venot, J.P., and Clement, F., Justice in development? An analysis of water interventions in the rural South. *Natural Resources Forum*, 37(1), pp. 19–30, 2013. DOI: <https://doi.org/10.1111/1477-8947.12010>
- [69] Sultana, F., and Loftus, A., The right to water: Prospects and possibilities. Routledge, London, 2012.
- [70] Boelens, R., Cultural politics and the hydrosocial cycle: Water, power and identity in the Andean highlands. *Geoforum*, 57, pp. 234–247, 2014. DOI: <https://doi.org/10.1016/j.geoforum.2013.02.008>
- [71] Perreault, T., What kind of governance for what kind of equity? Towards a theorization of justice in water governance. *Water International*, 39(2), pp. 233–245, 2014. DOI: <https://doi.org/10.1080/02508060.2014.886843>
- [72] Zwartveen, M.Z., and Boelens, R., Defining, researching and struggling for water justice: Some conceptual building blocks for research and action. *Water International*, 39(2), pp. 143–158, 2014. DOI: <https://doi.org/10.1080/02508060.2014.891168>
- [73] Budds, J., Contested H2O: Science, policy and politics in water resources management in Chile. *Geoforum*, 35(3), pp. 315–328, 2004. DOI: <https://doi.org/10.1016/j.geoforum.2003.08.002>
- [74] Linton, J., and Budds, J., The hydrosocial cycle: defining and mobilizing a relational-dialectical approach to water. *Geoforum*, 57, pp. 170–180, 2014. DOI: <https://doi.org/10.1016/j.geoforum.2013.10.008>
- [75] Bakker, K., Commons versus commodities: Charting the hydrosocial terrain of water privatization. *Progress in Human Geography*, 31(6), pp. 792–811, 2007. DOI: <https://doi.org/10.1177/0309132507083506>
- [76] Swyngedouw, E., Dispossessing H2O: the contested terrain of water privatization. *Capitalism Nature Socialism*, 16(1), pp. 81–98, 2005. DOI: <https://doi.org/10.1080/1045575052000335384>
- [77] Loftus, A., Rethinking political ecologies of water. *Third World Quarterly*, 30(5), pp. 953–968, 2009. DOI: <https://doi.org/10.1080/01436590902959198>
- [78] Swyngedouw, E., Liquid power: Water and contested modernities in Spain, 1898–2010. MIT Press, Cambridge, MA, 2015.
- [79] Bakker, K., The business of water: market environmentalism in the water sector. *Annual Review of Environment and Resources*, 38(1), pp. 469–494, 2013. DOI: <https://doi.org/10.1146/annurev-environ-022112-142244>
- [80] Castro, J.E., Systemic conditions and public policy in water and sanitation services. *Water Alternatives*, 2(1), pp. 1–23, 2009.
- [81] Tortajada, C., Water management and policy challenges in developing countries. *Water Resources Development*, 22(2), pp. 209–218, 2006. DOI: <https://doi.org/10.1080/07900620600648391>
- [82] Rogers, P., and Hall, A.W., Effective water governance. TEC Background Papers 7, Global Water Partnership, 2003.
- [83] Gleick, P.H., The changing water paradigm: a look at twenty-first century water resources development. *Water International*, 25(1), pp. 127–138, 2000. DOI: <https://doi.org/10.1080/02508060008686804>
- [84] Falkenmark, M., Freshwater as shared between society and ecosystems: From divided approaches to integrated challenges. *Philosophical Transactions of the Royal Society B: Biological Sciences*, 358(1440), pp. 2037–2049, 2003. DOI: <https://doi.org/10.1098/rstb.2003.1386>

R. Saldaña-Escorcía, received the BSc. Eng. in Environmental and Sanitary Engineer in 2021, from the Universidad Popular del Cesar, Aguachica, Colombia. Sp. in Preservation and Conservation of Natural Resources in 2023, from the Universidad Pontificia Bolivariana Bucaramanga, Colombia, and is in his last year of the Master in Governance of Protected Areas and Management of Biological Resources at the Universidad El Bosque, Bogotá, D.C., Colombia. He is currently assistant professor in the Department of Environmental and Sanitary Sciences at the Universidad Popular del Cesar, Aguachica. He is part of the research group on health and environmental studies, as well as the research group on environmental management and sustainable territories. His research interests include: water treatment, spatial analysis, natural resource management, water governance and economic valuation of environmental assets.

ORCID: 0000-0002-5290-7072

Synthesis of surfactants based on alkyl glyceryl ester /ether and evaluation as wax inhibitor

Denise Gentili Nunes^{a,*}, Giovani Cavalcanti Nunes^b, Elizabeth Roditi Lachter^c, Agatha Oliveira Santos^b, Rita de Cássia Pessanha Nunes^d & Elizabete Fernandes Lucas^{d,e}

^a Centro Federal de Educação, Tecnológica Celso Suckow da Fonseca, Rio de Janeiro, Brasil. * denise.nunes@cefet-rj.br

^b Universidade do Estado do Rio de Janeiro, Rio de Janeiro, Brazil. giovani.nunes@uerj.br; agathasantos25@gmail.com

^c Universidade Federal do Rio de Janeiro, Instituto de Química, Rio de Janeiro, Brasil. lachter@iq.ufrj.br

^d Universidade Federal do Rio de Janeiro, Instituto de Macromoléculas, Rio de Janeiro, Brasil. redpessanha@gmail.com

^e Universidade Federal do Rio de Janeiro, Programa de Engenharia Metalúrgica e de Materiais/COPPE, Rio de Janeiro, Brasil. elucas@metalmat.ufrj.br

Received: June 3rd, 2025. Received in revised form: October 10th, 2025. Accepted: October 22nd, 2025.

Abstract

This study evaluated glycerol esters (GEC12, GEC14) and ethers (GETC14, GETC18) as alternative paraffin inhibitors compared with a commercial product (PI-CX). Rheological tests were performed on two crude oils (A and C). A cold finger assay was performed to measure wax deposition in a model system. PI-CX showed the best performance overall, but the synthesized molecules were also effective for oil A, reducing gelation temperature, viscosity, and yield stress. GEC12 showed slightly superior performance among the synthesized inhibitors. In the model system these inhibitors had the same performance. Although PI-CX proved to be more efficient, the new compounds are low cost, biodegradable, and effective under severe conditions (5 °C). Oil C, which did not gel down to -5 °C, showed no improvement with inhibitors, indicating that not all oils require treatment. The results support the potential of these glycerol-based compounds as sustainable alternatives for paraffin inhibition in specific crude oils.

Keywords: petroleum; rheology; paraffin inhibitors; glycerol esters; glycerol ethers.

Síntesis de surfactantes basados en ésteres/éteres de alquil glicerilo y evaluación como inhibidores de ceras

Resumen

Este estudio evaluó los ésteres de glicerol (GEC12, GEC14) y los éteres (GETC14, GETC18) como inhibidores de parafina alternativos en comparación con un producto comercial (PI-CX). Se realizaron pruebas reológicas en dos petróleos crudos (A y C). Se realizó un ensayo de dedo frío para medir la deposición de cera en un sistema modelo. PI-CX mostró el mejor rendimiento en general, pero las moléculas sintetizadas también fueron efectivas para el petróleo A, reduciendo la temperatura de gelificación, la viscosidad y el límite elástico. GEC12 mostró un rendimiento ligeramente superior entre los inhibidores sintetizados. En el sistema modelo, estos inhibidores tuvieron el mismo rendimiento. Aunque PI-CX demostró ser más eficiente, los nuevos compuestos son de bajo costo, biodegradables y efectivos en condiciones severas (5 °C). El petróleo C, que no gelificó a -5 °C, no mostró ninguna mejora con los inhibidores, lo que indica que ni todos los petróleos requieren tratamiento. Los resultados respaldan el potencial de estos compuestos basados en glicerol como alternativas sostenibles para la inhibición de parafina en petróleos crudos específicos.

Palabras clave: petróleo; reología; inhibidores de parafina; ésteres de glicerol; éteres de glicerol.

1 Introduction

Wax deposition is one of the major flow assurance challenges. During crude oil transportation, the wax of paraffinic crudes can precipitate, form gel and deposit in pipelines. The problems can be greater depending on the content and type of wax. Higher wax content normally lead to higher viscosity, yield stress, pour point values. It also leads to a non-Newtonian behavior in temperatures below the crystallization temperature [1-3]. As to the type, wax can be of low molecular weight, which are linear wax (n-alkanes), called macrocrystalline or high molecular weight wax, which are non-linear wax (iso and cycloalkanes), known as microcrystalline. Macrocrystalline (linear waxes) consists of a distribution of carbon numbers from approximately C20 to C40 and tends to form plate or needle-like and harder crystals. Compared to the microcrystalline, these crystals can cause more problems during the flow. They can crystallize and agglomerate more easily due to their structural similarity, in addition to precipitating and depositing on the pipe walls. The microcrystalline (non-linear waxes) consists of a distribution of carbon numbers from approximately C30 to C70+ and tend to form smaller particles sized and spherical shape [4-7]. The paraffinic gel is composed of waxes that form a network that trap the oil, resulting in solid like plugs that settle. The thickness of this deposit tends to increase and harden with aging. The gel can form during the shut-in of wells. The major problem occurs during the restart process because the plug requires applied pressure to break the gel structure in order to flow. Kurniawan et al [8] studied the influence of macro and microcrystalline wax on gel strength. They found that microcrystalline (non-linear) wax does not have a solid fraction sufficient to form a gel with elastic properties, forming weak gels. While the macrocrystalline (linear) generates a strong physical gel with high elastic properties, forming harder gels. The methods used for paraffin deposition remediation can be thermal, mechanical, chemical or a combination thereof [4-6,9,10]. The thermal method includes insulation and heating of flow. The mechanical one is carried out by passing a pig (a polyurethane plug used to scrape off the paraffin deposited in the pipeline). The name of this practice is pigging. Chemical methods include wax inhibitors, dispersants and solvents. Inhibitors prevent deposits or form softer deposits. Dispersants and solvents help to remove deposits. Pigging often occurs after using these chemical remediation methods. It is a high-risk operation, and the inhibitors can help reduce the frequency of pigging [11,12]. Inhibitors can also have other benefits, they prevent the formation of paraffin networks because they modify the crystals, reduce the pour point, viscosity and yield stress besides preventing deposition by changing the wettability of the surface [13]. Polymers are widely applied as paraffin inhibitors of which poly(ethylene-co-vinyl acetate) (EVA) and poly(methyl acrylates) (MAC) are the most found in literature [3,12,14-17]. Surfactants are also used, but their application is still questioned and require more research. Ethoxylated surfactants are the most reported in literature [15]. Some classes, as ethers and esters are studied only as pour point depressant (PPD) [15,17].

Because petroleum is a complex mixture of many

compounds, there are many factors that influence the inhibitors' action. There are some reports in literature showing the importance of studying the correlation between the oil composition and wax deposition inhibitors [5-7,16]. The studies show that most inhibitors act best on low molecular weight waxes (C₃₄ and below) and less on high molecular weight waxes (C₃₅+) [5,15]. The more efficient analyses to evaluate the wax deposition inhibitors are cold finger, flow loop and rheology [2,4,12,14,18]. The aim of this work is to contribute to greater understanding of the surfactant's action mechanism. For that, alkyl glycerol ether and ester were synthesized and evaluated as paraffin deposition inhibitors. Their results were compared with a commercial polymeric inhibitor.

2 Experimental

2.1 Materials

The crude oils, called A and C, were provided by Rio Petroleo in Rio de Janeiro, Brazil, an engineering company specialized in services for oil producing operators. Oil A properties as well as the SARA value for the crude oils A and C are seen in Table 1 and 2 [19,20].

Methyl dodecanoate, methyl tetradecanoate, 1-bromotetradecane, 97%; 1-bromooctadecane, 97%; 1,2-isopropylidene-glycerol (solketal, 97%), and Amberlyst 15 (wet, hydrogen form) were purchased from Sigma-Aldrich, Rio de Janeiro, Brasil. Tetrabutylammonium bromide (99%), sodium hydroxide (NaOH, 97%), ethanol (95%), Sodium carbonate (Na₂CO₃) and ethyl ether were purchased from Vetec Química Fina, Duque de Caxias, Brasil. Sodium chloride (NaCl, 99%) and magnesium sulfate (MgSO₄, anhydrous) were acquired from Labssynth, São Paulo, Brasil. Deuterated chloroform (CDCl₃) was supplied by Tedia of Brazil, Rio de Janeiro, Brasil. Paraffin (mp 58-62°C) was purchased from sigma-Aldrich. Toluene PA was purchased from Synth. A commercial wax inhibitor, named EVA10, based on poly(ethylene-vinyl acetate), was supplied by Braskem, São Paulo.

Table 1
Crude oil A properties

Description	Method	Result	Units of measure
GT	Rheology	8.69 ± 0.34	°C
WAT	Rheology	14.36 ± 0.13	°C
WAT	DSC	17.52 ± 0.03	°C
Water content	ASTM D4377 [21]	0.42 ± 0.02	%m/m

GT – Gelation Temperature; WAT – Wax Appearance Temperature; μ DSC – differential scanning microcalorimetry

Source: own authorship.

Table 2.
SARA values for crude oil A and C

Sample	Oil Composition/ %m/m			
	Saturated	Aromatics	Resins	Asphaltenes
A*	46.7	45.4	7.9	<0.1
C**	59.87	30.57	9.35	0.21

* SARA obtained in a previous work [19]

** SARA obtained in a previous work [20]

Source: own authorship.

2.2 Synthesis

Two classes of surfactants were synthesized: Alkyl glycerol ester and alkyl glycerol ethers.

2.2.1 Alkyl glycerol esters

The alkyl glycerol esters were synthesized in two steps, esterification of the solketal and hydrolysis of the solketal ester (Fig. 1), following a procedure adapted from Yu et al [22].

In the first step, methyl esters of different fatty chain sizes (C12 and C14) and solketal with a molar ratio of 1/2 and Na_2CO_3 (1.7% m/m in relation to the mass of the solketal) were added to a flask. The reaction took place under stirring, for 5 h at 200 °C. After the reaction was completed, an excess of 1,2-*O*-isopropylidene glycerol was removed under vacuum (10 mmHg) distillation. The product was dissolved in ethyl ether and washed with water to remove Na_2CO_3 . Then the phases were separated and the ethyl ether was removed from the organic phase to obtain the esterified solketal. In the second step, solketal ester, ethanol 95% (proportion: 1g of the solketal ester and 4 mL of ethanol) and Amberlyst 15 resin (10% m/m in relation to the mass of solketal ester) were added to a flask. The mixture was kept under stirring for 3 h at 78 °C. The final mixture was filtered, and the ethanol was removed to obtain Alkyl Glycerol Esters [23]. The objective was to obtain only monoglycerides molecules (only one esterified hydroxyl group). The products were called GEC12 and GEC14 in this paper.

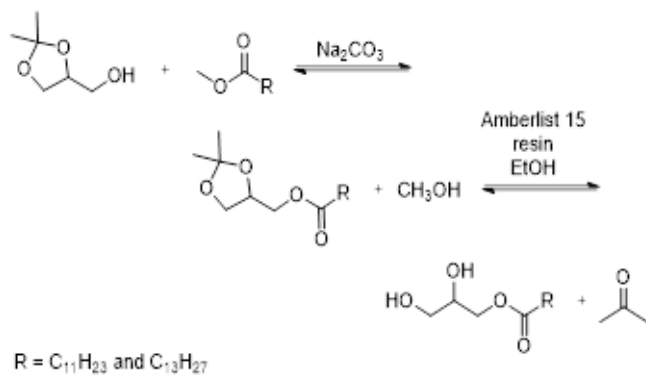


Figure 1. Alkyl glycerol esters reaction
Source: own authorship.

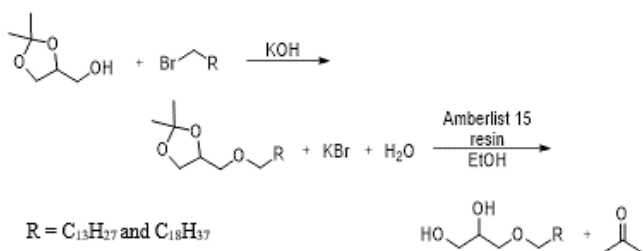


Figure 2. Alkyl glycerol ethers reaction
Source: own authorship.

2.2.2 Alkyl glycerol ethers

The alkyl glycerol ethers were also synthesized in two steps: Etherification of the solketal and hydrolysis of the solketal ether (Fig. 2) [24].

In the first step, a mixture of 0.05 mol of tetrabutylammonium bromide, 0.2 mol of solketal, and 36 mL of 33% (m/m) KOH solution was added to a flask and vigorously stirred for 15 min at ambient conditions. After that, 0.1 mol of alkyl bromide of different fatty chain sizes (C14 and C18) was added dropwise. The mixture took place under stirring for 48 h at 130 °C. The phases were separated. The organic phase had the etherified solketal. In the second step, solketal ether, ethanol (4.0 mL per 1 g of ether) and Amberlyst 15 resin (0.1 g per 1 g of ether) were added to a flask. The mixture was kept under stirring for 4 h at 100 °C. Soon after, the mixture was filtered, and the ethanol was removed to obtain Alkyl Glycerol Ethers [24]. The products were called GEtC14 and GEtC18 in this paper. The objective of this procedure was also to obtain glycerol ethers with only one esterified hydroxyl group.

2.3 Characterization of the synthesized surfactants

The reaction products were characterized by Fourier-transform infrared spectroscopy (FTIR), measured with a NICOLET Magna-IR 6700, and by ^{13}C nuclear magnetic resonance spectroscopy (NMR), using a BRUKER DRX-400 instrument.

2.4 Solubilization of commercial inhibitor EVA10 in toluene

The solubilization was carried out by dissolving 0.125g of EVA10 in 5ml of toluene PA, keeping it under stirring for 1.5h at 45°C. The oils were analyzed with 1000 ppm of this mixture, called PI-CX.

2.5 Evaluation of inhibitors' performance

The inhibitors' performance was verified by rheological assays (gelation temperature, viscosity and yield stress measurement) and cold finger analysis. All the rheological assays were performed in a Thermo Scientific HAAKE MARS II Rheometer with cone-plate geometry, C60 and they were performed in duplicate. The oil samples were analyzed without and with 1000 ppm of inhibitors (GEC12, GEC14, GEtC14 and GEtC18). The performance of the inhibitors was compared with the commercial polymeric inhibitor (PI-CX). The rheological procedures were described in detail by the group in previous work [19].

2.5.1 Gelation temperature measurement

The oil samples were initially heated from 20 to 60 °C in rotational mode, and then it was cooled from 60 to -5 °C at 1 °C min⁻¹, frequency 1.59 Hz, under a shear stress at 0.01Pa, in oscillatory mode. GT was measured for oil A without inhibitor and with all inhibitors. And for oil C only without inhibitor.

2.5.2 Viscosity measurement

The samples were heated from 20 to 60 °C and cooled from 60 to 5 °C, at 1 °C min⁻¹, both steps in rotational mode. Viscosity was measured for oils A and C without inhibitor and with all inhibitors. This test was also carried out for oil samples only in the presence of 1000ppm of toluene.

2.5.3 Yield stress measurement

The samples were heated to 40 °C and then cooled to 5 °C in rotational mode. Every 5 degrees, shear rates from 0.001 to 0.2 s⁻¹ were applied and the shear stress was measured in these conditions. Yield stress was measured only for oil A without inhibitor and with all inhibitors.

2.5.4 Cold finger assay

For the cold finger test, a paraffin model system was initially prepared, 40% m/m paraffin (mp 58-62°C) in toluene. The paraffin was solubilized in toluene at 45 °C for 90 min. Four samples were placed in the cold finger in duplicate, the model system without inhibitor and with 1000 ppm of the inhibitors GEC14, GEC14 and PI-CX, selected based on the first results. A Cold Finger from F5 Technology Model 62 was used. A temperature of 0°C was set in the cold finger to ensure paraffin precipitation and the bath in which the vials were placed was stabilized at a temperature of 50°C to ensure that the paraffin precipitated only on the finger and not on the walls of the vials. In addition, each vial had a magnetic stirrer to keep the sample homogenized. The equipment was programmed for a 24-hour test. After that, the vials were removed from the bath, keeping the fingers connected to maintain the precipitation of the paraffin. The deposited paraffin was dried and weighed.

3 Results and discussion

3.1 Alkyl glycerol esters characterization

The production of alkyl glyceryl esters was confirmed by FTIR and ¹³C NMR. As desired, only monoglycerides were obtained. The ¹³C chemical shifts were quite similar for the two different esters: We can see in Fig. 3, GEC12 ¹³C-NMR spectrum, $\delta = 174.4$ ppm (RCOOR') for the monoglycerides and absence of signals in 110 ppm (ketal group carbon) and 51.6 ppm (methyl carbon). The GEC12 FTIR spectrum (Fig. 4) presented characteristic peaks at 3411 cm⁻¹ (OH), 2922 and 2853 cm⁻¹ (CH), 1740 cm⁻¹ (C=O for the monoglycerides obtained. The results agree with the literature [25].

3.2 Alkyl glycerol ethers characterization

The production of alkyl glyceryl ethers was confirmed by FTIR and ¹³C NMR. As desired, only monoglycerides were obtained. The GEC14 ¹³C NMR spectrum presented that the complete ketal conversion (to diol) happened due to the absence of the signal in the at $\delta = 110$ ppm of the carbon in the ketal group. The alkyl bromide was consumed due to the absence of the chemical shift at $\delta = 33.5$ ppm which

corresponds to the carbon (CH₂) adjacent to the bromine atom. (Fig. 5). While the GEC14 FTIR spectrum of alkyl glyceryl ethers (Fig. 6), presented their characteristic peaks at 3313 cm⁻¹ (OH), 2918 and 2850 cm⁻¹ (CH), 1124 and 1060 cm⁻¹ (C-O). The results agree with the literature [24].

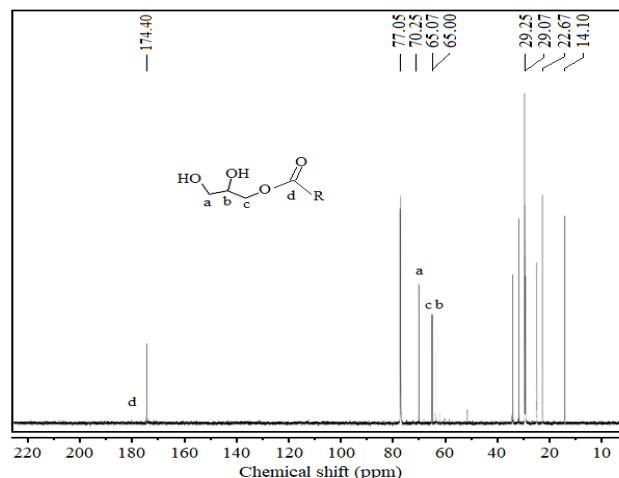


Figure 3. ¹³C-NMR spectrum of GEC12 inhibitor
Source: own authorship.

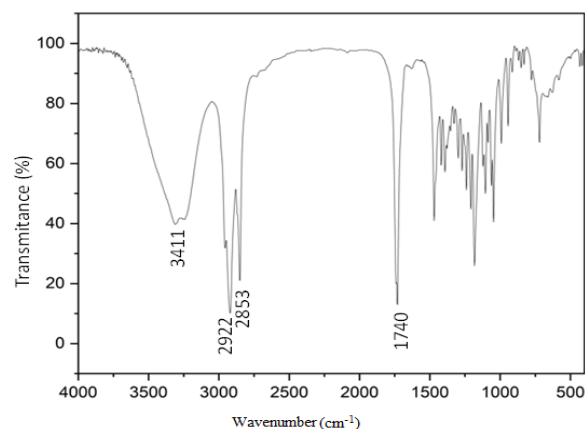


Figure 4. FTIR spectrum of GEC12 inhibitor
Source: own authorship.

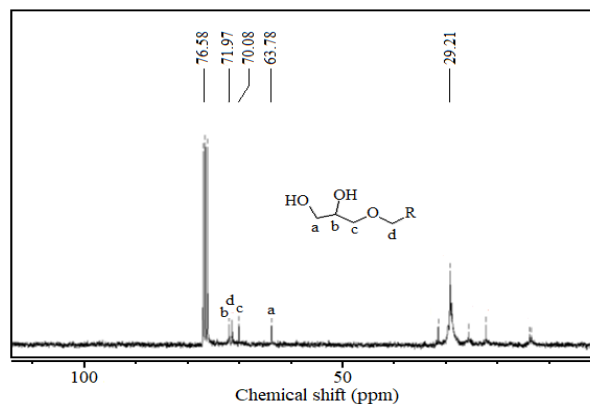


Figure 5. ¹³C-NMR spectrum of GEC14 inhibitor
Source: own authorship.

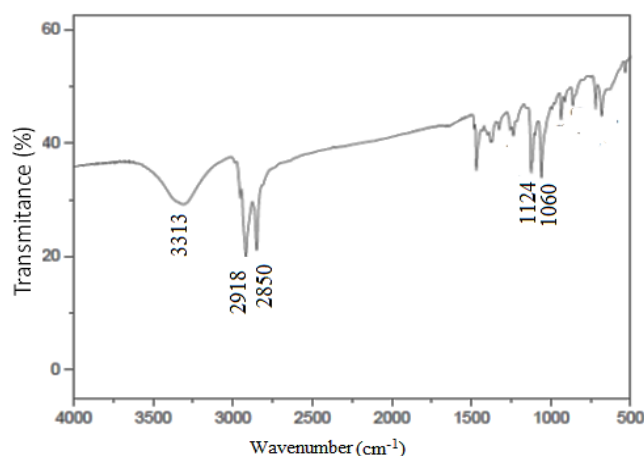


Figure 6. FTIR spectrum of GEC14 inhibitor
Source: own authorship.

3.3 Gelation temperature measurement

The assays were carried out under shear stress at 0.01Pa, the value which gel formation normally happens. Fig. 7 shows the graphs of G' and G'' as a function of temperature for oil A without inhibitor. The GT was obtained as the intersection point between the G' and G'' curves. For temperatures higher than the gelation temperature (GT), the G' value is lower than the G'' value.

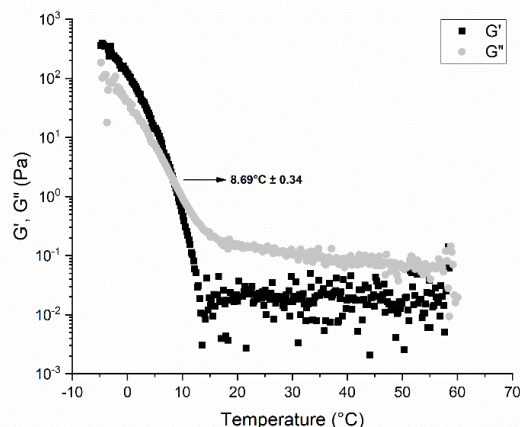


Figure 7. G' and G'' measurement in function of temperature of oil A without inhibitor at 0.01Pa
Source: own authorship.

Table 3.

Gelation Temperature measurement of oil A with and without inhibitors

Inhibitor (at 1000 ppm)	GT(°C)
No inhibitor	8.69 ± 0.34
GEC12	5.59 ± 0.33
GEC14	5.57 ± 0.33
GETC14	4.96 ± 0.31
GETC18	4.82 ± 0.16
PI-CX*	-21.49 ± 0.35

* GT obtained in a previous work [19]

Source: own authorship.

For temperatures lower than the GT, the G' value is greater than the G'' value [26]. G' is the storage modulus, it represents the elastic behavior of the fluid. G'' is the loss modulus which corresponds to the viscous behavior of the fluid. The dispersion of points at temperatures above the GT for the G' happens because the gel [27] has not yet formed. The oil sample without inhibitor and with the other inhibitors presented similar behavior. The GT values obtained for all samples of oil A are summarized in Table 3. This oil with inhibitors presented a reduction of GT. This suggests that the inhibitors were able to interfere with the wax crystallization mechanism, reducing the temperature of formation of the three-dimensional crystal network responsible for oil gelation. The GT for oil A without inhibitor was 8.69 °C, while for the oil in the presence of glycerol ester and glycerol ether additives were between 4.82 and 5.52 °C, respectively. This is the reason why the assays in the sequel will be executed at the range of 9 and 5 °C. All the inhibitors synthesized presented a good performance. They were able to reduce the gelation temperature of oil A around 44% and 36% for the oil in the presence of glycerol ester and glycerol ether, respectively. Considering the measurement errors, we can say that this difference in the performance is not significant. The size of the nonpolar chain also did not significantly interfere with the performance of the inhibitors. In previous work [19], it was observed a reduction in oil GT to -21.49, when using a commercial paraffin inhibitor (PI-CX) at the same concentration (1000 ppm), suggesting that this additive was able to further alter the shapes of the crystals, preventing the formation of paraffin gel.

The measurements of G' and G'' for oil C (Fig. 8) showed that this oil did not present GT until the final temperature of the test (-5 °C). There was no intersection between the curves. Because of this, samples were not made with additives containing inhibitors. Based on the SARA (Table 2) of oils and the literature [8], we can say that even though oil C presented a higher paraffin content than oil A, the paraffins must probably be of the microcrystalline type (with higher molecular weights) which have a lower tendency to form paraffin gels.

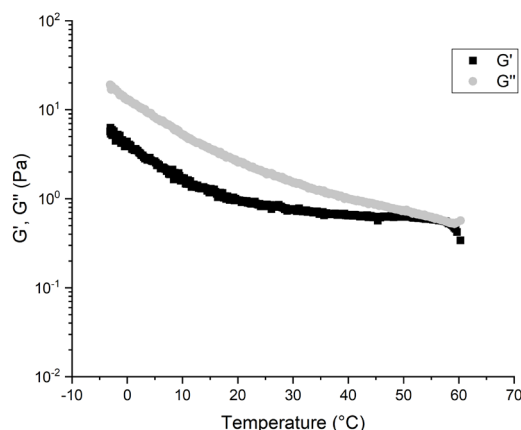


Figure 8. G' and G'' measurement in function of temperature of oil C without inhibitor
Source: own authorship.

3.4 Viscosity measurement

The viscosity measurements were carried out for the oils A and C without inhibitors and with the synthesized inhibitors. As the PI-CX inhibitor preparation is done using toluene, the viscosity measurement of the oils A and C were carried out also in the presence of toluene alone to study the influence of this solvent in the crudes viscosity.

According to the Figs. 9 and 10, for the oil A without inhibitor, the waxes dispersed in the medium influenced the oil rheology significantly increasing its viscosity as temperature decreases below GT, as predicted in the literature [28]. While for the oil with inhibitors, they were able to considerably avoid the increase of the oil viscosity in agreement with the literature where the inhibitors are known as rheological modifiers [29]. All the inhibitors had an excellent performance. Table 4 shows the viscosity values at 9 °C and 5 °C, which approximately corresponds to the oil GT with and without inhibitors. Among the synthesized inhibitors, GEC12 was the one that presented a slightly better behavior, at both 9 °C and 5 °C, with a reduction in oil viscosity at both temperatures of around 60%, indicating the formation of softer gels comparing to the others. This phenomenon can be attributed to the presence of the ester carbonyl which may be causing the formation of smaller crystals or crystal dispersion.

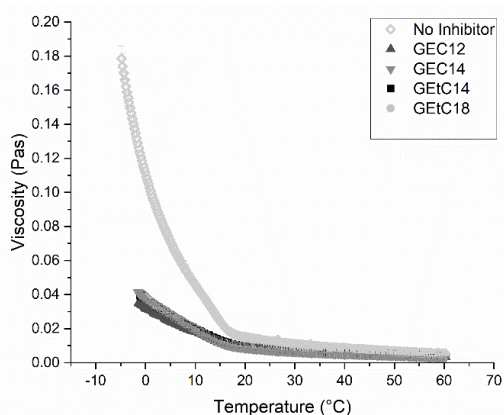


Figure 9. Viscosity measurement as a function of temperature of oil A with and without inhibitors

Source: own authorship.

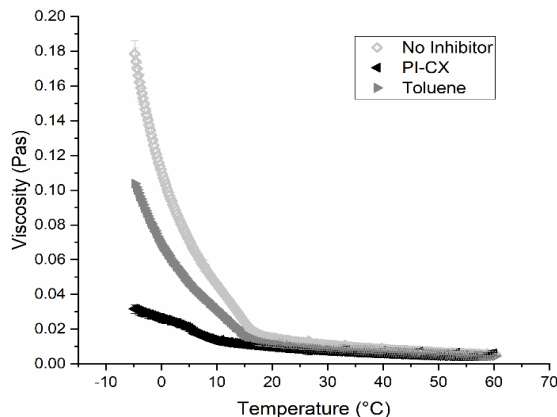


Figure 10. Viscosity measurement as a function of temperature of oil A with PI-CX inhibitor and in toluene

Source: own authorship.

Table 4.

Viscosity measurement of oil A at 9 and 5 °C with and without inhibitors and in toluene

Inhibitor (at 1000 ppm)	Oil A Viscosity (Pas)	
	9 °C	5 °C
No inhibitor	0.0498 ± 0.0012	0.0704 ± 0.0024
GEC12	0.0193 ± 0.0001	0.0248 ± 0.0003
GEC14	0.0213 ± 0.000	0.0284 ± 0.0003
GEtC14	0.0213 ± 0.006	0.0278 ± 0.0011
GEtC18	0.0205 ± 0.000	0.0279 ± 0.0003
PI-CX	0.0142 ± 0.0010	0.0210 ± 0.0020
Toluene	0.0344 ± 0.0004	0.0467 ± 0.0005

Source: own authorship.

According to the results, we conclude that probably the C12 carbon chain of the GEC12 ester has a greater attraction to the paraffins. Perhaps the smaller chain, when compared to C14 and C18, has an easier diffusion in the medium or it has greater solubility in the medium, favoring the interaction. Comparing the surfactants with a commercial polymeric inhibitor PI-CX, the latter reduced the viscosity around 70% at 9 °C and 5 °C. In Fig. 10 and Table 4, we can see that the toluene had an influence on the reduction of viscosity for the oil A, reducing this oil viscosity by 33% at 5 °C. Therefore, it is possible to verify that the reduction in PI-CX was only 37%. These results show that the glycerol esters and ethers inhibitors were more effective in reducing viscosity for oil A. The synthesized inhibitors were able to reduce the oil viscosity more than the commercial polymeric inhibitor, that is normally used by the industry. Despite presenting a small reduction in GT when compared to PI-CX, the gels formed presented a softer consistence, enabling the oil to flow even under severe temperature conditions (5 °C), which justifies its application instead of the commercial inhibitor.

For oil C, the viscosity measurements were carried out at 5 °C only. Although oil C does not present GT, the temperature of 5 °C was the same analyzed for oil A. As this temperature is considered a severe condition. The rheological curves for oil C are presented in Figs. 11 and 12. As seen in Table 2, oil C has more asphaltenes than oil A, which justifies the viscosity of oil C being higher than that of oil A. For oil

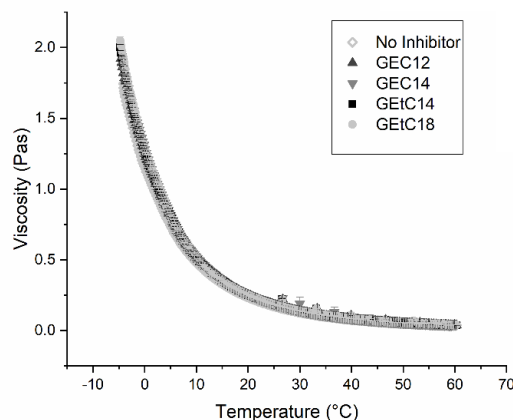


Figure 11. Viscosity measurement as a function of temperature of oil C with and without inhibitors

Source: own authorship.

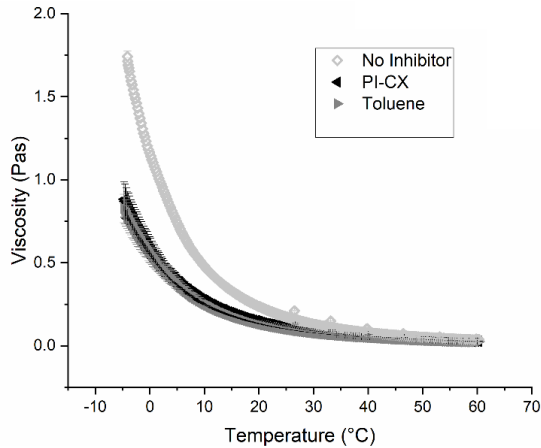


Figure 12. Viscosity measurement as a function of temperature of oil C with PI-CX inhibitor and in toluene
Source: own authorship.

Table 5.

Viscosity measurement of oil C at 5 °C with and without inhibitors and in toluene

Inhibitor (at 1000 ppm)	Oil C Viscosity (Pas)
	5 °C
No inhibitor	0.7341 ± 0.0096
GEC12	0.7918 ± 0.0253
GEC14	0.8049 ± 0.0078
GEtC14	0.8075 ± 0.0031
GEtC18	0.8047 ± 0.0136
PI-CX	0.3896 ± 0.0350
Toluene	0.3689 ± 0.0332

Source: own authorship.

C in the presence of synthesized inhibitors there was no reduction in oil viscosity. Since oil C does not have a gelation temperature, it is the type of oil that does not need paraffin inhibitor. In the presence of the commercial inhibitor (PI-CX), oil C showed a reduction in viscosity (Fig. 12). In this figure we can see that the toluene also had an influence on the reduction of viscosity for oil C. The reduction in viscosity was approximately the same for PI-CX and toluene (Table 5), proving that the efficiency effect was only due to toluene.

The change in behavior of the viscosity of oil A value under 15 °C is a typical behavior of oil when the paraffins appear, disperse in the medium, grow and agglomerate to form the gel and deposit in the pipelines. For this type of oil, the paraffin inhibitors were able to block the formation of the crystal network which, as a consequence generated a soft gel. Oil C does not have a gelation temperature and the increase in viscosity occurs with the decrease in temperature exponentially, without forming two straight lines. In this case, even though the paraffins do not form gel, they act on the increase of viscosity.

3.5 Yield stress measurement

To quantify the yield stress (gel breakdown), the shear stress was measured by varying the shear rate. These measurements were carried out at temperatures from 35 °C

to 5 °C every 5 °C for oil A samples without and with wax inhibitor (GEC12, GEC14, GEtC14, GEtC18 and PI-CX). The yield stress was determined when the shear stress value increased with the shear rate and reached a maximum value forming a plateau [2]. This behavior only occurred at 5 °C, both for the oil without and with inhibitors, but it was more evident in the system without the inhibitor. This result makes sense because according to Table 3, at 5 °C the oil without inhibitor has already formed a gel, the oils with synthesized inhibitors are starting to form a gel and the oil with PI-CX has not formed a gel. The other temperatures almost coincide with the x axis. The comparison of yield stress values at 5 °C for oil A samples without and with inhibitors can be seen in Table 6 and Fig. 13. The results of Table 6 show that the presence of inhibitors significantly reduced the yield stress by around 86% for glycerol esters, 70% for glycerol ethers and 98% for PI-CX. Among the synthesized inhibitors, GEC12 was the one that presented the best result according to the results found in viscosity measurements at 5 °C (Table 4). The results make sense since if the gel is softer, its viscosity and yield stress are lower. As for the commercial inhibitor, we can say that the oil doped with this inhibitor will have no problems restarting the flow after a production stoppage. Yield stress tests were not performed for oil C because this oil did not show a gelation temperature down to -5°C, and therefore did not form a gel.

Table 6.

Yield stress measurement of oil A with e without inhibitors

Inhibitor	Yield Stress (Pa)
No inhibitor	0.352 ± 0.003
GEC12	0.050 ± 0.001
GEC14	0.061 ± 0.005
GEtC14	0.096 ± 0.004
GEtC18	0.078 ± 0.006
PI-CX*	0.01 ± 0.01

* Yield stress obtained in previous work [19].

Source: own authorship.

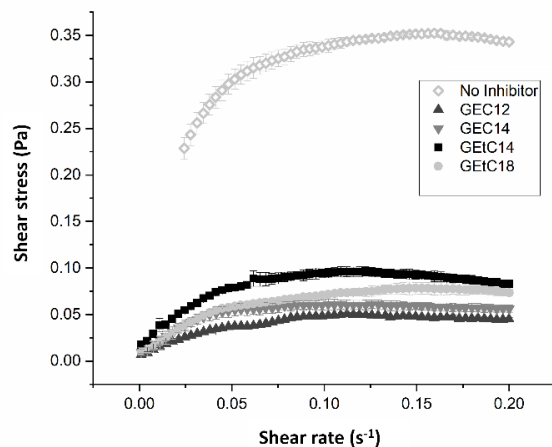


Figure 13 Yield stress measurement at 5 °C of oil A with e without inhibitors
Source: own authorship.

Table 7.

Model system wax deposition with GEC14 and GEtC14 inhibitors

Inhibitor	Wax deposition (g)
No inhibitor	6.05 ± 0.13
GEC14	3.98 ± 0.25
GEtC14	4.22 ± 0.12
PI-CX	1.38 ± 0.45

Source: own authorship.

3.6 Cold finger assay

Cold finger is an equipment to try to simulate the conditions where fluid flow is halted, as when a well shuts down. As the cold finger test requires a large amount of oil, the study of paraffin deposition was done with model system. And as we noticed that the size of the fatty chain has not shown a significant change in the performance of the inhibitors, only two synthesized inhibitors were chosen (GEC14 and GEtC14). In this case, maintaining the size of the fatty chain and varying only the polar segment of the surfactants (ether and ester). The results were compared with the commercial polymeric inhibitor. The masses after removing the model system from the cold finger, the deposited masses can be seen in Table 7. Analyzing the table, the inhibitors GEC14 and GEtC14 reduced the paraffin deposition (around 30%). For this wax type and amount, the cold finger results show that there was no significant change between ester and ether. While in the presence of PI-CX the mass deposited presented 77% of reduction (from 6.05 to 1.38).

4 Conclusion

Rheological and cold finger tests showed that both the synthesized inhibitors and the commercial inhibitor could act as excellent paraffin inhibitors for one of the oils tested (oil A), reducing all the parameters studied, as gelation temperature, viscosity, yield stress and wax deposition. Even though the efficiency of the polymeric inhibitor is much greater than that of glycerol ethers and esters, these surfactants presented a reduction in rheological parameters and wax deposition in cold finger assay sufficient to form soft gels which help the flow of the oil. Comparing the synthesized inhibitors, the efficiency in reducing GT was not significant between them. The glycerol ester with a chain length of 12 carbons (GEC12) reduced the viscosity and yield stress slightly more than the others. These two low rheological parameters are important to maintain the flow, especially when restarting the well. Both inhibitors (GEC14 and GEtC14) presented the same reduction in wax deposition. The tests on oil C, which did not show a gelation temperature down to -5°C, showed that not all oils need paraffin inhibitors. Paraffin inhibitors did not influence the behavior of this type of oil.

Surfactant-type inhibitors are not yet widely used as paraffin inhibitors because polymeric inhibitors tend to provide better results as seen in the tests performed. But besides glycerol esters and ethers being biodegradable, another great advantage is that the entire product is considered active material. The efficiency is due to the

surfactant-paraffin interaction. Polymeric inhibitors are usually sold on the market with low concentration of active material, requiring a large amount of product to be used to reach the required effect. Furthermore, it is usually prepared in toluene which promotes a reduction in viscosity masking the effect of the inhibitor.

From an industrial and economic perspective, comparing glycerol ester and ether, the first one is a more promising candidate for large-scale application. The esterification route requires fewer synthesis steps, milder reaction conditions, and employs cheaper and renewable reagents such as methyl esters (the main component of biodiesel) and glycerol, which is generated as a by-product in biodiesel production. On an industrial scale, synthesizing fatty-chain glycerol esters from these materials would be particularly attractive, as it would integrate wax inhibitor production into existing biodiesel production, enhancing both cost efficiency and sustainability.

Acknowledgments

FAPERJ (E-26/260.037/2023, E-26/204.066/2024, E-26/204.584/2024, E-26/204.172/2025), CNPq (305.565/2022-2), ANP, Rio Petroleo.

References

- [1] Zhao, Y., Paso, K., Kumar, L., Safieva, J., Sariman, M.Z.B., and Sjöblom, J., Controlled shear stress and controlled shear rate nonoscillatory rheological methodologies for gelation point determination. *Energy and Fuels*, 27(4), pp. 2025–2032, 2013. DOI: <https://doi.org/10.1021/ef302059f>.
- [2] Mahir, L.H.A., Vilas-Bôas-Fávero, C., Ketjuntwi, T., Fogler, H.S., and Larson, R.G., Mechanism of wax deposition on cold surfaces: gelation and deposit aging. *Energy and Fuels*, 33(5), pp. 3776–3786, 2019. DOI: <https://doi.org/10.1021/acs.energyfuels.8b03139>.
- [3] Erceg-Kuzmić, A., Radošević, M., Bogdanić, G., Srića, V., and Vuković, R., Studies on the influence of long chain acrylic esters polymers with polar monomers as crude oil flow improver additives. *Fuel*, 87(13-14), pp. 2943–2950, 2008. DOI: <https://doi.org/10.1016/j.fuel.2008.04.006>.
- [4] Jennings, D.W., and Weispfennig, K., Effect of shear on the performance of paraffin inhibitors: coldfinger investigation with Gulf of Mexico crude oils. *Energy and Fuels*, 20(6), pp. 2457–2464, 2006. DOI: <https://doi.org/10.1021/ef0602170>.
- [5] Zhang, F., Ouyang, J., Feng, X., Zhang, H., and Xu, L., Paraffin deposition mechanism and paraffin inhibition technology for high-carbon paraffin crude oil from the Kazakhstan PK oilfield. *Petroleum Science and Technology*, 32(4), pp. 488–496, 2014. DOI: <https://doi.org/10.1080/10916466.2011.596883>.
- [6] García, M.C., Carbognani, L., Urbina, A., and Orea, M., Correlation between oil composition and paraffin inhibitors activity. *SPE 49200-MS*, 1998. DOI: <https://doi.org/10.2118/49200-MS>.
- [7] Yang, F., Zhao, Y., Sjöblom, J., Li, C., and Paso, K.G., Polymeric wax inhibitors and pour point depressants for waxy crude oils: a critical review. *Journal of Dispersion Science and Technology*, 36(2), pp. 213–225, 2015. DOI: <https://doi.org/10.1080/01932691.2014.901917>.
- [8] Kurniawan, M., Subramanian, S., Norrman, J., and Paso, K., Influence of microcrystalline wax on the properties of model wax-oil gels. *Energy and Fuels*, 32(5), pp. 5857–5867, 2018. DOI: <https://doi.org/10.1021/acs.energyfuels.8b00774>.
- [9] Wang, K.S., Wu, C.H., Creek, J.L., Shuler, P.J., and Tang, Y., Evaluation of effects of selected wax inhibitors on paraffin deposition. *Petroleum Science and Technology*, 21(3-4), pp. 369–379, 2003. DOI: <https://doi.org/10.1081/LFT-120018526>.
- [10] Azevedo, L.F.A., and Teixeira, A.M., A critical review of the modeling of wax deposition mechanisms. *Petroleum Science and Technology*,

- 21(3-4), pp. 393–408, 2003. DOI: <https://doi.org/10.1081/LFT-120018528>.
- [11] Hoffmann, R., and Amundsen, L., Influence of wax inhibitor on fluid and deposit properties. *Journal of Petroleum Science and Engineering*, 107 pp. 12–17, 2013. DOI: <https://doi.org/10.1016/j.petrol.2013.04.009>.
- [12] Wei, B., Recent advances on mitigating wax problem using polymeric wax crystal modifier, *J Pet Explor Prod Technol* 5, pp. 391–401, 2015. DOI: <https://doi.org/10.1007/s13202-014-0146-6>.
- [13] Zhen-Hao, L., Said-Al-Salim, H., and Ridzuan, N., Science and Technology a review of the mechanism and role of wax inhibitors in the wax deposition and precipitation. *Pertanika Journal of Science and Technology*, 27, pp. 499–526, 2019.
- [14] Dubey, A., Chi, Y., Daraboina, N., and Sarica, C., Investigating the performance of paraffin inhibitors under different operating conditions. *SPE-187252-MS*, 2017.
- [15] Aiyejina, A., Chakrabarti, D.P., Pilgrim, A., and Sastry, M.K.S., Wax formation in oil pipelines: a critical review. *International Journal of Multiphase Flow*, 37(7), pp. 671–694, 2011. DOI: <https://doi.org/10.1016/j.ijmultiphaseflow.2011.02.007>.
- [16] Alves, B.F., Rossi, T.M., Marques, L.C.C., Soares, B.G., and Lucas, E.F., Composites of EVA and hydrophobically modified PAMAM dendrimer: effect of composition on crystallization and flow assurance of waxy systems. *Fuel*, 332(1), Art. 125962, 2023. DOI: <https://doi.org/10.1016/j.fuel.2022.125962>.
- [17] Jing, J., Cao, L., Shan, Y., Sun, J., and Tan J., Optimizing the low-temperature performance of high-wax-content crude oil with emulsion-based wax inhibitors: Mechanisms and efficacy. *AnnNYAcad Sci.*, 1541(1), pp. 255–265, 2024. DOI: <https://doi.org/10.1111/nyas.15248>.
- [18] Li, W., Li, H., Da, H., Hu, K., Zhang, Y., and Teng, L., Influence of pour point depressants (PPDs) on wax deposition: a study on wax deposit characteristics and pipeline pigging. *Fuel Processing Technology*, 217, Art. 106817, 2021. DOI: <https://doi.org/10.1016/j.fuproc.2021.106817>.
- [19] Nunes, D.G., Nunes, G.C., Lachter, E.R., Santos, A.O., Alves, B.F., and Lucas, E.F., The role of wax inhibitors for flow assurance below WAT in long tiebacks. *Arabian Journal of Science and Engineering*, 50, pp. 5021–5035, 2024. DOI: <https://doi.org/10.1007/s13369-024-09600-7>.
- [20] Nunes, D.G., Silva, J.C., Nunes, G.C., Silva, M.D.L., and Lucas, E.F., Crude oils mixtures: compatibility and kinetics of water-in-oil emulsions separation. *DYNA (Colombia)*, 89(223), pp. 67–74, 2022. DOI: <https://doi.org/10.15446/dyna.v89n223.99911>.
- [21] ASTM Internacional, ASTM D4377: Standard test method for water in crude oils by potentiometric karl fischer titration, west conshohocken, PA, USA, 2011.
- [22] Yu, C.C., Lee, Y.S., Cheon, B.S., and Lee, S.H., Synthesis of glycerol monostearate with high purity. *bulletin of the korean chemical society*, 24 pp. 1229–1231, 2003. DOI: <https://doi.org/10.5012/bkcs.2003.24.8.1229>.
- [23] Nunes, D.G., Da-Silva, A.D.P.M., Cajaiba, J., Pérez-Gramatges, A., Lachter, E.R., and Nascimento, R.S.V., Influence of glycerides-xanthan gum synergy on their performance as lubricants for water-based drilling fluids. *Journal of Applied Polymer Science*, 131(22), pp. 1–9, 2014. DOI: <https://doi.org/10.1002/app.41085>.
- [24] de-Paula, F.H., M., de-Freitas, F.A., Nunes, D.G., Iglauer, S., Gramatges, A.P., Nascimento, R.S.V., and Lachter, E.R., Alkyl glyceryl ethers as water-based lubricant additives in mixtures with xanthan gum. *Colloids and Surfaces A: Physicochemical Engineering Aspects*, 634, Art. 127881, 2022. DOI: <https://doi.org/10.1016/j.colsurfa.2021.127881>.
- [25] Ghandi, M., Mostashari, A., Karegar, M., and Barzegar, M., Efficient synthesis of α -monoglycerides via solventless condensation of fatty acids with glycerol carbonate. *Journal of the American Oil Chemists' Society*, 84(7), pp. 681–685, 2007. DOI: <https://doi.org/10.1007/s11746-007-1091-z>.
- [26] Venkatesan, R., Singh, P., and Fogler, H.S., Delineating the pour point and gelation temperature of waxy crude oils. *SPE Journal*, 7(4), pp. 349–352, 2002. DOI: <https://doi.org/10.2118/72237-PA>.
- [27] Venkatesan, R., Nagarajan, N.R., Paso, K., Yi, Y.B., Sastry, A.M., and Fogler, H.S., The strength of paraffin gels formed under static and flow conditions. *Chemical Engineering Science*, 60(13), pp. 3587–3598 2005. DOI: <https://doi.org/10.1016/j.ces.2005.02.045>.
- [28] Singh, P., Fogler, H.S., and Nagarajan, N., Prediction of the wax content of the incipient wax-oil gel in a pipeline: an application of the controlled-stress rheometer. *Journal of Rheology (NYNY)*, 43(6), pp. 1437–1459, 1999. DOI: <https://doi.org/10.1122/1.551054>.
- [29] Kok, M., Letoffe, J.M., Claudy, P., Martin, D., Garcin, M., and Volle, J.Z., Thermal characteristics of crude oils treated with rheology modifiers, 1997.

D.G. Nunes, received the BSc. in Chemistry in 2000, MSc. in Science and Technology of Polymers in 2002, PhD in Science and Chemistry in 2014, all of them from the Federal University of Rio de Janeiro. Postdoc at the University of Tulsa in the study of paraffin gelation and inhibition in 2022. Currently, she is associate professor in Federal Center for Technological Education of Rio de Janeiro (Cefet/RJ). She has experience in chemistry applied to the exploration and production of oil and gas. ORCID: 0000-0002-6251-7334

G.C. Nunes, received the BSc. Eng in Chemistry Engineering in 1986, from the state University of Rio de Janeiro (UERJ). MSc. in Modeling and Simulation of Three Phase Separator in 1994, from the Federal University of Rio de Janeiro (UFRJ). PhD in Multivariable Control of a Three-Phase Separator in 2000, from the University of Florida. Postdoc at the University of Tulsa in 2022. He worked 25 years at Petrobras as a processing engineer. Currently he is Adjunct Professor in the University of Rio de Janeiro (UERJ). He has experience in control, optimization, modeling in processing and reservoir. ORCID: 0000-0001-7567-0103

E.R. Lachter, received the BSc. Chemistry Engineering in 1978, MSc in Science in 1982, PhD in Science and Chemistry in 1988, all of them from the Federal University of Rio de Janeiro, Brazil. Currently, she is full professor in Chemistry Institute at Federal University of Rio de Janeiro, UFRJ, Brazil. She has experience in catalysis applied to synthesis of surfactant from biomass to the exploration and production of oil and gas. ORCID: 0000-0002-8101-7650

A.O Santos is currently graduating in Chemical Engineering from the University of the State of Rio de Janeiro, UERJ, Brazil. She was a technological initiation student from Faperj. Currently participating in the PRH ANP program at UERJ and at the stage in Iconic Lubrificantes. Tem experience in chemistry applied to the Petroleum industry. ORCID: 0009-0003-0290-0221

R.C.P. Nunes, has a BSc. Eng. in Industrial Chemistry in 2008, from the Federal Rural University of Rio de Janeiro, Brazil. MSc. in Polymer Science and Technology in 2011, and a PhD in Polymer Science and Technology in 2015, all of them from the Federal University of Rio de Janeiro, Brazil. She currently works as a researcher in the Macromolecules and Colloids Laboratory in the Oil Industry. She has experience in the field of chemistry, with an emphasis on polymers and colloids, working with polymers applied to oil exploration and production. ORCID: 0000-0002-4888-2247

E.F. Lucas, received the BSc. Eng in Chemistry Engineering in 1986, and MSc. in Science and Technology of Polymers in 1990, all of them from the Federal University of Rio de Janeiro, Brazil. Sp. in Polymers in 1992, from the University of Massachusetts, USA. PhD in Science and Technology of Polymers in 1994, from the Federal University of Rio de Janeiro, Brazil, and an Executive MBA from COPPEAD / UFRJ in 2002. Currently, she is full professor at the Federal University of Rio de Janeiro and coordinator of the Human Resources Program at ANP (PRH-16.1 IMA / COPPE / UFRJ). She participates as a permanent professor in the Polymer Science and Technology Program (IMA / UFRJ) and in the Metallurgical and Materials Engineering Program (COPPE / UFRJ). She has experience in Non-Metallic Materials (Polymers, Applications) and Chemistry (Polymers and Colloids), working mainly in polymers applied to the exploration and production of oil and gas. ORCID: 0000-0002-9454-9517

Mapping the evolution of drone-based last-mile delivery: a bibliometric analysis with field insights from Colombia

Luz Maribel Guevara-Ortega, Juan Enrique Hidalgo-Urrea, Luz Mireya Candil-Parra
& William Rafael Navarro-Zúñiga

Facultad de Ingeniería, Universidad EAN, Bogotá, Colombia. lmguevara@universidadean.edu.co, jhidalgo03762@universidadean.edu.co,
lcandil1@universidadean.edu.co, wnavarr77233@universidadean.edu.co

Received: May 16th, 2025. Received in revised form: October 24th, 2025. Accepted: October 31st, 2025.

Abstract

The article combines a bibliometric analysis of 301 studies (2019–2025) with a survey of 70 Colombian logistics leaders. It identifies an annual scientific growth rate of 14.96 %, with emerging emphasis on sustainability, optimized routes, and hybrid truck-drone fleets. Respondents report key barriers: air-space regulation (80 %), limited payload capacity (65.7 %), insufficient infrastructure (64.3 %), and concerns about security, privacy, and high up-front costs. Integrating both approaches, the authors propose an urban pilot inspired by Milan, tailored to the Colombian context, profitable even at 50 % utilization and yielding a return above 90 % in the first year. They conclude that last-mile drone adoption demands clear regulatory frameworks, infrastructure investment, and risk-management strategies to build trust among users and operators.

Keywords: drones; last-mile delivery; Colombia; urban logistics; implementation barriers; sustainability.

Evolución de la entrega con drones en la última milla: análisis bibliométrico con enfoque en Colombia

Resumen

El artículo combina un análisis bibliométrico de 301 estudios (2019-2025) con una encuesta a 70 líderes logísticos colombianos. Detecta un crecimiento científico anual del 14,96 %, con énfasis emergente en sostenibilidad, rutas optimizadas y flotas híbridas camión-dron. Los encuestados señalan como principales barreras la regulación del espacio aéreo (80 %), la escasa capacidad de carga (65,7 %), la falta de infraestructura (64,3 %), además de preocupaciones sobre seguridad, privacidad y altos costos iniciales. Integrando ambos enfoques, los autores proponen un piloto urbano inspirado en Milán, adaptado al contexto colombiano, rentable incluso con una utilización del 50 %, generando un retorno superior al 90 % en el primer año. Concluyen que la adopción de drones en la última milla exige marcos regulatorios claros, inversión en infraestructura y gestión de riesgos para generar confianza entre usuarios y operadores.

Palabras clave: drones; entrega de última milla; Colombia; logística urbana; barreras de implementación; sostenibilidad.

1 Introduction

The exponential growth of e-commerce and consumers' expectations for fast and efficient deliveries have radically transformed logistics dynamics in urban environments. The so-called "last mile," understood as the final delivery leg from the distribution center to the end customer, currently represents one of the main operational, environmental, and economic challenges for distribution companies [1,2]. In

Latin America, and particularly in Colombia, these challenges are exacerbated by structural conditions such as traffic congestion, uneven quality of urban infrastructure, and technological limitations of delivery fleets [3].

In this context, drones—or Unmanned Aerial Vehicles (UAVs)—are emerging as a disruptive technological alternative with the potential to transform last-mile logistics. Their ability to avoid traffic congestion, operate over short distances with greater energy efficiency, and reduce

How to cite: Guevara-Ortega, L.M., Hidalgo-Urrea, J.E., Candil-Parra, L.M., and Navarro-Zúñiga, W.R., Mapping the evolution of drone-based last-mile delivery: a bibliometric analysis with field insights from Colombia DYNA, (92)239, pp. 91-100, October - December, 2025.

environmental impact positions them as a viable and sustainable solution in urban and suburban settings [4,5]. However, implementing drones in the Colombian context requires overcoming various regulatory, technical, and social barriers, as well as adapting operational models to the country's geographic and demographic specificities [6,7].

Given this scenario, the present article aims to analyze the state of the art regarding the implementation of drones in last-mile logistics, with an emphasis on their applicability in urban areas of Colombia. To achieve this, a systematic review of recent international scientific literature (2019–2025) is conducted, considering technical, operational, regulatory, and environmental aspects. This analysis allows for the identification of major research trends, key challenges, and strategic opportunities for designing drone-based logistics solutions in the Colombian urban context.

This study also conducts a bibliometric analysis of drone use in last-mile deliveries, through an analysis of publications in Scopus [8] and a survey of logistics leaders in Colombia, offering a comprehensive view of the state of the art and contrasting local perceptions with global trends, to enable a deeper understanding of the topic.

2 Methodology

This research aims to conduct an exhaustive review of scientific literature and analyze the technical, legal, and environmental aspects related to drone technology. The study is framed as a descriptive and mixed-methods investigation, combining both qualitative and quantitative approaches. The methodology is based on previous research on the feasibility, barriers, opportunities, and challenges of using drones in last-mile logistics, adapted to the Colombian context.

2.1 Bibliometric analysis

This analysis aims to identify and synthesize global research trends and thematic priorities in the domain of drone logistics, with special attention given to last-mile delivery and its integration into urban environments.

It was structured into four methodological phases to ensure consistency and analytical rigor. First, the search criteria were defined using the Scopus database, selecting only peer-reviewed journal articles published between January 2019 and April 2025, using the following query: TITLE-ABS-KEY ("drone" AND "last mile delivery") AND (LIMIT-TO (DOCTYPE, "ar")). Second, metadata from 301 articles were extracted, including title, authors, affiliations, year of publication, abstract, author keywords, citation count, and corresponding author's country. The dataset was exported in a format compatible with Bibliometrix (RStudio). Third, data cleaning and standardization were performed, involving normalization of author and institution names, elimination of incomplete or duplicated records, and manual unification of semantically equivalent keywords. Finally, a comprehensive bibliometric analysis was conducted using Bibliometrix, which enabled the computation of descriptive metrics (e.g., annual scientific production, average citations, and collaboration rate), along with structural and network analyses such as thematic mapping, keyword co-occurrence, co-authorship and co-citation networks, and geographical distribution of scientific output.

2.2 Empirical survey on implementation barriers in Colombia

The survey was designed following the methodological guidelines proposed by [9] and aimed to assess the current state of drone use in last-mile logistics in urban Colombia.

The target population included companies and individuals involved in transportation and supply chain operations, particularly those familiar with drone technologies. The data collection was carried out through a structured survey, composed of 21 questions organized around six barrier categories adapted from [10]: privacy and security, regulatory, psychological, environmental, economic, and technical challenges. However, the conceptual framework for the survey also integrated insights from other recent studies on drone logistics adoption and diagnostic research methodologies [10-12].

A non-probabilistic convenience sampling method was used to select logistics professionals who were readily accessible and willing to participate [12]. The sample included 70 logistics process leaders from major Colombian cities such as Bogotá, Medellín, Cali, Barranquilla, Cartagena, and others. Notably, 85% of respondents had over five years of experience in logistics operations across various sectors, including freight transport, retail, e-commerce, pharmaceuticals, and courier services.

Before distribution, the survey underwent a content validation process through expert review by academics and professionals with at least a master's degree and experience in distribution logistics. The validated instrument was then deployed via Google Forms. To maximize reach and participation, a snowball sampling technique was also adopted [13], encouraging participants to share the survey within their professional networks, including via LinkedIn—mirroring the outreach strategy described by [9].

The empirical insights generated from this process allowed for a rich, context-specific understanding of the implementation barriers to drone-based last-mile delivery in Colombia, thereby offering a grounded counterpoint to the more generalized barriers identified in global literature.

3 Results

The bibliometric analysis was conducted on a curated dataset of 301 journal articles published between 2019 and 2025, retrieved from Scopus [8]. These documents were distributed across 138 different sources. Key descriptive indicators include an annual growth rate of 14.96%, an average document age of 2.17 years, and an average of 29.9 citations per document. A total of 12,963 references were analyzed. The dataset includes 871 unique author keywords and 1,693 Keywords Plus. A total of 927 authors contributed, with an average of 3.68 co-authors per document and an international collaboration rate of 32.56%.

These metrics reveal a growing and collaborative field, characterized by multi-authored contributions and a notable level of international scientific cooperation.

Scientific output showed a consistent upward trend over the seven-year period, peaking in 2024 and 2025. Authors such as Ghoniem A., Kong F., and Altinses D. were the most productive. The main journals published on this topic

included "Transportation Research Part E," "IEEE Internet of Things Journal," and "Expert Systems with Applications."

China, the United States, and the United Kingdom were the most prolific countries, reflecting strong investment in technological research and logistics innovation.

Highly cited articles addressed optimization problems, delivery models, and sustainability impacts. Among them, the paper titled "The multiple flying sidekicks traveling salesman problem" received 350 citations.

Collaboration networks revealed clusters of co-authorship primarily concentrated in Asia and Europe. The analysis of keyword co-occurrence identified core themes such as logistics, routing, optimization, and urban delivery. Recent years saw the emergence of terms like "sustainability" and "urban logistics," suggesting an increasing diversification of research agendas.

3.1 Evolution of scientific output over time

The temporal evolution of scientific publications on drones in last-mile delivery logistics, spanning from 2019 to 2025, reveals a strong upward trend in scholarly interest. In 2019, there were only 13 published articles; this number increased steadily in the subsequent years, reaching 25 in 2020, 26 in 2021, and 42 in 2022. A significant growth occurred in 2023 with 56 articles, culminating in a peak of 109 publications in 2024. As of April 2025, 30 articles have already been published, suggesting that the current year may surpass or match the previous year's total by the end of the period. This trend is illustrated in Fig. 1, which clearly reflects the exponential increase in academic output related to drone applications in urban logistics.

In terms of impact, measured by the average total citations per year, a declining trend is observed. While early publications in 2019 and 2020 achieved high citation averages (18.59 and 18.84 respectively), more recent publications such as those in 2024 and 2025 exhibit lower averages (2.28 and 0.10). This is expected, as newer articles typically require more time to accumulate citations. Nonetheless, the increase in output reflects a growing maturity and diversification of the field of research.

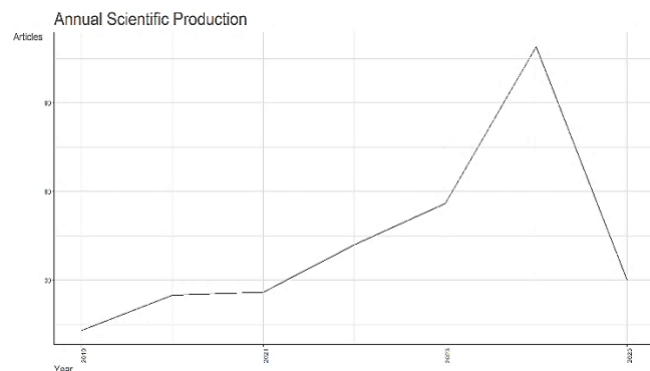


Figure 1. Annual Scientific Production.
Source: Scopus, 2025.

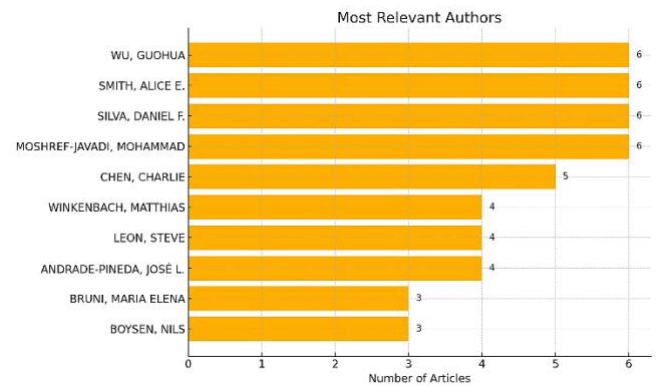


Figure 2. Most Relevant Authors.
Source: Scopus, 2025.

These findings underscore a progressive consolidation of drone-based delivery systems as a focal topic within logistics and transportation research, driven by both technological innovation and global interest in smart urban mobility solutions.

3.2 Most productive authors and institutions

The analysis of author productivity revealed that the most active contributors in the field of drones for last-mile delivery are Daniel F. Silva and Alice E. Smith. Both have contributed multiple articles between 2024 and 2025, including publications in top-tier journals such as *IEEE Transactions on Evolutionary Computation* and the *European Journal of Operational Research*. Their research focuses on optimization algorithms and logistics planning for truck-drone hybrid systems [14]. Fig. 2 visually highlights their leading roles, showing their high publication counts relative to other authors in the field.

Regarding institutional productivity, Central South University leads with 24 publications, followed by The Hong Kong Polytechnic University (22), National Technical University of Athens (21), and Beihang University (19). These institutions are predominantly located in Asia and Europe, reflecting the global distribution of drone-related logistics research hubs. Fig. 3 illustrates this ranking, emphasizing the dominant presence of Asian and European institutions in the scientific output on last-mile drone delivery.

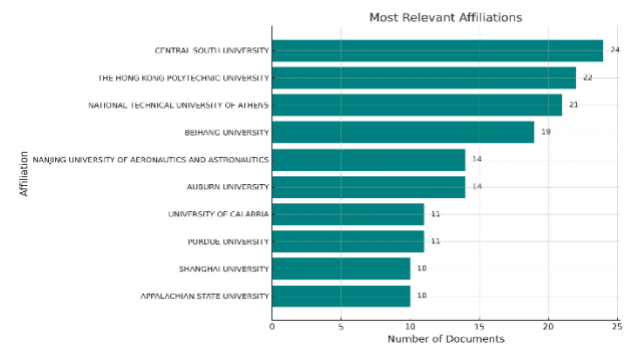


Figure 3. Most Relevant Affiliations.
Source: Scopus, 2025.

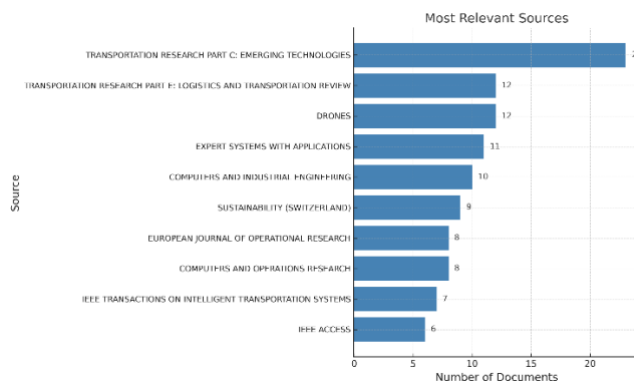


Figure 4. Most Relevant Sources.
Source: Scopus, 2025.

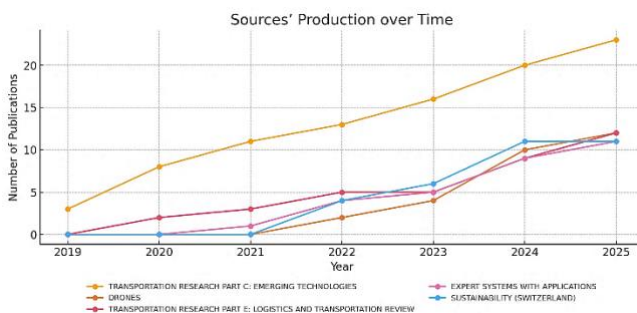


Figure 5. Sources' Production over Time.
Source: Scopus, 2025.

The data suggests that productive researchers are often embedded within highly active institutions, and their work is frequently published in high-impact journals. This correlation between author and institutional output underscores the importance of collaborative environments and research infrastructure in advancing the field.

3.3 Most relevant journals and thematic areas

The bibliometric analysis identified several academic journals that play a central role in disseminating research on drones in last-mile logistics. Fig. 4 presents the most relevant sources, highlighting Transportation Research Part C: Emerging Technologies as the most prolific, with 23 articles published on the topic during the 2019–2025 period. Fig. 5 complements this by illustrating the Sources' Production over Time, including Drones and Transportation Research Part E: Logistics and Transportation Review, each with twelve articles, and Expert Systems with Applications, which contributed eleven articles.

These journals indicate a multidisciplinary scope, where research, engineering, and intelligent systems intersect with logistics. Particularly, the prevalence of technology-focused and optimization-oriented outlets suggests that the field is still strongly driven by performance modeling, system design, and algorithm development.

The thematic areas addressed in these publications include autonomous vehicle routing, hybrid delivery

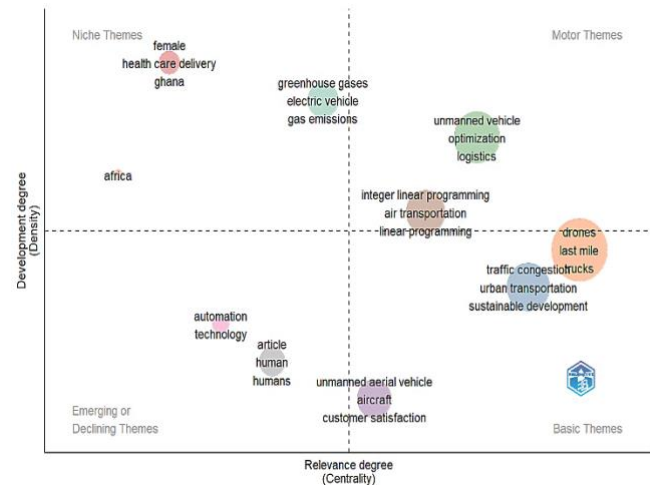


Figure 6. Thematic Map.
Source: Scopus, 2025.

systems, sustainability in logistics, and urban transportation networks. Fig. 6 displays the thematic map, which visually clusters these core areas based on co-word analysis, revealing the intellectual structure of the field. This diversity reflects an expanding academic interest in adapting drone technology to the practical challenges of urban distribution and smart city logistics.

While global academic literature frequently addresses drone logistics from the perspective of optimization and integration within smart urban systems, the work of [10] provides a valuable framework for analyzing the barriers to implementing drones in last-mile deliveries. Building on this, the fieldwork conducted in Colombia captures the perception of leaders in distribution and transportation logistics processes. Among surveyed logistics leaders, Fig. 7 illustrates security and privacy emerged as the most critical concern (68.6%).

These findings, particularly regarding risks such as hacking, cyberattacks, and physical interference with 77.1% also citing theft or damage to drones as shown in Fig. 8.

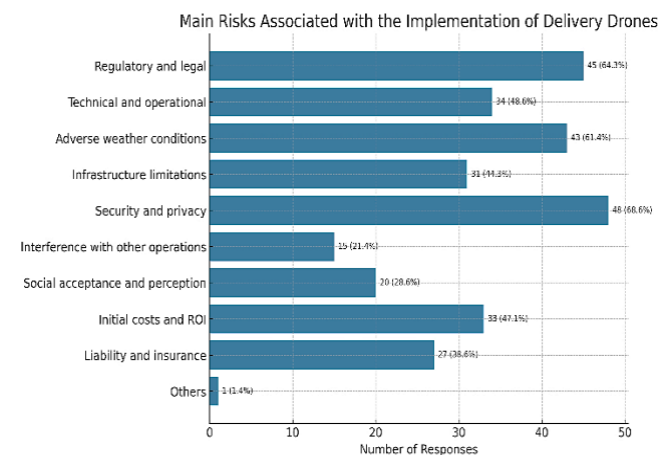


Figure 7. Most Critical Concerns.
Source: Own elaboration.

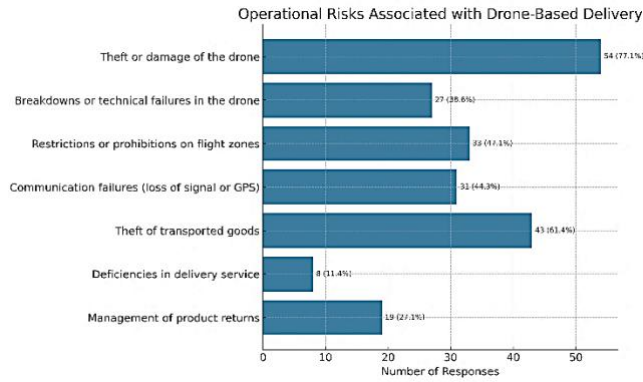


Figure 8. Most Critical Risk.
Source: Own elaboration.

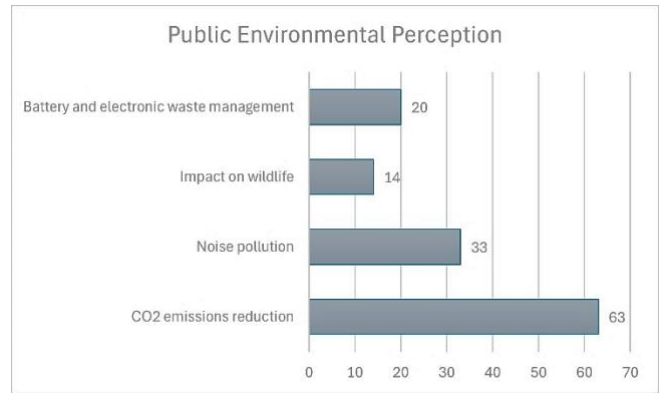


Figure 10. Public Environmental Perception.
Source: Own elaboration.

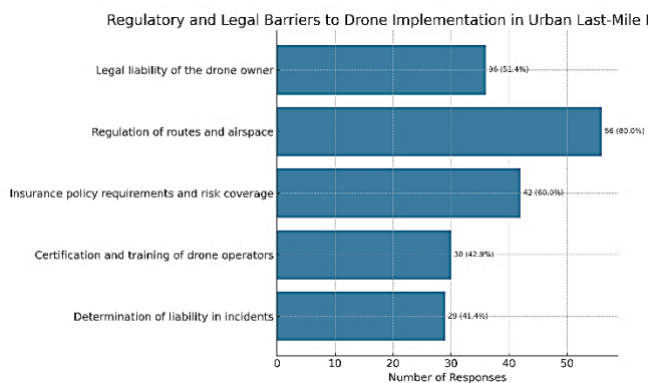


Figure 9. Regulatory Barriers.
Source: Own elaboration.

Regulatory hurdles were equally prominent, with 80% of participants identifying airspace regulation as a major constraint, and over 60% pointing to insurance and licensing requirements. Fig. 9 illustrates these regulatory barriers, emphasizing the need for clearer frameworks related to drone flight permissions, operator certification, and liability coverage in last-mile delivery operations.

Public perception posed additional resistance: 47.1% of respondents noted fear of accidents, and 34.3% questioned the reliability of drones. Fig. 9 illustrates these public perception challenges, showing that although 90% acknowledged the potential of drones to reduce CO₂ emissions, 47.1% expressed concern about noise pollution, and nearly 29% highlighted the issue of electronic waste.

From an economic standpoint, while 72.9% of logistics leaders expected drones to reduce operational costs, 41.4% identified high initial investment as a key barrier. Technological limitations were also evident: 65.7% of respondents considered load capacity insufficient, and 64.3% cited the lack of adequate infrastructure to support drone operations.

These findings contrast the optimism observed in global academic research by grounding the discussion in real-world barriers, as illustrated by Fig. 10. They highlight the multifaceted challenges that may inhibit the integration of drones into smart city logistics, particularly in emerging economies, where regulatory, infrastructural, and societal constraints are still prevalent.

3.4 Keyword co-occurrence analysis

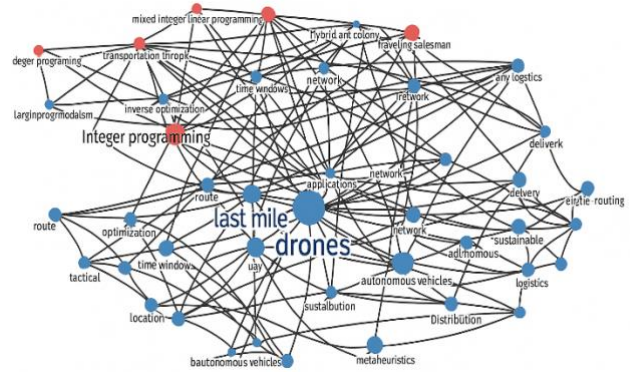


Figure 11. Co-occurrence Network.
Source: Scopus, 2025.

The analysis of keyword co-occurrence allows for the identification of the conceptual structure of the scientific literature on drones applied to last-mile delivery, by mapping the terms that most frequently appear together in indexed documents. This technique facilitates the detection of dominant themes, thematic connections, and emerging areas of research within the field. Fig. 11 presents the co-occurrence network, highlighting how clusters of related terms—such as optimization, routing, sustainability, and vehicle type—reveal the multidimensional nature of current research and its alignment with practical implementation challenges.

In this study, a co-occurrence network was constructed based on centrality metrics such as betweenness, closeness, and PageRank, which enabled the identification of the most influential nodes within the semantic network. The term “integer programming” emerged as the most central keyword, with a prominent score in betweenness centrality (49.3) and PageRank (0.057). This highlights the importance of mathematical modeling and algorithmic approaches as essential tools for solving complex logistical problems, particularly those related to route planning and resource allocation.

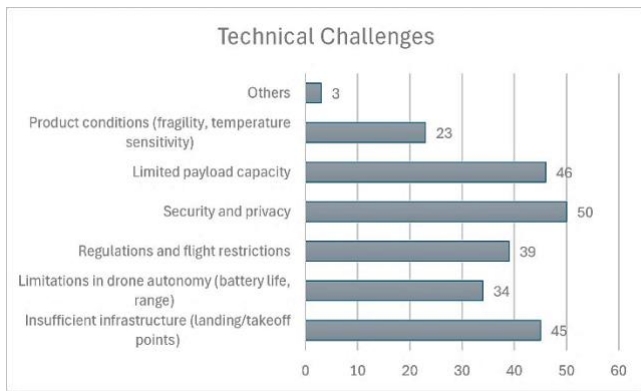


Figure 12. Technical Challenges.
Source: Own elaboration.

Other highly connected terms included “traveling salesman problem” [15], “automobiles,” and “routing”, all of which are grouped into a thematic cluster focused on operations research, logistics network optimization [16], and transportation analysis. These concepts reflect the central role of computational techniques in addressing efficiency challenges in urban deliveries, especially in scenarios where travel time [17], energy consumption [18] or carbon emissions [19], must be minimized.

This thematic structure directly echoes the findings from the fieldwork conducted in Colombia, where 70 leaders from logistics, manufacturing, and transportation companies were surveyed. Fig. 12 illustrates these technical challenges, revealing that the barriers to drone adoption for last-mile delivery are closely aligned with those identified in the academic literature: insufficient infrastructure (64.3%), limited payload capacity (65.7%), restricted drone autonomy (48.6%), and complexities in planning efficient routes in urban environments.

As a result, both academic research and business perception in the Colombian context converge on the idea that logistics optimization—understood as the integration of variables such as vehicle type, urban mobility conditions, and physical infrastructure constraints—is a top priority. The high interconnectivity among the key terms identified in the literature confirms that the field remains firmly rooted in quantitative models and algorithmic solutions, while the local empirical data reinforces the relevance of these approaches for addressing real-world implementation challenges of drones.

It is worth noting that although the thematic network is currently dominated by mathematical approaches, new keywords are beginning to emerge related to sustainability, public perception [16], regulations [20], and emerging technologies (such as AI and blockchain) [21], suggesting a gradual diversification in the analytical frameworks. This thematic evolution opens opportunities for future research to integrate both technical and social components into more holistic proposals for last-mile logistics design.

3.5 Co-authorship network analysis

Fig. 13 presents the co-citation network, offering insight into the structure of collaboration among researchers in the

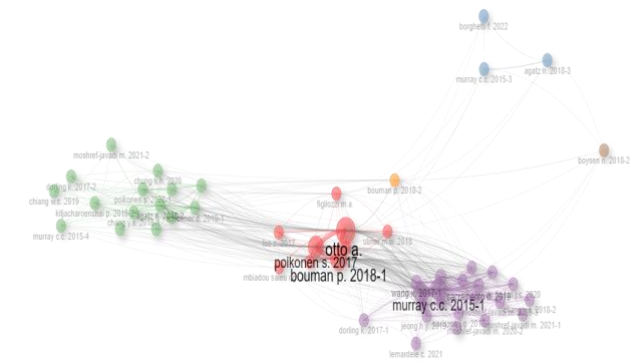


Figure 13. Co-citation Network.
Source: Scopus, 2025.

field of drones for last-mile delivery. Based on co-citation metrics and centrality indicators, the network highlights the most influential authors and the degree of their integration within the broader research community. This structure reveals not only the key intellectual contributors but also the formation of thematic clusters that shape the academic discourse on drone-based logistics solutions.

Otto A. emerges as the most central figure in the co-authorship network, showing the highest betweenness centrality (385.79), closeness (0.017), and PageRank (0.038). These metrics indicate that Otto A. plays a pivotal role in connecting different subgroups within the network. Other significant contributors include Bouman P. (2018), Poikonen S. (2017), and Figliozzi M.A., all of whom exhibit strong connectivity and influence.

The clustering of authors into distinct communities reveals thematic collaborations focused on vehicle routing, urban delivery frameworks, and algorithmic optimization. The presence of authors linked to foundational publications between 2017 and 2018 suggests that early contributions continue to anchor contemporary research.

Overall, the co-authorship structure demonstrates a moderately centralized network, with a few key authors acting as hubs of influence and collaboration. These hubs facilitate knowledge dissemination across research groups and support the consolidation of best practices in drone-based logistics.

3.6 Geographic analysis: countries with the highest production

The geographic distribution of publications reveals the countries that are driving research on drones in last-mile delivery logistics. Fig. 14 displays the distribution by corresponding author's countries, showing that the United States leads in scientific output with 57 publications, accounting for 18.9% of all documents in the dataset. It is followed by China with 49 publications (16.3%), while Italy, Germany, and the United Kingdom also figure among the most active contributors, reflecting a strong global interest concentrated in North America, Asia, and Europe.

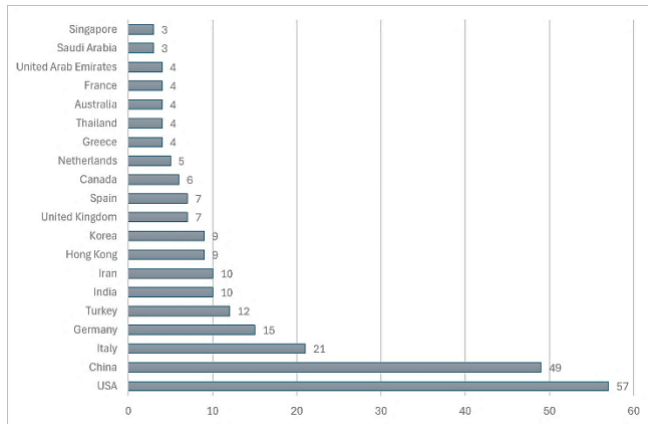


Figure 14. Corresponding Author's Countries.
Source: Scopus, 2025.

A deeper look at collaboration patterns distinguishes between single-country publications (SCP) and multiple-country publications (MCP). The United States had 37 SCPs and 20 MCPs, while China had 32 SCPs and 17 MCPs, indicating a balanced mix of domestic and international research efforts. Notably, Italy showed a high proportion of international collaboration, with 42.9% of its articles involving authors from other countries.

These trends underscore the global nature of drone-related research, with significant contributions from both Western and Asian countries. The high level of MCP in countries like Italy suggests an openness to cross-border collaboration, which can be crucial for advancing experimental implementations and policy alignment in smart logistics.

Italy stands out as one of the leading countries in research on drone-based last-mile delivery, and a representative example of this leadership is the case study conducted in Milan by [22]. Through a stated preference analysis and financial evaluation, the study demonstrated that autonomous drones are both technically feasible and economically sustainable for small parcel deliveries in urban environments, achieving profitability within three years. This empirical evidence provides a solid methodological foundation for replicating similar models in other urban contexts.

Building on the foundational work by [22], a pilot project was formulated in this research to assess the applicability of drone-based last-mile delivery in Colombian urban areas. The Milanese model served as a benchmark, demonstrating both technical and financial feasibility under real-world constraints. The proposed pilot mirrors key operational parameters—including drone specifications (octocopter design, 2.25 kg payload, 30-minute autonomy), delivery cycles, and depot structure—tailored to Colombia's urban logistics conditions. The plan aims to conduct over 32,000 deliveries with a fleet of 10 drones, and incorporates performance indicators such as service precision, delivery time, operational efficiency, and environmental impact. Financial projections under pessimistic, moderate, and optimistic utilization scenarios show that the initiative is profitable even at 50% operational capacity, achieving a first-

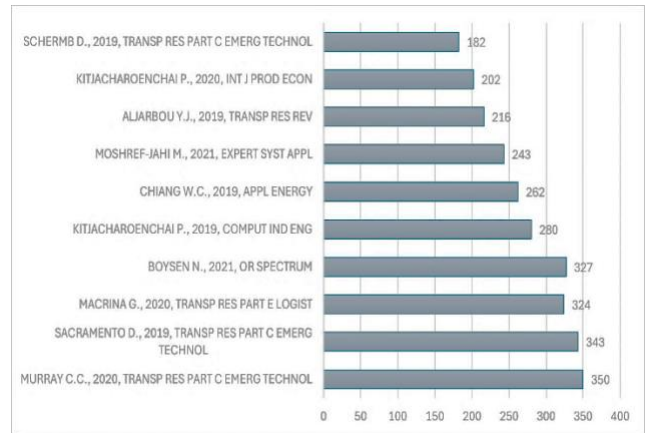


Figure 15. Most Global Cited Documents.
Source: Scopus, 2025.

year return on investment exceeding 90%. These results underscore the viability of drones as a scalable and sustainable solution to the growing challenges of last-mile delivery in Colombian cities.

3.7 Most cited documents

The most cited documents in the field of drone applications for last-mile delivery provide insight into foundational contributions and thematic influence within the research community. Based on total global citations, the top five articles represent a combination of methodological innovation and system-level analysis.

Fig. 15 highlights the most globally cited documents in the field of drones for last-mile delivery. Leading the list is the article by [23], published in *Transportation Research Part C: Emerging Technologies*, which received 350 citations, with an average of 58.3 citations per year. This paper presents a robust framework for hybrid drone-truck delivery systems and has become a foundational reference in studies focused on optimization algorithms and simulation-based logistics models, underscoring its critical role in shaping the academic discourse.

Following closely is an article by Sacramento, which received 343 citations and focuses on stochastic modeling of drone-based logistics under uncertainty. Other notable contributions include works that explore routing efficiency and the integration of drone systems with urban infrastructure. These influential studies—by [24, 25, 4] have significantly advanced the theoretical foundations of drone logistics and continue to shape current research in the field.

These highly cited papers not only serve as methodological benchmarks but also signal the primary axes of development in this field: route planning, hybrid fleet coordination, and smart infrastructure integration. Their prominence underscores the technical depth and applied potential of research in last-mile drone logistics.

4 Discussions

The findings of this study allow for an integrated understanding of global research trends on drones for last-mile deliveries and the contextual perception of logistics leaders in Colombia. The bibliometric evolution shows a sustained growth in scientific production in the field, peaking in 2024, with an increasing focus on topics such as sustainability, energy efficiency, route planning, and hybrid truck-drone systems [23,4]. This panorama reflects a consolidating field driven by technological developments and the pursuit of more sustainable and resilient urban logistics models [26].

However, the contrast between international literature and the results of the survey applied in Colombia reveals a significant gap between theoretical potential and practical feasibility. While studies such as those by [22, 27] highlight the technical and economic feasibility of drones for fast deliveries in densely populated urban areas, Colombian logistics leaders point out critical obstacles such as limited payload capacity (65.7%), insufficient infrastructure (64.3%), and regulatory constraints (80%), which align with the barriers identified by [10, 20].

Furthermore, risk perception and social concerns — including privacy, safety, and noise — emerge as significant barriers. These findings align with research such as [28], who warns of the social and labor impacts of drone deployment in African healthcare systems, and the study by [29], which highlights the negative effect of perceived risk on consumers' adoption intention.

From a technical perspective, the predominance of terms such as "integer programming" and "traveling salesman problem" in the co-occurrence analysis of keywords confirms the literature's emphasis on using mathematical models and optimization algorithms as fundamental tools. This is consistent with proposals such as those by [30], who validate hybrid scenarios as more cost-effective depending on demand density and territorial configuration.

Regarding sustainability, the positive impact of drone use on carbon emissions is widely [26,18] and recognized by 90% of respondents. However, emerging environmental concerns persist, such as noise, electronic waste, and limited autonomy under adverse weather conditions [31,21].

The case of Zipline in Rwanda [32] serves as empirical evidence of the viability of well-structured operational models, capable of drastically reducing delivery times and eliminating the waste of medical resources. However, its replicability in Colombia requires institutional, regulatory, and technical adaptations, particularly in more complex urban environments with less regulatory coverage.

Finally, the implementation of a pilot inspired by the Milan model —adapted to Colombian conditions— represents a strategic advance. Its financial projections, even under pessimistic scenarios, suggest that sustainable returns are achievable. This result confirms the proposal by [33] on the scalability potential of drone delivery when supported by existing infrastructure and territorial planning.

Overall, this discussion reveals a critical duality: on one hand, academic and technical support for the viability of

drones for urban deliveries; on the other, contextual barriers that still limit their effective adoption in countries like Colombia. Overcoming this gap will require a multi-stakeholder approach that articulates technological innovation, regulatory governance, urban infrastructure, and social acceptance.

5 Conclusions

The bibliometric analysis demonstrates the rapid consolidation of research on last-mile deliveries with drones between 2019 and 2025: scientific production has grown at an average annual rate of 14.96%, peaking in 2024, while diversifying towards topics such as sustainability, route planning, and hybrid truck-drone systems. These findings corroborate that urban aerial logistics has become a priority area within studies on smart mobility and emission reduction.

However, the survey applied to 70 Colombian logistics leaders reveals a gap between theoretical potential and practical adoption: 80% identify airspace regulation as the main barrier, 65.7% point to limited payload capacity, and 64.3% highlight the lack of support infrastructure. Additionally, concerns about security and privacy (68.6%) and the initial cost (41.4%) reinforce the need to address socio-technical factors before scaling pilot projects.

The integration of both approaches —bibliometric and empirical— enabled the proposal of a pilot project, inspired by the Milan case, adapted to Colombian urban conditions. Financial projections demonstrate profitability even at a 50% utilization level, achieving a return of over 90% in the first year, confirming the economic viability of the solution as long as supportive policies and infrastructure investment are articulated.

Among the study's limitations are convenience sampling and the self-reported nature of responses, which suggests caution when generalizing the findings. Future research should expand the sample to other stakeholders —aeronautical authorities, urban communities, and technology providers— as well as evaluate operational scenarios with demand simulations and climatic restrictions to strengthen decision-making.

Finally, although the literature supports the technical feasibility and environmental benefits of drones for last-mile delivery, their adoption in Colombia will depend on the ability to harmonize technological advancements with clear regulatory frameworks, adequate infrastructure, and risk management strategies that ensure trust among users and operators.

References

- [1] Lyons, T., and McDonald, N.C., Last-mile strategies for urban freight delivery: a systematic review. *Transportation Research Record: Journal of the Transportation Research Board*, 2677(1), pp. 1141-1156, 2022. DOI: <https://doi.org/10.1177/03611981221103596>
- [2] Lemardel, C., Estrada, M., Pagès, L. and Bachofner, M., Potentialities of drones and ground autonomous delivery devices for last-mile logistics. *Transportation Research Part E: Logistics and Transportation Review*, 149, art. 102325, 2021. DOI: <https://doi.org/10.1016/j.tre.2021.102325>

- [3] The Logistics World., El Auge del comercio electrónico en Latinoamérica: Cómo la Logística de última Milla Está Transformando El Sector. [online]. 2024. Available at: <https://thelogisticsworld.com/logistica-comercio-electronico/el-auge-del-comercio-electronico-en-latinoamerica-como-la-logistica-de-ultima-milla-esta-transformando-el-sector>
- [4] Boysen, N., Fedtke, S., and Schwerdfeger, S., Last-mile delivery concepts: a survey from an operational research perspective, *OR Spectrum*, 43, pp. 1–58, 2021. DOI: <https://doi.org/10.1007/S00291-020-00607-8>
- [5] Patella, S.M., Grazieschi, G., Gatta, V., Marcucci, E., and Carrese, S., The adoption of green vehicles in last mile logistics: a systematic review. *Sustainability*, 13(1), art. 6. 2021. DOI: <https://doi.org/10.3390/su13010006>
- [6] Muñoz-Villamizar, A., Solano-Charris, E., Reyes-Rubiano, L., and Faulin, J., Measuring Disruptions in Last-Mile Delivery Operations. *Logistics*, 5(1), art. 17, 2021. DOI: <https://doi.org/10.3390/LOGISTICS5010017>
- [7] Eskandaripour, H., and Boldsaikhan, E., Last-Mile Drone Delivery: past, present, and future. *Drones*, 7(2), Art. 77, 2023. DOI: <https://doi.org/10.3390/drones7020077>
- [8] Scopus, "Documents search results," Elsevier, [Online]. 2025. Available at : <https://www.scopus-com.bdbiblioteca.universidadean.edu.co/results/results.uri?st1=drone&st2=&s=%28TITLE-ABS-KEY%28drone%29+AND+TITLE-ABS-KEY%28last+mile+delivery%29%29&limit=10&origin=searchbasic&sort=plf-f&src=s&sot=b&sdt=b&sessionSearchId=5b92db2bb273c5e0c9f84bf31538547&yearFrom=2019&yearTo=2025&cluster=scosubtype%2C%22ar%22%2Ct>
- [9] Fehling, C., and Saraceni, A., Technical and legal critical success factors: feasibility of drones and AGV in the last-mile-delivery. *Research in Transportation Business and Management*, 50, Art. 101029, 2023. DOI: <https://doi.org/10.1016/j.rtbm.2023.101029>
- [10] Sah, B., Gupta, R., and Bani-Hani, D., Analysis of barriers to implement drone logistics, *International Journal of Logistics Research and Applications*, 24(6), pp. 531–550, 2020. DOI: <https://doi.org/10.1080/13675567.2020.1782862>
- [11] Pacheco, D.A.D.J., Sarker, S., Bilal, M., Chamola, V., and Garza-Reyes, J.A., Opportunities and challenges of drones and internet of drones in healthcare supply chains under disruption, *Production Planning and Control*, 36(15), pp. 2009–2031, 2024. DOI: <https://doi.org/10.1080/09537287.2024.2437041>
- [12] Hernández-Sampieri, R., and Mendoza Torres, C.P., Metodología de Investigación: la investigación, McGraw-Hill Interamericana, [online]. 2023. Available at: <https://www-ebooks7-24-com.bdbiblioteca.universidadean.edu.co/?il=31455>
- [13] Jalali, S., and Wohlin, C., Systematic literature studies: database searches vs. backward snowballing, *Proc. Int. Symp. on Empirical Software Engineering and Measurement*, pp. 29–38, 2012. DOI: <https://doi.org/10.1145/2372251.2372257>
- [14] Pina-Pardo, J.C., Silva, D.F., Smith, A.E., and Gatica, R.A., Fleet resupply by drones for last-mile delivery. *European Journal of Operational Research*, 316(1), pp. 168–182, 2024. DOI: <https://doi.org/10.1016/j.ejor.2024.01.045>
- [15] Nguyen, M.A., Luong, H.L., Hà, M.H., and Ban, H.B., An efficient branch-and-cut algorithm for the parallel drone scheduling traveling salesman problem, *4OR*, 21(4), pp. 609–637. 2023. DOI: <https://doi.org/10.48550/arXiv.2111.11307>
- [16] Bridgelall, R., Spatial analysis of middle-mile transport for advanced air mobility: A Case Study of Rural North Dakota, *Sustainability*, 16(20), art. 8949, 2024. DOI: <https://doi.org/10.3390/su16208949>
- [17] Peng, Y., Zhu, W., Yu, D.Z., Liu, S., and Zhang, Y., Multi-depot electric vehicle–drone collaborative-delivery routing optimization with time-varying vehicle travel time, *vehicles*, 6(4), pp. 1812–1842, 2024. DOI: <https://doi.org/10.3390/vehicles6040088>
- [18] Zhang, J., Campbell, J.F., Sweeney, D.C., and Hupman, A.C., Energy consumption models for delivery drones: a comparison and assessment, *Transportation Research Part D: transport and environment*, 90, art. 102668, 2021. DOI: <https://doi.org/10.1016/j.trd.2020.102668>
- [19] Peng, Y., Zhang, Y., Yu, D.Z., Liu, S., Zhang, Y., and Shi, Y., Optimizing multi-depot mixed fleet vehicle–drone routing under a carbon trading mechanism, *mathematics*, 12(24), art. 4023, 2024. DOI: <https://doi.org/10.3390/math12244023>
- [20] Madani, B., and Ndiaye, M., Drone delivery systems for logistics operations: identification of regulatory challenges, in *Proc. IEEE Int. Conf. on Engineering, Technology and Innovation (ICE/ITMC)*, pp. 1–7, art. 2420, 2023. DOI: <https://doi.org/10.1109/ICE/ITMC58018.2023.10332420>
- [21] Muñoz, G., Barrado, C., Çetin, E., and Salami, E., Deep reinforcement learning for drone delivery, *Drones*, 3(3), art. 72, 2019. DOI: <https://doi.org/10.3390/drones3030072>
- [22] Borghetti, F., Caballini, C., Carboni, A., Grossato, G., Maja, R., and Barabino, B., the use of drones for last-mile delivery: a numerical case study in Milan, Italy, *Sustainability*, 14(3), art. 1766, 2022. DOI: <https://doi.org/10.3390/su14031766>
- [23] Murray, C.C., and Raj, R., The multiple flying sidekicks traveling salesman problem: parcel delivery with multiple drones, *Transportation Research Part C: Emerging Technologies*, 110, pp. 368–398, 2020. DOI: <https://doi.org/10.1016/j.trc.2019.11.003>
- [24] Sacramento, D., Pisinger, D., and Røpke, S., An adaptive large neighborhood search metaheuristic for the vehicle routing problem with drones, *Transportation Research Part C: Emerging Technologies*, 102, pp. 289–315, 2019. DOI: <https://doi.org/10.1016/j.trc.2019.02.018>
- [25] Macrina, G., Di-Puglia-Pugliese, L., Guerriero, F., and Laporte, G., "Drone-aided routing: a literature review," *Transportation Research Part C: Emerging Technologies*, 120, Art. 102762, 2020. DOI: <https://doi.org/10.1016/j.trc.2020.102762>
- [26] Bao-D, Y., Yan, Li, Y., and Chu, J., "The Future of Last-Mile Delivery: lifecycle environmental and economic impacts of drone-truck parallel systems," *Drones*, 9(1), art. 54, 2025. DOI: <https://doi.org/10.3390/drones9010054>
- [27] Zhi-Hua, H., Huang, Y.L., Li, Y.N., and Bao, X.Q., Drone-based instant delivery hub-and-spoke network optimization. *drones*, 8(6), art. 247. 2024. DOI: <https://doi.org/10.3390/drones8060247>
- [28] E.A., Ameso., Digital entanglements: medical drones in African healthcare systems. *Global Public Health*, 19(1), art. 2405987, 2024 DOI: <https://doi.org/10.1080/17441692.2024.2405987>
- [29] Ganjipour, H., and Edrisi, A., Applying the integrated model to understanding online buyers' intention to adopt delivery drones in Iran. *Transportation Letters*, 15(2), pp. 98–110. 2022. DOI: <https://doi.org/10.1080/19427867.2022.2035130>
- [30] Choi, Y., and Schonfeld, P.M., A comparison of optimized deliveries by drone and truck. *Transportation Planning and Technology*, 44(3), pp. 319–336. 2021. DOI: <https://doi.org/10.1080/03081060.2021.1883230>
- [31] Aurambout, J., Gkoumas, K., and Ciuffo, B. Last mile delivery by drones: an estimation of viable market potential and access to citizens across European cities. *European Transport Research Review*, 11(30), pp.1-21, 2019. DOI: <https://doi.org/10.1186/s12544-019-0368-2>
- [32] Ackerman, E., and Koziol, M., "The blood is here: Zipline's medical delivery drones are changing the game in Rwanda," *IEEE Spectrum*, 56(5), pp. 24–31, 2019. DOI: <https://doi.org/10.1109/MSPEC.2019.8701196>
- [33] Tokosh, J., and Chen X., "Delivery by Drone: estimating market potential and access to consumers from existing Amazon Infrastructure," *Papers in Applied Geography*, 8(4), pp. 414–433, DOI: <https://doi.org/10.1080/23754931.2022.2105167>

L.M. Guevara-Ortega, is PhD. in Process Engineering from Universidad EAN, holds a MSc. in industrial Engineering from the Universidad Francisco José de Caldas. She has 20 years of professional and research experience in the fields of sustainable supply chains, procurement, process research, and organizational management. Currently, she serves as an Associate Professor at Universidad EAN, Colombia.
ORCID: 0000-0002-9883-4964

J.E. Hidalgo-Urrea, is a Sp. in Quality and Innovation Process Management and holds a MSc. in supply chain management from the Universidad EAN, Colombia. He has over 16 years of experience in the logistics and fast-moving consumer goods (FMCG) sector. Throughout his career, he has led production, warehousing, logistics, and transportation teams in companies such as Alpina S.A., and currently serves as the Logistics Director at Centurion Foods.

ORCID: 0009-0002-4771-3633

L.M. Candil-Parra, holds a BSc. in International Business, a Postgraduate Sp. in Quality and Innovation Process Management, and a MSc. in Supply Chain Management from the Universidad EAN, Colombia. She has over 17 years of experience in the humanitarian sector, collaborating with various

international organizations and focusing on emergency logistics and supply chain management. Her experience integrates operational best practices with strategic planning in complex environments.

ORCID: 0009-0005-3056-7627

W.R. Navarro-Zúñiga, holds a BSc in Industrial Engineering, a Postgraduate Sp. in Logistics, and MSc. in Supply Chain Management from the Universidad EAN, Colombia. He has over 12 years of experience in logistics and operations within industrial sectors of both national and international scope. Since 2014, he has held leadership positions at C.I. Energía Solar S.A.S. – ESWINDOWS, where he currently serves as Head of Distribution and Transportation.

ORCID: 0009-0000-6285-8588

Improvement of the efficiency of hospital care: a simulation-based approach

Katherine Tatiana Osorio-Canchig, John Paúl Reyes-Vásquez & Darwin Santiago Aldás-Salazar

Facultad de Ingeniería en Sistemas, Electrónica e Industrial, Universidad Técnica de Ambato, Ambato, Ecuador. kosorio0512@uta.edu.ec, johnpreyes@uta.edu.ec, darwinsaldas@uta.edu.ec

Received: May 5th, 2025. Received in revised form: October 9th, 2025. Accepted: November 4th, 2025.

Abstract

This article analyses the implementation of lean manufacturing tools integrated with industry 4.0 technologies, specifically with the discrete event simulation, to improve the operational performance of hospital processes. This study applied a quantitative and experimental methodological approach to the implementation of lean healthcare (LH) to reduce waste. Thus, statistical and scenario modelling tools called ExpertFit and Experimenter are employed using FlexSim software in the healthcare environment. Here, a detailed diagnosis of critical processes is performed, with emphasis on identifying bottlenecks in patient weighing, triage and surgery. The results reveal significant limitations in the responsiveness of the system to sudden increases in demand. The simulation model then proposes a structural intervention involving the addition of four nurses and three doctors. This reveals a potential increase in operational efficiency of up to 36.8% over the projected demand. Finally, this study highlights the relevance of the methodological integration of LH as a strategy for the systematic elimination of waste and the promotion of a culture of continuous improvement in decision-making. This multidimensional approach provides a transferable analytical framework for both academic researchers and healthcare professionals, contributing to the development of more efficient and adaptable hospital management models.

Keywords: industry 4.0; simulation; lean healthcare

Mejora de la eficiencia de la atención hospitalaria: un enfoque basado en la simulación

Resumen

Este artículo analiza la implementación herramientas lean manufacturing integradas con tecnologías de la industria 4.0, específicamente con la simulación de eventos discretos para la mejora del rendimiento operacional de procesos hospitalarios. Para el estudio se aplica un enfoque metodológico cuantitativo y experimental con la implementación lean healthcare (LH) que permite reducir los desperdicios. Así, se emplean herramientas estadísticas y de modelamiento de escenarios denominadas ExpertFit y Experimenter utilizando el software FlexSim en el entorno sanitario. Aquí, se realiza un diagnóstico detallado de los procesos críticos, con énfasis en identificar cuellos de botella en el pesaje de pacientes, triaje y cirugías. Los resultados revelan limitaciones significativas en la capacidad de respuesta del sistema ante incrementos súbitos de demanda. Luego, el modelo de simulación propone una intervención estructural que contempla la incorporación de cuatro profesionales de enfermería y tres facultativos doctores. Esto revela un incremento potencial de la eficiencia operativa de hasta 36.8% con respecto a la demanda proyectada. Finalmente, el estudio destaca la relevancia de la integración metodológica de LH como estrategia para la eliminación sistemática de desperdicios y la promoción de una cultura de mejora continua en la toma de decisiones. Este enfoque multidimensional proporciona un marco analítico transferible tanto para investigadores académicos como para profesionales del sector salud, contribuyendo al desarrollo de modelos de gestión hospitalaria más eficientes y adaptables.

Palabras clave: industria 4.0; simulación; atención sanitaria ajustada

1 Introduction

Lean manufacturing (LM) is a methodology originating from the automotive industry, which seeks to maximise value

by eliminating waste [1]. This focuses on improving operational efficiency by reducing activities that do not provide value to the end customer, ensuring a more agile and less costly production [1]. Thus, in healthcare, the concept of

How to cite: Osorio-Canchig, K.T., Reyes-Vásquez, J.P., and Aldás-Salazar, D.S., Improvement of the efficiency of hospital care: a simulation-based approach DYNA, (92)239, pp. 101-110, October - December, 2025.

lean healthcare (LH) seeks to optimise hospital processes to improve the quality of care and reduce costs by systematically eliminating waste in the management of healthcare services.

An efficient healthcare system requires advanced technological infrastructure, trained staff and optimised processes [2,3]. In this context, the need for innovative techniques to improve quality and patient safety has been emphasized [4]. However, hospitals must continuously refine the efficiency of their processes to respond to increasing demand and the addition of new services [5].

LH and Industry 4.0 (I4.0) are transforming healthcare systems by optimising processes without compromising service quality [6]. The application of lean principles has been shown to reduce process times [7] while digital simulation validates interventions prior to implementation [8]. In addition, the integration of LM tools with I4.0 technologies facilitates tactical and operational decision making, for example, through predictive analytics and workflow modelling in virtual environments to improve operational efficiency and reduce waiting times [9,10]. On the other hand, sustainability in healthcare systems is achieved by integrating quantitative models that optimise resources and reduce waste. This approach aligns with LH and I4.0 methodologies, which seek to improve operational efficiency and ensure an optimal experience for patients and medical staff [11].

Previous literature identifies operational waste such as unnecessary patient transfers and excessive specimen transport times [12,13]. Also, the integration of LH with I4.0 technologies allows addressing these issues through better resource allocation and workflow optimisation [14]. This drives a healthcare model that is more agile, efficient and better able to respond to changes in demand, ensuring an optimal experience for both patients and medical staff. In addition, operational waste affects service quality, increases costs and raises the risk of adverse events [15]. In this sense, LH principles are of particular importance in hospital management in terms of safety and quality of care [12].

Therefore, this paper aims to reduce hospital waiting times that currently affect operational efficiency and quality of care by generating delays in diagnosis and treatment. Our motivation is aligned with the growing challenges in health services management, where the demand for care often exceeds the operational capacity of hospitals. In that context, by identifying bottlenecks (BO) and optimising the use of resources through I4.0 technologies, such as simulation, more effective decisions can be implemented to improve operational efficiency. Also, the integration of methodologies such as LH contribute to the sustainability of the healthcare system, ensuring a better experience for both patients and medical staff [16]. Finally, this study provides new insights into the application of LH integrated with I4.0 in medical areas, with a special focus on the optimisation of hospital processes. Based on the identified situation in hospital process management, this study poses the following research questions: i) How can LH improve capacity in the current healthcare system and hospital service efficiency; ii) How can simulation, as an I4.0 technology, improve human resource allocation for proper decision making; and iii) How

can simulation, as an I4.0 technology, improve human resource allocation for proper decision making?

The rest of the article is structured as follows: section 2 presents a review of the relevant literature, providing the theoretical context and background of the study. Section 3 describes in detail the methodology adopted, including the procedures and tools used. Section 4 presents the results obtained, accompanied by their respective analysis and a discussion of the findings. Finally, section 5 offers the conclusions of the study, as well as possible lines of future research.

2 Theoretical background

2.1 The digital technologies of I4.0

I4.0 technologies have revolutionised industrial processes in traditional supply chains. So, raw material procurement, manufacturing and logistics are driven by the digitisation of business processes, for example, with the internet of things (IoT) [17]. IoT facilitates real-time monitoring of patients, equipment and supplies, improving decision-making and operational efficiency. Moreover, artificial intelligence (IA) plays a key role in analysing large volumes of data to forecast demands, optimise logistical routes and personalise patient care, improving responsiveness to unforeseen changes [17]. Cybersecurity becomes a critical aspect to ensure the protection of clinical information and the digital infrastructure of hospitals. In this context, autonomous robots optimise repetitive and high-precision tasks, reducing the burden on healthcare staff. Newly, simulation is crucial in validating processes to reduce waste because it allows modelling and optimising workflows in virtual environments before they are implemented. Also, it improves agility in decision-making and response to variations in demand without affecting service quality, e.g., for healthcare systems [18]. In addition, big data and the integration of universal systems allow optimising hospital management, improving communication between devices and responsiveness to variations in demand. In this context, the capacity of the healthcare system is fundamental to efficiently manage resources and avoid BO and maintain service quality, especially in times of high demand. Here, correct decision making is supported by technologies such as simulation [9]. In particular, three decision levels can be distinguished in terms of the decision to be made in a given time frame: strategic, tactical and operational [19]. These decisions can be oriented towards minimising costs in the selection of production sites, storage and distribution of products or raw materials.

On the other hand, sustainability in resource management seeks not only efficient use, but also continuous improvement. In this sense, they highlight the importance of integrating quantitative models to optimise the management of inventories and resource flows [11]. This is approached from several perspectives: economic, optimising operational costs without affecting quality; environmental, minimising ecological impact by reducing resources and energy; and social, ensuring an accessible and quality service for all patients [20]. Here, cloud computing enables scalable storage and processing of medical data, improving information access and management. Additive

manufacturing, through 3D printing, facilitates the customisation of prostheses and surgical tools, reducing costs and production times. Augmented reality and virtual reality improve medical training and procedure planning by providing accurate and interactive simulations [9].

In the context of simulation, this replicates a real process with sufficient fidelity to improve workflows. There are several types of simulation, such as discrete event simulation (DES), which models systems with changes at specific points in time [21], and continuous simulation, which uses equations to represent variables with constant changes. Other approaches include agent-based simulation (ABM), which models complex systems with autonomous interaction [21]. Monte Carlo simulation models uncertainty with random simulations, useful for risk analysis and economics. System dynamics (SD) studies the interaction of variables in non-linear systems, such as population growth. Optimisation simulation integrates simulation and optimisation techniques to improve complex processes [14]. Virtual simulation, which includes augmented and virtual reality, creates replicas of physical systems, useful for training and industrial simulation. Finally, stochastic Monte Carlo simulation explores systems with multiple random variables, using probabilistic methods [22].

In the clinical setting, simulation is essential for learning, recreating complex scenarios and evaluating performance in medical procedures [23]. Clinical simulation has proven to be essential in medical training, providing professionals with a controlled environment to deal with complex situations without the risks inherent in real practice. This improves decision-making, team coordination and quality of care [23]. In this context, FlexSim healthcare (FCH) is a specialised software for simulating the healthcare sector, offering advanced tools such as full-scale 3D visualisation and statistical analysis. Its use allows evaluating scenarios and optimising resources in environments with capacity constraints, such as the availability of beds, medical equipment and staff. This approach is essential to mitigate BO [18], where demand exceeds capacity, causing waiting times and reducing efficiency.

In environments of uncertainty, DES is suitable for optimising processes and improving the efficiency of the healthcare system by analysing and making decisions based on simulated data. This involves minimising waiting times, improving staff allocation and maximising medical equipment utilisation without compromising quality of care [18]. Also, simulation with deterministic demand plays a crucial role in operational planning and management. It is a demand that can be predicted with certainty, which facilitates optimal resource allocation [18]. However, when variability in medical care is high, such as in emergency units, uncertainty in demand creates additional challenges in maintaining efficient patient flow. From this perspective, projected demand is introduced, which refers to an advance estimate of the volume of medical care based on historical data and expected patterns. This type of demand allows for anticipating variations in the number of patients and optimising resource allocation, ensuring a more efficient response to fluctuations in demand [19].

The simulation process in FCH follows several sequential

steps to ensure an efficient analysis of the system: (i) system analysis, where simulation objectives are defined and critical areas are identified; (ii) data collection, considering initial conditions and internal variables; (iii) system model building using flow diagrams or networks to represent discrete events; (iv) simulation model development, defining its structure and software platform; v) validation of the model, ensuring its accuracy through testing and verification; vi) running the simulation, observing how the system responds to different inputs; and vii) obtaining and analysing results to evaluate system behaviour and look for optimisation opportunities [24].

2.2 *Lean healthcare*

LH is a key methodology for optimising processes and is focused on reducing waste and continuously improving clinical outcomes, which reduces costs and improves the quality of care [25]. Its integration with simulation, using tools such as FCH, allows modelling and analysis of processes, facilitating decision-making to improve the efficiency and productivity of the healthcare system [12]. Within this approach, operational decisions seek to minimise waste and waiting time. Also, tactical decisions are aimed at improving the productivity of the services provided in relation to the resources used. This monitors system performance in terms of quality and quantity of care [18].

A key aspect of LH is the elimination of waste through LM tools adapted to the hospital environment. Among them, 5S encourages workspace organisation; value stream mapping (VSM) allows visualisation of the value stream to identify improvements; kanban optimises inventory management under the just-in-time (JIT) model; and poka-yoke introduces error-proofing mechanisms in medical and administrative procedures [26].

Other effective strategies include kaizen, based on continuous improvement, and heijunka, which balances workload to avoid saturation. In addition, single-minute exchange of die (SMED) reduces changeover times between procedures, and total productive maintenance (TPM) ensures preventive maintenance of medical equipment, improving its availability and reliability [26].

Within the framework of LM thinking, the identification and elimination of waste is crucial to improve operational efficiency. Traditionally, seven types of waste have been identified: overproduction, excessive inventory, unnecessary movements, waiting times, defects, overprocessing and inefficient transportation. However, in modern environments, especially in the hospital setting and within the I4.0 paradigm, three additional wastes have been added: underutilisation of human talent, which refers to the underutilisation of staff competencies and skills; poor information management, which leads to delays and errors in decision-making; and poor quality of inputs or suppliers, which affects operational continuity and patient safety [26].

Effective LH implementation depends not only on the application of tools and strategies, but also on human capital. Through continuous training and the incorporation of new professionals, the flexibility of the system to adapt to the changing demands of the clinical environment can be

improved. Moreover, the flexibility and polyvalence of professionals allow for the optimisation of available resources, which favours the efficiency of the system in contexts with high variability of demand [27,28].

In this sense, system overload occurs when the amount of care required exceeds the system's capacity to manage it effectively. This phenomenon can lead to saturation of resources, increasing waiting times and affecting the quality of services. Consequently, the correct identification of these critical points and the implementation of preventive measures are essential to maintain adequate flow of care and operational efficiency [29]. Also, at LH, quality is an essential component that is ensured through the recruitment of highly qualified staff. This approach ensures that care is delivered in a safe, efficient and patient-centred manner. Other strategies, such as process standardisation and the adoption of advanced technologies, are also critical to improving outcomes [16]. In that sense, the business challenge lies in balancing these strategies to optimise both diagnostics and treatments as well as the patient experience, minimising medical errors and improving clinical efficiency.

It is important that all staff are actively involved in identifying inefficiencies and proposing solutions [27]. Here, continuous improvement (kaizen) provides effective strategies, such as constant feedback and training in best practices. While the incorporation of doctors and nurses can improve the flow of care and reduce waiting times, other approaches such as restructuring care processes and implementing flow management technologies can also be considered [28]. For that reason, any approach that allows for more efficient and faster care will be beneficial for the patient experience and hospital operations. Finally, the principle of workload levelling (heijunka) suggests that the equitable distribution of tasks is key to avoiding overload and maintaining optimal performance. Solutions such as reorganising shifts, adding more medical staff, implementing multifunctional teams and using scheduling tools can help to better balance demands and available resources [30].

3 Methodology

This study uses conceptual modelling to improve process performance by implementing I4.0 enabling technologies, specifically simulation [26]. Here, a quantitative and experimental approach is adopted to model hospital processes using FCH software. The design includes the creation of simulation models that represent the flow of patients from admission to discharge. Evaluation of key metrics (KPIs) considers all intermediate stages of care.

Regarding the implementation steps for LH and the details of the tools used, a conceptual framework for programming the simulation is presented in Fig. 1. First, data is collected and theoretical input calculations are performed for the simulation in Flexsim, i.e., performance measures, work-in-process inventories, and distributions of arrivals to each process. Next, the simulation model is constructed in the healthcare environment. Then, the experimental scenarios are tested to evaluate the impact of waiting time and efficiency. Here, the LM tools are incorporated. In the next step, scenarios are chosen for decision-making that eliminate

waste, optimisation of processes, and the promotion of a culture of continuous improvement in the organisation. Finally, these scenarios are evaluated considering KPIs to optimise resource allocation and system efficiency, facilitating strategic decision-making.

Data collection includes process times, care flows and resource utilisation. Interviews with medical staff, direct observations and review of hospital records are used. In this sense, the analysis of available data on the system to be simulated is a key task that must be carried out rigorously, as it simplifies and optimises the process of developing simulation models. So, the relevant information is identified, based on the objectives defined in the project. For the collection of data needed for the simulation, the care flows presented for patients are studied in order to obtain key information for modelling and analysis.

Table 1 shows the analysis of the activity times of the medical staff, in order to identify the BOs in the process.

To determine the arrival distributions for each process, the FCH ExperFit tool is used. This tool automatically and accurately generates a probability distribution that optimally represents a data set for the modelling and analysis of the simulated processes. Table 2 presents the fitted probability distributions for the different model parameters.

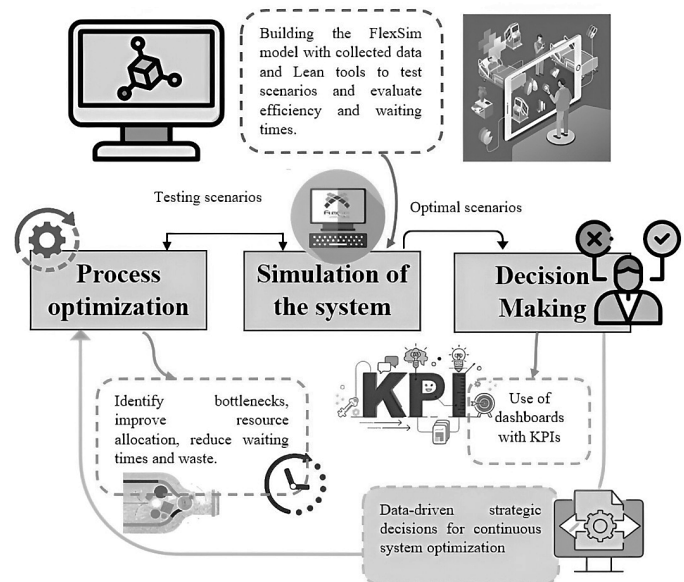


Figure 1. Conceptual framework for simulation

Source: Own elaboration.

Table 1.
Standard time for each process.

Process	Time (minutes)
Patient reception and initial evaluation	56.45
Diagnostics	70.45
Medical consultation	71.43
Tests and operation	108.75

Source: Own elaboration.

Table 2.
Probability distribution of each process, from FCH

Process	Distribution
Registration and transport	beta (41.451096, 112.979605, 37.523096, 33.290444, <stream>)
Transport to waiting room	beta (18.931491, 54.113646, 29.936199, 34.615791, <stream>)
Transport to emergency room	loglogistic (0.001362, 41.976442, 23.821625, <stream>) opc 2
Triaje	beta (3.294162, 1551.812034, 17.804659, 17.883504, <stream>)
Transfer to observation room	beta (15.518288, 73.273535, 53.957810, 51.952136, <stream>)
Emergency medical examination	weibull (1490.952979, 11.667304, 3.946799, <stream>) no
Emergency medical consultation	beta (525.319578, 659.245646, 31.778915, 25.224985, <stream>)
Location in the emergency operating room	lognormal2(0.000000, 300.004653, 0.009302, <stream>)
Emergency surgery	beta (3586.995716, 3609.383641, 67.328649, 40.671087, <stream>)
Emergency recovery room location	beta (276.598245, 316.566239, 40.216633, 22.607272, <stream>) opc2
Emergency patient exit	loglogistic (31.375206, 29.979410, 23.047032, <stream>)
Weighing in the balance	johnsonbounded (97.216798, 148.054684, -0.222860, 2.926063, <stream>)
Location in a hospital bed	beta (2.537234, 67.841892, 48.279582, 44.009175, <stream>)
Medical examination	beta (1639.514543, 1921.928166, 44.802877, 32.603515, <stream>)
Electrocardiogram	lognormal2(0.000000, 659.182762, 0.013292, <stream>)
X-rays	lognormal2(0.000000, 1501.033324, 0.003534, <stream>)
General consultation	johnsonbounded (574.469277, 632.364177, 1.032101, 4.300052, <stream>)
Patient exit	beta (41.853312, 69.975457, 42.834650, 38.970669, <stream>)

Source: Own elaboration.

Table 3.
Design of experiments

Scenario Code	Description	Increase in staff	Demand
E1	Base Condition (actual situation)	++	DI
E2	Increased demand	XO	DI
E3	Minimal staff expansion	XO	DI
E4	Moderate expansion of staff	XO	DI
E5	Exclusive increase of doctors	+O	DA
E6	Increase in nurses and doctors	XO	DA
E7	Maximum expansion of staff	XO	DA
E8	Optimised staff expansion	XO	DA

Note: ++ initial number of staff XO increase in nurses and doctors +O increase in doctors only DI initial patient demands DA increase in patient demand.

Source: Own elaboration.

In terms of scenario analysis, strategies proposed by the LH methodology are used to evaluate the impact of adding more medical and nursing staff in a hospital setting. So, the initial conditions are evaluated against the experiments. The simulation time corresponds to a week of 604,800 seconds (sec). These scenarios include variations in the number of patients, the availability of resources and the organisation of the workflow, allowing to evaluate how they affect the demand, the redistribution of resources and the implementation of operational improvements. Thus, eight scenarios are modelled in FCH with DES to analyse patient flow and resource allocation.

Table 3 presents the design of experiments with details of each scenario, highlighting the simulation conditions and key differences between them. This allows to assess the impact of each strategy on hospital capacity and system sustainability.

4 Results

4.1 Integral evaluation of production processes under initial conditions

To perform the analysis of times, throughput and resources under initial conditions. Fig. 2 presents the transit times of patients in different areas of the clinic. Administrative phases, such as patient registration (82.39 sec) and discharge (283.07 sec), show efficient times, indicating adequate management at these stages. However, significant delays were identified in the clinical stages. Waiting time for weighing in general consultation reaches an average of 5444.63 sec, and waiting time in the examination room until the arrival of the doctor is 1165.34 sec, suggesting BO in patient management and the availability of medical resources. As for diagnostic procedures, electrocardiogram takes 682.37 sec, while X-ray takes 1547.15 sec. In addition, the total X-ray process (3906 sec) is considerably longer than electrocardiogram (1216.85 sec), which could be attributed to equipment availability, logistics or complexity of the procedure.

Fig. 3 details the times recorded in the emergency area, where both strengths and opportunities for improvement in care management are identified. Initial activities show an

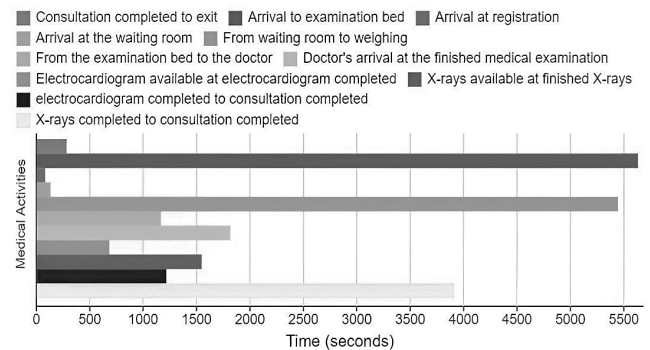


Figure 2. General consultation time intervals under initial conditions, from FCH

Source: Own elaboration.

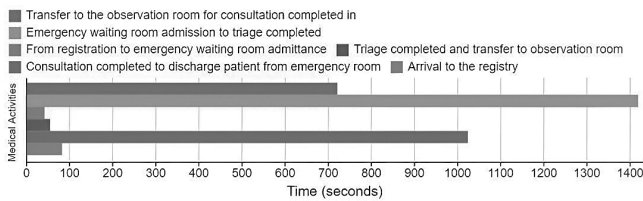


Figure 3. Emergency consultation time intervals under initial conditions, from FHC
Source: Own elaboration.

efficient flow: patient registration is completed in 82.39 sec, followed by admission to the waiting room (41.81 sec), which evidences a quick incorporation of patients into the system. In contrast, triage represents a critical point, with an average duration of 1418.44 sec. This delay can be attributed to the detailed assessment of patients or to BO in the availability of specialized staff and infrastructure.

Given its impact on the allocation of care, it is recommended that resources be optimized to reduce these times. The transfer to the observation rooms is agile, with an average of 54.57 sec, reflecting adequate logistics. Emergency medical consultation has an average duration of 720 sec, considered to be in accordance with the complexity of the cases attended. Consequently, patient discharge requires 1024.17 sec, time associated with final evaluations, documentation and coordination of transfers. Optimizing these processes would reduce delays in discharge and speed up the availability of resources for new admissions.

Finally, the findings highlight how simulation can provide key information to improve the allocation of human resources. By identifying critical areas, informed decisions can be made to optimise patient flow and minimise waiting times, which contributes to increased operability.

Regarding to BOs, in general practices the weighing of patients represents a BO due to the availability of only one scale, which slows down the flow of care. In emergencies, triage is also a BO, whose improvement could be achieved with more assessment stations to increase the capacity of the process. Also, the availability of a single operating theatre limits surgical capacity, suggesting the need for a second theatre to meet demand more efficiently. These improvements optimise resource utilisation and strengthen the economic sustainability of the system by maximising the use of existing infrastructure without compromising service quality. In conclusion, the simulation by managing the identified BOs facilitates tactical and operational decisions on how best to allocate staff. This ensures an efficient response in areas such as weighing or triage, improving care and reducing delays.

In terms of resource use, Fig. 4 shows the X-ray utilization for one week, with a total of 25 patients seen, reflecting the demand for this specific procedure. In addition, Fig. 5 shows the use of the wheelchair for the transfer of 50 patients, indicating that, although the patient flow is considerable, it is not high enough to require the use of other equipment or transfer methods. This suggests that transfer resources and diagnostic procedures are being used appropriately according to projected demand, without generating BO in these aspects of the flow of care.

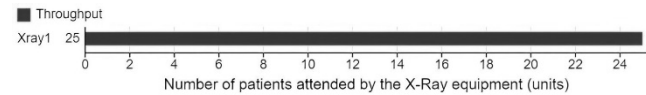


Figure 4. X-ray performance under initial conditions, from FCH
Source: Own elaboration.

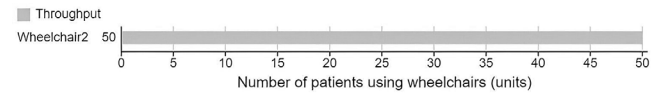


Figure 5. Wheelchair performance under initial conditions, from FCH
Source: Own elaboration.

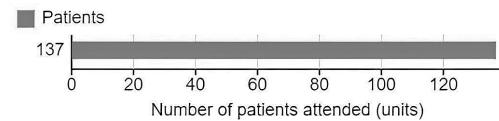


Figure 6. Patients attended under initial conditions, from FCH
Source: Own elaboration.

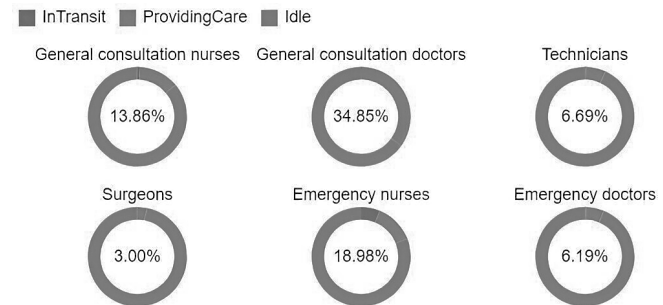


Figure 7. Staff utilization under initial conditions, from FCH
Source: Own elaboration.

Based on the staff available under initial conditions, the maximum care capacity is determined to be 137 patients, as shown in Fig. 6. This limit is due to the identified BOs and the restricted availability of resources, which directly impacts on the efficiency of the care system.

Fig. 7 presents a scorecard with various KPIs illustrating staff utilisation in the clinic. It shows that general practitioners have the highest percentage of utilisation, while nurses in this area have a lower workload, as health technicians are in charge of examinations. In the emergency area, nurses have a higher workload, participating in surgeries, while surgeons are more free. This distribution of tasks highlights the differences in staff responsibilities according to the type of medical care, suggesting the need for an adequate allocation of human resources to improve operational efficiency in both areas.

Fig. 7 also shows staff utilisation in the medical system, revealing a significant proportion of inactivity (Idle) in all roles, suggesting opportunities for optimisation in task allocation. On the one hand, general practice doctors spend the most time on direct care, with 34.85%, followed by emergency nurses (18.98%) and general practice nurses (13.86%). On the other hand, technicians (6.69%),

emergency doctors (6.19%) and surgeons (3.00%) have a lower participation in direct care, which is in line with the specialised nature of their functions. The category 'InTransit' (on the move) has a low incidence.

4.2 Experimentation of production processes with LH

For the execution of the experiments shown in Table 3, different scenarios were configured using LH principles in order to optimise human and operational resources. Through the DES performed with the FCH software, the flow of medical care is modelled. This approach, based on accurate data, facilitates tactical and operational decision making to improve the efficiency of the system in the short and medium term.

In Fig. 8, it is evident that, despite maintaining efficient times in processes such as patient registration (84.68 sec) and discharge (178.86 sec), significant delays were identified in the weighing in general consultation (2073.77 sec) and waiting in the examination room (2262.24 sec), suggesting the presence of wasted waiting time. To mitigate these delays, LM tools such as heijunka, which helps to level the workload and avoid unnecessary backlogs, and VSM, which allows visualising the flow of care and identifying optimisation opportunities, can be applied. In contrast, electrocardiogram (702.95 sec) and x-ray (1548.76 sec) procedures were managed efficiently, but the total consultation time for x-ray (1008.66 sec) exceeds that for electrocardiogram (867.75 sec), which could be related to logistical or complexity differences.

In Fig. 9, the times recorded in emergencies reveal efficient management of registration (84.68 sec) and admission to the waiting room (41.84 sec). However, triage (1448.12 sec) remains a BO, suggesting the need for optimisation in this process. Transfer to observation rooms is fast (56.75 sec) and emergency medical consultation (659.01 sec) remains within an adequate range. Discharge time (812.51 sec) also presents an opportunity for improvement in the discharge process.

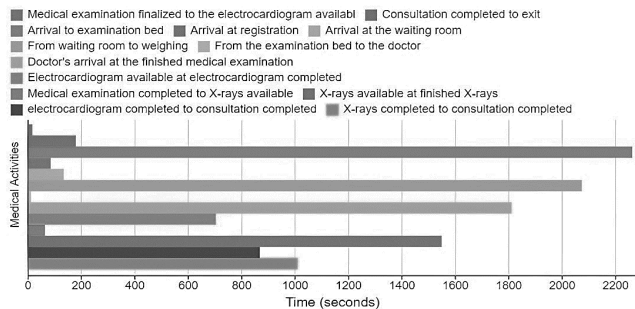


Figure 8. General consultation time intervals, from FCH
Source: Own elaboration.

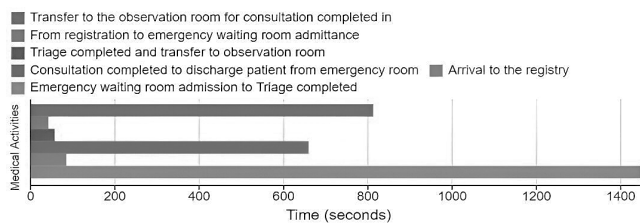


Figure 9. Emergency consultation time intervals, from FCH
Source: Own elaboration.

Experiment1

Warmup Time: 0.00 0:00:00 16/12/2024

Stop Time: 604800.00 0:00:00 23/12/2024

Replications per Scenario: 5

Parameters	Scenarios		
	Nurses	Doctors	Number of patients
<input checked="" type="checkbox"/> Parameters			
<input checked="" type="checkbox"/> Nurses			
<input checked="" type="checkbox"/> Doctors			
<input checked="" type="checkbox"/> Number of patients			
Scenario 1	3	2	20
Scenario 2	4	3	20
Scenario 3	5	4	20
Scenario 4	6	4	20
Scenario 5	3	3	50
Scenario 6	4	3	50
Scenario 7	5	4	50
Scenario 8	6	4	50

Figure 10. Experimental scenarios, from FCH
Source: Own elaboration.

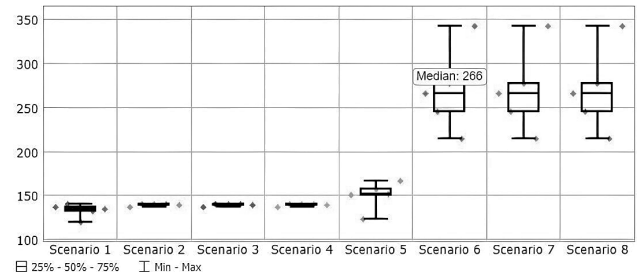


Figure 11. Patients seen according to E6, from FCH
Source: Own elaboration.

The simulation results show how different scenarios impact system capacity and demand. Fig. 10 presents different scenarios: standard operation with 20 patients per day, increasing staff (nurses and doctors) and increasing demand to 50 patients per day without changing the amount of resources.

In terms of system throughput, when the number of patients is maintained at 20 per day, the capacity of care varies between 120 and 140 patients per week in Scenario 1 (E1). In this initial scenario, the system throughput reaches 40.8%. In Scenarios E2, E3 and E4, where minimal or moderate expansion of staffing is implemented, capacity is maintained at a median of 139 patients. This indicates that these adjustments do not have a significant impact on operational efficiency. Consequently, when demand increases to 50 patients per day, E5 where only the number of doctors is increased shows a slight improvement. This suggests that the availability of doctors is not the only limiting factor in the system, but that other resources such as support staff and hospital infrastructure also play a role.

Fig. 11 shows that in the best-case scenario (E6), a significant improvement in the capacity of care is observed, along with a reduction in BO. From this scenario onwards, BO constraints are kept under control in subsequent scenarios, contributing to greater stability in system performance. With a simultaneous expansion of doctors and nurses, the system reaches a minimum of 214 patients seen weekly, with an average of 266 representing a throughput of 77.6% and a maximum of 343, at this being the total possible

capacity, the throughput reaches 100%. This increase reflects a significant improvement of 36.8% in operational efficiency, highlighting the positive impact of resource optimisation and staff expansion on hospital capacity. Thus, the results highlight the importance of balanced staff growth in optimising hospital care, far exceeding the efficiency achieved in scenarios with partial expansions.

By taking advantage of E6 to reach the maximum number of patients, it is revealed that the system manages to serve an average of 266 patients weekly, as illustrated in Fig. 12. Thus, applying LM tools, such as kaizen, through continuous improvement and staff feedback, would allow detecting and correcting inefficiencies to further increase the capacity of the system.

Fig. 13 presents staff utilisation as a function of E6. Here, there is a slight increase in the utilisation of general practitioners from 34.85% to 36.89%. Also, technicians experience a significant increase from 6.69% to 14.33%, and the utilisation of surgeons doubles. In addition, it is noted that physicians, technicians and surgeons all increase their time spent on direct care. In conclusion, there is an increase in staff utilisation due to the increase in the number of patients. Consequently, in the emergency area, nurses increase their share from 18.98% to 24.42%, while doctors increase from 6.19% to 9.94%. However, although some roles still show Idle, these changes reflect a better distribution of time towards direct care. Finally, it is identified that the use of LM tools such as heijunka can optimise load levelling, reducing these unproductive times and improving team performance.

Finally, Fig. 14 and 15 show the use of X-rays and wheelchairs, serving 52 and 104 patients respectively. This indicates a moderate workload that allows for efficient management of resources without generating excessive pressure.

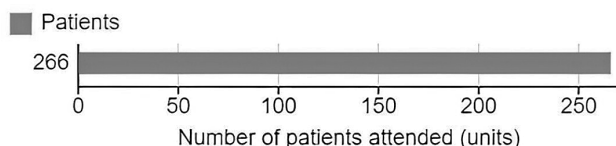


Figure 12. Total patients attended, from FCH
Source: Own elaboration.

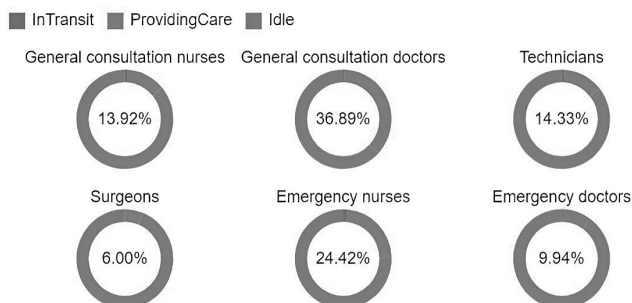


Figure 13. Staff utilization according to the parameters of E6, from FCH
Source: Own elaboration.

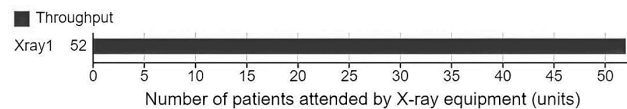


Figure 14. X-ray performance, from FCH
Source: Own elaboration.

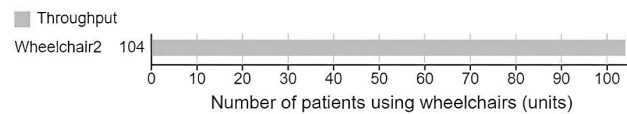


Figure 15. Wheelchair performance, from FCH
Source: Own elaboration.

4.3 Discussion of results

Analysis of the simulation results highlights the importance of optimising resources within the healthcare system. BO is identified in the process of weighing patients during general consultation and triage in emergencies, which has a negative impact on operational efficiency. In addition, it is observed that the addition of four nurses and three doctors significantly improves the capacity of care, increasing the number of patients seen weekly. In E6, the number of patients seen increases from a range of 157-166 in the initial conditions to a range of 214-343, reaching the maximum capacity of the system. This finding is in line with previous studies [31], where improved staff allocation results in an optimisation of resources and care times in an emergency hospital. Additionally, the results indicate that the efficient use of resources such as X-rays and wheelchairs avoids overloading the system. This is in line with other proposals [32], where the appropriate allocation of equipment and resources improves not only efficiency, but also the quality of service.

To further reduce waiting times and improve patient flow, we recommend applying the kaizen continuous improvement approach, implementing more weighing and triage stations, as well as the construction of a second operating theatre. Our simulation results are supported by other authors [33], who demonstrate how resource optimisation through simulation contributes to maintaining efficient flow in high-demand situations, such as health emergencies.

Implementing the recommendations derived from simulation not only reduces BO, but also optimises hospital operations, improving the allocation of staff and resources for more efficient care. This approach is especially relevant for economic sustainability, because increasing the capacity of care while reducing time wastage has a positive impact on KPIs, such as the system's profit to strengthen its long-term sustainability. In this sense, it reinforces the idea that appropriate resource allocation and improved operational efficiency not only reduce costs, but also contribute to economic stability and quality of care [34].

5 Conclusions

This study demonstrates that the combination of LH and DES can optimise efficiency and improve the allocation of

hospital resources. Reducing wasteful waiting times, increasing care capacity and providing system sustainability are critical aspects of success. This answers the research questions posed in this article.

How can LH improve the capacity in the current healthcare system and the efficiency of the hospital service? LH optimises hospital capacity by reducing operational waste, such as excessive waiting times and overloading of staff on certain shifts. LM tools such as VSM allow for the detection of BO in care flows, while kaizen drives continuous improvement in critical processes such as patient weighing, triage and surgeries. In addition, the application of heijunka, which focuses on workload levelling, allows balancing hospital demand, avoiding peaks of saturation and staff downtime. This optimises the availability of doctors and nurses without generating additional costs. The methodology applied through experimentation has been shown to reduce waiting times by 35% and increase operational efficiency by up to 36.8%. Consequently, these results show that strategic staff redeployment based on LM principles increases capacity to meet up to 77.6% of projected demand without compromising service quality. This is in line with theoretical studies concerning the impact on the sustainability of the hospital system [10]. Thus, the requirements associated with these improvements include the integration of digital and operational systems, the standardisation of processes, and alignment with healthcare performance indicators, such as monitoring response times, analysing patient flow, and allocating resources in real time, to ensure sustainable improvements in efficiency.

How can simulation, as an I4.0 technology, improve the allocation of human resources for appropriate decision-making? DES, as a key tool of I4.0, enables the evaluation of different care scenarios and optimisation of human resource allocation based on actual demand. Its application facilitates the identification of BO and the dynamic redistribution of staff, ensuring that the workload is efficient and equitable in each shift. From an economic and social perspective, the simulation allows decisions to be made based on key KPIs, such as capacity, waiting times and profit. This ensures a more efficient response to variations in demand. In this study, our results show that the combination of simulation and LH to reduce waste achieves optimal resource allocation in care systems. At the tactical level, simulation allows planning medium-term staffing strategies, optimising the number of doctors and nurses needed according to the expected workload. At the operational level, DES enables immediate adjustments in staff deployment based on real-time demand, ensuring that resources are used efficiently, and service quality is maintained. This study confirms that the combination of LH and DES is an effective strategy to optimise hospital efficiency, improving decision-making at different levels.

This study has several limitations. First, the data used in the simulation are restricted to operational decisions within a specific hospital, which may restrict the ability to generalize the results to other hospitals with different characteristics, such as size, infrastructure, or type of patients. Furthermore, the model has focused exclusively on maximizing operational efficiency, without considering additional factors

that could affect system performance, such as administrative processes, which are crucial for overall efficiency. For future research, it is recommended to integrate IA to optimize resource allocation in an adaptive way. IA would allow adjusting resources in real time, improving the flexibility of the system in the face of fluctuations in demand. Furthermore, it would be relevant to extend the model to different hospital contexts, evaluating hospitals with different characteristics to test the applicability and robustness of the model in different settings. It is also suggested to investigate the impact of the digitalization of administrative processes, as the automation of these processes could reduce waiting times, improve resource allocation and, in general, optimize the efficiency of the health system

References

- [1] Bhamu, J., and Sangwan, K.S., Lean manufacturing: literature review and research issues. *International Journal of Operations & Production Management*, 34, pp. 876–940, 2014. DOI: <https://doi.org/10.1108/IJOPM-08-2012-0315>
- [2] Rutberg, M.H., Wenzel, S., Devaney, J., Goldlust, E.J., and Day, T.E., Incorporating discrete event simulation into quality improvement efforts in health care systems. *American Journal of Medical Quality*, 30, pp. 31–35, 2013. DOI: <https://doi.org/10.1177/1062860613512863>
- [3] DeRienzo, C.M., Shaw, R.J., Meanor, P., Lada, E., Ferranti, J., and Tanaka, D., A discrete event simulation tool to support and predict hospital and clinic staffing. *Health Informatics Journal*, 23, pp. 124–133, 2016. DOI: <https://doi.org/10.1177/1460458216628314>
- [4] Devapriya, P., Strömblad, C.T.B., Bailey, M.D., Frazier, S., Bulger, J., Kemberling, S.T., et al., StratBAM: a discrete-event simulation model to support strategic hospital bed capacity decisions. *Journal of Medical Systems*, 39, p. 130, 2015. DOI: <https://doi.org/10.1007/s10916-015-0325-0>
- [5] Karakra, A., Fontanili, F., Lamine, E., Lamothe, J., and Taweel, A., Pervasive computing integrated discrete event simulation for a hospital digital twin. In *2018 IEEE/ACS 15th International Conference on Computer Systems and Applications (AICCSA)*, pp. 1–6, 2018. DOI: <https://doi.org/10.1109/AICCSA.2018.8612796>
- [6] Singh, A.R., Gupta, A., Satpathy, S., and Gowda, N., Study to assess the utility of discrete event simulation software in projection and optimization of resources in the out-patient department at an apex cancer institute in India. *Health Science Reports*, 5, pp. 1–8, 2022. DOI: <https://doi.org/10.1002/hsr2.627>
- [7] Ahn, C., Rundall, T.G., Shortell, S.M., Blodgett, J.C., and Reponen, E., Lean management and breakthrough performance improvement in health care. *Quality Management in Healthcare*, 30, pp. 6–12, 2021. DOI: <https://doi.org/10.1097/QMH.0000000000000282>
- [8] Quazi, F., Raju, N., and Viradia, V., Digital twin technology in healthcare: applications, challenges, and future insights. *International Journal of Global Innovations and Solutions*, pp. 1–13, 2024. DOI: <https://doi.org/10.21428/e90189c8.bdb0264f>
- [9] Ivanov, D., Dolgui, A., and Sokolov, B., The impact of digital technology and Industry 4.0 on the ripple effect and supply chain risk analytics. *International Journal of Production Research*, 57, pp. 829–846, 2019. DOI: <https://doi.org/10.1080/00207543.2018.1488086>
- [10] Sharma, V., Jamwal, A., Agrawal, R., and Pratap, S., A review on digital transformation in healthcare waste management: applications, research trends and implications. *Waste Management & Research*, 2024, art. 5420. DOI: <https://doi.org/10.1177/0734242X241285420>
- [11] Becerra, P., Mula, J., and Sanchis, R., Green supply chain quantitative models for sustainable inventory management: a review. *Journal of Cleaner Production*, 328, art. 129544, 2021. DOI: <https://doi.org/10.1016/j.jclepro.2021.129544>
- [12] García, S., and Montenegro, D., Implementation and evaluation of lean healthcare tools through the FlexSim simulator. *Proceedings of*

- the LACCEI International Multi-Conference for Engineering, Education and Technology, 2021, art. 594. DOI: <https://doi.org/10.18687/LACCEI2021.1.1.594>
- [13] Illusanguil-Corro, K.D., Villamarin-Jipa, V.V., Llerena-Rosado, E.D., and Saavedra-Freire, J.V., Impact of management models based on lean healthcare on the efficiency and quality of hospital services: a literature review. *Reincisol*, 3, pp. 5728–5739, 2024. DOI: [https://doi.org/10.59282/reincisol.V3\(6\)5728-5739](https://doi.org/10.59282/reincisol.V3(6)5728-5739)
- [14] Reyes, J., Mula, J., and Díaz-Madroño, M., Quantitative insights into the integrated push and pull production problem for lean supply chain planning 4.0. *International Journal of Production Research*, 62, pp. 6251–6275, 2024. DOI: <https://doi.org/10.1080/00207543.2024.2312205>
- [15] Rosas-Hernández, L.C., Limon-Romero, J., Baez-López, Y., Perez-Sánchez, A., and Tlapa-Mendoza, D., Lean healthcare and DMAIC to improve the supply process in a public hospital. *Dyna Management*, 9, pp. 1–16, 2021. DOI: <https://doi.org/10.6036/mn9986>
- [16] Cohen, R., Lean methodology in health care. *Chest*, 154, pp. 1448–1454, 2018. DOI: <https://doi.org/10.1016/j.chest.2018.06.005>
- [17] Ahsan, M.M., and Siddique, Z., Industry 4.0 in healthcare: a systematic review. *International Journal of Information Management Data Insights*, 2, pp. 1–20, 2022. DOI: <https://doi.org/10.1016/j.jjime.2022.100079>
- [18] Roy, S., Wuest, T., Ahmed, I., and Saldanha, J., Bottleneck management through strategic sequencing in smart manufacturing systems. *Graduate Theses*, West Virginia University, 2023.
- [19] Mula, J., Peidro, D., Díaz-Madroño, M., and Vicens, E., Mathematical programming models for supply chain production and transport planning. *European Journal of Operational Research*, 204, pp. 377–390, 2010. DOI: <https://doi.org/10.1016/j.ejor.2009.09.008>
- [20] Ghobakhloo, M., Fathi, M., Iranmanesh, M., Maroufkhan, P., and Morales, M.E., Industry 4.0 ten years on: a bibliometric and systematic review of concepts, sustainability value drivers, and success determinants. *Journal of Cleaner Production*, 302, art. 127052, 2021. DOI: <https://doi.org/10.1016/j.jclepro.2021.127052>
- [21] Anu, M., Introduction to modeling and simulation. In Healy, K., Withers, D., and Nelson, B. (eds.), *Winter Simulation Conference*, pp. 7–13, 1997. DOI: <https://doi.org/10.1145/268437.268440>
- [22] Carson, J.S., Introduction to modeling and simulation. In *Proceedings of the Winter Simulation Conference*, art. 4235, 2005. DOI: <https://doi.org/10.1109/WSC.2005.1574235>
- [23] López-Sánchez, M., Ramos-López, L., Pato-López, O., and López-Álvarez, S., Simulation-based training in medicine: a teaching tool. *CIR MAY AMB*, 18, pp. 25–29, 2012.
- [24] Zhu, X., Zhang, R., Chu, F., He, Z., and Li, J., A FlexSim-based optimization for the operation process of cold-chain logistics distribution centre. *Journal of Applied Research and Technology*, 12, pp. 270–278, 2014. DOI: [https://doi.org/10.1016/S1665-6423\(14\)72343-0](https://doi.org/10.1016/S1665-6423(14)72343-0)
- [25] Tlapa, D., Zepeda-Lugo, C.A., Tortorella, G.L., Baez-Lopez, Y.A., Limon-Romero, J., Alvarado-Iniesta, A., et al., Effects of lean healthcare on patient flow: a systematic review. *Value in Health*, 23, pp. 260–273, 2020. DOI: <https://doi.org/10.1016/j.jval.2019.11.002>
- [26] Reyes, J., Mula, J., and Díaz-Madroño, M., Development of a conceptual model for lean supply chain planning in industry 4.0: multidimensional analysis for operations management. *Production Planning & Control*, 34, pp. 1209–1224, 2023. DOI: <https://doi.org/10.1080/09537287.2021.1993373>
- [27] Fernandes, H.M.L.G., de Jesus, M.V.N., da Silva, D., and Guirardello, E.B., Lean healthcare in the institutional, professional, and patient perspective: an integrative review. *Revista Gaúcha de Enfermagem*, 41, pp. 1–12, 2020. DOI: <https://doi.org/10.1590/1983-1447.2020.20190340>
- [28] Pokinska, B.B., Fialkowska-Filipek, M., and Engström, J., Does lean healthcare improve patient satisfaction? a mixed-method investigation into primary care. *BMJ Quality & Safety*, 26, pp. 95–103, 2017. DOI: <https://doi.org/10.1136/bmjqs-2015-004290>
- [29] Oz, B., Shneer, S., and Ziedins, I., Static vs accumulating priorities in healthcare queues under heavy loads. *arXiv*, 2, pp. 1–11, 2020. DOI: <https://doi.org/10.48550/arXiv.2003.14087>
- [30] Régis, T.K.O., Gohr, C.F., and Santos, L.C., Lean healthcare implementation: experiences and lessons learned from Brazilian hospitals. *Revista de Administração de Empresas*, 58, pp. 30–43, 2018. DOI: <https://doi.org/10.1590/S0034-759020180103>
- [31] Bahari, A., and Asadi, F., A simulation optimization approach for resource allocation in an emergency department healthcare unit. *Global Heart*, 15, pp. 1–6, 2020. DOI: <https://doi.org/10.5334/GH.528>
- [32] Daldoul, D., Nouaouri, I., Bouchriha, H., and Allaoui, H., Simulation-based optimisation approach to improve emergency department resource planning: a case study of a Tunisian hospital. *International Journal of Health Planning and Management*, 37, pp. 2727–2751, 2022. DOI: <https://doi.org/10.1002/hpm.3499>
- [33] Melman, G.J., Parlikad, A.K., and Cameron, E., Balancing scarce hospital resources during the COVID-19 pandemic using discrete-event simulation. *Health Care Management Science*, 24, pp. 356–374, 2021. DOI: <https://doi.org/10.1007/s10729-021-09548-2>
- [34] Zhang, H., Best, T.J., Chivu, A., and Meltzer, D.O., Simulation-based optimization to improve hospital patient assignment to physicians and clinical units. *Health Care Management Science*, 23, pp. 117–141, 2020. DOI: <https://doi.org/10.1007/s10729-019-09483-3>

K.T. Osorio-Canchig, received the BSc. Eng. in Industrial Engineering from the Universidad Técnica de Ambato, Ecuador.
ORCID: 0009-0008-8590-0804

J.P. Reyes-Vásquez, received the PhD in Engineering and Industrial Production from the Universitat Politècnica de València, Spain. He is aggregate professor at the Universidad Técnica de Ambato, Ecuador. His research interests include information technologies, industrial engineering, supply chain management, operations planning, lean manufacturing tools, business process management, and modelling and simulation.
ORCID: 0000-0002-5446-5490

D.S. Aldas-Salazar, received the MSc in Industrial Management and Productive Systems, and is currently a PhD. student at the Universitat Politècnica de València. He works as a lecturer and researcher at the Faculty of Systems, Electronics, and Industrial Engineering, Universidad Técnica de Ambato. His research focuses on several projects related to supply chain management and industrial systems optimization.
ORCID: 0000-0001-8882-030X

Safety competency model for drillers in open-pit mines: application of functional analysis and developing a curriculum in Mexican mining

Graciela Rodríguez-Vega^a, María Alejandra Valenzuela-Soto^a & Dora Aydee Rodríguez-Vega^c

^a Industrial Engineering Department, University of Sonora, Hermosillo, Sonora, Mexico. graciela.rodriguez@unison.mx, a216204266@unison.mx

^b Mechatronic Faculty, Polytechnic University of Sinaloa, Mazatlán, Sinaloa, Mexico. drodriguez@upsin.edu.mx

Received: July 24th, 2025. Received in revised form: November 4th, 2025. Accepted: November 10th, 2025.

Abstract

Although mining is a primordial economic activity in Mexico, it presents high-rate occupational risks, especially in drilling operations. Only 1% of the workforce is involved in this activity, yet it accounts for 8% of fatal occupational accidents. The objective of this study is to identify the safety competencies required for the driller profile and to evaluate the impact of training designed based on the identified competencies. The implemented methodology combines the International Labor Office's recommendations for identifying critical job competencies and functional analysis with the Developing a Curriculum matrix. Diagnostic examination instruments were developed. The evaluation applied to eight drillers indicated that 75% met the required competencies; non-competent personnel received the corresponding training to achieve competency. The results show a decrease in safety indicators, such as injuries and accidents.

Keywords: competency; training; safety; open-pit mines; accidents; incidents; drillers; functional analysis; developing a curriculum.

Modelo de competencias de seguridad para perforistas en minas a cielo abierto: aplicación de análisis funcional y desarrollo de un curriculum en la minería Mexicana

Resumen

A pesar de que la minería representa una actividad clave para la economía mexicana, presenta altos riesgos de trabajo, en especial en actividades de perforación. Solo el 1% de la fuerza laboral participa en esta actividad, concentrando el 8% de los accidentes ocupacionales fatales. El objetivo del este trabajo es identificar las competencias de seguridad del puesto de perforista y evaluar el impacto de la capacitación creada a partir de las competencias identificadas. La metodología empleada combina las recomendaciones de la Organización Internacional del Trabajo para identificar competencias críticas, el análisis funcional y la matriz Desarrollo de un Curriculum. Se diseñaron instrumentos de evaluación diagnóstica de los perforistas. La evaluación aplicada a ocho perforistas indica que el 75% cumplía con las competencias requeridas, el personal no competente recibió la capacitación correspondiente para acreditar la competencia. Los resultados indican una disminución en los indicadores de seguridad, tales como lesiones y accidentes.

Palabras clave: competencia; capacitación; seguridad; minas a cielo abierto; accidentes; incidentes; perforista; análisis funcional; desarrollo de un curriculum.

1 Introduction

The mining industry plays a fundamental role in the economy of various countries; however, extraction activities

involve significant risks to workers' safety, especially during the drilling process [1]. These tasks are characterized by high levels of exposure to physical and mechanical hazards, which have contributed to an increase in the incidence of

How to cite: Rodríguez-Vega, G., Valenzuela-Soto, M.A., and Rodríguez-Vega, D.A., Safety competency model for drillers in open-pit mines: application of functional analysis and developing a curriculum in Mexican mining DYNA, (92)239, pp. 111-117, October - December, 2025.

occupational accidents [2]. Although the mining sector employs only 1% of the labor force, it accounts for approximately 8% of occupational accidents with fatal outcomes [3].

Mining is a fundamental pillar of the national economy of Mexico. According to data from the National Institute of Statistics and Geography, in 2021, the mining and metallurgical sector contributed 8.6% to the industrial Gross Domestic Product and 2.5% to the National Gross Domestic Product [4]. Furthermore, statistics from the Mexican Social Security Institute indicated that, in 2023, extractive industries presented an incidence rate of 2.0 occupational accidents per 100 workers [1]. In addition, reports from the Mexican Mining Chamber (Camimex) show that affiliated mining and metallurgical companies recorded an incidence rate of 0.90 accidents per 100 workers in 2022. During the same year, Camimex reported a total of 4,247 non-disabling accidents, 981 reportable accidents (969 disabling and 12 fatal), and 209,804 lost workdays (137,804 days lost due to accidents and 72,000 days lost due to fatal accidents) [1].

In the literature, four stages are commonly recognized in the development of occupational safety research within the mining industry: (1) safety engineering, (2) policies and procedures, (3) behavior-based safety, and (4) behavior-based safety culture [5]. According to Bloch [6], approximately 95% of accidents and incidents occurring during the first two stages can be attributed to human error. Ismail et al. [5] classify the main causes of mining-related accidents into 16 categories, including: human error, unsafe behavior, unsafe acts, lack of safety training, insufficient safety education, worker inexperience, poor supervisory leadership, mechanical failures, organizational deficiencies, geological factors, inadequate working conditions, and the absence of a safety culture. Fu et al. [7] argue that human safety skills—such as knowledge, habits, and psychological factors—alongside safety culture, tend to be overlooked components. Additionally, lack of work experience—understood as the set of skills and knowledge acquired by a worker in a specific activity over a given period—is regarded as one of the most prevalent causes of accidents across multiple sectors [3, 8]. Moreover, several authors highlight that human error remains one of the primary risk factors in occupational accidents, often resulting from inadequate training and the absence of a structured system for competency assessment in safety practices [7,9,10].

Several studies have identified a direct correlation between worker age and work experience, suggesting that although aging may increase accidents severity and rates—due to the decline in motor skills and physical capabilities—experience can help reduce both the frequency and severity of risks [3,8,11]. Nuñez and Prieto [12] point out that workers lacking the necessary skills to perform their tasks may focus excessively on meeting performance targets, while neglecting occupational hazards and the proper use of safety equipment. This behavior increases the likelihood of work-related injuries. Moreover, Nuñez and Prieto [12] and Rahman et al. [13] emphasize that the incidence of accidents and fatalities can be reduced through appropriate training and the proper installation and maintenance of safety devices—areas in which safety competencies play a critical role.

This study aims to identify the core safety competencies associated with the job profile of open-pit mine drill operators, using DACUM (Developing a Curriculum) and functional analysis as methodological frameworks.

1.1 Risks in mining

Mining is a multidisciplinary industry that operates under dynamic conditions within a complex sociotechnical system, where human interactions with technical processes pose significant challenges to the development of effective risk management policies [14], particularly in the identification and assessment of risks [15].

A typical mining project life cycle is divided into four main phases: exploration (7–10 years), development (5–10 years), operation (2–20 years), and closure (2–10 years) [15]. The exploration phase includes activities aimed at identifying the materials to be extracted and supports both cost–benefit analysis and the documentation required for the business plan. The development phase begins with the planning and construction of the project. It is characterized by the recruitment of various industrial profiles (civil, mechanical, electrical engineers, geologists, among others), making it the most resource-intensive phase. It is during this stage that the drill operator becomes directly involved. The third phase is mainly concerned with the commercialization of production, while the final closure phase consists of dismantling and relocating facilities and equipment.

Occupational health and safety issues are present throughout all stages of the mining cycle and can be classified into the following categories: hazardous substances, use of explosives, heat stroke and electrical hazards, physical hazards, ionizing radiation, thermal stress, noise and vibration, as well as hazards specific to underground mining such as fire, explosions, confined spaces, and atmospheres with insufficient oxygen levels [16]. Workers are also exposed to airborne dust and gases generated during blasting or rock drilling, the adoption of non-ergonomic working postures, and the operation of heavy machinery and vehicles, among other risks [14].

Zhou et al. [17] report that among drilling tasks, the most significant hazards include entrapment by objects, equipment-related injuries, and physical overexertion, while hazards involving lower levels of risk include exposure to substances or environmental conditions, as well as to fire and explosions.

1.2 Safety competencies

Safety culture is defined as the combination of a set of values and behaviors that determine how a safety process is managed within organizations [18]. However, despite the strong interest of companies in promoting and implementing safety culture and behavior-based safety programs, workplace accidents will continue to occur if workers still lack safety competencies [19,20]. According to Tetzlaff et al. [21] the absence of risk awareness, poorly designed training systems, and occupational stressors are pre-existing hazards that make organizational systems vulnerable and cause failures. Therefore, the authors recommend implementing

training programs to produce qualified personnel who are fully aware of occupational hazards.

The Mine Safety and Health Administration (MSHA) indicates that the adoption of safe work practices, such as workplace examinations, is crucial to protect mining workers from the hazards to which they are exposed [22]. In this context, MSHA standards emphasize the need for competent personnel to perform such examinations.

A competent worker is defined as someone who possesses the skills and experience that fully qualify them to perform their assigned tasks [23]. Additionally, such a worker must be capable of identifying hazards and adverse conditions that either an average worker may recognize or that a worker familiar with the mining industry could reasonably predict [22]. Competency is understood as the combination of knowledge, skills, abilities, and attitudes required to perform a task efficiently [18]. In this regard, competencies enable organizations to make better-informed decisions and increase the likelihood that individuals faced with abnormal situations will have the knowledge and skills necessary to respond appropriately [24].

1.3 Techniques for identifying competencies

There are various analytical techniques used to identify occupational competencies, including Developing a Curriculum (DACUM), the AMOD model, the Studied Typical Employment Method (ETED), and Functional Analysis [25].

The DACUM technique enables a practical and rapid description of occupational content based on three core principles: (1) expert workers can describe their work more accurately than anyone else; (2) an occupation can be defined by describing the tasks performed by expert workers; and (3) all tasks require the application of knowledge, behaviors, and skills, as well as the use of tools and equipment. The AMOD technique is a variant of DACUM, distinguished by organizing tasks according to their complexity [26]. Functional analysis is a logical-deductive process that allows the progressive breakdown of functions performed within an organization or productive sector [25]. The ETED technique is a constructivist approach that emphasizes the variability of work and prioritizes technical aspects such as the use of machinery, implementation of work methods, regulatory compliance, and material [27].

According to the International Labor Organization (ILO) [25], the methodology for developing a technical competency standard requires:

1. Identifying the relationships between functions and the activities that constitute a productive function.
2. Standardizing the identified competencies.
3. Validating the standard with a technical or standardization committee.

1.4 Current regulations

In Mexico, the Secretariat of Labor and Social Welfare (STPS) is the authority responsible for regulating working conditions through the enforcement of mandatory labor regulations. In the mining sector, the STPS issued the Official

Mexican Standard NOM-023-STPS-2012, which governs the operation of both underground and open-pit mines [28]. Section 5 of this standard outlines employer obligations, while section 9.2 provides specific guidelines for conducting excavations in open-pit mining. However, these provisions are general in nature and must be complemented by detailed and effective training programs to ensure the safe execution of mining activities.

At the international level, various standards exist to support hazard identification and risk assessment in the workplace. One such standard is ISO 45001, which establishes the requirements for the implementation of an Occupational Health and Safety Management System. The standard emphasizes the importance of adopting a systematic approach to hazard identification, risk assessment and control, as well as ensuring the active participation of workers in occupational health and safety management [29].

2 Methodology

To determine the safety competencies associated with the drill operator profile, the methodology proposed by the ILO [25] was adapted. This methodology implements a mixed-methods approach based on functional analysis and the DACUM technique, as illustrated in Fig. 1 and described in the following sections.

2.1 Description of the work procedure

Table 1 presents each of the sequential stages involved in the drill operator's work using portable equipment.

2.2 Development of the process network

This step identifies the drill operator's involvement in operational activities and allows for visualization of how the drill operator profile interacts with other roles (Table 2). In this study, it is possible to observe the interactions of the drill operator with their assistants (two, according to the working scheme of the company analyzed) and with the drill pattern supervisors.

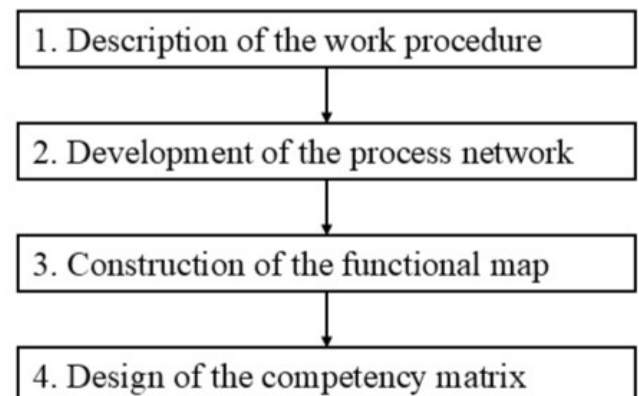


Figure 1. Mixed-methods approach based on functional analysis and the DACUM.

Source: Author's own creation

Table 1.
Portable Drilling Procedure.

Step Sequence	Responsible Party
1. Conduct checklist verification.	Drill operator
2. Transport equipment to drilling site.	Drill operator, assistants, operations and safety personnel
3. Align drilling machine.	Drill operator, assistants
4. Prepare the drill pattern.	Drill operator and assistants
5. Assemble core barrel.	Drill operator and assistants
6. Assemble inner tube.	Drill operator and assistants
7. Place barrel onto head and foot clamp.	Drill operator and assistants
8. Start drilling (bit entry).	Drill operator
9. Retrieve inner tube.	Drill operator and assistants
10. Assemble second inner tube.	Drill operator's assistant
11. Inject water to reach bottom of hole.	Drill operator
12. Prepare additional tube.	Drill operator and assistants
13. Empty inner tube.	Drill operator's assistants
14. Arrange rock samples in boxes.	Drill operator's assistant
15. Secure boxes for client delivery.	Drill operator's assistant

Source: Author's own creation

Table 2.
Process network.

Subprocess	Procedure	Main Activities	Job Profile
Site Preparation	Drill pattern marking	Drill pattern layout, materials transport, use of pack animals	Drill pattern supervisors
Equipment Installation	Drilling machine setup	Wireline cable installation, drill rig alignment, pipe adjustment	Drill operator and assistant
Operation and Drilling	Handling of rods and tools	Use of polymers, hand tools, rod feeding, diamond drilling	Drill operator and assistant
Safety and Procedures	Safe operation of drilling equipment	Operation of portable, mobile, underground, pneumatic, and hydraulic drill rigs	Drill operator and assistant
Recovery and Deinstallation	Recovery and disassembly of equipment	Core and pipe retrieval, pipe rescue, drill rig removal	Drill operator and assistant

Source: Author's own creation

2.3 Construction of the functional map

A functional map is a graphical representation that breaks down the key objective of the job profile into specific activities. Within this methodology, the main and basic functions of the drilling process were identified (Fig. 2).

2.4 Identification of critical competencies

Using the DACUM methodology, this stage involves identifying the corresponding process phase for each competency, detailing the related tasks and activities, required skills and knowledge, tools and equipment utilized, as well as associated risks and the necessary safety measures.

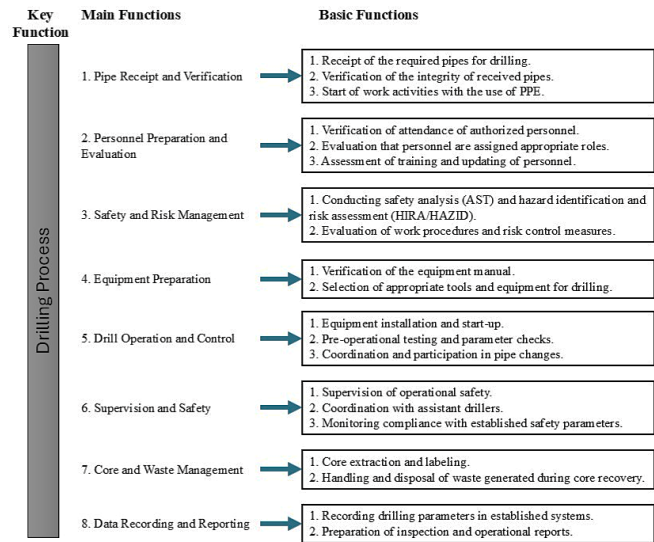


Figure 2. Functional map for the drill operator.

Source: Author's own creation.

2.5 Design and validation of the assessment instrument

The assessment instrument was developed with 23 items, of which completion of at least 19 is required to consider a worker competent. Given the presence of critical competencies, certain evaluation criteria were established: the mandatory use of personal protective equipment, ensuring that only authorized personnel perform specific tasks, and conducting machine operational tests are essential prerequisites for competency certification. Conversely, failure to maintain continuous supervision over the installation of safety guards is deemed sufficient grounds to classify a worker as not competent.

For validation purposes, the instrument was reviewed by the company's most experienced drilling personnel, who provided valuable feedback on the terminology and critical elements of the tool. In total, three experts (drill operators) with more than 12 years of experience and certifications in drilling machinery operation, as well as training in industrial safety provided by international mining companies and STPS, participated in the review process.

3 Results

Table 3 presents the competencies identified for each of the main and basic functions outlined in Fig. 1. These competencies are described in terms of the skills and knowledge necessary to safely perform the tasks or activities. The skills and knowledge considered include effective communication, knowledge of roles and responsibilities, competency assessment, safety and task-specific risks knowledge, waste management, documentation, among others.

In relation to NOM-023-STPS-2018, the matrix presented in Table 3 supports compliance with the employer's obligation to identify and evaluate the risks to which workers

Table 3.
Competency Matrix for the Drill Operator Profile.

Process Stage	Tasks and Activities	Skills and Knowledge	Tools and Equipment	Hazards / Risks
Receipt and Verification of Core	<ol style="list-style-type: none"> 1. Receipt of core 2. Verification or confirmation of core 3. Start activity with PPE 	<ul style="list-style-type: none"> - Identification of drilling materials - Effective communication - Entry logbook - Radio communication for core reporting - Visual and documentary review 	<ul style="list-style-type: none"> - Entry logbook - Radio to communicate core status 	<ul style="list-style-type: none"> - Providing incorrect location or activity information - Visual and documental revise - Risk of run-over if site operators do not identify the core team
Personnel Preparation and Evaluation	<ol style="list-style-type: none"> 1. Review attendance lists of authorized personnel 2. Verify work team attendance 3. Complete equipment checklist 4. Review training and authorization of personnel. 	<ul style="list-style-type: none"> - Knowledge of roles and responsibilities - Competency assessment - Knowledge of job requirements - Safety knowledge - Equipment knowledge - Attention to detail 	<ul style="list-style-type: none"> - Authorized personnel lists - Attendance lists 	<ul style="list-style-type: none"> - Errors in task assignment - Non-compliance with safety regulations
Safety and Risk Management	<ol style="list-style-type: none"> 1. Conduct Risk Analysis before starting activities 2. Identify and evaluate potential operational risks 	<ul style="list-style-type: none"> - Knowledge of specific drilling risks - Control measures evaluation - Knowledge of unsafe acts and conditions - Risk and hazard awareness 	<ul style="list-style-type: none"> - Risk documents and control measures 	<ul style="list-style-type: none"> - Exposure to hazardous conditions - Non-compliance with safety protocols
Equipment Preparation	<ol style="list-style-type: none"> 1. Verify manual and select tools 2. Select drilling tools and supplies. 	<ul style="list-style-type: none"> - Interpretation of equipment manuals - Knowledge of drilling tools 	<ul style="list-style-type: none"> - Equipment manuals - Lists of tools and supplies 	<ul style="list-style-type: none"> - Equipment damage due to incorrect use - Selection of inappropriate tools
Drill Operation and Control	<ol style="list-style-type: none"> 1. Move equipment in case of new drill site 2. Machine alignment 3. Installation, testing, and coordination in drilling 4. Equipment installation and tests 5. Coordination and participation in steel changes 	<ul style="list-style-type: none"> - Specific operational skills - Coordination with assistants and operators - Use of alignment tools - Ability to adjust and align machine - Knowledge of topographic plans 	<ul style="list-style-type: none"> - Drilling equipment - Alignment equipment 	<ul style="list-style-type: none"> - Accidents during drilling - Failures in operational coordination
Supervision and Safety	<ol style="list-style-type: none"> 1. Monitor conditions and incident recording 2. Stop activities if dangerous or risky conditions are found 3. Document any anomalies during activities 	<ul style="list-style-type: none"> - Supervision skills - Safety data recording 	<ul style="list-style-type: none"> - Safety data recording formats 	<ul style="list-style-type: none"> - Risks associated with supervision - Incidents not properly recorded
Core and Waste Handling	<ol style="list-style-type: none"> 1. Store cores according to client specifications 2. Register cores according to client specifications 	<ul style="list-style-type: none"> - Knowledge of core and waste handling - Information recording 	<ul style="list-style-type: none"> - Storage containers 	<ul style="list-style-type: none"> - Contamination due to improper handling - Loss of critical information
Data Recording and Reporting	<ol style="list-style-type: none"> 1. Record data and prepare reports of meters drilled, recirculated water, and amount of additives used 	<ul style="list-style-type: none"> - Documentation skills - Use of recording systems - Use of digital tools to send documentation 	<ul style="list-style-type: none"> - Recording formats 	<ul style="list-style-type: none"> - Documentation errors - Loss of important data

Source: Author's own creation

are exposed, as well as to communicate these hazards to the occupationally exposed personnel. Competency assessment also enables the definition of a training program by identifying weaknesses in competency fulfillment, in addition to establishing the mandatory theoretical and practical knowledge regarding the use of personal protective equipment (PPE) and safety procedures.

Regarding international standards such as ISO 45001, which focuses on Occupational Health and Safety

Management Systems, the proposed model and the identified competencies facilitate systematic risk management and encourage the active participation of exposed personnel in hazard identification and risk assessment, emphasizing the importance of each safety aspect considered in the execution of their activities. Once the competencies presented in Table 3 were established, a sample of eight drill operators was selected to complete the assessment instrument through a theoretical-practical evaluation. The results indicate that 75%

of the evaluated operators meet the required competencies to perform drilling activities safely (Table 4). Operators who did not achieve competence in safe work were subsequently trained on the relevant topics and successfully approved the competency evaluation in a second assessment. occupationally exposed personnel. Competency assessment also enables the definition of a training program by identifying weaknesses in competency fulfillment, in addition to establishing the mandatory theoretical and practical knowledge regarding the use of personal protective equipment (PPE) and safety procedures.

Regarding international standards such as ISO 45001, which focuses on Occupational Health and Safety Management Systems, the proposed model and the identified competencies facilitate systematic risk management and encourage the active participation of exposed personnel in hazard identification and risk assessment, emphasizing the importance of each safety aspect considered in the execution of their activities.

Once the competencies presented in Table 3 were established, a sample of eight drill operators was selected to complete the assessment instrument through a theoretical-practical evaluation. The results indicate that 75% of the evaluated operators meet the required competencies to perform drilling activities safely (Table 4). Operators who did not achieve competence in safe work were subsequently trained on the relevant topics and successfully approved the competency evaluation in a second assessment.

In Table 5, the impact of competency-based training on the company's safety indicators is shown. It is possible to observe a decrease in lost-time injuries and restricted work cases after implementing the evaluation instrument and providing training to non-competent workers.

Table 4.
Evaluation results.

Drill operator	Item							Result	
	1	3	11	12	16	Other	Total	Conclusion	
1	1	1	1	1	1	18	23	Competent	
2	1	1	1	1	1	18si q	23	Competent	
3	0	0	0	0	1	18	19	Not competent	
4	0	0	0	0	1	18	19	Not competent	
5	1	1	1	1	1	18	23	Competent	
6	1	1	1	1	1	18	23	Competent	
7	1	1	1	1	1	18	23	Competent	
8	1	1	1	1	1	18	23	Competent	

Source: Author's own creation.

Table 5.
Impact of Competency-Based Training on Safety Indicators

Safety Indicator	2023 Before Training	2024 After Competency Evaluation
LTI (Lost Time Injury)	2	0
RWI (Restricted Work Injury)	3	0
MTI (Medical Treatment Injury)	1	1

Source: Author's own creation.

4 Conclusions

This study proposes a set of competencies for open-pit mine drilling personnel, described in terms of skills, knowledge, tools, and specific hazards to which workers are exposed. The competence model developed provides a formal basis for the safe execution of drilling activities, supports efficient risk management, and facilitates compliance with national regulations (NOM-023-STPS-2012) and international occupational health and safety standards (ISO 45001).

Furthermore, the methodology applied (integrating DACUM and functional analysis) is effective in identifying the key tasks, tools, and knowledge gaps associated with the drill operator role. The use of these techniques allows companies to design training and assessment programs tailored to their operational realities, thereby improving individual and organizational outcomes.

The results suggest that the professionalization and empowerment of workers through continuous skills development and active worker participation in risk identification and mitigation improves mining safety culture and ultimately reduce not only the frequency but also the severity of occupational injuries.

Due to the nature and duration of mining projects, the results were obtained from a small sample of workers from a company in the northwest region of Mexico. Therefore, it is recommended to replicate the study in other companies within the region to increase the number of workers involved. This approach could enable the generalization of the findings. Finally, continuous evaluation and training should be viewed as a dynamic component of the mining safety policy and culture.

References

- [1] Camimex, Seguridad. Incidentes en la industria minera, [online]. 2025. Disponible en: <https://www.camimex.org.mx/index.php/estadisticas/Seguridad>
- [2] Navarro-Valdiviezo M.A., Cultura de seguridad y su influencia en los accidentes laborales con maquinaria pesada en las minas de Shougang Hierro Perú. Bs. Eng. Thesis, Universidad Nacional San Luis Gonzaga, Perú, 2019.
- [3] Baraza, X., Cugueró-Escofet, N., and Rodríguez-Elizalde, R., Statistical analysis of the severity of occupational accidents in the mining sector. *Journal of Safety Research*, 86, pp. 364-375, 2023. DOI: <https://doi.org/10.1016/j.jsr.2023.07.015>
- [4] Secretaría de Economía. Minería. [online]. 2024. Disponible en: <https://www.gob.mx/se/acciones-y-programas/mineria>
- [5] Ismail, S.N., Ramli, A., and Aziz, H.A., Influencing factors on safety culture in mining industry: a systematic literature review approach. *Resources Policy*, 74, art. 102250, 2021. DOI: <https://doi.org/10.1016/j.resourpol.2021.102250>
- [6] Bloch Lance. The 4TH Wave: culture-based behavioural safety. [online]. The Southern African Institute of Mining and Metallurgy Platinum, [consulted, March 30th, 2025]. 2012. Available at: https://www.saimm.co.za/Conferences/Pt2012/163-176_Bloch.pdf
- [7] Fu, G., Xie, X., Jia, Q., Tong, W., and Ge, Y., Accidents analysis and prevention of coal and gas outburst: understanding human errors in accidents. *Process Safety and Environmental Protection*, 134, pp. 1-23, 2020. DOI: <https://doi.org/10.1016/j.psep.2019.11.026>
- [8] Bande, R., and López-Mourelo, E., The Impact of worker's age on the consequences of occupational accidents: empirical evidence using Spanish Data. *Journal of Labor Research*, 36(2), pp. 129-174, 2015. DOI: <https://doi.org/10.1007/s12122-015-9199-7>

- [9] Reyes-Martínez, R.M., Maldonado-Macías, A., and Prado-León, L.R., Human factors identification and classification related to accidents' causality on hand injuries in the manufacturing industry. *Work*, 41(1), pp. 3155-3163, 2012. DOI: <https://doi.org/10.3233/WOR-2012-0577-3155>
- [10] Salminen, S., and Tallberg, T., Human errors in fatal and serious occupational accidents in Finland. *Ergonomics*, 39(7), pp. 980-988, 1996. DOI: <https://doi.org/10.1080/00140139608964518>
- [11] Margolis, K.A., Underground coal mining injury: a look at how age and experience relate to days lost from work following an injury. *Safety Science*, 48(4), pp. 417-421, 2010. DOI: <https://doi.org/10.1016/j.ssci.2009.12.015>
- [12] Nuñez, I., and Prieto, M., The impact of skills mismatches on occupational accidents: An analysis of the effectiveness of organizational responses. *Safety Science*, 170, Art. 106349, 2024. DOI: <https://doi.org/10.1016/j.ssci.2023.106349>
- [13] Rahman, F.A., Arifin, K., Abas, A., Mahfudz, M., Cyio, M.B., Khairil, M., Ali, M.N., Lampe, I., and Samad, M.A., Sustainable Safety Management: a safety competencies systematic literature review. *En Sustainability (Switzerland)* 14(11), art. 16885, 2022. DOI: <https://doi.org/10.3390/su14116885>
- [14] Baghaci-Nacini, S.A., and Badri, A., Identification and categorization of hazards in the mining industry: a systematic review of the literature. *En International Review of Applied Sciences and Engineering*, 15(1), pp. 1-19, 2024. DOI: <https://doi.org/10.1556/1848.2023.00621>
- [15] Badri, A., Nadeau, S., and Gbodossou, A., a mining project is a field of risks: a systematic and preliminary portrait of mining risks. *International Journal of Safety and Security Engineering*, 2(2), pp. 145-166, 2012. DOI: <https://doi.org/10.2495/SAFE-V2-N2-145-166>
- [16] International Finance Corporation. *Environmental, Health and Safety Guidelines for Mining*. [online]. [consulted, February, 15th, 2025], 2007. Available at: <https://www.ifc.org/content/dam/ifc/doc/2000/2007-mining-ehs-guidelines-en.pdf>
- [17] Zhou, A., Wang, K., and Zhang, H., Human factor risk control for oil and gas drilling industry. *Journal of Petroleum Science and Engineering*, 159, pp. 581-587, 2017. DOI: <https://doi.org/10.1016/j.petrol.2017.09.034>
- [18] Revez, D., and Mendes-Silva, G.P., Development and application of process safety competency framework in agroindustry: A case study. *Process Safety Progress*, 42(1), pp. 103-109, 2023. DOI: <https://doi.org/10.1002/prs.12553>
- [19] Axley, L., Competency: a concept analysis. *nursing forum*, [online]. 43(4), pp. 214-222, 2008. Available at: <http://m-w.com/dictionary/>
- [20] Chang, S.H., Chen, D.F., and Wu, T.C., Developing a competency model for safety professionals: correlations between competency and safety functions. *Journal of Safety Research*, 43(5-6), pp. 339-350, 2012. DOI: <https://doi.org/10.1016/j.jsr.2012.10.009>
- [21] Tetzlaff, E.J., Goggins, K.A., Pegoraro, A.L., Dorman, S.C., Pakalnis, V., and Eger, T.R., Safety Culture: a retrospective analysis of occupational health and safety mining reports. *safety and health at work*, 12(2), pp. 201-208, 2021. DOI: <https://doi.org/10.1016/j.shaw.2020.12.001>
- [22] Mine Safety and Health Administration. *Program Policy Letter P15-V-01 - Examination, Evaluation and Effectiveness*, [online]. 2015. Available at: https://www.jacksonlewis.com/sites/default/files/docs/PPL18002_0.pdf
- [23] Hrica, J.K., and Eiter, B.M., Competencies for the Competent Person: defining workplace examiner competencies from the health and safety leader's perspective. *Mining, Metallurgy and Exploration*, 37(6), pp. 1951-1959, 2020. DOI: <https://doi.org/10.1007/s42461-020-00275-w>
- [24] Abikenova-Sholpan K., Oshakbayeva-Zhuldyz O., Bekmagambetov-Alimzhan B., and Sarybayeva-Inara E., View of the role of professional competencies in developing a culture of safety in the workplace. *European Journal of Sustainable Development*, 12(4), pp. 237-246, [online]. 2023. Available at: <https://ecsdev.org/ojs/index.php/ejsd/article/view/1461/1434>
- [25] International Labour Organization (ILO). *Equipo técnico de trabajo decente y oficina de países para América Central, H.P., y R., Dominicana*, [en línea]. metodologías para la elaboración de normas técnicas, diseños curriculares y evaluaciones por competencias laborales, [en línea]. 2014. Disponible en: <https://www.oitcinterfor.org/metodolog%C3%ADas-elaboraci%C3%B3n-normas-t%C3%A9cnicas-dise%C3%B1os-curriculares-evaluaciones-competencias-laborales>
- [26] Irigoien, M., and Vargas, F., *Competencia laboral: manual de conceptos, métodos y aplicaciones en el sector salud*. Oficina Internacional del Trabajo, CINTERFOR, 2002.
- [27] El-Assafiri-Ojeda, Y., Medina-Nogueira, E., Medina-León, A., Nogueira-Rivera, D., and Medina-Nogueira, D., Método developing a curriculum para el análisis ocupacional. Acercamiento a la gestión del conocimiento developing a curriculum method for occupational analysis, [online]. *An Approach to Knowledge Management. Ingeniería Industrial*, XL (2), pp. 161-170, 2019. Available at: <http://www.rii.cujae.edu.cu>
- [28] STPS. *NORMA Oficial Mexicana NOM-023-STPS-2012, Minas subterráneas y minas a cielo abierto - Condiciones de seguridad y salud en el trabajo*, [online]. 2012. Available at: https://dof.gob.mx/nota_detalle.php?codigo=5272056&fecha=11/10/2012#gsc.tab=0
- [29] ISO 45001:2018 *Sistemas de gestión de seguridad y salud en el trabajo- Requerimientos con guías para uso*. International Standardization Organization. 2018.

G. Rodríguez-Vega, received the BSc. Eng in Industrial Engineering in 2005 from the Technological Institute of Los Mochis, México. MSc. in Industrial Engineering in 2008 from the Technological Institute of Hermosillo, México, and PhD in Information Sciences in 2022 from the Autonomous University of Sinaloa, Mexico. Currently, she is a fulltime professor in the Industrial Engineering Department, Engineering Interdisciplinary Faculty, University of Sonora. México. Her research interests include occupational safety and health and multivariate analysis. ORCID: 0000-0001-7366-1107

M.A. Valenzuela-Soto, received the BSc. Eng in Industrial and Systems Engineering in 2026, and MSc. in Systems and Technology Engineering 2025, all of them from the University of Sonora, Mexico. She worked in programs and projects of the mining area, with emphasis on environmental management and since 2023. She is currently coordinator 5s program in a mining company. ORCID: 0009-0003-0929-1262

D.A. Rodríguez-Vega, received the BSc. Eng in Electronic Engineering in 2002, from the Technological Institute of Los Mochis, MSc. in Electronic Engineering in 2004, from the Technological Institute of Chihuahua, and PhD in Information Sciences in 2018 from Autonomous University of Sinaloa, all of them from Mexico. Currently, she is a fulltime professor in the Faculty of Mechatronics, Polytechnic University of Sinaloa. Her research interests include robotics, human-robot interactions, multivariate anthropometry and occupational safety and. ORCID: 0000-0002-6521-7978

Technical and economic analysis of alternatives for the construction of tertiary roads in Colombia

Zully Palomeque-Sánchez^a, Juan Gabriel Bastidas-Martínez^b & Jessica Rincón-Esteva^c

^a Facultad de Ingeniería, Universidad Militar Nueva Granada, Bogotá, Colombia. Zully.palomeque@unimilitar.edu.co

^b Facultad de Estudios a Distancia, Universidad Militar Nueva Granada, Bogotá, Colombia. juan.bastidas@unimilitar.edu.co

^c Grupo Enel, Bogotá, Colombia. Jessica.rincon@enel.com

Received: August 26th, 2025. Received in revised form: October 10th, 2025. Accepted: November 4th, 2025.

Abstract

This article aims to describe the design methods for the construction of tertiary roads in Colombia. A detailed compilation of alternatives currently recommended in technical documents was carried out. Subsequently, pavement designs were developed considering different soil types, traffic levels, climatic conditions, and materials. In total, 410 alternatives were obtained, including pavements with surface treatments, flexible, semi-rigid, rigid, and plain-concrete strip structures. Based on critical conditions (soil, traffic, and climate), seven alternatives were selected for economic analysis. Multi-criteria analyses using the Selection by Advantage method were conducted to identify the best alternative from the technical, environmental, and economic perspectives. Results indicate that semi-rigid pavements present greater feasibility compared to current practices, as they exhibit lower thicknesses, reduced costs, and higher potential for material recycling at the end of their service life.

Keywords: low-volume roads; plain-concrete strip road; camera-ready manuscript; soil improvement techniques; geosynthetics.

Análisis técnico y económico de alternativas para la construcción de vías terciarias en Colombia

Resumen

Este artículo tiene como objetivo describir los métodos de diseño para la construcción de vías terciarias en Colombia. Se efectuó una compilación detallada de alternativas actualmente recomendadas en documentos técnicos. Posteriormente se realizó el diseño de pavimentos considerando diferentes tipos de suelo, niveles de tránsito, clima y materiales. En total, fueron obtenidas 410 alternativas que involucran pavimentos con tratamientos superficiales, flexibles, semirrígidos, rígidos y placa huella. A partir de las condiciones críticas (suelo, tránsito y condiciones climáticas) se seleccionaron siete alternativas en las cuales fueron realizados análisis económico. Análisis multicriterio bajo el método de selección por ventaja fueron realizados para seleccionar la mejor alternativa desde el punto de vista técnico, ambiental y económico. Resultados indican que pavimentos semirrígidos se presentan mayor viabilidad en referencia a las técnicas actuales, dado que exhiben menores espesores, costo y mayor capacidad de reciclaje de materiales al final de su vida útil.

Palabras clave: vías terciarias; placa huella; análisis multicriterio; técnicas de mejoramiento de suelos; geosintéticos.

1 Introducción

Las vías terciarias son importantes, dado que enlazan principalmente poblaciones rurales y centros de producción agrícola, mejorando el acceso a servicios de salud, educación, comercio, entre otros [1,2]. Adicionalmente, se emplean en el sector de minería, hidrocarburos, energía, parques solares,

entre otros. Datos del Ministerio de Transporte indican que la red vial colombiana se compone por aproximadamente 205.875 km de carreteras, de las cuales, 7% son primarias, 25% secundarias y 70% corresponden a vías terciarias [3]. Según datos del Instituto Nacional de Vías INVIAS, la red vial no pavimentada 54.43% se encuentra en estado malo-muy malo, 36.66% regular y únicamente 8.91% en estado

How to cite: Palomeque-Sánchez, Z., Bastidas-Martínez, J.G. and Rincón-Esteva, J., Análisis técnico y económico de alternativas para la construcción de vías terciarias en Colombia DYNA, (92)239, pp. 118-129, October - December, 2025.

bueno-muy bueno [4]. Por tanto, es necesaria la creación de políticas que fomenten su construcción y mantenimiento. En Colombia han creado diversos planes nacionales para el fortalecimiento de vías terciarias. En 1960 se creó el Fondo Nacional de Caminos Vecinales en Colombia mediante los Decretos 1650 de 1960 y 1084 de 1961 adscrito al Ministerio de Obras Públicas [5]. Su propósito fue el mejoramiento y conservación de los caminos verdaderos del país o regionales mediante la cooperación entre los Departamentos y Municipios. Sin embargo, en el año 2003 fue liquidado mediante Decreto Nacional 1790 y transferido a INVIAS. Entre los años 2003 y 2019 fue creado el plan 2500 que tenía como objetivo la pavimentación, reconstrucción y/o repavimentación de 2500 km de carreteras para el desarrollo regional buscando conectividad de regiones apartadas del país [6]. Este plan contempló los lineamientos del Consejo Nacional de Política Económica y Social CONPES 3311 de 2004 con recursos de 1.8 billones de pesos. En el año 2011 se ejecutó el programa Caminos para la prosperidad que tenía como objetivo la invención de 50.000 km de vías terciarias. Paralelamente, se creó el Sistema General de Regalías SGR que busca la repartición de recursos económicos generados por regalías de petróleo en todos los Departamentos para la financiación de proyectos, mediante el Órgano Colegiado de Administración y Decisión OCAD.

En 2016, fueron definidas las zonas más afectadas por el conflicto armado, por sus siglas ZOMAC considerando 344 Municipios de 19 Departamentos. A partir de lo anterior se creó el Plan 50/51 que buscó la intervención de los 50 corredores más productivos y 51 proyectos estratégicos para mejorar la conectividad rural en ZOMAC. Se establecieron estrategias de financiamiento a través de obras por impuestos mediante la Ley 1819 de 2016 que busca la financiación de obras en ZOMAC a partir de impuestos de obras [6]. Asimismo, surgieron Programas de Desarrollo con Enfoque Territorial PDET que buscan intervenciones, tales como la construcción de vías terciarias en zonas afectadas por conflicto armado. A pesar de la existencia de planes para el fortalecimiento de vías terciarias, en la literatura técnica consultada no se reportan cifras exactas de los kilómetros de vías intervenidas.

1.1 Documentos técnicos para diseño y construcción de estructuras para vías terciarias en Colombia

A fin de garantizar las condiciones técnicas y económicas de proyectos de infraestructura, algunas entidades públicas disponen de documentos técnicos que proporcionan diversas alternativas de pavimentación para vías de bajo volumen de tránsito tales como: i) Manual de diseño de pavimentos asfálticos para vías con bajos volúmenes de tránsito publicado por INVIAS en el año 2007 [7]. El objetivo de ese documento es proporcionar espesores de estructuras pavimentos flexibles para vías rurales mediante cartas de diseño. Estas cartas de diseño corresponden a espesores determinados mediante la metodología AASHTO 1993 [8]; ii) Manual de diseño de pavimentos de concreto para vías con bajos, medios y altos volúmenes de tránsito, desarrollado en el año 2008 por el Instituto Colombiano de productores de cemento ICPC con participación de INVIAS y del Ministerio

de transporte [9]. Ese documento suministra el espesor de la losa de concreto a partir de las variables de diseño; iii) Guía de diseño de pavimentos con placa huella publicada por INVIAS en el año 2015 [10]. La placa huella es un conjunto de elementos que conforman la estructura para el tránsito de vehículos en vías rurales. Entre los elementos que conforman la placa huella se tiene: placas en concreto reforzado, separador central y sobreanchos en concreto ciclópeo, elementos de confinamiento tipo riostras y bordillos, transvásales y longitudinales al eje de la vía y elementos de drenaje tipo cunetas. Estos elementos se encuentran apoyados sobre un material de subbase granular [11,12]. En la Fig. 1 se presenta una estructura típica de placa huella; iv) Cartilla de obras menores de drenaje y estructuras viales del programa de Colombia Rural en el año 2020. En este documento se presentan diseños tipo de estructuras de pavimento flexible, semirrígidos, rígidos, placa huella y caminos ancestrales [13]; v) Documento para la formulación de proyectos tipo para el mejoramiento de vías terciarias del Departamento Nacional de Planeación DNP en el año 2021 que proporciona soluciones estructurales y funcionales basadas en estabilización de materiales con cemento o materiales asfálticos, lechadas asfálticas, tratamientos superficiales, entre otros. Adicionalmente, algunos documentos proporcionan lineamientos técnicos para la construcción de elementos de drenaje superficial, subsuperficial, muros de contención, puentes, entre otros. Asimismo, se proporcionan especificaciones de construcción y técnicas para el mantenimiento rutinario [14].

1.2 Variables de diseño

Las metodologías para el diseño y construcción de vías terciarias involucran factores o variables que buscan garantizar aspectos de estructurales, funcionales y durabilidad durante el periodo de diseño. Las principales metodologías incluyen: i) Tránsito: generalmente es definido por el número de ejes equivalentes de 80 kN en el carril de diseño durante el periodo de diseño; ii) Subrasante: definida



Figura 1. Estructura en placa huella.
Fuente: Autores.

Tabla 1.

Consideraciones de documentos técnicos para el diseño de vías terciarias en Colombia.

Documento	Entidades u organizaciones	Periodo (años)	Variables de diseño				Tipos de pavimentos				
			Tránsito	Subrasante	Clima	Materiales	PTS	PF	PS	PR	PH
Manual de diseño de pavimentos asfálticos para vías con bajos volúmenes de tránsito	INVIAS 2007	10	x	x	x	MDC-MDF-TSD-BG-BEC-BEE-SBG-AFR	x	x	x		
Manual de diseño de pavimentos de concreto para vías con bajos, medios y altos volúmenes de tránsito	ICPC -INVIAS- Ministerio de Transportes 2008	20	x	x		C-BG-BEC				x	
Guía de diseño de pavimentos con placa huella	INVIAS 2015	20	x	x		C-SBG					x
Cartilla de obras menores de drenaje y estructuras viales del programa de Colombia Rural	INVIAS 2020	10	x	x	x	C-MDC-TSD-TSA-BG-SBG-SCE-SCA	x	x	x	x	x
Cartilla de Proyectos tipo para el mejoramiento de vías terciarias	DNP e INVIAS 2021	5*	x	x		C-TSD-LA-BEC-BEE-BEM	x		x		x

*Periodo de diseño mínimo.

Fuente: Autores.

como la capacidad de soporte del suelo de fundación que comúnmente se determina según los ensayos de California Bering Ratio CBR o módulo resiliente; iii) Clima: determinada a partir del nivel de precipitación anual y de la temperatura media ponderada del lugar donde se pretende construir el pavimento; iv) Materiales para la conformación de las capas de pavimentos dependen de la disponibilidad del sitio, procesos constructivos, costos, entre otros. Cada documento técnico proporciona algunas recomendaciones, destacando: mezclas asfálticas densa en caliente MDC o en frío MDF; tratamientos superficiales dobles TSD; tratamiento superficial con asfaltita (asfalto natural) TSA; lechadas asfálticas LA, base granular BG; base estabilizada con cemento BEC, emulsión BEE o mecánicamente BEM; subbase granular SBG; Afirmado AFR; concreto C; suelos estabilizados con cemento SEC o cal SEC, entre otros. En la Tabla 1 se presenta una descripción de las variables de diseño contempladas en los documentos técnicos para el diseño de vías terciarias en Colombia. Asimismo, se presenta el periodo de diseño y los tipos de alternativas recomendadas en cada documento que incluyen: pavimento con tratamiento superficial PTS, pavimento flexible PF, pavimento semirrígido PS, pavimento rígido PR y placa huella PH

1.3 Nuevas tecnologías

A nivel nacional, en el año 2022, INVIAS incorporó el artículo 237 dentro de su normativa técnica, con el propósito de promover el desarrollo y la implementación de tecnologías emergentes para la estabilización de subrasantes en estructuras de pavimento, particularmente en vías de bajo volumen de tránsito [15]. Esta especificación contempla la utilización de aditivos químicos no convencionales orientados al mejoramiento de las propiedades geotécnicas de los materiales locales. Los estabilizantes considerados incluyen: i) emulsiones enzimáticas, que inducen una reducción en la plasticidad y la permeabilidad de los suelos; ii) materiales puzolánicos, que mejoran la capacidad portante mediante el incremento de la rigidez del sistema suelo-estabilizante; iii) polímeros y organosilanos, los cuales

incrementan la impermeabilidad y confieren características hidrofóbicas; iv) sales inorgánicas, empleadas como tratamiento supresor de polvo; y v) aceites sulfonados y sales orgánicas, que contribuyen al control de la expansión en suelos con potencial de hinchamiento.

Adicionalmente, en Colombia se encuentran vigentes especificaciones técnicas para la construcción de carreteras que contemplan diversas soluciones constructivas [16]. Estas incluyen: i) el uso de geotextiles tejidos o no tejidos en subrasantes blandas con altos contenidos de humedad y valores de CBR entre 1 % y 3 %, así como la incorporación de agentes estabilizantes como cal o cemento; ii) la utilización de mezclas asfálticas naturales, tales como asfaltita, mapia, gilsonita, entre otras, que pueden emplearse en la conformación de capas estructurales como subbases, bases o capas de rodadura; iii) la ejecución de capas granulares estructurales tratadas con cemento Portland o emulsiones asfálticas, con el objetivo de mejorar su capacidad mecánica y durabilidad; y iv) la aplicación de tratamientos superficiales o lechadas asfálticas para la conformación de superficies de rodadura, con el fin de brindar protección e impermeabilización a la estructura vial. Algunas investigaciones en laboratorio con materiales locales indican buen desempeño de estas tecnologías [17,18]. A nivel internacional, las tendencias emergentes en ingeniería de pavimentos se orientan hacia el desarrollo de materiales con capacidad de auto reparación, los cuales permiten prolongar la vida útil de las estructuras viales al reducir la necesidad de intervenciones frecuentes. Asimismo, se promueve el aprovechamiento de subproductos industriales en la construcción de capas de pavimento, tales como plásticos reciclados, bio-asfaltos, materiales asfálticos reciclados (RAP, por sus siglas en inglés: *Recycled Asphalt Pavement*), residuos de construcción y demolición (RCD), residuos de concreto y escorias derivadas de procesos siderúrgicos, entre otros. Paralelamente, se investiga el diseño de materiales asfálticos de alto desempeño mediante la incorporación de aditivos especiales que mejoran significativamente las propiedades mecánicas, la resistencia al envejecimiento y la durabilidad del pavimento [19].

1.4 Objetivo del estudio

En síntesis, el desarrollo de proyectos de construcción de vías terciarias es crucial para el desarrollo, crecimiento económico e integración regional. Actualmente, existen documentos técnicos que proporcionan algunas recomendaciones técnicas (alternativas, materiales, procesos constructivos, entre otros) para el diseño y construcción para estructuras de vías terciarias en Colombia. Sin embargo, la selección de la mejor alternativa depende principalmente de factores económicos. Actualmente, en la práctica de la ingeniería existe una tendencia a desarrollo y construcción de estructuras en placa huella para las vías terciarias, principalmente por la disponibilidad de materiales y la facilidad de los procesos constructivos. Por tanto, este artículo realiza un análisis detallado de las alternativas contempladas en los diversos documentos técnicos, a fin de seleccionar la alternativa a partir de un análisis multicriterio que contemplan aspectos técnicos, ambientales y económicos.

2 Metodología

La metodología adoptada en este estudio es de enfoque mixto, combinando elementos cuantitativos y cualitativos para el diseño de alternativas constructivas de un tramo de vía terciaria. Esta se estructuró en cuatro etapas principales. En la primera, se identificaron y describieron las variables fundamentales para el diseño de pavimentos en este tipo de vías, incluyendo tránsito, capacidad de soporte de la subrasante, características de los materiales y condiciones climáticas. La segunda etapa consistió en la determinación de los espesores de pavimento con base en las recomendaciones y materiales descritos en los documentos técnicos vigentes para vías terciarias, considerando pavimentos con tratamientos superficiales, flexibles, semirrígidos, rígidos y estructuras tipo placa huella. En la tercera etapa, se seleccionaron las alternativas de diseño más representativas para la condición más crítica —definida por el mayor nivel de tránsito, el clima más severo y la menor capacidad portante de la subrasante—, realizando un análisis económico para estimar los costos de construcción mediante los análisis de precios unitarios INVIAS 2025. Finalmente, la cuarta etapa comprendió un análisis multicriterio, empleando metodologías de gestión de proyectos, con el propósito de identificar la alternativa viable desde los puntos de vista técnico, ambiental y económico.

2.1 Variables de diseño de pavimentos

2.1.1 Tránsito

En relación con el tránsito, los documentos técnicos consultados presentan los siguientes criterios: i) el manual de diseño de Pavimentos flexibles INVIAS, 2007 clasifica el tránsito en dos niveles, definidos por el número de ejes equivalentes de 80 kN: T1 (<150.000) y T2 (entre 150.000 y 500.000); ii) el manual de diseño de pavimentos de concreto de INVIAS 2008 contempla una única categoría para vías terciarias, con $T_0 < 1.000.000$, definida para un tránsito promedio diario

inferior a 200 vehículos; iii) la cartilla de del programa Colombia rural establece tres categorías: N1 (<150.000), N2 (entre 150.000 y 300.000) y N3 (entre 300.000 y 500.000); iv) la cartilla de proyectos tipo para el mejoramiento de vías terciarias del DNP define un tránsito máximo de 500.000 ejes equivalentes. Finalmente, la Guía de Diseño de Pavimentos con Placa Huella de INVIAS 2015 no establece un nivel de tránsito específico, dado que los análisis estructurales se realizan considerando cargas últimas para camiones de dos y tres ejes; no obstante, recomienda su aplicación en proyectos con tránsito inferior a 500.000 ejes equivalentes.

En síntesis, las metodologías revisadas para el diseño de vías terciarias utilizan las repeticiones de carga calculadas mediante el método de ejes equivalentes de 80 kN. Para pavimentos flexibles y semirrígidos, se contempla un tránsito de hasta 500.000 ejes equivalentes en un periodo de diseño de 10 años, mientras que, para pavimentos de concreto, el límite es de 1.000.000 de ejes equivalentes en 20 años. Con base en estos criterios, en el presente estudio se definieron cuatro categorías de tránsito, conforme se presenta en la Tabla 2.

2.1.2. Subrasante

De forma general, todos los documentos técnicos indican que el valor mínimo de CBR para el diseño y construcción de estructuras de vías terciarias corresponde a 3.0%, excepto el manual de diseño de pavimentos de concreto INVIAS 2008 que contempla valor mínimo 2%. En la Tabla 3 se presentan las categorías de subrasante (S) definidas en las metodologías de diseño a partir de resultados del ensayo de CBR. A partir de lo anterior, para este estudio fueron definidas cuatro tipos de subrasante con valores de 3.0%, 5.0%, 7.0 y 10.0%

2.1.3. Condiciones climáticas

El manual de diseño de pavimentos flexibles INVIAS 2007 contempla el cálculo del índice de Thornthwaite IT a partir de índices de humedad y aridez que permiten clasificar las categorías climáticas donde se presente construir el pavimento, conforme se presenta en la Tabla 4.

Tabla 2.
Nivel de tránsito contemplados en este estudio.

Categoría	Ejes equivalentes de 80 kN	Consideraciones
NT1	150000	
NT2	300000	
NT3	500000	
NT4	1000000	Diseño de pavimentos rígidos

Fuente: Autores.

Tabla 3.
Nivel de tránsito contemplados en este estudio.

Tipo de subrasante	Pavimentos flexibles	Pavimentos rígidos	Colombia Rural
S1	≤ 3.0	< 2.0	3.0 a 5.0
S2	3.0 a 5.0	2.0 a 5.0	5.0 a 7.0
S3	5.0 a 10.0	5.0 a 10.0	7.0 a 10.0
S4	≥ 10.0	10.0 a 20.0	10.0 a 15.0
S5		> 20.0	

Fuente: Autores.

Tabla 4.
Clasificación del clima por IT.

Categoría	Descripción	IT
Árido	Muy pocas lluvias, alta evaporación	-100 a -61
Semi-árido	Pocas lluvias	-60 a -21
Subhúmedo	Lluvia moderada o lluvia fuertemente estacional	-20 a 19
Húmedo	Lluvia estacional calurosa moderada	20 a 100
Super húmedo	Lluvias con alta frecuencia o muchos días con superficie húmeda	>100

Fuente: Autores a partir de INVIAS 2007.

Tabla 5.
Clasificación de clima por temperatura.

Categoría del clima	T7 días (°C)
Frío	< 20
Templado	20 a 30
Cálido	> 30

Fuente: Autores a partir INVIAS 2007

Tabla 6.
Parámetros de temperatura y precipitación según guía de Colombia rural.

Temperatura media anual ponderada (°C)	Precipitación media anual (mm/año)	Sistema de subdrenaje
≤ 13	≤ 2000	Con/sin
13 a 20	2000 a 4000	Con/sin
20 a 30	4000 a 6000	Con/sin

Fuente: Autores.

Este valor se determina a partir de datos históricos de precipitación y temperatura. Adicionalmente, este método permite clasificar el clima por temperatura, a partir del promedio de temperatura de los siete días consecutivos más calientes del año (T7 días) conforme se presenta en la Tabla 5. La cartilla de obras menores de drenaje y estructuras viales del programa de Colombia rural INVIAS 2022 contempla la temperatura media anual ponderada y el nivel de precipitación media anual, conforme Tabla 6. Adicionalmente, contempla la alternativa del sistema de subdrenaje.

En este estudio fueron considerados tres escenarios, representando clima frío, templado y cálido con temperaturas de 10°C, 20°C y 30°C, respectivamente. Los valores de precipitación adoptados en este estudio para estos climas corresponden a 1500, 3000 y 5000 mm/año, respectivamente. Estos valores se asocian con climas áridos, húmedos y muy húmedos, los cuales pueden representar las condiciones climáticas típicas de una región fría seca, templada semihúmeda y cálida muy húmeda en regiones Colombia.

2.2 Alternativas de diseño

A partir de las variables, se procedió a realizar el cálculo de espesores de las capas del pavimento para una vía terciaria contemplando alternativas de los documentos técnicos que corresponden a: i) Pavimentos con tratamiento superficial PTS; ii) Pavimentos flexibles empleando mezclas asfálticas en caliente y en frío PF; iii) Pavimentos semirrígidos PS; iv) Pavimentos rígidos PR; v) Placa huella PH. En la Tabla 7 se presentan los materiales que componen la alternativa de diseño según cada metodología de diseño. Para todas las opciones se consideró el periodo de diseño de 10 años, excepto para la opción en pavimento de concreto que se consideró 20 años.

La determinación de los espesores para pavimentos flexibles y semirrígidos según INVIAS 2007 se realizó mediante la herramienta PAV-NT1. Este software hace parte del manual de diseño de pavimentos asfálticas para vías con bajos volúmenes de tránsito (ver Fig. 2) y contiene el algoritmo para cálculo de espesores de la metodología AASHTO 1993. En total, fueron diseñadas 180 estructuras de pavimentos con tratamientos superficiales, flexibles y semirrígidos producto de las cinco (5) alternativas contempladas en la metodología, tres (3) niveles de tránsito, cuatro (4) valores de suelo de subrasante y tres (3) consideraciones de clima. Los diseños de pavimento de concreto según el manual de diseño INVIAS 2008 y la guía de Colombia rural de INVIAS 2022 no contemplan la acción

Tabla 7.
Alternativas de diseño.

Metodología	Metodología	Alternativas									
		PTS		PF		PS		PR		PH	
Manual de diseño de pavimentos asfálticos para vías con bajos volúmenes de tránsito INVIAS 2007	AASHTO 1993	TSD	TSD	MDF	MDC	MDC	MDF				
		BG	BG	BG	BG	BG	BEE				
		SBG	BEC	SBG	SBG	BEC	SBG				
Manual de diseño de pavimentos de concreto para vías con bajos, medios y altos volúmenes de tránsito INVIAS 2008								C	C	C	
								SN	BG	BEC	
Guía de diseño de pavimentos con placa huella INVIAS 2015	Carga última										C
											SBG
Cartilla de obras menores de drenaje y estructuras viales del programa de Colombia Rural INVIAS 2020		TSD o TSA			MDC	MDC	MDC	C	C	C	C
		SCE			BG	BG	BG	SN	SBG	SEC	SBG
Cartilla de Proyectos tipo para el mejoramiento de vías terciarias INVIAS DNP 2021	AASHTO 1993	TSD o LA	TSD o LA								
		BG	BEC o BEE								

Dónde: TSD Tratamiento Superficial Doble; TSA Tratamiento Superficial Asfáltica; LA Lechada Asfáltica; MDC Mezcla Densa en Caliente; MDF Mezcla Asfáltica a Frío; BG Base Granular; BEC Base Estabilizada con Cemento; BEE Base Estabilizada con Emulsión; SCE Suelo Cemento; SCA Suelo Cal; SN suelo natura; C Concreto.

Fuente: Autores.



Figura 2. Herramienta PAV-NT1.

Fuente: INVIAS 2007 [7].

del clima (temperatura y precipitaciones). Estas metodologías tampoco se contemplan la influencia de los alabeos térmicos del concreto. Sin embargo, se observa el efecto del confinamiento de las losas, que puede ser originado por la presencia de bermas, bordillos u otro elemento. En este estudio se adoptó que la resistencia del concreto definida por el módulo de rotura (MR) concierne a 3.8 MPa, dado que puede ser fabricado en obra. Empleando la metodología INVIAS 2008 fueron diseñadas 12 estructuras correspondiente a tres (3) soportes de la losa de concreto (SN, BGC y BEC), cuatro (4) tipos de suelos de subrasante y un (1) nivel de tránsito correspondiente a 1.000.000 de ejes equivalentes de 80 kN para 20 años (Categoría N4). Para los diseños según la guía de Colombia rural, fueron diseñadas 36 estructura considerando tres (3) soportes de losa de concreto (SN, SBG y SCE), tres (3) niveles de tránsito, cuatro (4) tipos de subrasante. En ambas metodologías, los espesores fueron obtenidos de las tablas o cartas establecidos en los documentos. En total fueron diseñadas 48 estructuras de pavimento rígido.

Para el cálculo de los espesores de las estructuras de pavimento flexibles y semirrígidos contempladas en la Cartilla de obras menores de drenaje y estructuras viales del programa de Colombia Rural se analizaron tres (3) categorías del tránsito, cuatro (4) tipos de subrasante, tres (3) condiciones climáticas y cinco (5) opciones de pavimentos (flexibles y semirrígidos). En total, fueron determinas 180 estructuras. No se emplearon las recomendaciones de la cartilla de proyectos tipo para el mejoramiento de vías terciarias INVIAS DNP 2021, dado que las mismas se encuentran referidas en el manual de diseño de pavimentos flexibles INVIAS 2007.

2.3 Evaluación económica

A partir los espesores de pavimentos calculados para diferentes tipos de subrasantes, niveles se transitó, condiciones de clima y materiales, se procedió a determinar siete alternativas de diseño asumiendo las condiciones más críticas. Estas condiciones fueron establecidas a partir de la menor capacidad de la subrasante (CBR=3%), mayor nivel de tránsito y clima más riguroso. Para el caso de las estructuras de pavimentos rígidos se diseñaron considerando periodos de 10 y 20 años. Posteriormente, para cada alternativa se determinó el costo de obra por 100 ml asumiendo un ancho de calzada de 6 metros. Para la alternativa en placa huella se contempló un ancho de 5.5 metros, dado que corresponden a vías unidireccional.

Los costos fueron determinados de los análisis de precios unitarios APU disponibles por INVIAS 2025 para 138 provincias de 30 Departamentos que conforman el territorio colombiano. En este estudio no fueron considerados los APU para el Departamento del Amazonas y San Andrés, dado que los mismos difieren significativamente del promedio. Cada APU contempla costos de equipos, materiales, mano de obra y transporte. En todas las actividades de construcción, en el transporte se contempla la distancia en un tramo de 1 km desde la fuente del material al lugar de la obra. Fueron consideradas las actividades de construcción relacionadas con la construcción de capas para pavimentos de vías terciarias. Es decir, en este estudio no se consideraron actividades relacionadas con actividades de explanaciones (cortes y/o terraplenes), estructuras de contención, obras de drenaje superficial o subsuperficial, señalización y demarcación, entre otras. Lo anterior, dado que el objetivo principal fue realizar un estudio comparativo de las alternativas de estructuras de pavimentos.

2.4 Análisis multicriterio para la selección de alternativas

Dado que este tipo pavimentos tiene diferentes periodos de diseño, materiales y técnicas constructivas, se puede generar efectos que impactan en términos económicos. Por tanto, considerando las alternativas se realizó un análisis multicriterio bajo el método de selección por ventaja [20]. Esta metodología permite crear una matriz de comparación de criterios, en la cual se asignan valoraciones bajo la escala Likert. En este estudio se evaluaron aspectos técnicos (vida útil), ambientales (volumen de materiales naturales empleados y volumen de materiales reciclados) y

Tabla 8.

Definición de valoración para los criterios analizados.

Valoración	Técnico	Ambiental		Económico
	Vida útil (años)	Volumen de materiales (m ³)	Volumen de reciclaje (m ³)	Costo (US\$)
5 (muy alto)	5 a 10	> 350	<90	>22000
4 (alto)	10 a 15	275-300	90-150	18000-22000
3 (moderado)	10 a 15	200-275	150-250	14000-18000
2 (moderado-bajo)	15 a 20	100-200	250-350	10000-14000
1 (bajo)	>20	<100	>350	<10000

Fuente: Autores.

económicos (costo de construcción). Como resultado se obtiene la sumatoria de importancia de los aspectos evaluados. El método de selección por ventaja permite hacer una evaluación cualitativa y cuantitativa objetiva con alto grado de certeza, debido a que se consideran los criterios relevantes y se analizan de forma sistemática [21]. En la Tabla 8 se presentan la valoración para cada uno de los criterios analizados.

3 Resultados

3.1 Pavimentos con tratamientos superficiales

En la Tabla 9 se presenta los espesores en centímetros de las capas de los pavimentos que contemplan el uso de tratamientos superficiales TSD. En todos los casos, el espesor del tratamiento superficial corresponde a 3.0 cm y no genera aporte estructural al pavimento. La cartilla Colombia rural propone el uso de una capa estructural compuesta por SCE con un espesor comprendido entre 25 y 30 cm. Esta técnica no es aplicable a suelos con baja capacidad de soporte (CBR del 3%) en condiciones de tránsito N2 y N3. Para suelos con mayor capacidad (CBR del 7% al 10%) y bajo nivel de tránsito (N1), se recomienda un espesor de 25 cm, mientras que para los demás casos se sugiere un espesor de 30 cm. Por su parte, el manual de diseño de pavimentos flexibles INVIAS (2008) contempla estructuras conformadas por dos capas: base granular (BG) y subbase granular (SBG). Una de las alternativas incluye el tratamiento de la subbase con cemento, denominándose en este caso como BEC. Para esta configuración, se recomienda un espesor de 20 cm sobre suelos con CBR del 5% y 7%, independientemente del nivel de tránsito y del clima. El espesor de la capa BG en esta opción varía entre 15 y 30 cm, dependiendo de las condiciones de subrasante y tránsito. En una segunda opción, se considera una capa de BG de 20 cm, apoyada sobre una

subbase granular con espesor variable entre 17 y 52 cm. En este caso, los mayores espesores de la BG se asocian con niveles de tránsito elevados, suelos de menor CBR y climas cálidos.

3.2 Pavimentos flexible

En las Tablas 10 y 11 se presentan los espesores en centímetros de las capas de pavimentos flexibles con MDC y MDF, respectivamente. En términos generales, ambas metodologías generan espesores similares para la capa asfáltica, con valores que oscilan entre 7.5 cm y 11 cm. Estas variaciones se atribuyen principalmente a las condiciones climáticas y al nivel de tránsito. En particular, se requieren mayores espesores en escenarios con tránsito tipo N3 y clima cálido, debido a la mayor susceptibilidad de la mezcla asfáltica a la deformación bajo cargas elevadas y temperaturas altas. Esta tendencia es consistente, dado que ambas metodologías se basan en los lineamientos del diseño AASHTO 1993. Con respecto a los materiales granulares (BG + SBG), la cartilla de Colombia rural contempla espesores variables por capa, entre 15 cm y 30 cm, mientras que el manual de diseño de pavimentos Flexibles del INVIAS (2008) establece espesores constantes de 15 cm, con excepción de los casos en los que la subrasante presenta un CBR del 3% y niveles de tránsito N2 o N3. Además, la cartilla de Colombia rural propone una alternativa consistente en una única capa granular de BG con espesores entre 15 cm y 30 cm, lo cual permite una reducción en la cantidad total de materiales empleados. En el caso de los pavimentos con MDF, se recomiendan espesores para la capa de rodadura que oscilan entre 8 cm y 12 cm, en función del nivel de tránsito y las condiciones climáticas. Independientemente del escenario evaluado, las estructuras incluyen capas granulares BG y SBG con espesores constantes de 15 cm cada una.

Tabla 9.
Espesores de pavimentos con tratamientos superficiales.

		SCE (INVIAS 2020)								
Tránsito	Capa	N1	N2	N3	N1	N2	N3	N1	N2	N3
			Frio			Templado			Cálido	
3.0	SCE	30	NA	NA	30	NA	NA	30	NA	NA
5.0	SCE	30	30	30	30	30	30	30	30	30
7.0	SCE	25	30	30	25	30	30	25	30	30
10.0	SCE	25	30	30	25	30	30	25	30	30
		BG + BEC (INVIAS 2008)								
5.0	BG	17.3	21.7	25.2	18.2	22.8	26.5	20.4	25.5	29.7
	BEC	20	20	20	20	20	20	20	20	20
7.0	BG	15.1	19.3	22.6	15.9	20.3	23.8	17.7	22.7	26.6
	BEC	20	20	20	20	20	20	20	20	20
		BG + SBG (INVIAS 2008)								
3.0	BG	20	20	20	20	20	20	20	20	20
	SBG	29.9	35.9	40.7	32.7	39	44.1	39.2	46.3	52
5.0	BG	20	20	20	20	20	20	20	20	20
	SBG	23.8	29.3	33.7	26.3	32.1	36.7	32.2	38.6	43.7
7.0	BG	20	20	20	20	20	20	20	20	20
	SBG	20.2	25.3	29.4	22.5	27.9	32.2	27.9	33.9	38.7
10.0	BG	20	20	20	20	20	20	20	20	20
	SBG	17	22,5	26.4	19.7	24.9	29	24.8	30.6	35.2

Fuente: Autores.

Tabla 10.

Espesores de pavimentos flexibles con MDC.

MDC+BG+SBG (INVIAS 2020)										
CBR (%)	Capa	Frio			Templado			Cálido		
		N1	N2	N3	N1	N2	N3	N1	N2	N3
3.0	MDC	8	9	10	9	10	10	10	N/A	N/A
	BG	15	15	15	15	20	25	30	N/A	N/A
	SBG	20	20	25	25	25	25	30	N/A	N/A
5.0	MDC	8	9	10	9	10	10	10	10	10
	BG	20	25	25	25	30	15	15	25	30
	SBG						25	25	25	30
7.0	MDC	8	9	10	9	10	10	10	10	10
	BG	15	15	15	20	20	25	15	20	25
	SBG							15	25	30
10.0	MDC	8	9	10	9	10	10	10	10	10
	BG	15	15	15	20	20	25	15	20	20
	SBG							15	20	25
MDC+BG (INVIAS 2020)										
3.0	MDC	8	9	10	N/A	N/A	N/A	N/A	N/A	N/A
	BG	30	30	30	N/A	N/A	N/A	N/A	N/A	N/A
5.0	MDC	8	9	10	9	10	10	N/A	N/A	N/A
	BG	20	25	25	25	30	30	N/A	N/A	N/A
7.0	MDC	8	9	10	9	10	10	10	N/A	N/A
	BG	20	20	20	20	25	30	30	N/A	N/A
10.0	MDC	8	9	10	9	10	10	10	N/A	N/A
	BG	15	15	15	20	20	25	30	N/A	N/A
MDC+BG+SBG (INVIAS 2008)										
3.0	MDC	7.5	8.2	9	7.7	8.8	9.7	8.6	9.8	10.7
	BG	15	15	15	15	15	15	15	15	15
	SBG	15	15	15	15	15	15	15	16.6	19
5.0	MDC	7.5	8.2	9	7.7	8.8	9.7	8.6	9.8	10.7
	BG	15	15	15	15	15	15	15	15	15
	SBG	15	15	15	15	15	15	15	15	15
7.0	MDC	7.5	8.2	9	7.7	8.8	9.7	8.6	9.8	10.7
	BG	15	15	15	15	15	15	15	15	15
	SBG	15	15	15	15	15	15	15	15	15
10.0	MDC	7.5	8.2	9	7.7	8.8	9.7	8.6	9.8	10.7
	BG	15	15	15	15	15	15	15	15	15
	SBG	15	15	15	15	15	15	15	15	15

Fuente: Autores.

Tabla 11.

Espesores de pavimentos flexibles con MDF.

CBR (%)	Capa	Frio			Templado			Cálido		
		N1	N2	N3	N1	N2	N3	N1	N2	N3
3.0	MDF	7.9	9	9.9	8.6	9.8	10.7	9.3	10.6	11.7
	BG	15	15	15	15	15	15	15	15	15
	SBG	15	15	15	15	15	15	15	15	15
5.0	MDF	7.9	9	9.9	8.6	9.8	10.7	9.3	10.6	11.7
	BG	15	15	15	15	15	15	15	15	15
	SBG	15	15	15	15	15	15	15	15	15
7.0	MDF	7.9	9	9.9	8.6	9.8	10.7	9.3	10.6	11.7
	BG	15	15	15	15	15	15	15	15	15
	SBG	15	15	15	15	15	15	15	15	15
10.0	MDF	7.9	9	9.9	8.6	9.8	10.7	9.3	10.6	11.7
	BG	15	15	15	15	15	15	15	15	15
	SBG	15	15	15	15	15	15	15	15	15

Fuente: Autores.

3.3 Pavimento semirrígidos

En la Tabla 12 se presentan los espesores en centímetros de las capas que conforman los pavimentos semirrígidos. El manual de diseño de pavimentos flexibles INVIAS 2008 considera estructuras compuestas de MDC, BG y BEC. Los

espesores de la capa de rodadura oscilan entre 7.5 cm a 10.7 cm y depende del nivel del tránsito y clima. Los espesores de las capas granulares son constantes y corresponden a 15 cm y 20 cm de BG y BEC, respectivamente. Se evidencia que los espesores no cambian por el tipo de CBR. Por su parte, la guía de Colombia rural plantea dos opciones. La primera

Tabla 12.
Espesores de pavimentos semirrígidos.

Espesores de pavimentos semirrigidos.

CBR (%)	Capa	Frio			Templado			Cálido		
		N1	N2	N3	N1	N2	N3	N1	N2	N3
MDC+BG+BEC (INVIAS 2008)										
3.0	MDC	7.5	8.2	9	7.7	8.8	9.7	8.6	9.8	10.7
	BG	15	15	15	15	15	15	15	15	15
	BEC	20	20	20	20	20	20	20	20	20
5.0	MDC	7.5	8.2	9	7.7	8.8	9.7	8.6	9.8	10.7
	BG	15	15	15	15	15	15	15	15	15
	BEC	20	20	20	20	20	20	20	20	20
7.0	MDC	7.5	8.2	9	7.7	8.8	9.7	8.6	9.8	10.7
	BG	15	15	15	15	15	15	15	15	15
	BEC	20	20	20	20	20	20	20	20	20
10.0	MDC	7.5	8.2	9	7.7	8.8	9.7	8.6	9.8	10.7
	BG	15	15	15	15	15	15	15	15	15
	BEC	20	20	20	20	20	20	20	20	20
MDC+SEC (INVIAS 2020)										
3.0	MDC	6	8	8	6	8	8	6	8	8
	SCE	20	20	25	25	25	30	25	30	30
5.0	MDC	6	8	8	6	8	8	6	8	8
	SCE	15	15	20	20	20	20	20	20	25
7.0	MDC	6	8	8	6	8	8	6	8	8
	SCE	15	15	15	15	15	20	20	20	20
10.0	MDC	6	8	8	6	8	8	6	8	8
	SCE	15	15	15	15	15	15	15	20	20
MDC+BG+SCA (INVIAS 2020)										
3.0	MDC	8	8	9	9	9	10	10	10	N/A
	BG	20	20	20	20	20	25	30	30	N/A
	SCA	20	20	20	20	20	25	20	20	N/A
5.0	MDC	8	9	9	9	10	10	10	N/A	N/A
	BG	20	20	20	20	25	25	30	N/A	N/A
	SCA	20	20	20	20	20	20	20	N/A	N/A

Fuente: Autores.

opción contempla una capa estructural de SCE, con espesores que varían entre 15 cm a 30 cm. Los mayores espesores están asociado a mayores niveles de tránsito y menor capacidad de resistencia de la subrasante. La segunda opción considera dos capas granulares BG y SAC. El espesor de BG oscila entre 20 a 30 cm, mientras que el espesor de SAC es constante y corresponde a 20 cm, excepto para pavimento con CBR 3%, clima templado y nivel de tránsito N3, en el cual se recomienda 25 cm. Sin embargo, esta opción es válida para suelos con CBR 3% y 5%. En todas las dos configuraciones se incluye una capa MDC como superficie de rodadura.

3.4 Pavimento rígido

En la Tabla 13 se presentan los resultados de espesores en centímetros de losa de para pavimentos rígidos, considerando que se soporta directamente en la subrasante (suelo natural SN), 15 cm SBG o 15 cm SEC.

Espesores obtenidos según el manual de pavimentos de concreto INVIAS 2008 oscilan entre 18 cm a 23 cm y son mayores debido al periodo de diseño de 20 año. Por su parte, los espesores obtenidos según la guía de Colombia rural oscilan entre 16 cm a 21 cm. De forma general, el espesor de la losa depende de la capacidad de la subrasante, nivel de tránsito y material de apoyo de la losa. Es decir, el espesor aumenta con el nivel de tránsito y con el aumento del CBR.

Tabla 13.
Espesores de losa para pavimento rígido.

CBR (%)	INVIAS 2020									INVIAS 2008		
	SN			SBG			SEC			SN	SBG	SEC
	N1	N2	N3	N1	N2	N3	N1	N2	N3	N4	N4	N4
3.0	21	20	21	20	20	21	18	17	18	23	22	19
5.0	19	20	20	19	20	20	17	17	18	21	21	18
7.0	19	20	20	19	19	20	16	17	17	21	21	18
10.0	19	19	20	18	19	19	16	16	17	19	18	18

Fuente: Autores.

3.5 Placa huella

Guía de diseño de pavimentos con placa huella INVIAS 2015 contempla una única estructura compuesta por huellas de espesor de 15 cm reforzadas longitudinalmente con barras #4 cada 15 cm y transversalmente con barras #2 cada 30 cm. La guía de Colombia rural considera opciones de placa huella para la circulación de vehículos livianos y comerciales (buses y camiones). En la primera opción, considera un espesor de 15 cm con barras #3 longitudinales y transversales cada 20 cm. La segunda opción considera espesores de 15 cm y 20 cm con barras #4 longitudinales y transversales cada 15 cm y 20 cm, respectivamente.

3.6 Alternativas de diseño

De acuerdo con lo descrito en la metodología, en esta sección se presentan las alternativas de diseño desarrolladas para las condiciones más críticas, correspondientes a una subrasante con CBR del 3 % y el mayor nivel de tránsito proyectado. Se evaluaron diferentes tipologías estructurales, incluyendo pavimentos con tratamientos superficiales (PTS), pavimentos flexibles contruidos con mezclas asfálticas en caliente (PF-1) y en frío (PF-2), pavimentos semirrígidos conformados por estructuras de dos (PS-1) y tres capas (PS-2), pavimentos rígidos diseñados para periodos de servicio de 10 (PR-1) y 20 años (PR-2), así como estructuras tipo placa huella con espesores de 15 cm (PH-1) y 20 cm (PH-2). En la Fig. 3 se presenta el resumen de las alternativas.

3.7 Evaluación económica y análisis multicriterio de las alternativas de diseño

En la Fig. 4 se presentan los resultados de la evaluación de económica referente a los costos de construcción por 100 metros y el análisis multicriterio de las alternativas. De forma general, considerando los valores promedios, se puede evidenciar que las alternativas de pavimentos con tratamientos superficiales, flexibles y semirrígidos presentan costos similares. Las alternativas en concreto exhiben mayores costos de construcción, debido a los costos del concreto y acero de refuerzo para el caso de las alternativas en placa huella, a pesar de que el ancho se limitó a 5.5 metros. En todos los casos, la alternativa en pavimento de concreto diseñada a 20 años exhibió el mayor costo. Por tanto, desde el punto de vista económico la alternativa PS-2 (semirrígido compuesto de 8 cm de MDC y 30 cm de SCE) resulta en la mejor alternativa. Este resultado es coherente con el obtenido en el análisis multicriterio que involucra aspectos técnicos, y ambientales. Por otro lado, las estructuras de pavimentos rígidos y en placa huella presentan menores valores de la sumatoria de importancia, debido principalmente a los altos costos de construcción y baja capacidad de reciclaje de los materiales.

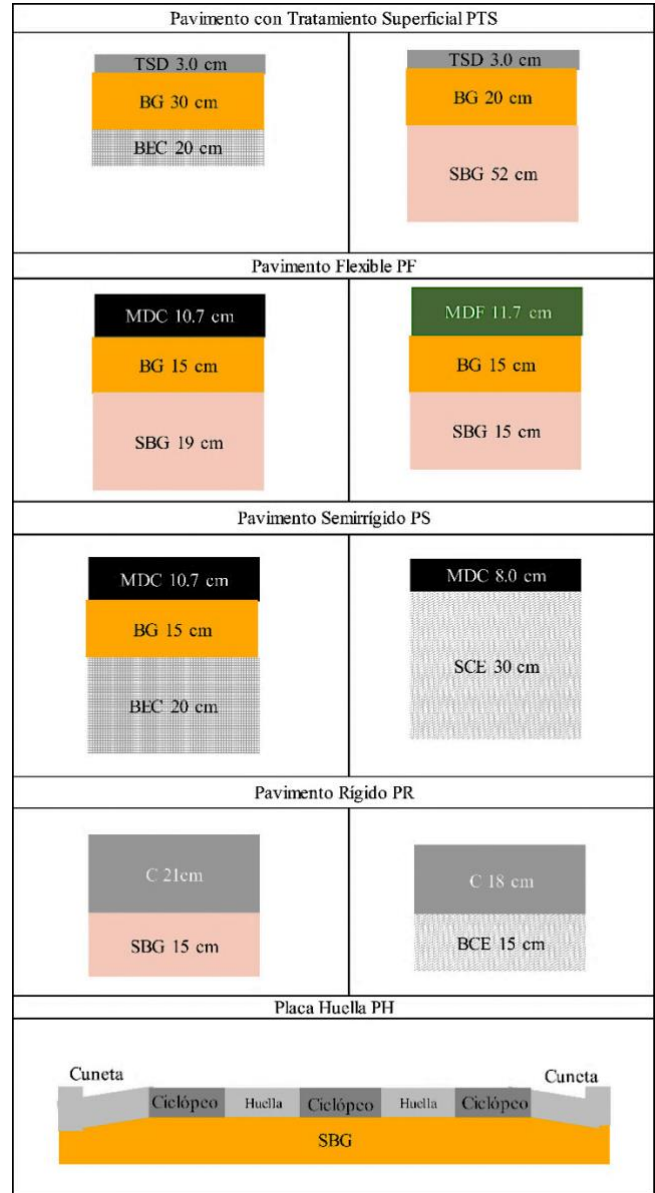


Figura 3. Alternativas de diseño.
Fuente: Autores.

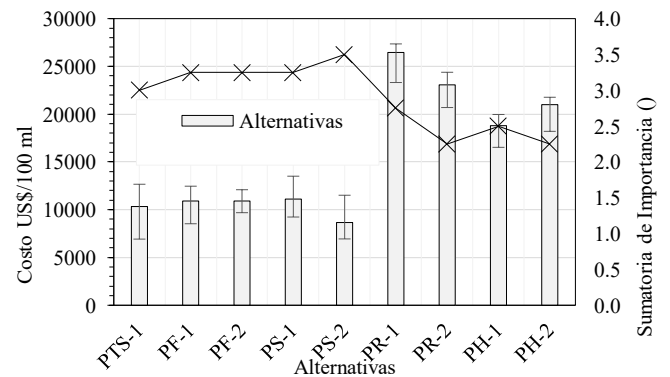


Figura 4. Alternativas de diseño.
Fuente: Autores.

4 Discusión de resultados

El análisis técnico de las alternativas para la construcción de vías terciarias desarrollado en este estudio consideró las condiciones críticas de subrasante, tránsito y clima, permitiendo identificar diferencias significativas en desempeño y viabilidad económica. A partir de este estudio, se aplicó un análisis multicriterio que integró aspectos técnicos, ambientales y económicos. Los resultados permiten concluir que el pavimento semirrígido es la opción más viable frente a otras alternativas evaluadas (flexibles, rígidos, placa huella, entre otros). Este resultado se fundamenta en la capacidad del pavimento semirrígido para ofrecer un balance óptimo entre durabilidad, resistencia y costo, especialmente en contextos rurales con bajo volumen de tránsito. No obstante, dado que el análisis se restringió a vías terciarias, futuros trabajos podrían enfocarse en la caracterización detallada de materiales locales, evaluación de cargas del tránsito reales con diversas condiciones climáticas actuales y análisis de ciclo de vida. Asimismo, sería pertinente ampliar la línea de investigación a nuevas tecnologías y procesos constructivos que apunten a recomendaciones técnicas para el mejoramiento de vías terciarias.

5 Conclusiones

El objetivo de este estudio fue realizar un análisis detallado de las alternativas contempladas en los actuales documentos técnicos para la construcción de vías terciarias. A partir de las condiciones críticas referentes a la subrasante, tránsito y clima. Se realizó un análisis multicriterio para seleccionar la mejor alternativa. A partir de los resultados se puede concluir:

- La alternativa de pavimento semirrígido exhibe mayor importancia en el análisis multicriterio. Es decir, tiene mayor viabilidad en referencia a los aspectos técnicos, ambientales y económicos ante las otras alternativas. Sin embargo, es necesario analizar las condiciones locales referente a la obtención de materiales, diseño del material granular tratado con cemento, mano de obra, equipos, costos de construcción, entre otros. Asimismo, condiciones sociales, principalmente los aspectos de movilidad del tramo vial durante la etapa constructiva.
- Este estudio analizó las alternativas para la construcción de vías terciarias según los lineamientos técnicos en Colombia. En este estudio no fueron incluidas vías de otros sectores, tales como explotaciones mineras a cielo abierto, parques solares, entre otros, los cuales requieren circulación de vehículos extrapesado o extra dimensionados.

Futuras investigaciones que apunten al fortalecimiento de las vías terciarias deben enfocarse al estudio y caracterización de materiales locales, tales como subrasantes, materiales granulares, aditivos, polímeros, entre otros, a fin de proporcionar valores de rigidez considerando la acción de carga del tránsito y las condiciones climáticas.

Referencias

- [1] Hafez, M., Ksaibati, M., and Atadero, R. Pavement maintenance practices of low-volume roads and potential enhancement: the regional experience of Colorado pavement management system, *International Journal of Pavement Engineering*, 22 (6), pp. 718–731, 2021. DOI: <https://doi.org/10.1080/10298436.2019.1643021>
- [2] Hauser, J., Ševelová, L., Matula, R., and Zedník, P. Optimization of low volume road pavement design and construction, *Journal of forest science*, 64 (2), pp. 74–85, 2018. DOI: <https://doi.org/10.17221/109/2017-JFS>
- [3] Ministerio de Transporte de Colombia. Anuario Nacional de Transporte [Online], Bogotá, Colombia, 2020. [Consultado Agosto 19, 2024]. Disponible en: <http://www.mintransporte.gov.co>
- [4] INVIAS Instituto Nacional de Vías, Estado de la red vial. [Online], Bogotá, Colombia, 2020. [Consultado Agosto 19, 2024]. Disponible en: <https://www.invias.gov.co/index.php/informacion-institucional/2-principal/57-estado-de-la-red-vial>
- [5] Ospina-Ovalle, G. El papel de las vías secundarias y los caminos vecinales en el desarrollo de Colombia, *Revista de Ingeniería*, 1(44), pp. 20–27, 2016. DOI: <https://doi.org/10.16924/revinge.44.3>
- [6] Cea, S., and Espinosa, S.I., El acuerdo de paz y las vías terciarias en Colombia, *Bitacora Urbano Territorial*, 32(1), pp. 149–160, 2022. DOI: <https://doi.org/10.15446/bitacora.v32n1.98480>
- [7] INVIAS, Manual de diseño de pavimentos asfálticos para vías con bajos volúmenes de tránsito, INVIAS, 2007, 103 P.
- [8] AASHTO, Guide for design of pavements structures, AASHTO, 1993, 624 P.
- [9] INVIAS, Manual de diseño de pavimentos de concreto para vías de bajos, medios y altos volúmenes de tránsito, INVIAS 2008, 114 P.
- [10] INVIAS, Guía de diseño de pavimentos con placa huella, INVIAS, 2015, 244 P.
- [11] Orobio, A., and Orobio, J.C. Pavimentos con placa-huella de concreto simple: Análisis con elementos finitos 3D, *Revista DYNA*, 83(199), pp. 9–18, 2016. DOI: <https://doi.org/10.15446/dyna.v83n199.55350>
- [12] Orobio, A., Orobio, J.C. and Mosquera, J.M., Recomendaciones de diseño y construcción de pavimento en placa-huella de concreto reforzado, *Revista ingenierías Universidad de Medellín*, 17(32), pp. 69–83, 2018. DOI: <https://doi.org/10.22395/riurum.v17n32a4>
- [13] INVIAS, Cartilla de obras menores de drenaje y estructuras viales, INVIAS, 2020, 180P.
- [14] DNP, Mejoramiento de vías terciarias vías de tercer orden, versión 3.0, DNP, 2021, 74 P.
- [15] INVIAS, Artículo 237 Estabilización de suelos con productos químicos no tradiciones, INVIAS 2022.
- [16] INVIAS, Especificaciones Generales para Construcción de Carreteras, INVIAS, 2022, 1345 P.
- [17] Bastidas-Martínez, J. G., Ruge, J.C., and Herrera-Cano, C.H., Mechanical performance of an asphalt stabilized base with natural asphalt, hydrated lime and Portland cement. *Construction Buildings Materials*, 446, pp. 137938, 2024. DOI: <https://doi.org/10.1016/j.conbuildmat.2024.137938>
- [18] Bastidas-Martínez, J.G., Herrera-Cano, C.E., and Bautista-Tapias, H.J. Performance of an unpaved roads reinforced with geogrid: construction of a physical model in laboratory and numerical validation, *Revista DYNA* 91(231), pp. 153–162, 2024. DOI: <https://doi.org/10.15446/dyna.v91n231.112274>
- [19] Cavalli, M.C., et al. Review of advanced road materials, structures, equipment, and detection technologies, *Journal of roads engineering*, 4(3), pp. 360–468, 2023. DOI: <https://doi.org/10.1016/j.jreng.2023.12.001>
- [20] Miranda-Quñones, S., Herrera, R.F., Atencio, E., Muñoz-La Rivera, F., and Arroyo, P., An update of the choosing by advantages (CBA) method from a probabilistic perspective: The selection of a heating system in a residential building, *Ain Shams Engineering Journal*, 15(10), pp. 102977, 2024. DOI: <https://doi.org/10.1016/j.asej.2024.102977>
- [21] Nnaji, C., Lee, H. W., Karakhan, A., and Gambatese, J., Developing a Decision-Making Framework to Select Safety Technologies for Highway Construction, *Journal of Construction Engineering and*

Management, 144(4), pp. 04018016, 2018. DOI: [https://doi.org/10.1061/\(ASCE\)CO.1943-7862.0001466](https://doi.org/10.1061/(ASCE)CO.1943-7862.0001466)

Z.A. Palomeque Sánchez, Ingeniera Civil de la Universidad Católica de Colombia. MBA y Especialista en Sistemas Integrados de Gestión Calidad, Seguridad y Medio Ambiente de la Universidad Viña del Mar en Chile, actualmente Docente de la Universidad Militar Nueva Granada-Programa de Ingeniería Civil y Líder de Semillero de Investigación PCGG-360
ORCID: 0000-0002-2403-6230.

J.G. Bastidas-Martínez, Ingeniero Civil de la Universidad del Cauca Colombia. MSc. en Geotecnia y PhD. en Geotécnica de la Universidad de Brasilia, Brasil. Profesor de la Pavimentos en cursos de pregrado y posgrado. Premio Nacional de Ingeniería Diodoro Sánchez otorgado por la Sociedad Colombiana de Ingenieros en 2021.
ORCID: 0000-0002-6818-0322.

J.A. Rincón-Esteva, Ingeniera Civil de la Universidad Militar Nueva Granada Colombia. MSc. en Ingeniería Civil con énfasis en Infraestructura Vial de la Pontificia Universidad Javeriana. Actualmente se desempeña como Especialista Infraestructural para el desarrollo y construcción de proyectos de parques solares en Colombia y Centroamérica del grupo Enel.
ORCID: 0009-0004-5519-9050.

Dam break analysis in Andean mountainous areas using numerical simulation in Iber

Paulina Elizabeth Suárez-Naranjo, Patricio Rubén Ortega-Lara & Patricia Lorena Haro-Ruiz

Departamento de Ingeniería Civil y Ambiental, Escuela Politécnica Nacional, Quito, Ecuador. paulina.suarez@epn.edu.ec, patricio.ortega@epn.edu.ec, patricia.haro@epn.edu.ec

Received: February 24th, 2025. Received in revised form: September 8th, 2025. Accepted: September 15th, 2025.

Abstract

Currently, dams are subject to new requests such as overtopping or dam break. In Andean cities above 2800 meters above sea level the topographic, hydrological and geological conditions differ from those in flatter regions. This study proposes the numerical simulation in the Iber software of a dam break situated in the central Andes of Ecuador. The passage of the flood wave downstream of the dam will be analyzed to identify potential impact zones in the urban area and civil infrastructure, considering clear water and clear water with sediment transport. Additionally, a hazard and impact assessment will be conducted using two international codes: the Spanish code RD9/2008 and the code from the U.S. Federal Emergency Management Agency (FEMA). The results obtained show a similarity with other studies regarding the breach hydrograph with and without sediments; Furthermore, the impact zones and the differences in the analyzed hazard codes can be observed.

Keywords: Iber; dam break; sediment transport; RD9/2008; FEMA.

Análisis de rotura de presas en zonas montañosas Andinas mediante simulación numérica en Iber

Resumen

Actualmente las presas están sujetas a nuevos escenarios como el sobrevvertido por coronación o la rotura de la presa. En ciudades andinas que se encuentran por encima de los 2800 m.s.n.m. las condiciones topográficas, hidrológicas y geológicas son diferentes con otras regiones más planas. Este estudio plantea la simulación numérica en el software Iber de la rotura de una presa implantada en los andes centrales del Ecuador. Se analizará el tránsito de esta crecida hacia aguas abajo de la presa, a fin de identificar posibles zonas de afectación a la zona urbana e infraestructura civil considerando agua clara y agua clara con transporte de sedimentos. Además, se realizará un análisis de peligrosidad y grado de afectación utilizando dos códigos internacionales, los cuales son: el código español RD9/2008 y el código de la Agencia Federal para el manejo de Emergencias norteamericano FEMA. Los resultados obtenidos muestran similitud con otros estudios en cuanto al hidrograma de rotura con y sin sedimentos; adicionalmente se puede evidenciar las zonas de afectación y las diferencias de los códigos de peligrosidad analizados.

Palabras clave: Iber; rotura de presa; transporte de sedimentos; RD9/2008; FEMA.

1 Introducción

Las presas son fundamentales para el desarrollo de la sociedad, siendo estructuras de gran importancia para el abastecimiento de agua potable, sistemas de irrigación, control de inundaciones, generación hidroeléctrica y recreación. En este sentido, un correcto funcionamiento de la

presa durante toda su vida útil es fundamental para garantizar el acceso al agua para diversos propósitos, lo cual está en concordancia con los Objetivos de Desarrollo Sostenible (ODS) planteados por los estados miembros de las Naciones Unidas. Las regulaciones y reglamentaciones actuales para el diseño, construcción y operación de las presas han sufrido cambios, adecuándose a las condiciones hidrológicas

actuales. Estos escenarios al ser más exigentes también han ocasionado una re-evaluación de la capacidad de descarga de aliviaderos y órganos de desagüe de presas ya construidas [1,2]. En España, las Normas Técnicas de Seguridad de grandes presas y embalses (NTS, aprobadas el 14 de abril del 2021 mediante Real Decreto 264/2021, BOE-A-2021-5867) establecen exigencias de seguridad mínimas que deben cumplir las presas actualmente.

Fenómenos como el sobrevvertido por coronación en una presa [3-5] o la rotura de presas considerando aterramiento [6] son fenómenos que deben ser considerados actualmente durante las fases de diseño o de evaluación de una presa existente. Estudios realizados en los últimos cinco años [6-8] proponen metodologías para el análisis de la rotura de una presa y balsas mediante el empleo de modelación numérica. Uno de estos estudios propone una metodología nueva para el análisis de rotura de presas mediante simulación numérica unidimensional y bidimensional, demostrando que existe notables diferencias entre analizar la rotura de una presa considerando el tránsito de un evento hidrológico y el de considerar también el aterramiento del material y la dinámica del sedimento aguas abajo del embalse.

Otros estudios de inundabilidad han analizado la influencia de las Zonas de Inundación Peligrosa y de la Vía de Intenso Desagüe en la delimitación de la Zona de Flujo Preferente [9]. En un contexto acorde a las nuevas tecnologías, estudios actuales proponen el empleo de técnicas de supercomputación y machine learning junto con un nuevo modelo de transporte de sedimentos para la calibración de un modelo numérico bidimensional en un embalse [10].

En el caso específico de Ecuador, este país posee condiciones hidrometeorológicas, topográficas y sísmicas diferentes dada su posición geográfica. Actualmente, se están construyendo presas de materiales sueltos en zonas montañosas andinas con cotas por encima de los 3800 m.s.n.m., y es necesario profundizar en el análisis de fenómenos como una eventual e hipotética rotura de presa o el desbordamiento del nivel del embalse por coronación. De los estudios analizados sobre rotura de presas muy pocos consideran el aterramiento de material en el embalse, el transporte de material de fondo, y su influencia en el hidrograma durante la rotura.

En 1993, en la zona sur del Ecuador, específicamente en el cantón Paute, sector La Josefina (Figs 1 y 2), se produjo un aluvión de tierra (por fallas geológicas) sobre el cauce natural del río Cuenca que obstruyó la unión de los ríos Paute y Jadán. Este aluvión generó un dique artificial de tierra que almacenó 200 millones de metros cúbicos de agua. La rotura y el posterior tránsito de esa crecida extraordinaria, ocasionó la muerte y desaparición de aproximadamente 150 personas, 7,000 personas damnificadas, múltiples daños a zonas pobladas y cultivos; y pérdida de animales de granja [11].

Estudios previos de roturas de presas en Ecuador [12-15] han simulado numéricamente la rotura de una presa, considerando agua clara sin transporte de sedimentos. Herbozo et al. [16] realizó un análisis asociado a fenómenos hidrológicos extremos (producto del cambio climático) y su afectación en el diseño de la presa Sube y Baja (Santa Elena, Ecuador), donde fue necesario definir técnicas de adaptación dentro del marco de gestión del riesgo.



Figura 1. Desfogue del río Cuenca por rotura del dique artificial
Fuente: Barreto et al. [17]



Figura 2. Posterior inundación sector la Josefina, Cuenca, Ecuador (29/03/1993)
Fuente: iagua [18].

En este contexto, el objetivo del presente trabajo es realizar la simulación numérica 2D de la rotura de una presa ubicada en una zona montañosa andina y analizar su propagación aguas abajo de la misma. Además, se analizará las zonas de peligrosidad empleando dos códigos internacionales: el código español RD9/2008 y el código de la Agencia Federal para el manejo de Emergencias norteamericano FEMA. Finalmente, se considerará el transporte de sedimentos de fondo a lo largo de toda la zona de estudio y su efecto en este tipo de cuencas montañosas. Estos estudios, buscan ser un complemento a las fases de diseño y una herramienta útil para la gestión del riesgo y la planificación territorial ordenada.

2 Materiales y métodos

2.1 Zona de estudio

El caso de estudio está ubicado en la zona montañosa central de los Andes en Ecuador (Figs 3 y 4), específicamente en la provincia de Tungurahua. La presa está rodeada por las estribaciones montañosas del volcán Carihuayrazo (5018 m.s.n.m.) sobre una depreciación topográfica denominada Chiquicahua (N 9850154.96; E 748919.21; UTM, 17S). Esta presa actualmente se encuentra en fase de construcción.

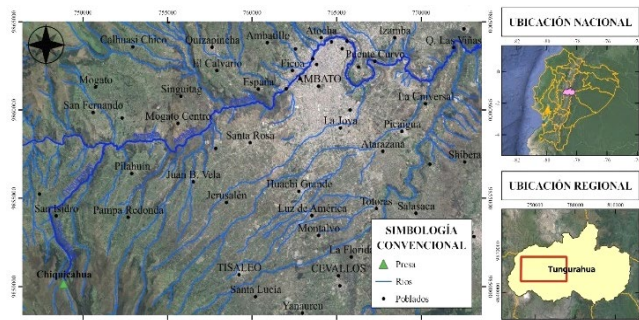


Figura 3. Ubicación de la presa y de la zona de estudio
Fuente: Elaboración propia



Figura 4. Sitio de implantación de la presa
Fuente: Banco de Desarrollo del Ecuador [20].

La presa de materiales sueltos cuenta con un núcleo de hormigón asfáltico o bituminoso, compuesto por un agregado de asfalto y minerales mezclados (Fig. 5). La altura total de la presa es de 39.0 m medidos desde la cota 3751.0 m.s.n.m. hasta la cota de coronación de la presa. El nivel máximo de operación de la presa se encuentra en la cota 3788.0 m.s.n.m., y el volumen del embalse útil es de 3.1 hm³ [19]. El propósito de la presa es abastecer de agua potable y riego a varias zonas aledañas.

La ciudad de Ambato es un núcleo urbano consolidado y de gran importancia empresarial. La cota promedio de la ciudad es 2580 m.s.n.m., posee 165 185 habitantes y se ubica a 22 kilómetros de la presa. El lugar de implantación de la



Figura 5. Visualización 3D de la presa y el embalse del proyecto
Fuente: Honorable Gobierno Provincial de Tungurahua [21].

presa corresponde a páramos de montaña que son extremadamente sensibles al acumular agua y regular los flujos hídricos. Estos medios se forman por los bosques andinos a alturas mayores de 3750 m.s.n.m., su clima es frío a lo largo de todo el año y poseen suelos de origen volcánico. Según la Secretaría Nacional de Gestión de Riesgo de Ecuador, Ambato es una de las ciudades que se encuentra en una zona con gran riesgo sísmico y presencia de fallas geológicas activas, donde han ocurrido fuertes terremotos, como el acaecido el 5 de agosto 1949.

2.2 Información base y flujo de trabajo

La información base para el estudio, ha sido obtenida de los organismos gubernamentales del Ecuador; la misma ha sido analizada, tabulada y depurada para disponer de una información confiable; y se detalla a continuación:

- Cartografía a escala 1:50.000 y 1:25.000, perteneciente al Instituto Geográfico Militar (IGM).
- Modelo Digital del Terreno (MDT) de 3 x 3 m de resolución por píxel proporcionado por SIG Tierras del Ministerio de Agricultura de Ecuador.
- Registros meteorológicos de las cuencas adyacentes a la zona del estudio. Esta información fue obtenida a través del Honorable Gobierno Provincial de Tungurahua (HGPT) y el Instituto Nacional de Meteorología e Hidrología (INAMHI).
- Estudios técnicos a nivel de diseño definitivo del proyecto facilitados por parte del HGPT.

La Fig. 6 indica el flujograma de trabajo de las actividades realizadas en el presente estudio, para llevar a cabo las simulaciones numéricas en el programa Iber V2.6

2.3 Modelación numérica

Para el análisis de la rotura de la presa se utilizó el modelo numérico bidimensional Iber V2.6 [22,23]. que analiza el efecto de rotura de presa mediante la formación de una brecha, el tránsito de la crecida aguas abajo en el cauce natural del río y el modelo de transporte de sedimentos con

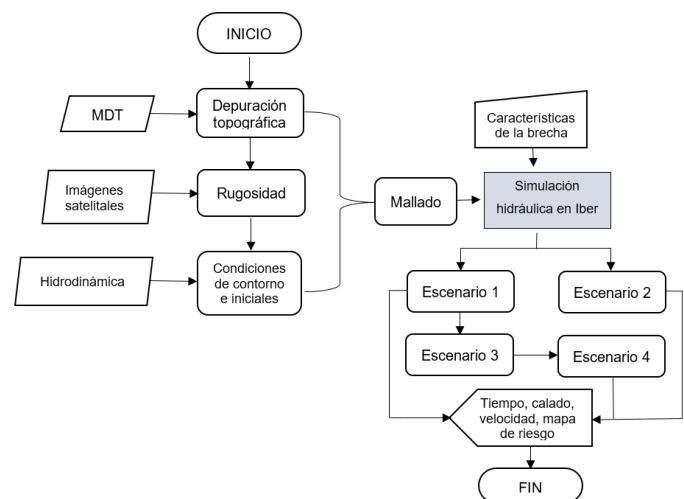


Figura 6. Flujograma de trabajo
Fuente: Elaboración propia

lecho móvil [24,25], la ecuación empleada para el transporte de sedimentos con fondo móvil fue la propuesta por Meyer-Peter y Müller [26].

La extensión de la zona de estudio es de 22 km desde la presa (3788.0 m.s.n.m.) hasta la zona urbana de la ciudad de Ambato (2580 m.s.n.m.). Luego de esto, se tiene un tramo encañonado (no considerado parte del dominio computacional). Se utilizó un Modelo Digital del Terreno MDT de 3 x 3 m de resolución por píxel, el cual mediante el programa SAGA se extrajo la red de drenaje para conocer el recorrido del cauce y posteriormente sea interpretado en el software Iber en formato .asc. El dominio computacional consta de 2 058 000 elementos, la malla es no estructurada. Para optimizar el tiempo de cálculo se ha utilizado 5 tamaños de malla distintos: zona del embalse (21 m), presa (3 m), aguas abajo de la presa (9 m), zona rural (15 m) y zona urbana (6 m). Para la asignación de los coeficientes de Manning se utilizó un mapa de uso de suelo a partir del análisis de ortofotografías y de la información base (Fig. 7). Los parámetros utilizados para el sedimento son: $D_{50} = 0.43$ mm, porosidad de 0.4, y ángulo de fricción interna de 0.50. Estos datos de suelo corresponden a la zona del embalse e implantación de la presa [19].

Los escenarios de simulación fueron cuatro, que corresponde a escenarios de funcionamiento normal y extraordinario, considerando agua clara y agua clara con transporte de sedimentos, los cuales se detallan en la Tabla 1.

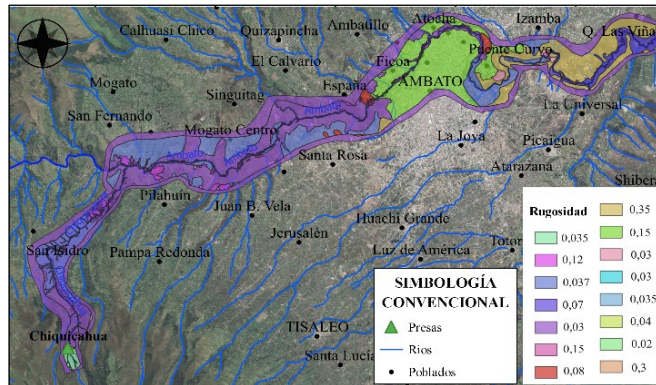


Figura 7. Mapa de uso de suelo con el valor de rugosidad asignado.

Fuente: Elaboración propia

Tabla 1.
Escenarios de simulación.

Escenario	Descripción
1A	Rotura de presa en su máximo nivel de operación con agua clara, se utiliza el criterio del código español RD9/2008.
1B	Rotura de presa en su máximo nivel de operación con agua clara, se utiliza el criterio del código norteamericano FEMA.
2A	Rotura de presa con avenida hidrológica de 1000 años con llenado completo, se clasifica la peligrosidad en función del código RD9/2008.
2B	Considera transporte de sedimentos de fondo, este escenario ocupa los datos del escenario 2A, más la información referente a los sedimentos.

Fuente: Elaboración propia

Tabla 2.

Criterios de análisis de peligrosidad código español RD9/2008.

CRITERIO		AFECCIÓN
Calado (m)	Velocidad (m/s)	
1.0	1.0	No grave
> 1.0	> 1.0	Grave

Fuente: Elaboración propia

Tabla 3.

Criterios de análisis de peligrosidad código norteamericano FEMA.

CRITERIO		AFECCIÓN
Calado (m)	Velocidad (m/s)	
0.9	3.0	Baja
1.4	4.0	Media
> 1.5	> 4.0	Alta

Fuente: Elaboración propia

Para los criterios sobre el análisis de peligrosidad se han utilizado dos normas: (a) norma española RD9/2008 (Tabla 2); (b) norma norteamericana FEMA 2009 (Tabla 3).

3 Resultados

De los resultados obtenidos, se puede evidenciar que existe zonas sin afectación y zonas vulnerables a este evento. El tránsito de la crecida afectaría a la infraestructura civil como: puentes, zona urbana, captaciones de agua y plantas de tratamiento durante los aproximadamente 22 km de recorrido, desde la zona del embalse hasta la salida del área urbana. Considerando las características hidráulicas, en algunos sitios se obtendría calados de 11.0 m, velocidades de hasta 19,0 m/s y números de Froude mayores a 5.0. El tiempo que transcurre desde el inicio de la rotura de la presa y la llegada de la crecida a la zona urbana sería de 48.0 min aproximadamente. La estimación de este periodo de tiempo es importante para gestionar los distintos planes de mitigación y emergencia que se deberían proponer ante una hipotética rotura de la presa. El área rural y urbana afectada sin considerar el cauce normal del río fue de 417.8 ha, de los cuales 90 ha corresponden únicamente a la zona urbana consolidada. La Figs. 8a y 8b muestra los mapas de velocidad y calado para el escenario 1A. Como se puede evidenciar, los rangos de velocidad alcanzarían los 12.0-14.0 m/s con calados de agua de hasta 10.0 m en el cauce principal de la zona urbana.

Para los mapas de peligrosidad el código RD9/2008 considera afección grave y no grave (Fig. 8c), mientras que el código FEMA la afección es baja, media y alta (Fig. 8d). La principal diferencia se encuentra en que el código RD9/2008 cuenta con dos categorías a diferencia del código FEMA que contempla tres categorías de peligrosidad. En cuanto a los rangos de calado y velocidad estos difieren, por ejemplo, la afección “no grave” del código RD9/2008 se presenta para calados de 1 m y velocidades de 1 m/s; mientras que la afección “baja” del código de la FEMA el calado es de 0.9 m y una velocidad de 3 m/s. Se observa en la Fig. 6c que el código RD9/2008 abarca una mayor área de peligrosidad grave en comparación con el código FEMA (Fig. 8d). Esta diferencia de rangos provoca que el Código

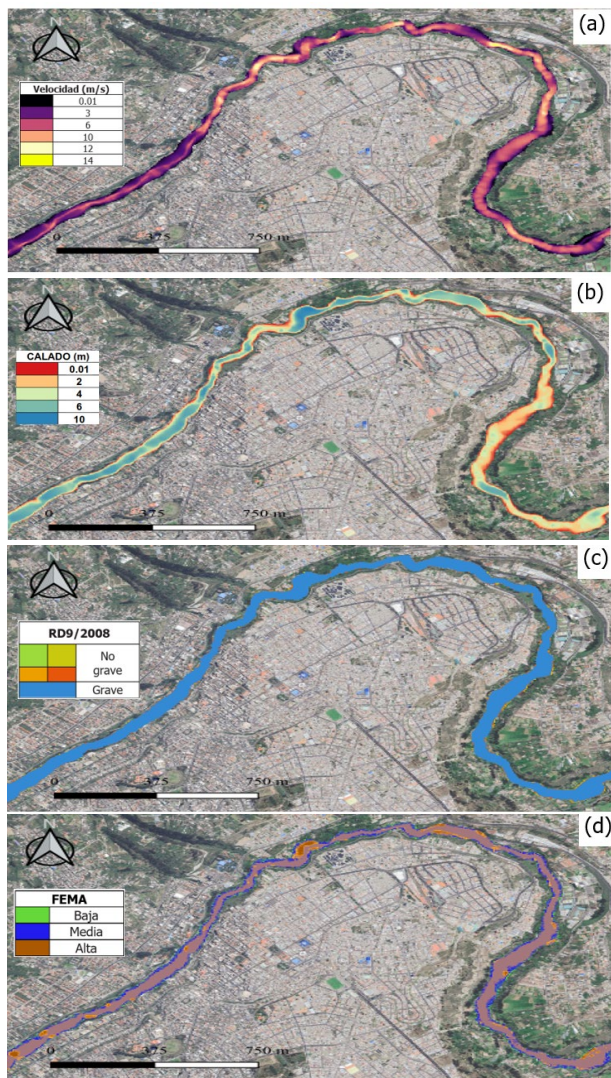


Figura 8. (a) Escenario 1A, mapa de velocidades, zona urbana; (b) Escenario 1A, mapa de calados, zona urbana; (c) Escenario 1A, clasificación de peligrosidad código RD9/2008, zona urbana; (d) Escenario 1B, clasificación de peligrosidad código FEMA, zona urbana; Fuente: Elaboración propia

FEMA categoriza áreas con afección media y el código RD9/2008 lo considerando como afección grave. Tomando en cuenta que, desde el punto de vista de la gestión del riesgo, calados mayores a 1.0 m ya ocasionarían problemas en las zonas urbanas. El código de peligrosidad RD9/2008 muestra ser más claro a la hora de delimitar estas áreas afectadas.

El escenario 2B parte de los mismos parámetros iniciales del escenario 1A, pero se ha incorporado el caudal de máxima crecida. En regiones andinas de alta montaña (cotas superiores a 3000 m.s.n.m.) las áreas de drenaje son menores dado la cercanía a la línea de cumbre de las montañas y la presencia de pajonales andinos cuya función es retener y almacenar agua. En este sentido, el caudal de máxima crecida para un periodo de retorno de 1000 años es de $7.41 \text{ m}^3/\text{s}$ según el estudio hidrológico proporcionado [19]. La rotura de presa se produce con el embalse lleno por donde está circulando un caudal extraordinario, la brecha y el tiempo de

formación de la misma, se determinó mediante las consideraciones de la Guía Técnica Española, dando una duración de 15 minutos y siendo el ancho superior e inferior de la brecha de 86.0 m y 43.0 m respectivamente.

Adicionalmente, se simuló el transporte de sedimentos, con un diámetro medio de partícula de 0.43 mm, el tiempo de simulación para este escenario fue alrededor de 8.5 horas. Se obtuvo los resultados de erosión y sedimentación a lo largo de todo el tramo de análisis, desde el embalse hasta la salida del núcleo urbano. Para la zona cercana al puente vial (punto 1) que está aproximadamente 3 km aguas abajo de la presa, se observa una mayor dinámica entre la sedimentación y la erosión (Fig. 9a). Para la zona urbana los valores de erosión oscilarían entre 1.0 y 2.0 m mientras que los valores de sedimentación alcanzarían valores de hasta 1.5 m. Estos valores de sedimentación en la zona urbana (2580 m.s.n.m.) son mucho menores que en la parte alta del cauce (punto 1) dado que las condiciones de pendiente longitudinal y ancho del río son distintas, evidenciando que gran parte del material se queda depositado en la parte alta de la cuenca (3750 m.s.n.m.). La diferencia de cotas entre la zona de la presa-embalse y la zona urbana es de 1170 m aproximadamente.

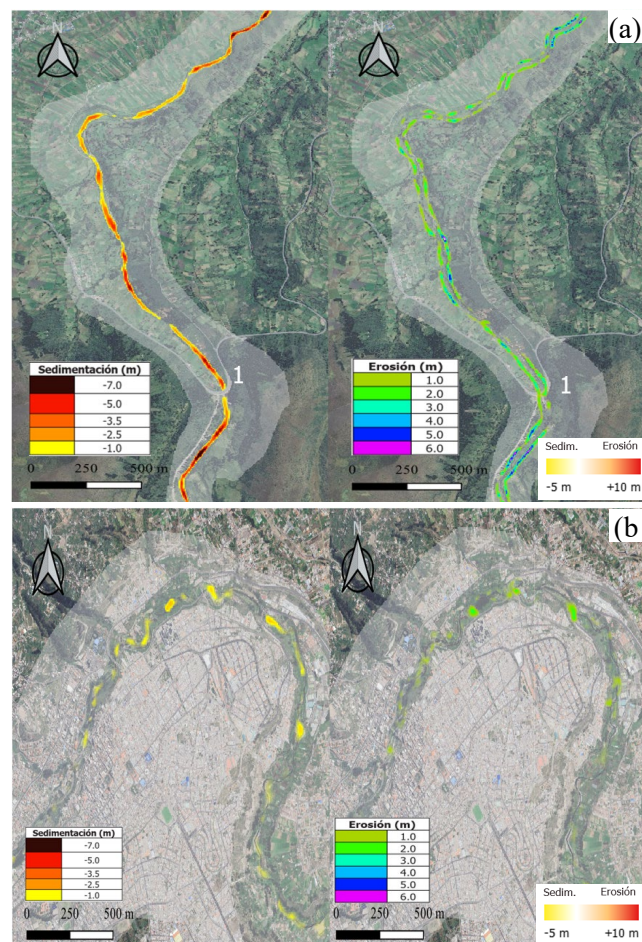


Figura 9. (a) Escenario 2B, mapa de erosión y sedimentación, zona a 3 km aguas debajo de la presa; (b) Escenario 2B, mapa de erosión y sedimentación, zona urbana.

Fuente: Elaboración propia

La Fig. 10 indica la evolución del fondo del río desde la zona del embalse hasta aguas abajo del mismo, llegando hasta la zona de un puente vehicular, el mismo que trabaja como sección de control. El tiempo total de simulación fue de aproximadamente 8 horas para el tránsito de toda la crecida. La brecha se empieza a formar a partir de 25 min, antes de este tiempo no existe transporte de sedimentos en el lecho. A partir de este tiempo, empieza la rotura de la presa y se activa el módulo de transporte de sedimentos.

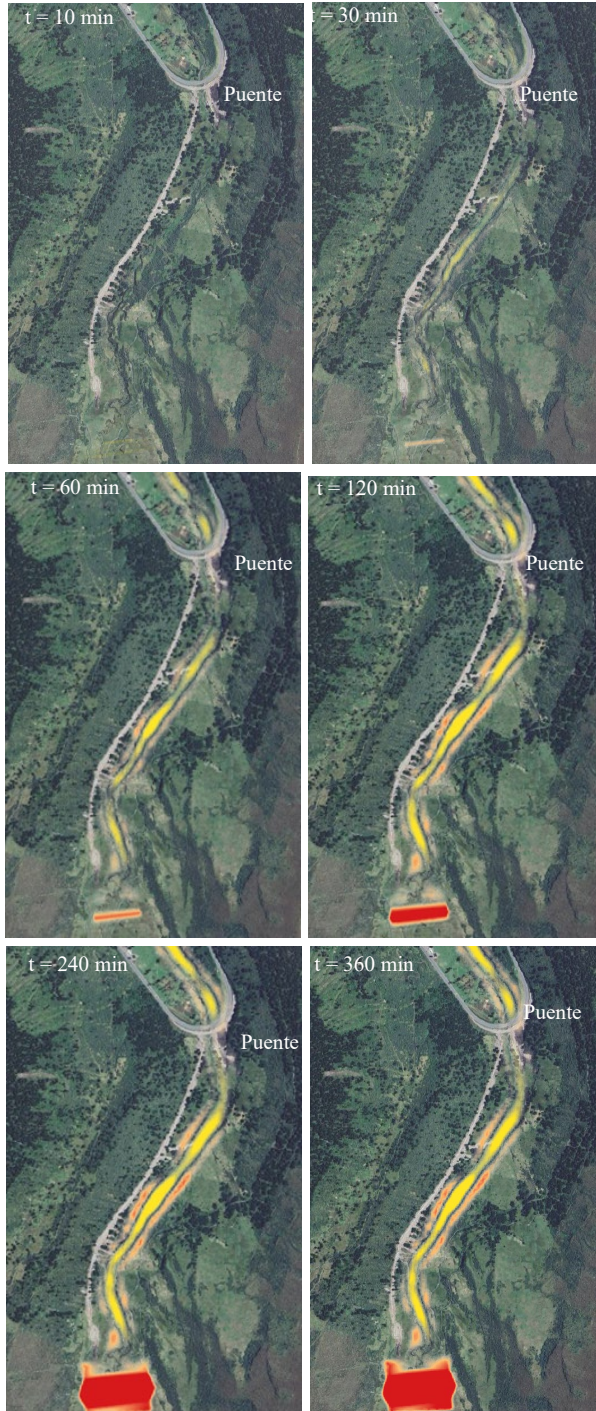


Figura 10. Variación del lecho de fondo aguas abajo del embalse. Mapa de erosión (+) y sedimentación (-) para distintos tiempos de análisis
Fuente: Elaboración propia

El transporte de sedimentos se hace notorio a partir de 30 min (cercano al tiempo de formación de la brecha), aguas arriba de la presa alcanzaría un valor de 1.25 m de erosión, en el instante inicial. Se puede observar que el material erosionado se ha depositado aguas abajo de la presa.

El lecho del río ha alcanzado su equilibrio a partir de las 4 h, para el tiempo transcurrido de 6 h aguas abajo de la presa el material sedimentado alcanzaría los 5 m de altura (color amarillo), en el margen izquierdo el proceso erosivo sería entre 4 a 5 metros (color naranja), lo cual podría provocar daños en la vía adjunta a esta margen. El tiempo de llegada de la crecida al puente sería de 5 min y la velocidad de alrededor de 18 m/s. En las cercanías de la presa, los calados de agua alcanzarían los 16.0 m y velocidades de hasta 35.0 m/s.

Se realizó la comparación entre el hidrograma tras la rotura considerando fondo fijo y fondo móvil (Fig. 11). Existe una diferencia entre los dos escenarios, el hidrograma considerando el transporte de sedimentos es mayor. En este caso, el caudal fue de 238.0 m³/s mayor que el caudal para el evento extraordinario de 1000 años. Esto supone un incremento del 4.3 % con respecto a la simulación con fondo fijo. Estos resultados muestran concordancia con los obtenidos en trabajos previos como Sanz-Ramos et al. [6], cuyos resultados en el hidrograma de rotura muestran un incremento del 4.1 % respecto al hidrograma de rotura considerando únicamente fondo fijo. Por lo tanto, analizar un evento de rotura de presa considerando el transporte de fondo móvil influye directamente en el hidrograma de rotura, con la característica de que el sedimento se deposita hacia aguas abajo.

La Fig. 12 indica la evolución del fondo del río producto del tránsito de la crecida por la rotura de presa en una sección ubicada a 5 km de la presa y 3 km del puente vehicular. Se puede observar que después de transcurrida 1 hora del evento, la erosión tendería al margen derecho del río, alcanzando valores máximos de 1.8 m. La Fig. 13 muestra la variación del calado de agua en el tiempo para la misma sección, desde el tiempo inicial de rotura hasta un valor de 30 min, se evidencia una elevación del flujo de 4.0 m de agua entre los 13 min y 20 min para posteriormente decrecer. Es decir que, el caudal máximo descargado, llega en un tiempo de alrededor de 20 minutos. También existiría un equilibrio entre los valores de erosión y sedimentación luego de 5 horas de simulación, cuyos valores alcanzaría los 2 y 3 m.

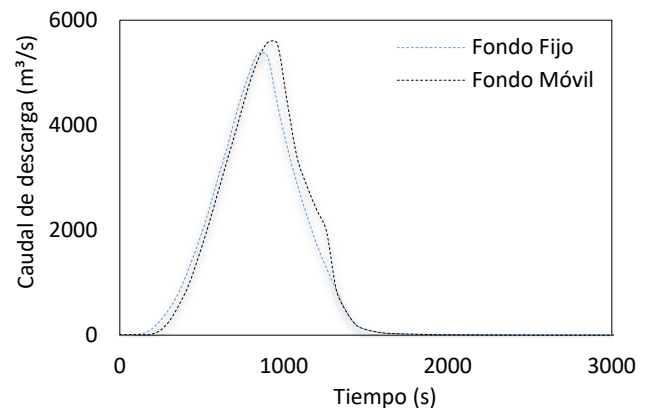


Figura 11. Hidrograma tras la rotura de la presa considerando fondo fijo y móvil.
Fuente: Elaboración propia

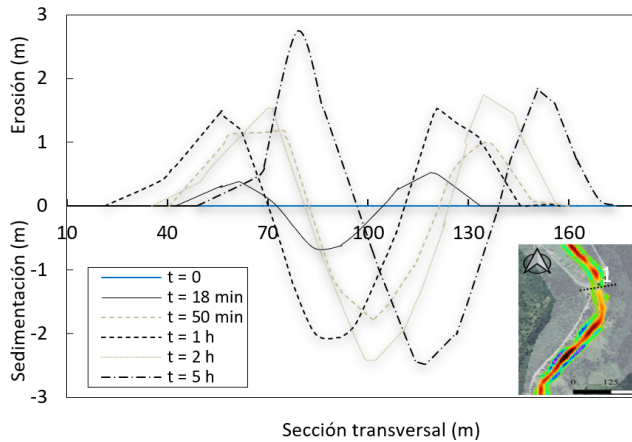


Figura 12. Evolución del fondo del cauce en el tiempo, Punto 1 a 5km de la presa
Fuente: Elaboración propia

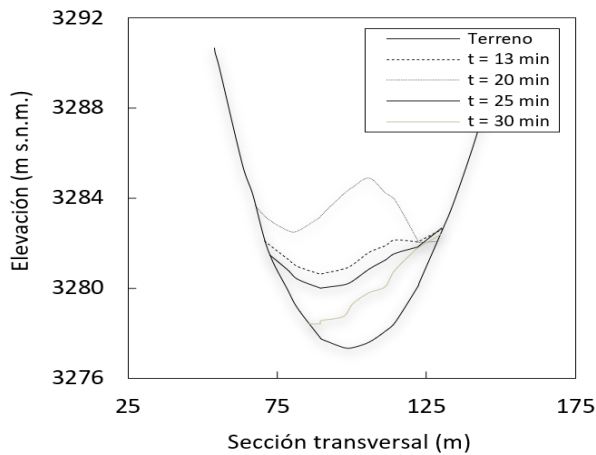


Figura 13. Variación del calado de agua en el tiempo.
Fuente: Elaboración propia

Tabla 4.

Criterios para la categorización de la presa

Datos	Altura mínima (m)	Volumen de almacenamiento (m³)	Longitud de coronación (m)	Área afectada (ha)
Guía Técnica Española	> 10.0	>100.000	> 500	> 5000
Proyecto	39.0	3'065.000	380	417,8

Fuente: Elaboración propia

Una vez determinados los parámetros necesarios para la clasificación de la presa y, en base a lo expuesto acerca de la Guía Técnica Española se establece, en la Tabla 4, la siguiente clasificación:

Al cumplirse dos de los parámetros establecidos, se determina que la presa se clasifica dentro del grupo de “grandes presas”. De igual forma, a la presa se la considera según el riesgo potencial dentro de la “Categoría A”, en razón que:

- Existe afectación al núcleo urbano.
- Afectación a servicios esenciales.
- Posibles daños materiales a infraestructura civil.

4 Discusión

El presente estudio aplica la metodología propuesta por Sanz-Ramos et al. [19] para la evaluación de rotura de presas y el análisis de transporte de sedimentos aguas abajo de la presa. En este caso, para un proyecto implantado en una zona de alta montaña (3800 m.s.n.m.) y el tránsito de la crecida abarca 22 km de distancia hasta la zona vulnerable urbana (2750 m.s.n.m.). En función de los resultados obtenidos y en concordancia con trabajos previos [19], existe una diferencia entre el análisis de la rotura considerando el fondo fijo y un fondo móvil. Este tipo de proyectos deben ser complementados con escenarios hipotéticos como la rotura de una presa y apoyados con criterios y normativas como la expuesta en la Guía Técnica de España y el código norteamericano FEMA. Además, de otras consideraciones como el transporte de material de fondo y su influencia en el hidrograma de rotura. Si bien las formulaciones empíricas empleadas en el modelo numérico poseen un rango de aplicación, estas pueden variar con las del proyecto, ya que dichas formulaciones son obtenidas bajo parámetros y condiciones específicas. Esto genera la necesidad de que el modelo numérico sea calibrado y validado con datos experimentales obtenidos durante el evento. En este sentido, es necesario una extensa campaña experimental de recolección de datos de sedimento para toda la longitud de análisis. Además, de considerar una granulometría variable en el modelo numérico. Al ser la rotura de presa un hecho hipotético y que se espera nunca ocurra, si es necesario disponer de mediciones en tiempo real del tránsito de la crecida y así retroalimentar el modelo numérico para reducir la incertidumbre de los resultados.

La pendiente media longitudinal del río en la parte urbana es alrededor del 4 %, la cual influye directamente en los rangos de velocidad registrados durante la crecida, cuyo valor alcanzaría los 15 m/s y calados de agua que podrían afectar principalmente la zona urbana más cercana al cauce principal. El tiempo de llegada de la crecida luego de rotura al núcleo urbano sería de 48 minutos. En este tiempo, todas las zonas posibles de afectación deberán ya haber evacuado e informado con algún sistema de alerta temprana a la población. En lo referente a los resultados obtenidos considerando el transporte de sedimentos de fondo, existe un incremento del 4.3 % en el hidrograma tras la rotura considerando el transporte de sedimentos, respecto a la simulación con fondo fijo. Respecto a la comparación de los códigos de peligrosidad, el código español RD9/2008 muestra ser más claro a la hora de delimitar estas áreas afectadas como graves, tomando como referencia un calado de 1 m y una velocidad de 1 m/s; cuyos valores según la gestión del riesgo son acordes para zonas urbanas con alta densidad poblacional, servicios básicos, puentes, etc.

5 Conclusiones

El presente estudio analiza la rotura de presa para distintos escenarios, que contempla escenarios de funcionamiento normal y con crecida extraordinaria, análisis de los mapas de peligrosidad con el código español RD9/2008 y el código de la Agencia Federal para el manejo

de Emergencias norteamericano FEMA. En función de los resultados obtenidos, la presa analizada es catalogada dentro del grupo de “grandes presas” y en función del riesgo potencial como presa “Categoría A”. El hidrograma de rotura con la inclusión del transporte de sedimentos resulta ser mayor que el hidrograma con agua clara, lo cual muestra una concordancia con trabajos previos. Dado las altas velocidades y el régimen supercrítico del flujo durante la propagación de la onda de crecida, la afectación a la infraestructura civil sería considerable, sobre todo en los servicios básicos esenciales de la zona urbana, como se ha podido observar en eventos anteriores en zonas montañosas como el denominado “Desastre de la Josefina” (aproximadamente 2250 m.s.n.m.) en Cuenca, Ecuador. El sedimento desplazado se ubica predominantemente aguas abajo de la presa y en menor cantidad en la zona baja de la cuenca correspondiente a la parte urbana de la ciudad de Ambato. Sin embargo, existen áreas puntuales en la zona urbana afectadas por la acumulación de sedimento como el caso de tomas de agua o plantas de tratamiento. Estos criterios plantean nuevos escenarios que deben ser considerados en Ecuador, bien sea para la fase de diseño de una presa, o para la evaluación de presas existentes. En este sentido, este estudio subraya la relevancia de adaptar metodologías nuevas a condiciones geográficas y normativas locales específicas, enfatizando la necesidad de datos precisos y actualizados para mejorar la capacidad predictiva de modelos numéricos en situaciones críticas como la rotura de presas en zonas vulnerables y así evitar lo sucedido como en eventos pasados.

Agradecimientos

Los autores expresan su agradecimiento al Honorable Gobierno Provincial de Tungurahua del Ecuador por prestar las facilidades para el acceso a la información técnica base del caso de estudio.

Referencias

- [1] Wahl, T., Prediction of embankment dam breach parameters a Literature Review and Needs Assessment. U.S. Department of the Interior, Bureau of Reclamation, Dam Safety Office, USA, 1998.
- [2] Federal Emergency Management Agency. FEMA. P-1015 Technical Manual: overtopping protection for dams. US Department of Homeland Security, USA, 2014.
- [3] Castillo, L.G., Carrillo, J.M., and Blázquez, A., Plunge pool mean dynamic pressures: a temporal analysis in nappe flow case. *Journal of Hydraulic Research*, 53(1), pp. 101–118, 2015. DOI: <https://doi.org/10.1080/00221686.2014.968226>
- [4] Carrillo, J.M., Metodología numérica y experimental para el diseño de los cuencos de disipación en el sobrevuerto de presas de fábrica. Universidad Politécnica de Cartagena, Cartagena, España, 2014.
- [5] Ortega, P.R., Análisis de la lámina vertiente en el sobrevuerto de presas de fábrica. Universidad Politécnica de Cartagena, Cartagena, España, 2022.
- [6] Sanz-Ramos, M., Olivares, G., and Bladé, E., Metodología para el análisis de rotura de presas con aterramiento mediante simulación con fondo móvil, *Revista Iberoamericana del Agua*, pp. 138-147, 2019. DOI: <https://doi.org/10.1080/23863781.2019.1705198>
- [7] Sanz-Ramos, M., Bladé, E., Silva, N., Salazar, F., López, D., and Martínez, E., A probabilistic approach for off-stream reservoir failure flood hazard assessment. *water*, 15(12), pp. 1–19, 2023. DOI: <https://doi.org/10.3390/w15122202>
- [8] Sanz-Ramos, M., Blade, E., Silva, N., and Salazar, F., Avances en iber para la clasificación de balsas: proyecto acropolis. *Ingeniería del Agua*, 28(1), pp. 47–63, 2024. DOI: <https://doi.org/10.4995/ia.2024.20609>
- [9] Sanz-Ramos, M., Bladé, E., Escolano, E., Optimización del cálculo de la vía de intenso desagüe con criterios hidráulicos. *Ingeniería del agua*, 24(3), pp. 203–218, 2020. DOI: <https://doi.org/10.4995/ia.2020.13364>
- [10] López-Gómez, D., De-Blas-Moncalvillo, M., Cuéllar-Moro, V., Herramientas para la gestión sostenible de la sedimentación en el embalse de Marmolejo (España). *Ingeniería del Agua*, 28, pp. 1–16, 2024. DOI: <https://doi.org/10.4995/ia.2024.20376>
- [11] Zeas, R., El deslizamiento de la Josefina tragedia nacional, proceedings Seminario internacional sobre aludes torrenciales, Galileo, pp. 87–98, Venezuela, 2019.
- [12] Palavecino, A., Modelación bidimensional del flujo generado por rotura de una presa de tierra, utilizando el programa Iber. Escuela Politécnica Nacional, Quito, Ecuador, 2015.
- [13] Acero, A., Modelación numérica bidimensional del flujo generado por rotura de la presa Mulacorral mediante Hec-Ras 5.0. Escuela Politécnica Nacional, Quito, Ecuador, 2019.
- [14] Toapaxi, J., and Acero, A., Análisis de inundación por rotura de presa utilizando el Modelo HEC-RAS 2D: caso de estudio de la presa mulacorral, Provincia de Tungurahua, *Revista Politécnica*, 48(1), pp. 51–64, 2021. DOI: <https://doi.org/10.33333/rp.vol48n1.05>
- [15] López, A., Análisis de la amenaza por inundación en caso de rotura de la represa Chiquiurcu, en el cantón Ambato, provincia de Tungurahua Ambato. Universidad Central del Ecuador, Quito, Ecuador, 2022.
- [16] Herbozo, J.E., Muñoz, L.E., Guerra, M.J., Minaya, V., Haro, P., Carrillo, V., Manciat, C., Campozaño, L., Non-Stationary hydrological regimes due to climate change: the impact of future precipitation in the spillway design of a reservoir, case study: sube y baja dam, in Ecuador. *Atmosphere* 13, Art. 828, 2022. DOI: <https://doi.org/10.3390/atmos13050828>
- [17] Barreto, J., Matute, R., Tenezaca, R., La Josefina, quince años después. Universidad del Azuay, Cuenca, Ecuador, 2008.
- [18] iagua., El gobierno de Ecuador pone en marcha el Plan de Manejo de la zona especial de La Josefina, [online], 2013. Available at: <https://www.iagua.es/noticias/ecuador/13/05/06/el-gobierno-de-ecuador-pone-en-marcha-el-plan-de-manejo-de-la-zona-especial-de-la-josefina-30009>.
- [19] Honorable Consejo Provincial de Tungurahua. Estudios y diseños definitivos embalse Quebrada Chiquicahua. Ambato, Ecuador, 2022.
- [20] Banco de Desarrollo del Ecuador, [online], 2022. Available at: <https://twitter.com/BDEcuadorBP/status/1548114024633491458/photo/2>
- [21] Honorable Consejo Provincial de Tungurahua. Un hito de ingeniería y esperanza emerge en Tungurahua. Ambato, Ecuador, 2023.
- [22] Bladé, E., Modelación del flujo en lámina libre sobre cauces naturales. Análisis integrado con esquemas en volúmenes finitos en una y dos dimensiones. Tesis doctoral. Universidad Politécnica de Catalunya, Barcelona, España, 2005.
- [23] Bladé, E., Cea, L., Corestein, G., Escolano, E., Puertas, J., Vázquez-Cendón, E., Dolz, J., Coll, A., Iber: herramienta de simulación numérica del flujo en ríos. *Revista Internacional de Métodos Numéricos para Cálculo y Diseño en Ingeniería*, CIMNE (Universitat Politécnica de Catalunya) 30, pp. 1–10, 2014.
- [24] Corestein, G., Bladé, E., Validación del módulo de transporte de sedimentos de fondo-modelo iber. *Proceedings III Jornadas de Ingeniería del Agua: La Protección Contra Los Riesgos Hídricos JIA*. Valencia, 23 y 24 de octubre, pp. 27–34, 2013.
- [25] Corestein, G., Bladé, E., Niñerola, D., Modelling bedload transport for mixed flows in presence of a non-erodible bed layer. *River Flow*, CRC Press, pp. 1611–1618, 2014.
- [26] Meyer-Peter, E., and Müller, R., Formulas for bed load transport. *proceedings of 2nd meeting of the international association for hydraulic structures research, delft*, 7 june, pp. 39–64, 1948.

P.E. Suárez-Naranjo, obtuvo el grado de Ingeniera Civil por la Universidad Técnica de Ambato en 2019. En 2023, obtuvo el grado de MSc. en Hidráulica, con mención en Diseño de Obras Hidráulicas, por la Escuela Politécnica Nacional. Se designó como Analista de Infraestructura en el Ministerio de Transporte y Obras Públicas (MTOP) en la provincia de

Cotopaxi y como Supervisora Encargada de Conservación Vial en la Zonal 1 (Esmeraldas, Carchi, Imbabura y Sucumbios) en la matriz del MTOP en Quito. Actualmente, es docente en la Carrera de Ingeniería Civil de la Universidad Politécnica Salesiana, sede Quito, campus Sur. Sus áreas de interés incluyen la hidráulica aplicada, la dinámica de fluidos y la modelación numérica de procesos hidráulicos, con un enfoque en el análisis de peligrosidad hidrológica, la delimitación de áreas de inundación y la evaluación de riesgos asociados a eventos extremos.
ORCID: 0009-0002-9298-9778

P.R. Ortega-Lara, es Ingeniero Civil de la Universidad Central del Ecuador, MSc. en Diseño de Proyectos Hidráulicos en la Escuela Politécnica Nacional y un doctorado en la Universidad Politécnica de Cartagena (España) en el tema de flujos multifase en chorros de vertido libre en presas. Actualmente, se desempeña como Profesor Titular Tiempo Completo de la Facultad de Ingeniería Civil y Ambiental de la Escuela Politécnica Nacional. También fue presidente de la Young Professionals Network EPN de la IAHR. Realizó una estadia de investigación con el IHE (Delft, Países Bajos). Es editor asociado de la Revista Hidrolatinoamericana IAHR y de la Revista Ingeniería del Agua (España). Sus áreas de interés son la Dinámica de Fluidos Computacional, modelación física experimental, flujos multifase agua-aire, presas y diseño de estructuras hidráulicas.
ORCID: 0000-0003-2697-3268

P.L. Haro-Ruiz, obtuvo el grado de Ingeniera Civil por la Escuela Politécnica Nacional en 2007. En 2010 obtuvo el Grado de Magister en Ingeniería de los Recursos Hídricos y Ciencias del Agua, Mención Diseño de Proyectos Hidráulicos por la Escuela Politécnica Nacional. El grado de PhD en Tecnología y Modelización en Ingeniería Civil, Minera y Ambiental lo obtuvo por la Universidad Politécnica de Cartagena (UPCT) en 2019 en Cartagena - España. Se desempeñó como Analista de Expansión en el Ministerio de Electricidad y Energía Renovable desde 2008 hasta 2014, participando en la supervisión de los estudios y construcción de centrales hidroeléctricas como Sopladora, Minas – San Francisco, Coca Codo Sinclair, Cuenca Alta del Guayllabamba, y proyectos Geotérmicos como Chachimiro. Actualmente, es Subdecana y Profesora Titular Auxiliar en la Facultad de Ingeniería Civil y Ambiental de Escuela Politécnica Nacional (EPN) en Quito – Ecuador. A lo largo de su carrera académica, se ha desempeñado como Coordinadora de la Maestría en Hidráulica del Departamento de Ingeniería Civil y Ambiental.
ORCID: 0000-0001-5612-3075

Methods for determining the structural strength of reinforced concrete beams with hybrid nodes

Yordy Miele-Bravo^a & Gema Zambrano-Baque^b

^a Facultad de Ingeniería y Ciencias Aplicadas, Universidad Técnica de Manabí, Portoviejo, Ecuador. yordimiele@gmail.com

^b Facultad de Ciencias Básicas, Universidad Técnica de Manabí, Portoviejo, Ecuador. monserrate.zambrano01@utm.edu.ec

Received: February 3th, 2025. Received in revised form: July 30th, 2025. Accepted: August 19th, 2025.

Abstract

Hybrid nodes of concrete beams and secondary steel beams cause disturbance and reductions in the load-bearing capacity of the cross-section, which can be compensated for by using suspension stirrups in the node area. These elements allow cracking to be controlled and redirect loads from the tension area to the compression zone, significantly improving the overall strength of the assembly. The stress-strain study, conducted using Abaqus software, supports experimental observations by providing insight into the stress trajectories. This integration with the cracking study led to the formulation of a structural model based on the strut-and-tie model, which was applied to the design of the structural node. A procedure is also proposed for calculating the structural capacity of reinforced concrete beams with hybrid connections and suspended stirrups, based on the theoretical strength of the reinforced concrete beam's cross-section.

Keywords: hybrid nodes; suspender stirrups; tensor strut; nominal resistance.

Métodos para determinar la resistencia estructural en vigas de hormigón armado con nudos híbridos

Resumen

Los nudos híbridos de vigas de hormigón y vigas secundaria de acero originan una perturbación y reducción de la capacidad resistente de la sección transversal, lo cual puede compensarse mediante el uso de estribos suspensores en la zona del nudo. Estos elementos permiten controlar la fisuración y redirigir las sollicitaciones desde el área traccionada hacia la zona comprimida, mejorando notablemente la resistencia del conjunto. El estudio tenso - deformación realizado con apoyo del software Abaqus, respalda las observaciones experimentales comprendiendo las trayectorias de esfuerzos. Esta integración con el estudio de fisuración llevó a la formulación de un modelo estructural basado en el modelo de bielas y tirantes aplicado al diseño del nudo estructural. Asimismo, se plantea un procedimiento para calcular la capacidad estructural de vigas de hormigón armado con conexiones híbridas y estribos suspendidos, basado en la resistencia teórica de la sección transversal de la viga de hormigón armado.

Palabras clave: nudos híbridos; estribos suspensores; Puntal Tensor; resistencia nominal.

1 Introducción

Una referencia clave para el desarrollo de la presente investigación el sismo ocurrido el 16 de abril de 2016, con magnitud 7,8 Magnitud de momento (Mw) y epicentro en la costa de la provincia de Manabí. Este evento fue consecuencia del proceso de subducción de la placa de Nazca con la placa Sudamericana, fenómeno que comparte origen y ubicación geográfica con otros terremotos registrados en la zona, como los

de enero de 1906 (Mw 8,8), mayo de 1942 (Mw 7,8), enero de 1958 (Mw 7,8), diciembre de 1979 (Mw 8,1) y agosto de 1998 (Mw 7,1) [1]. Después del sismo del 16 de abril de 2016 se observó el comportamiento de edificios con nudos híbridos como los de la Fig. 1, información presentada por [2,3]. Constituido en un gran laboratorio a escala natural, fueron localizados los fallos, los modos de agrietamiento de los nudos, las bondades y desventajas de diferentes tipologías utilizadas en numerosas edificaciones, entre otros aspectos de interés.

How to cite: Miele-Bravo, Y. y Zambrano-Baque, G., Métodos para determinar la resistencia estructural en vigas de hormigón armado con nudos híbridos DYNA, (92)239, pp. 139-149, October - December, 2025.

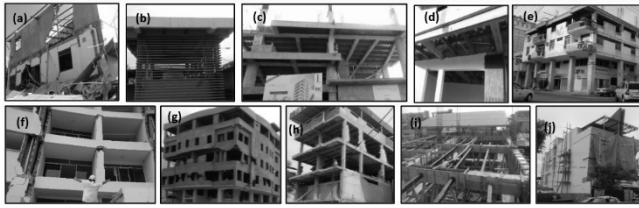


Figura 1. Edificios con nudos híbridos inspeccionados luego del sismo. (a). Baque. (b). Hospital Verdy. (c). Torremolinos. (d). Nouva Plaza. (e). Sabando. (f). Narea. (g). Omnilife. (h). Gym 3MP. (i). Montesdeoca. (j). Seny.

Fuente: Elaboración propia.

En síntesis, se puede indicar que la mayor parte de las edificaciones presentaron un buen desempeño sísmico, pero algunos fueron demolidos por fallas primarias no imputables al nudo híbrido relacionadas con aspectos como: i) la intensidad del sismo, evidenciada en los espectros de respuesta registrados en la ciudad de Portoviejo, fue significativamente superior especialmente en el intervalo de períodos cercanos a 0,5 en comparación con los espectros establecidos por el Código Ecuatoriano de la Construcción del 2000, [4] así como por las Normas Ecuatorianas de la Construcción de 2011 y 2015; [5,6], ii) la edificación de niveles adicionales sobre construcciones existentes sin realizar un refuerzo estructural adecuado; iii) estructuras con gran flexibilidad que experimentaron desplazamientos considerables y iv) una tipología estructural particular que exige una planta con una altura de 5 m y de mezzanines.

Por otro lado, los errores estructurales más frecuentes fueron principalmente fallas por columna corta, configuración de columna débil y viga fuerte, deficiencias en detallado del acero de refuerzo, ausencia de confinamiento adecuado en las uniones viga - columna y en las vigas y columnas, piso blando, fenómenos de licuefacción de suelos, entre otros [2,3,7].

1.1 Diseño del experimento para la modelación del comportamiento global de edificaciones con nudos híbridos

A los efectos de valorar la influencia del tipo de nudo (empotrado o articulado) se concibió y puso en práctica un diseño de experimentos factorial que consta de tres variables independientes y dos niveles cada una, a ser desarrollado por medio de modelación numérica.

La modelación numérica realizada, por medio del software ETABS desarrollado por Computers and Structures, Inc. (CSI 2015) [8], consideró las combinaciones de cargas gravitatorias y sísmicas del Instituto Americano del Concreto 318 (ACI 318) [9]. Como variables de respuesta se valoró las solicitaciones actuantes de momento, cortante y fuerza axial de las vigas ubicada en la zona del nudo híbrido y como parámetro de daño global de la estructura se evaluó la deriva de piso, que es dependencia entre el desplazamiento lateral y la altura de una estructura. Mientras más flexible es una estructura más desplazamiento lateral y daño tendrá, la deriva de piso es un parámetro efectivo para controlar el daño ante fuerzas laterales, motivo por el cual las normas la limitan a valores de entre el 1 y el 2 %. [10,11]

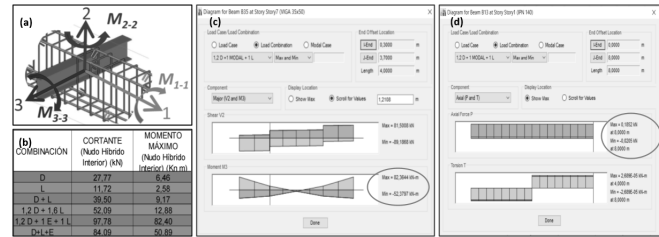


Figura 2. (a) Ejes referenciales de la viga (b) Valores máximos de las combinaciones de carga (c) Momento máximo para la combinación con sismo (d) Axial máximo en vigas.

Fuente: Elaboración propia.

A partir del análisis estadístico realizado, en el caso de nudos empotrados las variables independientes consideradas resultaron ser significativas en la respuesta. La Fig. 2 (b) indica los valores máximos de cortante y momentos obtenidos de los modelos numéricos para diferentes combinaciones de carga y en Fig. 2 (c) el gráfico de mayor momento y cortante para la combinación de carga permanente, carga viva y sismo. Los valores de momento y cortante del nudo se modifican por la longitud de espaciamiento de las vigas secundarias, de manera que se usó la separación de 1,60 m, distancia que se encuentra dentro de los rangos recomendados por los fabricantes de la lámina colaborante (steel deck) de la empresa Novacero la cual que cumple con la Norma Técnica Ecuatoriana del Instituto Ecuatoriano de Normalización 2397 (NTE INEN 2397), Norma de la Sociedad Americana para Pruebas y Materiales A653 (ASTM A653) y la Norma conjunta del Instituto Nacional Estadounidense de Estándares y de la Sociedad Americana de Ingenieros Civiles ANSI/ ASCE 3-91 (ANSI/ ASCE 3-91).

Los modelos numéricos y el tratamiento estadístico del diseño de experimento confirman que los momentos flectores alrededor del eje 3 Fig. 2 (a), son los que gobiernan en la viga, de manera que los análisis de resistencia deben estar relacionados con ese eje. El máximo axial en la viga de acero pasante en todos los modelos de nudos es de 0,18 kN y se muestran en la Fig. 2 (d), valor de poca consideración atribuible a la poca rigidez de la viga metálica con respecto a la viga de concreto reforzado paralela a ella y la presencia de la losa infinitamente rígida en su plano que toma la carga lateral. Por ese motivo, los axiales de la viga secundaria no influyen de manera significativa en la resistencia del nudo.

Se concibe un diseño experimental estadístico de tipo factorial, considerando tres variables independientes con dos niveles cada una, una réplica y la inclusión de cuatro especímenes de control, lo que da un total de 20 muestras ensayadas. Las variables independientes seleccionadas fueron: la relación entre momento flector y fuerza cortante, la relación entre la altura del nudo y la altura de la viga de hormigón y la utilización de estribos sensores. También se consideró la posibilidad de incluir la variable resistencia del hormigón a la compresión, pero se decidió su evaluación posterior por medio de modelación numérica, de cara a la reducción del número de especímenes experimentales. Se evaluó el impacto de estas variables sobre los principales comportamientos de la viga de hormigón armado (HA),

incluyendo la resistencia a momento flector, la resistencia al cortante, la rigidez, la fisuración y los modos de fallos.

1.2 Modelo con el método Puntal-Tensor (MPT) simplificado (bielas y tirantes)

El Modelo Puntal-Tensor (MPT) permite representar la distribución y trayectoria de las fuerzas por medio de puntales y tensores, incluso en condiciones de diseño complejos. El MPT permite representar el flujo de las fuerzas dentro de un elemento o región, permite comprender claramente los diversos elementos resistentes y destaca la necesidad de detallar cuidadosamente la armadura en ciertas regiones claves [12].

En las regiones B se utiliza la teoría clásica de flexión aplicada al hormigón armado, junto con el método convencional de diseño para el cortante basado en la suma de las contribuciones del concreto y del acero de refuerzo ($V_c + V_s$). En cambio, en las regiones tipo D, una parte significativa de la carga se transfiere directamente a los apoyos mediante fuerzas de compresión en el hormigón y las fuerzas de tracción en la armadura, lo que hace necesario aplicar un enfoque de diseño diferente. Estas regiones D pueden representarse mediante modelos de reticulados ideales, formados por puntales comprimidos de hormigón y tensores traccionados de acero, los cuales se conectan en zonas denominadas nodos [13].

1.3 Fundamentos teóricos del método de Bielas y Tirantes (STM)

Los orígenes del Método de Bielas y Tirantes (STM) se remontan a finales del siglo XIX, coincidiendo con las primeras publicaciones sobre el hormigón armado. En 1899, Wilhelm Ritter presentó un artículo titulado “Die Bauweise Hennbique”, en el cual introdujo un modelo de armadura para analizar vigas fisuradas y explicar su comportamiento frente a esfuerzos cortantes. Ritter presentó un modelo de armadura en el que se permiten observar vigas agrietadas y explicar la resistencia al cortante de vigas con barras de acero longitudinal y estribos, dando a lugar la primera ecuación de diseño para este tipo de estructuras. En lo posterior, en el año 1902, la obra de Emil Morsch titulada “Der Eisenbetonbau” revalida las ideas de Ritter aportando evidencia experimental y desarrollando el modelo clásico de armadura en 45° para vigas. El modelo con algunas adaptaciones sigue siendo la base del diseño al cortante de vigas de HA según la mayoría de los reglamentos actuales. A pesar de lo mencionado, la teoría actual surge en 1987 en el artículo “Toward a Consistent Design of Structural Concrete” de los autores Schlaich y Jennewein [14].

La técnica reemplaza las zonas de discontinuidad en la estructura donde se concentran esfuerzos tensionales, por una armadura hipotética de barras articuladas ya sean planas o espaciales denominadas bielas si están comprimidas, o tirantes si actúan a tracción y los nudos representan a los puntos de encuentro entre bielas y tirantes, en los cuales deben equilibrarse las cargas externas y los esfuerzos internos de la región [15,16]. El método STM permite interpretar de forma adecuada el comportamiento de nudos y

zonas de discontinuidad, conocidas como regiones D, además constituye una herramienta útil para diseñar uniones que no están contempladas en los códigos convencionales y también proporciona una alternativa para diseñar regiones sin discontinuidad denominadas regiones B [17].

Cuando se conoce cómo se distribuye dentro de una región D, es posible aplicar el método STM y así integrar el diseño con las regiones B y D continuas. En la zona de transición entre ambas regiones, es necesario asegurar el equilibrio de las cargas aplicadas, los esfuerzos exteriores y las reacciones [12,18,19]. La trayectoria que siguen los esfuerzos permite determinar la posición adecuada de las bielas y tirantes dentro del modelo [20].

La formulación de un modelo para una región D se vuelve considerablemente más sencilla cuando se dispone de información sobre las tensiones elásticas y las direcciones principales de esfuerzo. Este proceso se ha visto facilitado en las últimas décadas gracias al desarrollo de numerosos programas de análisis estructural basados en el Método de los Elementos Finitos (MEF), los cuales permiten visualizar de manera efectiva estos esfuerzos [16]. A partir de dichos análisis, las bielas pueden orientarse dentro de un margen de $\pm 15^\circ$ respecto a las direcciones principales de compresión, mientras que los tirantes se alinean en un rango similar con respecto a las tensiones de tracción [20]. El refuerzo, así como los tirantes pueden disponerse considerando criterios prácticos de construcción, ya que la estructura tiende a ajustarse al esquema interno de esfuerzos asumidos al modelo. Adaptar la geometría del sistema estructural propuesto a la distribución de tensiones elásticas contribuye significativamente a la eficacia del modelo [21].

En caso de no contar con herramientas de análisis avanzadas, es posible desarrollar un modelo de bielas y tirantes a partir del denominado “camino de cargas”. Este enfoque exige cumplir con el equilibrio externo de la región D, lo que implica identificar todas las cargas aplicadas y reacciones presentes. En la frontera entre la región B y la región D, la primera transmite las cargas a la segunda, por lo que es necesario subdividir el diagrama de esfuerzos de modo que las acciones en un lado de la estructura sean equilibradas por las del lado opuesto. El camino de carga se traza desde el centro de gravedad de los diagramas de tensión, siguiendo la dirección de las cargas aplicadas o de las reacciones, y las bielas y tirantes se orientan a lo largo del recorrido más directo posible entre esos puntos [16].

2 Evidencias experimentales de la evolución de las fisuras y los mecanismos de falla

A partir del patrón de daños registrado en la cara frontal de cada espécimen, asociado a los niveles de carga aplicados y su contraste con las restantes mediciones, se realizó una caracterización detallada de la evolución del daño y se identificó el efecto de las variables independientes analizadas sobre el comportamiento de los especímenes. A modo de ilustración, en la Fig. 3 se presentan, parcialmente, los patrones de fisuración correspondientes a los especímenes E 5.1 y E 5.2 para el ciclo de carga de la primera fisura, el ciclo de carga al 50 % de carga de fallo del espécimen y la fisuración para el fallo dúctil.

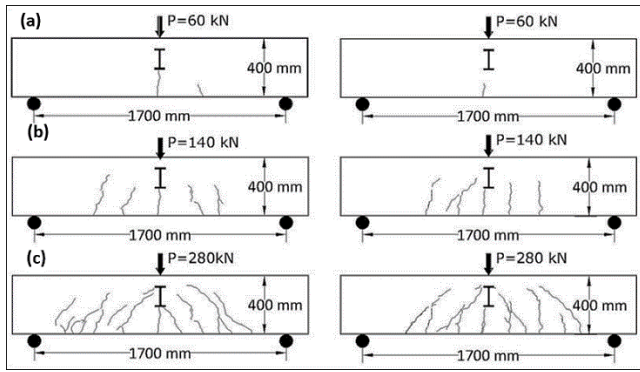


Figura 3. Patrones de fisuración del experimento E 5: (a) Formación de primera fisura. (b) Fisuración al 50 % de la carga de fallo por fluencia. (c) Fisuración para el ciclo de carga de fluencia.
Fuente: Elaboración propia.

La evolución y el tipo de fisuración durante los ensayos en ambos especímenes es similar y revela la uniformidad y consistencia de los resultados; lo anterior se manifiesta de igual forma en las restantes parejas de especímenes ensayados, donde se incluyen los patrones de daño de la totalidad de los elementos ensayados. Seguidamente se realizan contrastes de los resultados, con la intención de fundamentar las principales regularidades identificadas.

2.1 Fisuración en vigas con $\frac{M}{V} = 0,85 \text{ m}$

Para caracterizar la fisuración de todos los especímenes de luz corta, se ensayaron dos vigas patrones de control sin nudo híbrido denominadas E 9.1 y E 9.2. Fig. 4 cuya carga de fallo por fluencia del acero se la nombró como “fallo de control” y fue 221,05 kN y 221,66 kN respectivamente, mientras la carga de fallo teórica es de 221,10 kN. La aparición de la primera fisura principal de flexión ocurre al 27 % de la carga de fallo experimental con una longitud del 35 % del peralte de la viga y de 0,1 mm de, se trata de una fisura capilar por el desplazamiento súbito del eje neutro que causa la rotura por tracción del hormigón y que se corrobora por las curvas carga deformación. Las fisuras predominantes son de flexión-cortante y aparecen a medida que se incrementa la carga desde su punto de aplicación hacia los apoyos hasta distancia aproximada de 1,25 veces el peralte de la viga.

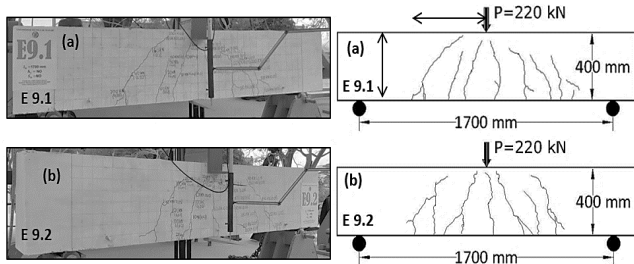


Figura 4. Patrón de fisuración para el fallo por fluencia del experimento E 9: (a) Especimen E 9.1. (b) Especimen E 9.2.
Fuente: Elaboración propia.

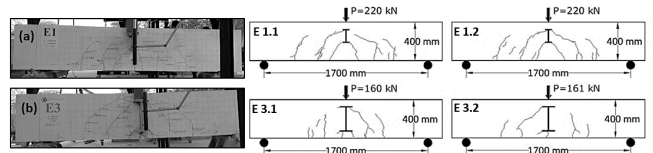


Figura 5. Patrones de fisuración para la carga de fallo: (a) Especimen E 1.1 y E 1.2. (b) Especimen E 3.1 y E 3.2.
Fuente: Elaboración propia.

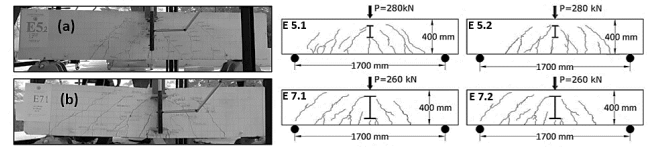


Figura 6. Patrones de fisuración para carga de fallo por fluencia: (a) Especimen E 5.1 y E 5.2. (b) Especimen E 7.1 y E 7.2.
Fuente: Elaboración propia.

2.2 Fisuración en vigas sin estribos suspensores

La Fig. 5 (a) muestran los especímenes E1 de luz corta, nudo bajo, sin suspensor, con una primera fisura de flexión y longitud del 30 % del peralte de la viga que se hace visible a un 27 % de la carga de fallo de control. Al superar el 27 % e incrementar la carga, aparecen otras fisuras de flexión que luego evolucionan a flexión-cortante y que se propagan desde el centro de la luz hasta 1,40 veces el peralte de la viga en dirección del apoyo. En los especímenes E3 de nudo alto ilustrados en la Fig. 5 (b), la fisuración es más acentuada y de mayor ancho a etapas más tempranas del ensayo, pues la primera fisura es visible en torno al 13 % de la carga de fallo de control, atribuible a la mayor perturbación del nudo alto y porque la (puntual) tiene menos hormigón bajo el ala inferior de la viga pasante.

2.3 Fisuración en vigas con estribos suspensores

Para los especímenes E5 de luz corta, nudo bajo y con estribos suspensores mostrados en la Fig. 6 (a), la primera fisura es visible al 27% de la carga de fallo de control, con un comportamiento similar a la viga patrón y al experimento E1. Al continuar incrementando la carga, las fisuras se propagan 2 veces el peralte de la viga desde el centro de la luz hasta la cercanía del apoyo, detalle que las diferencias de las vigas de control y vigas sin estribo suspensor, tal como se evidencia en la Fig. 6 (a, b). Esto es atribuible a la transferencia de la carga de los estribos suspensores desde el puntal que se desarrolla debajo del ala de la viga pasante hasta la parte superior de la viga, con un tensor que entrega parte de la carga a zonas cercanas al apoyo.

Para los especímenes E7 de luz corta, nudo alto y con estribos suspensores mostradas en la Fig. 6 (b), el agrietamiento ocurre al 16 % de la carga de fallo de control. A diferencia de la viga sin estribos suspensores, la zona fisurada se propaga hasta los apoyos. En este tipo de especímenes las puntales de compresión aparecen nuevamente bajo el ala del nudo pasante, pero al tener menos hormigón bajo la puntual, esta se fisura a menor carga, punto a partir del cual los estribos suspensores empieza a aportar.

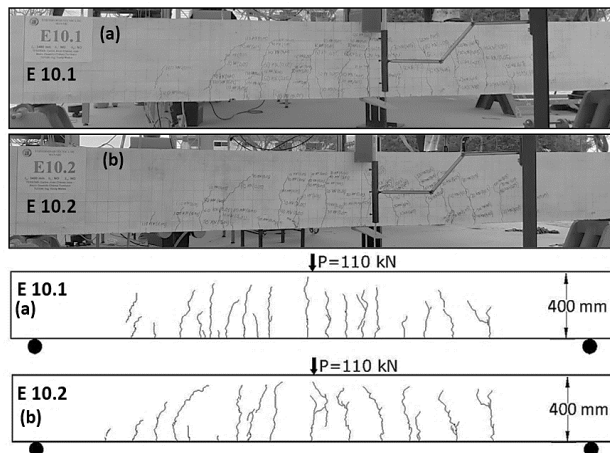


Figura 7. Fisuración para la carga de fallo por fluencia: (a) Especímen E 10.1 (b) Especímen E 10.2.

Fuente: Elaboración propia.

2.4 Fisuración en vigas con relación $\frac{M}{V} = 1,70 m$

Para caracterizar la fisuración de los especímenes con nudo híbrido pasante de luz larga, se ensayaron dos vigas patrones de control sin nudo híbrido denominadas E 10.1 y E 10.2 Fig. 7 con una carga de fallo por fluencia del acero a tracción que se nombró como “fallo de control” de 107,35 kN y 107,01 kN respectivamente, mientras la carga de fallo teórica es de 110,55 kN. Las fisuras predominantes son de flexión y se extienden hacia ambos lados del centro de la luz una longitud cercana a tres veces la altura de la viga. La aparición de la primera fisura principal (tipo capilar) de flexión ocurre al 26 % de la carga de fallo de control.

2.5 Fisuración en vigas sin estribos suspensores

En los especímenes E2 mostrados en la Fig. 8 de luz larga, nudo pequeño y sin estribos suspensores las grietas que predominan son las fisuras de flexión. En la zona ubicada desde el centro de la luz hasta una vez el peralte de la viga, las fisuras son de flexión hasta valores cercanos al 50 % de la carga de fallo primaria. Al aumentar la carga, las fisuras evolucionan a flexión-cortante y comienzan a aparecer desde el centro de la viga hacia ambos apoyos en una distancia cercana a 3 veces el peralte de la viga.

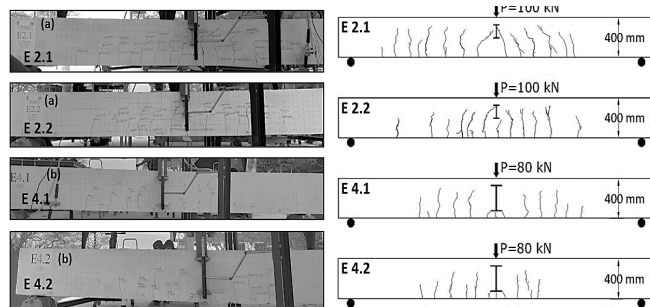


Figura 8. Patrones de fisuración para carga de fallo por fluencia: (a) Especímen E 2 (b) Especímen E 4.

Fuente: Elaboración propia.

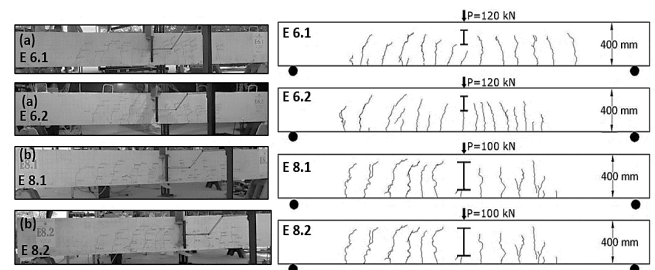


Figura 9. Patrones de fisuración a carga de fallo por fluencia: (a) Especímen E 6 (b) Especímen E 8.

Fuente: Elaboración propia.

2.6 Fisuración en vigas con estribos suspensores

En los especímenes E6 mostrados en la Fig. 9 de luz larga, nudo bajo y estribos suspensores la primera fisura ocurre a un 26 % de la carga de fallo de control. A partir de esa etapa la longitud de fisuras es menor comparada a vigas con las mismas características, pero sin estribos suspensores e iguales rangos de carga. Para las vigas E8 de luz larga, nudo alto y estribos suspensores la primera fisura de flexión se observa al 19 % de la carga de control. Para ambos tipos de especímenes E6 y E8 se observó fisuras desde el centro de la luz hasta 3 veces el peralte de la viga en dirección del apoyo, con fisuras predominantes de flexión tal como evidencia la Fig. 9

3 Evidencias de la fisuración

A continuación, se tomará de referencia la Fig. 10 para realizar las evidencias de la fisuración cuyo detalle es el siguiente:

- En todos los especímenes del experimento en la zona denominada A como se observa en la Fig. 10 se presenta la primera fisura de flexión, de tipo capilar de 0,1 mm de espesor. El patrón de fisuras en la parte inferior de la zona A, evidencia claramente la formación de puntales en forma de abanico para incrementos de carga cercanos a la falla por fluencia.
- Para las zonas B, C y D las fisuras de flexión se presentan luego que se ha llegado a un promedio del 30 % de la carga de fallo de control y cambian a inclinadas para cargas mayores al 45 % en todos los casos a excepción del experimento E8 que se forman al 33 % por tener la combinación de variables independientes más desfavorables.
- Se presentan fisuras de cortante en la zona C de las vigas cortas y D de las vigas largas a cargas mayores al 70 % de la carga de fallo de control.
- En todas las vigas con estribos suspensores las fisuras se propagan a mayor distancia desde el centro de la luz hacia el apoyo en comparación con las vigas sin estribos suspensores. Para la luz corta y con estribos suspensores las fisuras se propagan incluso a toda la viga.
- Luego del incremento de carga que causa la fluencia el acero a tracción (fallo primario), las grietas se ensanchan hasta llegar a la carga que causan el colapso del hormigón comprimido en la parte superior de la sección

(fallo secundario) el cual se manifiesta como un levantamiento del bloque de compresiones que se despega del acero a compresión superior y que clasifica como fisura de adherencia por cortante. Finalmente debido a la presencia de estribos que confinan el hormigón se puede llegar al arrancamiento del acero a tracción en la parte final del ensayo.

A partir de la valoración de los resultados de la experimentación y de la evolución de las fisuras en particular, se puede inferir la formación de puntales observada en todas las vigas del experimento e indican la formación de un primer puntal nombrado como puntal 1 en la Fig. 11 (a) y después ante al incremento de cargas aparece el puntal 2. Cuando se completa la fisuración del puntal de compresiones 2, los estribos suspensoros (si existen) transmiten la carga hacia la parte superior de la viga mediante el tensor indicado en la Fig. 11 (b) y propaga las fisuras hacia zonas más cercanas al apoyo ganando además resistencia.

3.1 Modelo M5

El comportamiento tenso-deformacional del experimento E5 está representado por el modelo M5 de la Fig. 12. Las características tenso-deformacionales inician con un puntal en forma de abanico bajo el nudo híbrido. Hasta la etapa elástica del hormigón a tracción no existe ninguna diferencia con la distribución de tensiones respecto a su semejante del modelo M1 (viga sin estribos suspensoros) mostrada en la Fig. 12 (a). Al 50 % de la carga de fallo [Fig. 12 (b)] la distribución de tensiones se vuelve turbulenta y diferente a la distribución de tensiones del modelo análogo M1 en la misma etapa. Se destaca en la Fig. 12 (b) que los puntales inician en el ala superior de la viga pasante y se apoyan en los estribos suspensoros.

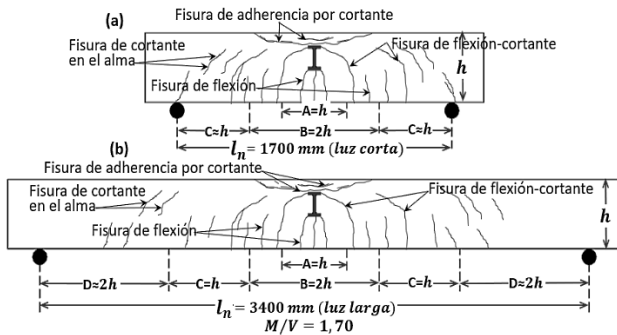


Figura 10. Fisuración típica en vigas con nudos híbridos: (a) $M/V = 0,85$ m (b) $M/V = 1,7$ m. Fuente: Elaboración propia.

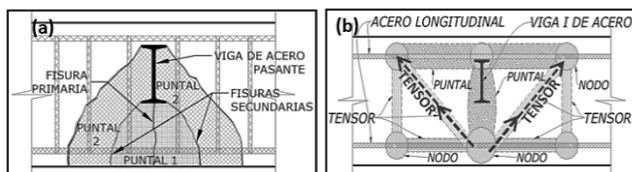


Figura 11. Puntal y tensor que esbozan las fisuras: (a) Puntal de compresiones 1 y 2. (b) Tensor formado por los estribos suspensoros. Fuente: Elaboración propia.

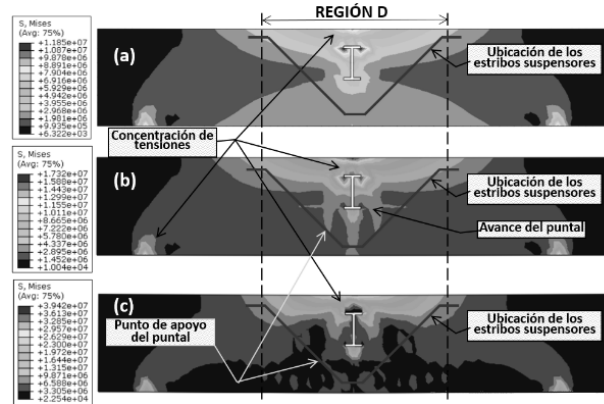


Figura 12. Distribución de tensiones en el hormigón del modelo M5: (a) 30 % de su capacidad máxima, (b) 50 % de su capacidad máxima (c) 100 % de su capacidad máxima. Fuente: Elaboración propia.

La parte (c) de la Fig. 12, corresponde a la etapa de fallo por fluencia del acero a tracción. El diagrama de Mises del hormigón muestra que se comporta como una viga atirantada, con un arco a compresión y tirante desde un apoyo hasta otro, diferente del modelo M1 para la etapa de fallo mostrada en Fig. 12 (c), la misma que tiene puntales bajo el ala de la viga pasante. Este cambio en M5 se debe a que los estribos suspensoros transfieren las cargas hacia la parte superior. La Fig. 12 contiene la evolución de las tensiones en el refuerzo hasta la etapa de fallo por fluencia. En la parte (c) de la Fig. 12 los estribos suspensoros registran esfuerzos similares que el acero a tracción longitudinal, diferente a las etapas previas mostradas en la parte (a) y (b) de la Fig. 12. En la Fig. 12(c) se visualiza el punto de apoyo del puntal en el acero de los estribos suspensoros.

En la Fig. 13(a) se muestra la viga M5 antes de rebasar el límite elástico del hormigón a tracción (30 % de la carga de fallo), con una distribución de tensiones lineal. Al 50 % de la máxima resistencia se observa claramente la creación de un puntal de compresión con forma de botella desde el área que confinan las alas de la viga de acero pasante hasta el nodo que forma el tensor del acero longitudinal y los estribos suspensoros. Para la máxima resistencia (100 % de la carga de fallo por fluencia) la distribución de tensiones alrededor del nudo es turbulenta y se conserva el puntal de compresiones de la etapa previa.

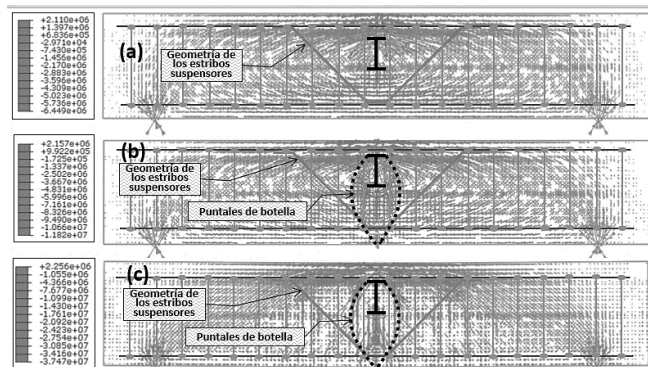


Figura 13. Trayectoria de esfuerzos del modelo M5: (a) 30 % de la carga de fallo (b). 50 % de la carga de fallo. (c) 100 % de la carga de fallo. Fuente: Elaboración propia.

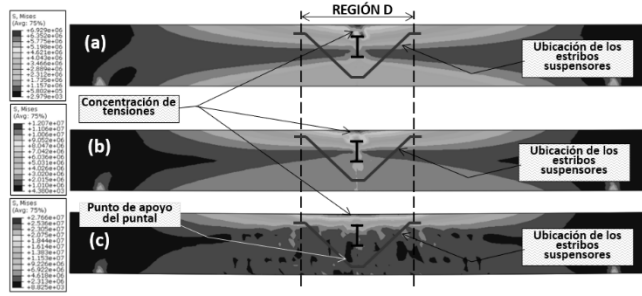


Figura 14. Distribución de esfuerzos en el hormigón del modelo M6: (a) 30 % de la capacidad máxima. (b) 50 % de la capacidad máxima (c) 100 % de la capacidad resistente.
Fuente: Elaboración propia.

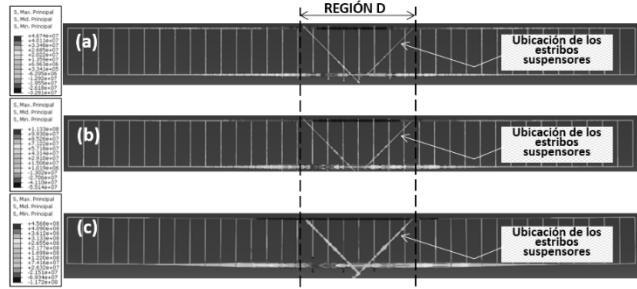


Figura 15. Distribución de tensiones del refuerzo del modelo M6: (a) 30 % de la capacidad máxima. (b) 50 % de la capacidad máxima (c) 100 % de la capacidad máxima.
Fuente: Elaboración propia.

3.2 Modelo M6

El comportamiento tenso-deformacional del modelo M6 indica que hasta la etapa elástica del hormigón a tracción [ver la Fig. 14 (a)], el puntal en forma de abanico es semejante a su modelo análogo sin estribos suspensores (modelo M2) de la Fig. 14 (a). Para tensiones mayores al 50 % de la carga de fallo, las tensiones se diferencian del modelo M2 y, para la etapa de fluencia del refuerzo a tracción (100 % de la carga de fallo) el hormigón registra menor esfuerzo en la zona de tracción y mayor esfuerzo en la zona de compresión en comparación a su par sin estribos suspensores.

La tensión en el refuerzo se presenta en la Fig. 15. En comparación de las vigas cortas de relación $M/V=0,85$ con estribos suspensores M5 de la Fig. 13, los estribos suspensores del modelo M6 de M/V 1,70 no alcanzan la fluencia, mientras que el refuerzo longitudinal a tracción si alcanza la fluencia. Esto indica que los estribos suspensores contribuyen más en vigas con mayor acción de cortante.

4 Métodos para calcular la capacidad resistente de vigas que incorporan estribos suspensores

El método que se propone, parte de los valores de la capacidad resistente nominal a flexión para vigas con nudo híbrido y suspensores (M_{nnh}) y de la resistencia teórica a flexión (M_n) de una viga sin perturbaciones por regiones D e igual a $M_n = A_s f_y \left(d - \frac{a}{2} \right)$; ambos valores nominales sin

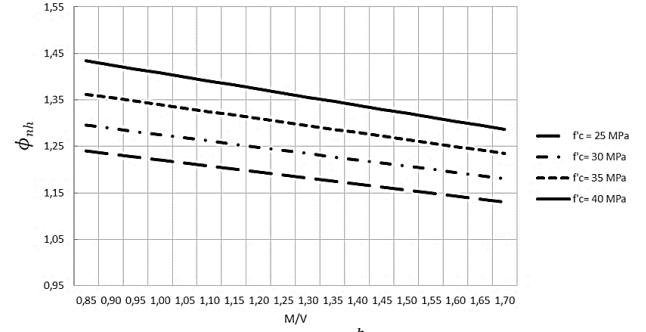


Figura 16. Valor del coeficiente ϕ_{nh} para $\frac{h_c}{h} = 0,35$.
Fuente: Elaboración propia.

aplicar el factor de reducción ϕ , como corresponde. Seguidamente se realizan interpolaciones sucesivas para obtener:

- Valores de la relación $\frac{M_{nnh}}{M_n}$ para valores intermedios de $\frac{M}{V}$, para cada relación $\frac{h_c}{h}$, (0,35 y 0,65) por separado.
- Valores de la relación $\frac{M_{nnh}}{M_n}$ para valores intermedios de $\frac{h_c}{h}$, para cada relación $\frac{M}{V}$, (0,85 y 1,7) por separado.
- Valores de las relaciones $\frac{M_{nnh}}{M_n}$ para valores intermedios de $\frac{h_c}{h}$ para relaciones $\frac{M}{V}$ intermedias entre (0,85 y 1,7).

4.1 Procedimiento para la utilización del método:

4.1.1 Definir los datos de entrada

- f'_c : resistencia del hormigón a la compresión, expresada en MPa.
- f_y : Límite de fluencia del acero, medido en MPa.
- h_c : altura de la viga pasante, en metros.
- h : peralte de la viga, en metros.
- $\frac{M}{V}$: relación entre el momento y el cortante o $\frac{l}{2}$, en metros
- l : distancia desde el nudo hasta el apoyo o nudo siguiente (m)
- A_s : área del refuerzo longitudinal a tracción, en m^2
- b : base de la viga, en metros.

4.1.2 Con la relación $\frac{h_c}{h}$ del caso, seleccionar el gráfico correspondiente. En caso de ser un valor intermedio seleccionar el gráfico del valor de $\frac{h_c}{h}$ inmediato superior.

4.1.3 En la Fig. 16 se debe entrar en la recta correspondiente a la resistencia del hormigón con el valor de M/V (con los valores del caso) y determinar el valor de ϕ_{nh} .

4.1.4 Determinar el valor de M_n por la ec. (1)

$$M_n = A_s f_y \left(d - \frac{a}{2} \right) \quad (1)$$

4.1.5 Determinar el valor de M_{nh} por la ec. (2)

$$M_{nh} = \phi_{nh} \cdot M_n \quad (2)$$

5 Métodos de estimación de la capacidad resistente en nudos con STM

Diversas normativas adoptan el enfoque del modelo de bielas y tirantes (STM), y establecen formulaciones para casos específicos [9,22,23]. Seguidamente se describen algunos de los principales procedimientos recomendados para el diseño de zonas de discontinuidad en las normativas antes citadas.

En términos generales puede establecerse que los pasos sugeridos para diseñar regiones D, con el enfoque STM, son los siguientes: [9].

1. Definir la región o regiones D, en zonas tales como nudos, cargas concentradas, variaciones en la sección, aberturas, entre otras, y a continuación establecer su alcance mediante la aplicación del principio de Saint Venant.
2. Determinar las fuerzas resultantes en los límites de cada región D, donde pueden presentarse tres tipos de esfuerzos externos:
 - Acciones exteriores, como por ejemplo cargas concentradas o fuerzas de pretensado.
 - Reacciones exteriores resultantes del cálculo normal de la estructura.
 - Esfuerzos provenientes de las regiones B adyacentes, tales como esfuerzos cortantes, momentos flectores y fuerzas axiales, que intervienen en el equilibrio de la región D.
3. Escoger un modelo de armadura y calcular las fuerzas resultantes en las bielas y tirantes para transmitir las fuerzas resultantes dentro de la región D. Deben satisfacerse los principios básicos siguientes:
 - El STM debe estar en equilibrio con las cargas de diseño. El cálculo de las reacciones y fuerzas debe cumplir con las leyes de la estática.
 - Las capacidades resistentes de las bielas y tirantes deben ser iguales o superiores a las fuerzas que reciben y las zonas nodales deben ser capaces de soportar o superar las fuerzas que concurren. Si se cumplen estas condiciones la estructura garantiza una distribución segura de las resistencias.
 - En una primera etapa es suficiente considerar los ejes de las bielas y tirantes, luego al diseñar se deben considerar sus anchos, las zonas nodales y las regiones de apoyo.
 - Las bielas no deben cruzarse ni superponerse, en cambio los tirantes pueden superponerse entre sí o cruzar otros tirantes.
 - El ángulo formado entre una biela y un tirante conectados en un nodo debe ser mayor o igual que 25° .
4. Diseñar los puntales, tensores y zonas nodales asegurando que tengan la capacidad resistente necesaria.

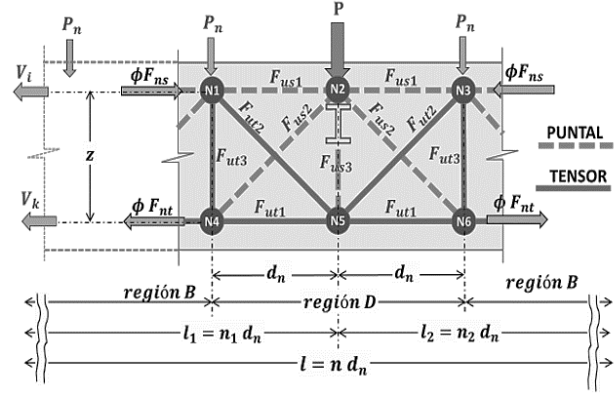


Figura 17. Modelo puntal tensor (MPT) del nudo híbrido.

Fuente: Elaboración propia.

6 Desarrollo del modelo

Las estructuras buscan soportar las cargas con la mínima menor deformación posible, utilizando tensores de menor longitud, ya que los puntales de hormigón son muy rígidos y contribuyen poco al esfuerzo interno [17], por lo cual la geometría y posición de los puntales y tensores deben ser la adecuada. Lo anterior se logra con observación de la fisuración experimental y los modelos matemáticos de ABAQUS de distribución, trayectoria y orientación de las tensiones, lo cual fue utilizado para ubicar los puntales y tensores del nudo híbrido mostrado en la Fig. 17.

En el modelo de la Fig. 17, F_{us1} es el puntal superior del nudo, F_{ut1} es el tensor inferior; F_{ut2} representa el tensor que forman los estribos suspensores, F_{ut3} son los estribos, P es la carga mayorada que transmite el nudo híbrido por la losa que sostiene; P_n es la carga mayorada por peso propio del tramo de la viga de hormigón y área cooperante de la losa que le corresponda; z es la altura del brazo de palanca entre el puntal superior F_{us1} y el tensor inferior F_{ut1} y d_n es la distancia horizontal entre nodos.

Las variables N1, N2... N6, son los nodos del MPT; l es la longitud del tramo de viga de influencia del nudo híbrido en consideración, l_1 y l_2 es la distancia desde el nudo híbrido al apoyo o siguiente nudo híbrido en la viga, V_t y V_k son las fuerzas que transmite el apoyo o un nudo aledaño al tramo de viga si los tuviera. Otras variables utilizadas son F_{ns} y F_{nt} , que representan la resistencia de puntales y tensores respectivamente en las fronteras entre la región B y D. La variable n es el número total de tramos de nodos de la viga; n_1 y n_2 son el número de tramos de nodos que se forman a cada lado del nudo híbrido hasta el siguiente apoyo o longitud de influencia del nudo híbrido aledaño.

El bloque de compresiones debe resistir una fuerza igual al puntal F_{us1} :

$$F_{us1} = n_1 \cdot R_i \frac{(d_n)^2}{z \cdot d_n} - \frac{n_1(n_1 + 1)}{2} \cdot P_n \frac{d_n}{z} + V_t \quad (3)$$

El puntal diagonal denominado F_{us2} se calcula como:

$$F_{us2} = R_i \frac{d_h}{z} - n_1 \cdot P_n \frac{d_h}{z} \quad (4)$$

Para representar el puntal bajo el nudo observado en los ensayos y el estudio tenso-deformacional, el MPT generalizado tiene un puntal F_{us3} igual:

$$F_{us3} = P$$

El refuerzo longitudinal a tracción debe resistir la fuerza del tensor

$$F_{ut1} = n_1 \cdot R_i \frac{(d_n)^2}{z \cdot d_h} - \frac{n_1(n_1 + 1)}{2} \cdot P_n \frac{d_n}{z} + V_k \quad (6)$$

El MPT de la Fig. 17 contiene un tensor dado por los estribos suspensores F_{ut2} cuyo refuerzo diagonal debe resistir:

$$F_{ut2} = R_i \cdot \frac{d_n}{d_h} - n_1 \cdot P_n \quad (7)$$

El refuerzo transversal (estribos o cercos) debe ser capaz de resistir la fuerza del tensor vertical F_{ut3} :

$$F_{ut3} = R_i - n_1 \cdot P_n \quad (8)$$

A partir de la fuerza de los puntales y tensores que definen las fuerzas anteriores, es posible diseñar el nudo. Para encontrar el área de refuerzo de cualquier tensor se emplea la ec. (9).

$$\phi F_{nt} = \phi A_{ts} f_y \quad (9)$$

Se debe cumplir que $\phi F_{nt} \geq \phi F_{ut}$, de manera que es posible reemplazar $F_{nt} = F_{ut1}$ en la ec. (9) y al despejar A_{st1} se obtiene el refuerzo longitudinal a flexión bajo el nudo:

$$A_{st1} = \frac{F_{ut1}}{\phi f_y} \quad (10)$$

De igual manera, por reemplazo en la ec. (10), se puede encontrar el acero de los estribos suspensores o de los estribos (cercos) al hacer $F_{nt} = F_{ut2}$ o $F_{nt} = F_{ut3}$. Se pueden realizar reemplazos en la ec. (11), y se obtiene el ancho del puntal w_s . Se debe cumplir que $\phi F_{ns} \geq \phi F_{us}$ donde $\phi F_{ns} = \phi 0,85 \beta_s \beta_c f'_c w_s b$ de manera que si se toma $F_{ns} = F_{us}$ y se despeja de w_s de la ec. (11) se puede determinar el ancho de los puntales, pues el resto de las variables son conocidas.

$$\phi F_{us} = \phi 0,85 \beta_s \beta_c f'_c w_s b \quad (11)$$

Los anchos de las zonas nodales deben resistir los esfuerzos de los puntales y tensores que convergen en ese nudo, para lo cual se debe satisfacer que $\phi F_{nn} \geq F_{us}$, pero $F_{nn} = f_{ce} A_{nz}$, siendo $f_{ce} = 0,85 \beta_c \beta_n f'_c$ y A_{nz} el ancho de la zona nodal e igual a $A_{nz} = w b$, donde w puede ser el ancho de un puntal " w_s " o el ancho de un tensor " w_t ". Al reemplazar las ecuaciones y despejar w se obtiene la ec. (12), que comprueba que el ancho de los puntales y tensores

satisfacen la resistencia de las zonas nodales.

$$w \geq \frac{F_{nt1}}{\phi f_{ce} b_s} \quad (12)$$

El ancho del ala b_f de la ec. (13), actúa como una placa de apoyo frente la acción de la carga P en la zona nodal 2 de la Fig. 17. Ese nodo debe garantizar que la resistencia del hormigón sea igual o superior a la fuerza de compresión generada por la carga P y cumpliendo la condición $\phi F_{nn} \geq F_{us}$, donde F_{nn} representa la resistencia en la superficie de la zona nodal hidrostática N_2 . De la ec. (5) se tiene que $F_{us3} = P$, entonces $P \leq \phi f_{ce} \cdot A_{vp}$, donde A_{vp} es el área contacto de la viga pasante con el hormigón e igual a $A_{vp} = b \cdot b_f$, siendo b es el ancho de la viga de hormigón.

$$b_f \geq \frac{P}{\phi f_{ce} b} \quad (13)$$

El ancho del ala b_f de la viga pasante tipo IPN es apropiado, si es mayor o igual al obtenido con la ec. (13), ya que esto garantiza que la capacidad resistente de diseño en la cara del nodo 2 será mayor que las fuerzas ejercidas por el nudo pasante.

7 Diagrama de flujo

La Fig. 18 presenta un diagrama de flujo para calcular el MPT del nudo híbrido mostrado en la Fig. 17.

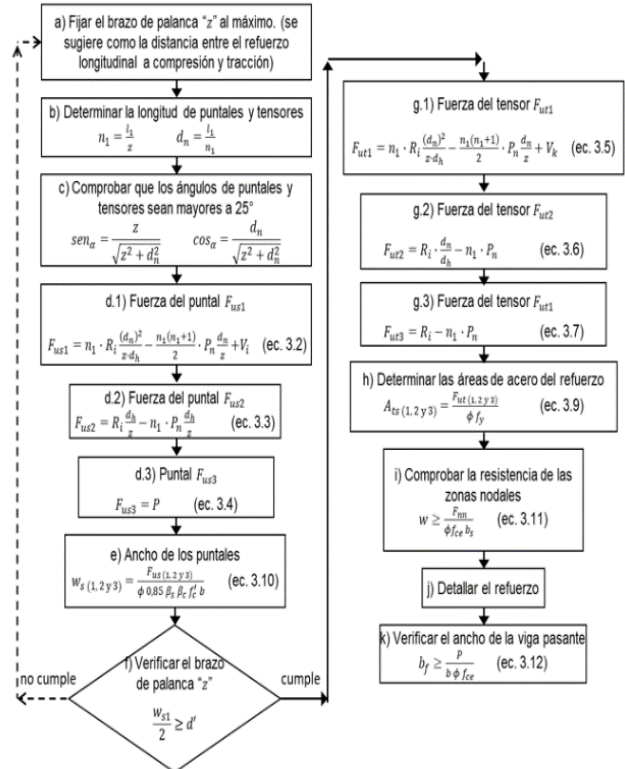


Figura 18. Diagrama de flujo para diseñar un nudo híbrido de viga pasante mediante MPT.

Fuente: Elaboración propia.

8 Conclusiones

- En todas las vigas con nudo híbrido, para esfuerzos menores al 30 % de la carga de fallo existe una concentración de tensiones en el hormigón alrededor de las dos alas de la viga pasante, que se distribuye hacia la parte inferior del peralte de la viga de hormigón con un puntal en forma de abanico y trayectorias de esfuerzos continuas y similares a una viga sin nudo híbrido.
- Para cargas mayores al 30 % de la carga de fallo, los puntales se apoyan en la zona confinada por las alas de la viga de acero y los esfuerzos evolucionan con una concentración de tensiones de compresión.
- Los estribos suspensores conducen las cargas hacia la parte superior, facilitando la distribución del esfuerzo sobre un área mayor de la región superior de la viga de HA, razón por la cual el esfuerzo en el hormigón disminuye, pues ahora la misma carga se reparte en una región mayor de la zona comprimida o traccionada de la viga cuando se alcanza el fallo por fluencia, en contraste con una viga equivalente que no cuenta con estribos suspensores.
- Los estribos suspensores en modelos con $M/V=1,70$ no alcanzan la fluencia a diferencia de los modelos con $M/V=0,85$, lo cual indica que los estribos suspensores contribuyen más en vigas con mayor predominio del cortante.
- En vigas con relaciones $M/V=0,85$, los estribos suspensores con una rama inclinada a 45° , aportan mayor resistencia que los estribos suspensores inclinados 90° , 75° , 60° , 21° y 0° , siendo 0° una barra horizontal paralela al acero longitudinal en toda la longitud de la viga de HA, del mismo diámetro que los estribos suspensores.
- Se demuestra por vías numéricas que la resistencia a momento flector se incrementa con la utilización de mayores resistencias a la compresión del hormigón, con un comportamiento aproximadamente lineal. La ecuación de regresión (2) muestra que la utilización de los estribos suspensores y la resistencia a la compresión del hormigón son las variables de mayor influencia en la resistencia a flexión. Se ratifica también que las variables M/V y h_c/h son significativas al 95 % de confianza.
- El estudio tenso-deformacional realizado permite conocer las trayectorias de los esfuerzos, junto con las fisuras observadas en los ensayos, llevaron a proponer un modelo fundamentado en el Método Puntal Tensor (MPT) para el diseño del nudo mediante ecuaciones para el cálculo del refuerzo longitudinal, transversal y estribos suspensores.

References

- [1] IG-EPN, I.G., Informe sísmico especial [online], 2016., Disponible en: <http://www.igepn.edu.ec/servicios/noticias/1324-informe-sismico-especial-n-18-2016>, 2016.
- [2] Castañeda, E., and Mieles, Y., Reflexiones sobre daños observados en edificios de vigas con nudos híbridos y losas "steel deck" ante el sismo del 16 de abril de 2016. paper presented at the proceedings of the "first annual state-of-the-art in civil engineering structures and materials", Quito, art. 1607, 2016. DOI: <https://doi.org/10.13140/RG.2.2.24934.01607>
- [3] Castañeda, E., and Mieles, Y., Una mirada al comportamiento estructural de columnas, vigas, entresijos y edificaciones durante el sismo de Ecuador 2016. *Revista Ingeniería de la Construcción*, 32(3), art. 157, 2017. DOI: <https://doi.org/10.4067/S0718-50732017000300157>
- [4] M., Ministerio de desarrollo urbano y vivienda, código Ecuatoriano de la construcción 2002-Peligro Sísmico, 2000.
- [5] INEN-NTE-2167, varilla de acero con resaltes, laminados en caliente soldables, microalabeadas o termotratadas, para hormigón armado. Requisitos. Quito, 2011.
- [6] INEN-NTE-1855-1, Hormigones. hormigón premezclado. Requisitos. (INEN Ed.). Quito, 2015.
- [7] Aguiar, R., and Mieles, Y., Análisis de los edificios que colapsaron en Portoviejo durante el terremoto del 16 de abril de 2016. *Revista Internacional de Ingeniería de Estructuras*, 20(3), pp.1-39, 2016. DOI: <https://doi.org/10.13140/RG.2.2.15108.12161>
- [8] CSI, C., Analysis reference manual for SAP2000, ETABS, SAFE and CSI Bridge. Computers and Structures, Inc., Berkeley, CA, USA, 2015
- [9] American Concrete Institute, Building code requirements for structural concrete (ACI 318-14). [Online], 2014. Disponible en https://www.concrete.org/store/productdetail.aspx?ItemID=318U14&Language=English&Units=US_Units.
- [10] NEC-SE-HM, Norma Ecuatoriana de la Construcción, 2015.
- [11] Penelis, G.G., and Penelis, G.G., Concrete buildings in seismic regions: CRC press, art. 2364, 2018. DOI: <https://doi.org/10.1201/b22364>
- [12] Cook, W., and Mitchell, D., Studies of disturbed regions near discontinuities in reinforced concrete members. *ACI Structural Journal*, 85(2), pp. 206-216, 1988. DOI: <https://doi.org/10.14359/2772>
- [13] ACI-318S-19, Requisitos de Reglamento para Concreto Estructural. Farmington Hills: American Concrete Institute, art. 6937, 2019. DOI: <https://doi.org/10.14359/51716937>
- [14] Borja, F., López, A., and Bañón, L., Apuntes de hormigón armado. adaptados a la instrucción EHE-08. Obras de Hormigón. Repositorio Institucional de la Universidad de Alicante. [online], 2012. Disponible en: <http://hdl.handle.net/10045/25610>, 2012.
- [15] Darwin, D., Dolan, C.W., and Nilson, A.H., Design of concrete structures: McGraw-Hill Education. [Online], 2016, Disponible en: <https://www.mheducation.com/highered/product/Design-of-Concrete-Structures-16e-Darwin.html>, 2016.
- [16] Schlaich, J., Schäfer, K., and Jennewein, M., Toward a consistent design of structural concrete. *PCI journal*, 32(3), pp. 74-150, Art. 150, 1987. DOI: <https://doi.org/10.15554/pci.05011987.74.150>
- [17] Dewobroto, W., and Reineck, K.H., Viga con cargas y apoyos indirectos. Diseño de Vigas de Hormigón usando Bielas y Tirantes, 2002.
- [18] Novak, L., SP-273: Further Examples for the design of structural concrete with strut-and-tie models. special publication, 273, art. 323, 2010. DOI: <https://doi.org/10.14359/51682323>
- [19] Wight, J.K., and Parra-Montesinos, G.J., Strut-and-tie model for deep beam design. *Concrete International*, 25(5), pp. 63-70. [online], 2003. Disponible en: https://www.concrete.org/store/productdetail.aspx?ItemID=RPRINT_CIP-6974&Format=DOWNLOAD&Language=English&Units=US_Unit, 2003.
- [20] Wight, J., and MacGregor, J., Reinforced Concrete Mechanics and Design (P. Education Ed. Sixth ed.), 2012.
- [21] Morales Beyer, E.M., Diseño de discontinuidades en vigas de hormigón estructural con modelos puntal-tensor [Tesis de pregrado, Universidad Austral de Chile]. Repositorio Institucional Cybertesis UACH. [online], 2007. Disponible en: <http://cybertesis.uach.cl/tesis/uach/2007/bmfcm828/doc/bmfcm828.d.pdf>, 2007.
- [22] Ministerio de Fomento, Instrucción de hormigón estructural (EHE-08) (Real Decreto 1247/2008, de 18 de julio; BOE de 22 de agosto de 2008). [online], 2008. Disponible en: <https://www.aparejadoresmadrid.es/documents/20194/36447/Instrucció%C3%B3n+de+Hormig%C3%B3n+Estructural+EHE+08.pdf/817f8b8b-d2d3-46c9-be47-a99896ca5b02>, 2008.

- [23] UNE-EN 1992-1-1:2010, Eurocódigo 2: Proyecto de estructuras de hormigón. Parte 1-1: Reglas generales y reglas para edificación [Norma UNE-EN]. UNE. [online], 2010. Disponible en: <https://tienda.aenor.com/norma-une-en-1992-1-1-2010-n0045553>, 2010.

Y. Mieles-Bravo, recibió el título de Ingeniero Civil en 2001 y la Maestría en Ciencias de la Ingeniería con mención en Estructuras en 2008, ambos otorgados por la Universidad Técnica de Manabí, Portoviejo, Manabí, Ecuador. En 2022, recibió el Doctorado en Ciencias Técnicas (CECAT) en la Universidad Tecnológica de la Habana (cuya tesis se enfoca en nudos híbridos en vigas de hormigón). Desde 2009 se desempeña como docente en

el área de estructuras del Departamento de Construcciones Civiles, Facultad de Ingeniería y Ciencias Aplicadas, Universidad Técnica de Manabí. Sus intereses de investigación incluyen: análisis estructural experimental de vigas de hormigón armado con nudos híbridos, modelación numérica en ABAQUS y diseño sísmico de estructuras de concreto reforzado.
ORCID: 0000-0002-2864-2625

G.M. Zambrano-Baque, recibió el título de Ingeniera Civil (Construcciones Civiles) en 2021. Actualmente, desde octubre de 2023, se desempeña como docente técnico en el Departamento de Física de la Universidad Técnica de Manabí, ubicada en Portoviejo, Manabí, Ecuador. Además, desde 2023 está cursando una Maestría en Física en la Facultad de Posgrado de dicha universidad.
ORCID: 0009-0005-7802-6168

Entregando lo mejor de los **colombianos**



Línea de atención al Cliente Nacional: **01 8000 111 210**


Línea de atención al Cliente Bogotá: **(57-1) 472 2000**

► www.4-72.com.co

DYNA

DYNA 92 (239), October - December, 2025
is an edition consisting of 100 printed issues
which was finished printing in the month of December of 2025
in Todograficas Ltda. Medellín - Colombia

The cover was printed on Propalcote C1S 250 g,
the interior pages on Propal Beige 90 g.
The fonts used are Times New Roman, Imprint MT Shadow

- 
- A scenic landscape featuring a wide, muddy river in the foreground, with steep, forested mountains rising in the background under a cloudy sky. The river's banks are covered in dense green vegetation, and a small bridge or structure is visible in the distance. The overall scene is a natural, mountainous environment.
- Impact of printing strategies and thermal debinding atmosphere on the microstructure and mechanical properties of M2 tool steel produced via fused filament fabrication
 - A mathematical model for optimizing the milk and cheese production chain in southern Nariño, Colombia
 - Experimental analysis and computational simulation of heat transfer in a radiator
 - Methodology for evaluating the effectiveness of clay inhibition treatments in injection wells: a case study in a colombian field
 - Proposals for improving acoustic comfort at the Be Live Experience Tuxpan hotel
 - ADKT: a support tool for reducing architectural knowledge evaporation in software projects
 - Effectiveness of 2-Layered grounding grids in high voltage GIS substations and new design considerations using FEM
 - Governance and participatory strategies in sustainable water management: a systematic analysis
 - Synthesis of surfactants based on alkyl glyceryl ester /ether and evaluation as wax inhibitor
 - Mapping the evolution of drone-based last-mile delivery: a bibliometric analysis with field insights from Colombia
 - Improvement of the efficiency of hospital care: a simulation-based approach
 - Safety competency model for drillers in open-pit mines: application of functional analysis and developing a curriculum in Mexican mining
 - Technical and economic analysis of alternatives for the construction of tertiary roads in Colombia
 - Dam break analysis in Andean mountainous areas using numerical simulation in Iber
 - Methods for determining the structural strength of reinforced concrete beams with hybrid nodes

- Impacto de las estrategias de impresión y de la atmósfera de despolimerización térmica en la microestructura y las propiedades mecánicas del acero de herramientas M2 producido mediante fabricación por fusión de filamentos
- Un modelo matemático para optimizar la cadena de producción de leche y queso en el sur de Nariño, Colombia
- Análisis experimental y simulación computacional de la transferencia de calor en un radiador
- Metodología para la evaluación de la eficacia de tratamientos de inhibición de arcilla en pozos inyectoros: caso de estudio en un campo colombiano
- Propuestas para la mejora del confort acústico en el hotel Be Live Experience Tuxpan
- ADKT: una herramienta para la reducción de la evaporación del conocimiento arquitectónico en proyectos software
- Eficacia de redes de puesta a tierra de dos capas en subestaciones GIS de alta tensión y consideraciones de diseño mediante FEM
- Gobernanza y estrategias participativas en la gestión sostenible del agua: un análisis sistemático
- Síntesis de surfactantes basados en ésteres/éteres de alquil glicerilo y evaluación como inhibidores de ceras
- Evolución de la entrega con drones en la última milla: análisis bibliométrico con enfoque en Colombia
- Mejora de la eficiencia de la atención hospitalaria: un enfoque basado en la simulación
- Modelo de competencias de seguridad para perforistas en minas a cielo abierto: aplicación de análisis funcional y desarrollo de un curriculum en la minería Mexicana
- Análisis técnico y económico de alternativas para la construcción de vías terciarias en Colombia
- Análisis de rotura de presas en zonas montañosas Andinas mediante simulación numérica en Iber
- Métodos para determinar la resistencia estructural en vigas de hormigón armado con nudos híbridos